

**Geometrically Non-linear Analysis of Plane
Frames Composed of Prismatic
and Tapered Sections.**

Gurinder Singh Bawa

Doctor of Philosophy

**The University of Aston in Birmingham
December 1988**

This copy of the thesis has been supplied on condition that anyone who consults it is understood to recognise that its copyright rests with its author and that no quotation from the thesis and no information derived from it may be published without the author's prior, written consent.

The University of Aston in Birmingham

**GEOMETRICALLY NON-LINEAR ANALYSIS OF PLANE FRAMES
COMPOSED OF PRISMATIC AND TAPERED SECTIONS.**

by
Gurinder Singh Bawa

Doctor of Philosophy.

1988

Summary

The geometrically non-linear analysis of plane frames is studied using the finite element technique. Stiffness matrices for a constituent prismatic member are first formulated from both derived and approximate displacement functions, the axial force being considered both constant and flexurally dependent.

Both direct and Newton-Raphson type iteration methods are invoked as solution methods, the latter being used in the tangential stiffness matrix approach.

The development is then extended to the study of non-prismatic frames. The use of derived functions in this case proved intractable and formulation was based on the derived functions for the geometrically linear behaviour of a non-prismatic member, this being an approximation to the true non-linear descriptions.

Again direct and Newton-Raphson iteration techniques are used for solution.

In addition to nodal loading, the effect of distributed and non-nodal loading is described, this being reduced to the application of equivalent fixed-end forces.

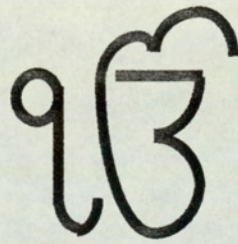
Supporting experimental work is presented for frames composed of both prismatic and tapered members to assess the accuracy of the theoretical solutions with respect to both deflections and bending moments, these tests indicating generally that axial forces should be considered as flexurally dependent. It can be noted that the literature survey showed very little experimental work of this nature.

Several examples are presented to demonstrate the range of problems appertaining to the theoretical developments, of particular note being those describing the behaviour of frames containing initial imperfections.

Further recommendations for study are given, these including the examination of plastic behaviour in conjunction with geometrically non-linear effects.

KEY WORDS

GEOMETRICAL
NON-LINEAR
FRAME
PRISMATIC
NON-PRISMATIC
STIFFNESS
MATRIX



**To the Almighty ONE, my Parents,
Brother and Sister.**

Acknowledgements.

I wish to express my sincere gratitude to Doctor D.J. Just for his supervision, encouragement and unfailing interest throughout the course of this work and during the writing of this thesis, for which I am indebted and much appreciated.

I would also like to thank the University of Aston in Birmingham and the Department of Civil Engineering for providing the finance and research studentship for this study.

Finally, I am most grateful to my very kind parents for their moral support through my studies and wish to thank my family for their encouragement.

List of Contents

	<u>Page</u>
Title Page	1
Summary	2
Dedications	3
Acknowledgements	4
List of Contents	5
List of Figures	13
List of Graphs & Tables	16
Nomenclature	17
<u>CHAPTER 1</u> - Historical Review and Literature Survey.	20
1.1. Historical Review.	21
1.2. Prismatic Sections.	23
1.3. Non-prismatic Sections.	25
1.4. Scope of Work.	27
<u>CHAPTER 2</u> - Introduction to the Finite Element Method.	29
2.1. Equilibrium Method.	32
2.1.1. Construction of the Flexural Stiffness Matrix for Straight Prismatic Beam.	33
2.1.1.1. Formulation of Lateral Deflection Function.	33

2.1.1.2. Calculation of Nodal Displacements From Arbitrary Constants.	34
2.1.1.3. Relationship between Stress Resultants & Nodal Displacements.	36
2.1.1.4. Formulation of Stiffness Matrix.	37
2.1.2. Construction of the Axial Stiffness Matrix for a Prismatic Bar.	38
2.1.3. Combined Stiffness Matrix for Flexural & axial Behaviour.	40
2.2. Work Method.	41
2.2.1. Construction of Flexural Stiffness Matrix for a Straight Tapered Rectangular Beam of Constant Breadth.	42
2.2.1.1. Relationship between Strains and Nodal Displacements.	43
2.2.1.2. Relationship between Stress Resultants and Strains.	43
2.2.1.3. Formation of Stiffness Matrix $[K_b]$.	45
2.2.1.4. Construction of Axial Stiffness Matrix $[K_a]$ for a Tapered Rectangular Beam.	46
2.2.1.5. Combined Stiffness Matrix for Flexural & Axial Behaviour.	47
2.3. Summary of the Two Methods.	49
2.3.1. Equilibrium Method.	49
2.3.2. Work Method.	49
<u>PART A</u> - Geometrically Non-linear Analysis of Prismatic Sections.	50
<u>CHAPTER 3</u> - Matrix Formulation.	51
3.1. Equilibrium Method.	53

3.1.1. Non-linear Matrix with Mutually Independent Flexural & Axial Components for Member in Compression.	54
3.1.2. Non-linear Matrix with Mutually Independent Flexural & Axial Components for Member in tension.	61
3.1.3. Limitations of the Non-linear Matrices so far Described.	65
3.1.4. Modification of Axial Strain Expression due to Finite Lateral Displacements.	66
3.1.5. Non-linear Stiffness Matrix with Coupled Flexural & Axial Components.	69
3.1.6. Formulation of Lateral Deflection Effects on Axial force for Member in Compression.	71
3.1.7. Formulation of Lateral Deflection Effects on Axial force for Member in Tension.	75
3.2. Work Methods.	76
3.2.1. Non-linear Stiffness Matrix with Mutually Independent Flexural & Axial Components.	77
3.2.2. Non-linear Stiffness Matrix with Coupled Flexural & Axial Components (Tangential Stiffness Matrix).	82
3.2.2.1. Relationship between Strains & Nodal Displacements.	82
3.2.2.2. Relationship between Stress Resultants and Strains.	84
3.2.2.3. Formulation of Tangential Stiffness Matrix.	85
3.2.2.3.1. Evaluation of $[K_L]$.	92
3.3. The Displacement Transformation Matrix.	96
3.4. Formulation of the Global Stiffness Matrix.	99

<u>CHAPTER 4</u> - Construction of Stiffness Matrices & Methods of Solution.	103
4.1. Construction of Global Equations for the Structure.	104
4.1.1. Linear Element.	104
4.1.2. Non-linear Element.	109
4.2. Imposition of Known Displacements	112
4.3. Solution of Linear Equations.	114
4.3.1. Cholesky Decomposition Method.	115
4.4. Solution of Non-linear Equations.	116
4.4.1. Elements obtained from Equilibrium and Work Processes in which Axial & Flexural Effects are Independent.	117
4.4.2. Elements obtained from Equilibrium in which Axial & Flexural Effects are Coupled.	117
4.4.3. Element Formulation Through a Tangent Stiffness Matrix.	118
4.5. Flow Charts for Programs.	120
4.5.1. Exact Solution using Coupling Factors.	120
4.5.2. Tangential Stiffness Matrix.	121
<u>CHAPTER 5</u> - Treatment of Non-nodal & Distributed Loading.	123
5.1. Non-nodal Point Load.	124
5.2. Distributed Loading.	129
5.3. Evaluation of Fixed end Moments.	132

5.3. Modification to the Program.	134
<u>PART B</u> - Geometrically Non-linear Analysis of Non-prismatic Sections.	135
<u>CHAPTER 6</u> - Matrix Formulation.	136
6.1. Formation of the Exact Stiffness Matrix for Geometrically Linear Behaviour of a Non-prismatic Beam.	138
6.1.1. Development of the Flexural Stiffness Matrix.	138
6.1.1.1. Formulation of the Lateral Deflection Function.	139
6.1.1.2. Calculation of Nodal Displacements from the Arbitrary Constants.	141
6.1.1.3. Relationship between Stress Resultants and Nodal Displacements.	142
6.1.1.4. Formulation of Stiffness Matrix $[K_b]$.	143
6.1.2. Construction of the Axial Stiffness Matrix $[K_a]$ for a Non-prismatic Bar.	145
6.1.3. Combined Stiffness Matrix for Flexural and Axial Behaviour.	147
6.1.4. Formulation of Stiffness Matrix for Rectangular and I-sections.	149
6.1.4.1. Rectangular Section.	149
6.1.4.2. I-section.	151
6.1.5. Formulation of Stiffness Matrix for a General Shape of Section.	154
6.2. Formulation of Exact Deflection Function for Non-linear Behaviour.	157
6.2.1. Formation of Lateral Deflection Function.	157

6.3. Formulation of Non-linear Stiffness Matrix with Mutually Independent Flexural & Axial Components.	161
6.3.1. Rectangular Section.	162
6.3.2. General Section (Power Function).	165
6.4. Non-linear Stiffness Matrix with Coupled Flexural and Axial Components (Tangential Stiffness Matrix).	166
6.4.1. Relationship Between Strains and Nodal Displacements.	166
6.4.2. Relationship Between Stress Resultants and Strains.	168
6.4.3. Formulation of Tangential Stiffness Matrix.	168
6.4.3.1. Evaluation of $[K_L]$.	170
<u>CHAPTER 7</u> - Non-nodal Loadings for Non-prismatic Sections.	173
7.1. Point Loads	175
7.2. Uniform Distributed Loadings.	176
<u>PART C</u> - Results, discussions and Conclusions.	177
<u>CHAPTER 8</u> - Experimental Verifications.	178
8.1. Description of Experimental Work.	179

8.1.1. Experimental Objectives.	179
8.1.2. Determination of Elasticity Modulus (E).	181
8.1.2.1. For Prismatic Sections.	183
8.1.2.2. For Non-prismatic Sections.	184
8.1.2.3. Tensile Results for Material Specimens.	185
8.1.3. Method of Testing.	187
8.2. Prismatic Section Results.	194
8.2.1. Discussion.	202
8.3. Tapered Section results.	204
8.3.1. Discussion.	211
<u>CHAPTER 9</u> - Application to Framework Behaviour.	213
9.1. Comparative Behaviour of Multi-storey Frames.	214
9.1.1. Load/Deflection Characteristics with Point Loads.	214
9.1.2. Load/Deflection Characteristics with UDL.	221
9.2. Analysis of Pitched Portal Frames subjected to High Column Loads via a Gantry Crane.	225
9.2.1. Frame composed of Prismatic I-sections.	225
9.2.2. Frame composed of Tapered I-sections.	230
9.3. Effects of Initial Imperfections on the Non-linear Behaviour of Pitched Portal Frames.	235
9.3.1. Effect of Lack of Straightness in Prismatic Frames.	235

9.3.2. Effect of Constructional Tolerances. 240

CHAPTER 10 - Summary, conclusions and Future work. 245

10.1. Summary. 246

10.2. Conclusions. 247

10.2.1. Frames with Prismatic Members. 247

10.2.2. Frames with Non-prismatic Members. 249

10.2.3. Practical examples of Geometrically Non-linear behaviour. 250

10.3. Recommendations for Future Research. 252

REFERENCES. 257

APPENDICES.

Appendix 1

Appendix 2

Appendix 3

Appendix 4

List of Figures.

- 2.1. Illustration Showing System of Elements and Nodal Points.
- 2.2. Straight Beam Showing positive Values of Nodal Forces.
- 2.3. Diagram Showing Stress Resultants and External Forces.
- 2.4. Diagram Showing Stress Resultants and Nodal Forces.
- 2.5. Tapered Beam Showing Positive Values of Nodal Forces.
- 2.6. Tapered Beam Showing a General Depth at Distance x .

- 3.1. Diagram Showing the Nodal Forces on the Deformed Member.
- 3.2. Diagram Showing the Element in its Deformed State in Compression.
- 3.3. Diagram Showing the Element in its Deformed State in Tension.
- 3.4. Diagram Showing Member under Lateral Loading.
- 3.5. Diagram Showing Element Deformation Due to Lateral Displacements.
- 3.6. Diagram Showing the Element in its Deformed State in Compression.
- 3.7. General Deformation of Member.
- 3.8. Displacement Components.
- 3.9. Forces in Local and Global Coordinate System.

- 4.1. Diagram showing Nodal External Forces to Their corresponding Displacements.
- 4.2. Diagram Showing Joint External Nodal Loadings.
- 4.3. Construction of Overall Stiffness Matrix and Formation of Global Equations.
- 4.4. Method of Imposing Zero Displacements.

- 5.1. Decomposition of Effect of Non-nodal Point Load.

- 6.1. Tapered Beam Showing positive Values of Nodal Forces.
 - 6.2. Stress Resultants on Element.
 - 6.3. Diagram Showing Stress Resultants and Nodal Forces.
 - 6.4. Tapered Beam Showing a General Depth at Distance x .
 - 6.5. Showing typical I-section.
 - 6.6. Non-prismatic Member Under Axial loading.
 - 6.7. Diagram Showing the Element in its Deformed State in Compression.
-
- 8.1. Diagram of the two Frames Considered in Experiment.
 - 8.2. Showing Four point Bending Test.
 - 8.3. Strain Gauge Positioning.
 - 8.4. Showing the fixing of test Frame to base of rig.
 - 8.5. Diagram showing Metal Fitment.
 - 8.6. Showing Positioning of Dial Gauges.
 - 8.7. Arrangement of apparatus with Strain recorder.
 - 8.8. Load/Deflection for Frame composed of Prismatic Sections.
 - 8.9. Load/Deflection for Frame composed of Prismatic Sections.
 - 8.10. Load/Moment at Joint 1 for Prismatic Sections.
 - 8.11. Load/Moment at Joint 2 for Prismatic Sections.
 - 8.12. Load/Moment at Joint 3 for Prismatic Sections.
 - 8.13. Convergence of Solution as Number of Elements Increases.
 - 8.14. Load/Deflection for Frame composed of Tapered Sections.
 - 8.15. Load/Deflection for Frame composed of Tapered Sections.
 - 8.16. Load/moment at Joint 1 for Tapered Sections.
 - 8.17. Load/moment at Joint 2 for Tapered Sections.
 - 8.18. Load/moment at Joint 3 for Tapered Sections.

- 9.1. Multistorey Frames under Study.
- 9.2. Sectional properties of Beams and Columns.
- 9.3. Frames showing System of Loadings.
- 9.4. Reduction in Stiffness with increase of Loading for two- and four storey frames.
- 9.5. Deflection and Moment Diagram.
- 9.6. Frames with Uniformly Distributed loadings.
- 9.7. Load/Deflection Characteristics for 2 and 4 Storey Frames.
- 9.8. Deflection and Moment Diagram.
- 9.9. Typical Workshop Portal Frame with Column Loadings.
- 9.10. Showing Horizontal and vertical deflections at Apex as Crane moves across span for Prismatic Frame.
- 9.11. Frame Deflection as Crane Load moves from one Column to the other.
- 9.12. Frame Joint Moments as Crane Load moves from one Column to the other.
- 9.13. Typical workshop Portal Frame with tapered members.
- 9.14. Dimension of I-section.
- 9.15. Showing Horizontal and vertical deflections at Apex as Crane moves across span for Tapered Frame.
- 9.16. Frame Deflection as Crane Load moves from one Column to the other.
- 9.17. Frame Joint Moments as Crane Load moves from one Column to the other.
- 9.18. Frame composed of Prismatic Sections with Imperfections in Members.
- 9.19. Graph of Load/Deflections due to Imperfections.
- 9.20. Deflections and Moments of Frame with Member Imperfections.
- 9.21. Frame Composed of Tapered Members with initial Joint Displacements.
- 9.22. Graph of Load/Deflection due to initial Joint Displacements.
- 9.23. Deflection and Moments of Frame with Joint Imperfections.

- 10.1. Showing the Idealisation of curved members.
- 10.2. Showing Frame with plastic hinge.

List of Graphs.

- 8.1. Load v Central Deflection for Prismatic Material.
- 8.2. Load v Central Deflection for Non-prismatic Material.

List of Tables.

- 8.1. Table of load and Deflection for Prismatic Frame Material.
- 8.2. Table of load and Deflection for Non-prismatic Frame Material.
- 8.3. Results from the Tensile Test.
- 8.4. Tabulated Results for the Coupled Stiffness Matrix.
- 8.5. Tabulated Results for the Tangential Stiffness Matrix.

Nomenclature.

Roman Alphabet.

a	Arbitrary Constant.
x	Horizontal Axis.
y	Vertical Axis.
u	Axial Deformations.
v	Lateral Deformations.
L	Length of Element.
M	Moments.
S	Shear Force.
E	Modulus of Rigidity.
A	Cross-sectional Area.
I	Second Moment of Area.
P	Axial Force.
t	Depth of Tapered Beam.
b	Breadth of Tapered Beam.
ds	Deformed Length of Element.
W	Load.
h_f	Thickness of Flange.
h_w	Thickness of Web.

Matrices.

- [A] Displacement Transformation Matrix.
- [B] Relationship between strains and Nodal displacements.
- [C] Relationship between arbitrary constants and Nodal displacements.
- [D] Relationship between stress resultants and strains.
- [H] Relationship between stress resultants and Nodal displacements.
- [K] Relationship between Nodal forces and Nodal displacements.
- [S] Relationship between Global Nodal forces and Global Nodal displacements.

Vectors.

- {a} Arbitrary Constants.
- { Δ } Nodal Displacements.
- {P} Nodal Forces.
- { ϵ } Strains
- { σ } Stress Resultants.
- {L} Global Forces.
- {X} Global Displacements.

Suffices.

- a Axial Behaviour.
- b Flexural Behaviour.
- 0 Linear Stiffness Matrix.
- s Initial Stress Matrix
- L Large Deflection Matrix.

Chapter 1

Historical Review and Literature Survey.

1.1. Historical Review.

The concepts of framework analysis emerged during the period of 1850 to 1875 predominantly through the work of J.C.Maxwell, A.Castigliano and O.Mohr. At this time the concepts of matrices were also being introduced and defined by Silvester, Hamilton and Caley. Their work became the foundation of matrix structural analysis, although it was not to find practical application for nearly 80 years.

Between 1875 and 1920, little progress was made in the development of theory and the analytical techniques subsidiary to matrix structural analysis. This was no doubt due mainly to the practical intractability of solving algebraic equations with more than a few unknowns. For the structures of primary interest in this period, trusses and frames, an analytical approach based on member forces as unknowns was universally employed. Analytical techniques such as the principle of polygon of forces, free-body diagrams, method of joints, method of sections, etc were employed where the unknowns were the axial forces in the members.

About 1920, as a result of work by Maney in the U.S.A. and Osterfeld in Denmark, the basic ideas of a truss and framework analysis approach based on displacement parameters as unknowns took form. It was Maney who in 1915 presented the Slope Deflection method ⁽¹⁾ as a general procedure to be used in the analysis of rigid jointed structures. The method involved the setting up of a number of simultaneous equations with unknowns taken as angular rotations and displacements at each joint. The solution of these equations enabled the moments and shear forces to be evaluated at each joint. It was this work that represents the forerunner of matrix structural analysis of today. However severe limitations on the size of problems that could be analysed still remained as the work involved in solving the simultaneous equations became prohibitive on large

structures.

This problem was overcome in 1932, when Hardy Cross introduced the Moment Distribution ⁽²⁾ method. This method made feasible the solution of problems of a greater order of complexity than the most sophisticated problems treatable by prior approaches. The method was simple to use and gave the results in a tabulated form. This process became the staple method of structural framework analysis for the next 25 years.

Today, both Slope Deflection and Moment Distribution are useful for the analysis of small problems as an aid in visualising behaviour, but they are primitive in power compared to computer methods and have been superseded by them in the solution of large complex problems.

The association between the mathematical concepts of matrix theory and the engineering concepts of structural analysis appeared in the 1930's through the work of Frazer, Duncan and Collar ⁽¹⁾. The liaison developed erratically through the 1940's, but there was no motivation for a firm union of the two concepts until the birth of the digital computer in the 1950's. Individuals who foresaw the impact of computers on both theory and practice then undertook the codification of the well established framework analysis procedures in the format best suited to the computer.

Two important publications on the association of these concepts were those of Argyris and Kelsey ⁽³⁾ and Turner, Clough, Martin and Topp ⁽⁴⁾. These publications wedded the concepts of framework analysis and continuum analysis and cast the resulting procedure in matrix format. This led to the first Finite Element techniques where the slope deflection equations were formulated in matrix format. However further

development of finite elements took form with 2 and 3D continua being considered.

With further advancement in both computer technology and software, Finite Element techniques (5,6,7,8) are now the most versatile and most widely used methods in structural analysis today. This has also enabled further complex behaviour to be studied where previously the mathematics were either too complex or the simultaneous equations impossible to solve.

The literature survey which concludes this chapter is presented in two sections, the first being concerned with the stability of frames with prismatic sections and the second with the stability of frames with tapered (non-prismatic) sections. Both are discussed separately below for clarity.

1.2. Prismatic Sections.

During the 1950's and 1960's the stability of frames was studied intensively and several well known texts (9,10,11,12) were published to reflect this interest.

Several research papers were published (13,14,15,16,27) in the mid 1960's to early 1980's concerned with the geometrically non-linear behaviour of frameworks. However it was only in the late 1960's that the matrix method of solution was first widely used in framework analysis and several texts have been published (17,18,19,20,21) since then.

It was Hartz (22) who first applied the standard work-based finite element process to a simple beam subjected to both flexural and axial load and produced stiffness matrices to

show non-linear behaviour. The method, using an approximation to the deformed geometry of the structure, produces results similar to those obtained by the standard stability functions ⁽¹²⁾ which were developed earlier ⁽²³⁾. The relationship between the axial force and the lateral deflections induced in the member due to bending was not considered and hence there was no direct linkage between the axial and flexural stiffness matrices.

Bunce and Brown ⁽²⁴⁾ divided the frame into several small elements and employed an alternative numerical method of finite deflection analysis. They used Dynamic Relaxation techniques where the static problem is represented by a fictional dynamic problem with viscous damping. This enabled easy solution and avoided the use of stability functions. However, because large number of elements need to be considered, it involves a large amount of data input and computer time.

Harald et al ⁽²⁵⁾ developed stiffness matrices using the stability (s and c) functions and produced similar results to those produced by Majid ⁽¹²⁾. However he also developed further components which could be added to the existing stiffness matrix to represent a plastic hinge. The method is useful in investigating plastic bending behaviour but again axial and flexural behaviour are considered independently of each other.

Zienkiewicz ⁽⁴⁵⁾ took the study of geometric non-linearity further by using the work process to develop the 'tangential stiffness matrix' for the study of plate stability. The text extended the previous work done by producing matrices which add on to the existing flexural and axial stiffness matrices and coupled the two independent portions. The formulation was such that the solution can be ideally effected using the Newton-Raphson technique. Further to this Wood and Zienkiewicz ⁽²⁶⁾ produced a

general modified tangential stiffness matrix for one dimensional elements such as arches and axisymmetric shells.

Chajes and Churchill (27) took the work of Wood and Zienkiewicz (26) and applied it to the simple prismatic beam member using a cubic deflection function. They produced the tangential stiffness matrix for the non-linear axial and flexural behaviour of beams, and showed how the Newton-Raphson technique can be adapted to obtain an iterative solution. They developed three matrices, ie the simple linear matrix and two extra additions, these being dependent on the axial force in the member and the lateral deflections induced in the structure. The tangential stiffness matrix is formed from a combination of all three matrices.

1.3. Non-prismatic Sections.

From the literature survey it was noticed that although much work had been carried out on the geometrically non-linear behaviour of individual beams and columns, relatively little appertained to the stability of frames composed of tapered (non-prismatic) members and hardly anything on the use of finite elements to study this behaviour.

From the 1950's to late 1970's various authors developed the linear analysis of non-prismatic sections. Moment distribution techniques (39) were employed to find the behaviour of non-prismatic members in frames. Also much work was done on the stability (29,30,31,32,33,34,35) of non-prismatic beams, columns and beam-columns. Simultaneously research was being carried out into the stability of frames composed of tapered members (36,37,38) employing the standard slope deflection technique to obtain the solutions.

It is only recently that, with the rapid development of computer technology, the matrix method can be used effectively in the study of framework stability. During the 1970's some progress was made in the application of the finite element technique to both the linear and non-linear analysis of frames incorporating non-prismatic sections.

Just ⁽⁴⁰⁾ used the exact and approximate deflection profiles and the standard finite element method to develop flexural and axial stiffness matrices to represent the linear behaviour of non-prismatic members in frames. He also developed equivalent fixed end shears and moments for loads which were not applied at the nodes of the element. This paper set the foundation for his next paper ⁽⁴¹⁾ where the method was further extended to box and I-sections respectively. Further equivalent nodal loads were developed for uniformly distributed loads and triangular loads and several examples evaluated to show the versatility of the matrices developed.

Brown ⁽⁴²⁾ and Karabalis⁽⁴³⁾ presented the linear flexural and axial matrices produced by Just ^(40,41) but using the approximate cubic deflection function to represent the deflected form of the non-prismatic section. This procedure, although simple to formulate, requires that the frame be divided into smaller elements and hence takes up much computer storage and time. However the results showed that for design office use, the accuracy and the convergence obtained from the approximate stiffness matrices is adequate with a small number of elements.

Recently Karabalis and Beskos ⁽⁴⁴⁾ used the approximate, cubic, deflection profile and developed stiffness matrices to represent geometric non-linear behaviour. This again requires that the framework be sub-divided into smaller elements and hence the need for large amount of data preparation and computer time.

1.4. Scope of Work.

Although non-prismatic members can be approximated by a number of stepped prismatic elements, such an approximation may require a considerable quantity of data preparation and computer time. Hence there exists a strong motivation to obtain accurate stiffness matrices for both prismatic and non-prismatic elements for geometrically non-linear analysis.

An understanding of prismatic members is a prerequisite to the understanding of non-prismatic members, and therefore a general study of the geometrically non-linear behaviour of prismatic members is first presented. Both the 'equilibrium method' and 'work method' are presented so that the reader may become fully acquainted with the principles of the finite element method.

For the prismatic section, the exact linear and corresponding exact non-linear deflection profiles are employed to develop the flexural and axial stiffness matrices respectively. The development leads to a solution procedure in which the load vector is progressively modified, a technique which appears not to have been considered in previous research. The results from this method are considered to represent most closely the non-linear behaviour of prismatic frames and the accuracy of the more approximate techniques is assessed by comparison with it. Similarly for the non-prismatic section approximate and exact deflection functions are used to derive the matrices for linear and non-linear behaviour.

Further to this the equivalent nodal forces (for uniformly distributed loading and inter joint loading) are presented for both prismatic and non-prismatic sections.

A brief outline is given of the main program and the development of useful routines which were employed in setting up the stiffness matrices. Also efficient, time saving, solution routines are presented which were used in the program.

Supporting experimental work is described with details of instrumentation. Several examples are presented to show both the versatility of the program and the finite element method in non-linear analysis, and also to examine the effect of non-linear behaviour in practical complex frameworks.

Chapter 2

Introduction to the Finite Element Method.

As outlined in chapter 1, the development of computer technology has enabled systematic analytical techniques involving large numbers of equations to be applied to the solution of continuum problems of great complexity and of these methods the finite element method is perhaps the most versatile at the present time.

The method is similar to the finite difference method in as much as the continuum is divided into a mesh and equations set up at every node, but differs from it in the manner in which the continuum is modelled. Whereas in the method of finite differences the governing differential equations of the continuum are replaced by difference equations which enable nodal equations to be constructed, in the finite element method the continuum is divided into a number of elements, each of these elements being connected to its neighbours at the nodes, as shown in Fig. 2.1.

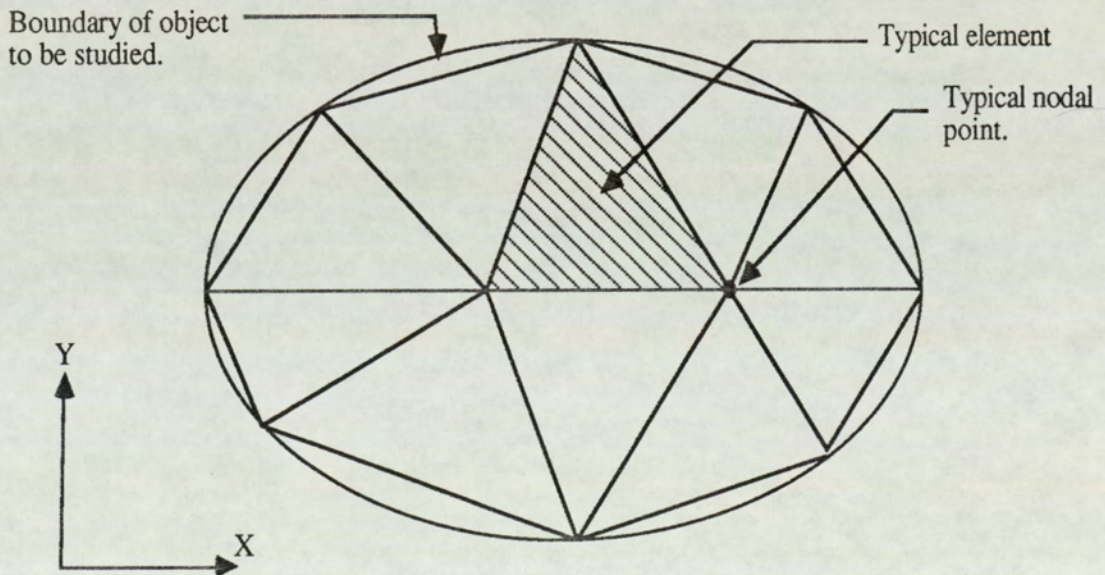


Fig. 2.1. Illustration Showing System Of Elements And Nodal Points.

In a structural problem, the determination of the force/displacement characteristics of a single element, ie by the obtaining of its stiffness properties, enables equilibrium equations to be set up at each node from which the nodal displacements may be obtained. Once these displacements have been obtained the nodal forces and stress distributions throughout the model can be obtained by back substitution into the original force/displacement relationships.

The method thus consists of the determination of the stiffness characteristics of the element and this may be obtained via the displacement field of the element. Generally this profile is either impossible or impractical to obtain exactly and therefore must be assumed.

This inherent approximation means that the stiffness characteristics of the element are themselves approximate and must be obtained via a work formulation with a suitable choice of displacement profile. The effect of the approximation on the accuracy of the analysis can be reduced by finer subdivision of the continuum.

Although the finite element method is primarily understood in relationship to 2 and 3D continua, the method can be equally well applied to essentially one dimensional structures. In this case, since the displacements are functions of one variable only, it is possible to obtain precise formulations which are not dependent upon subdivision for their accuracy.

Indeed because of this ability to determine the displacement field exactly, the derivation of the stiffness matrix when applied to one-dimensional elements can be obtained from direct equilibrium and can be much more concise compared with the standard work process used with approximate displacement functions.

To illustrate the process using derived functions and to compare it with the standard work process, the derivation of the bending and axial stiffness matrices for the straight prismatic beam shown in Fig. 2.2 will be presented using both methods.

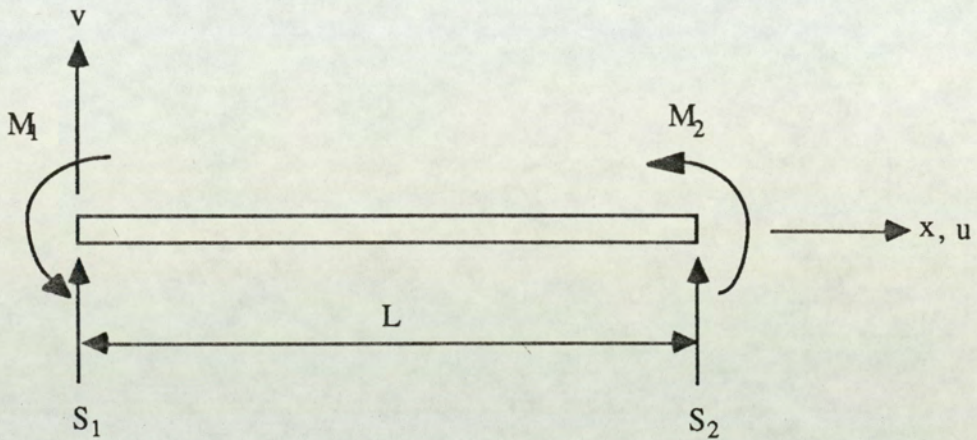


Fig 2.2. Straight Beam Showing Positive Values of Nodal Forces.

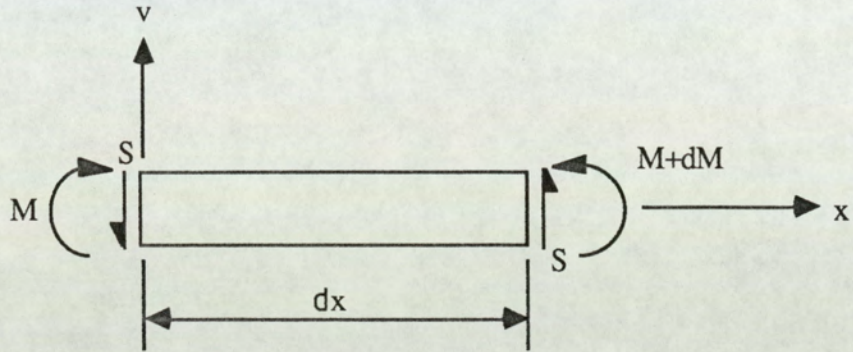
2.1. Equilibrium Method.

As previously mentioned this method depends on the ability to obtain the precise manner in which the element deforms and if this can be achieved, then the exact stiffness matrix can be obtained in a particularly precise manner. The advantage of an exact solution is that no increase in accuracy ensues on subdivision of the element and hence large elements can be used, thus reducing the amount of data required.

Construction of the Flexural Stiffness Matrix $[K_b]$ for a Straight Prismatic Beam.

2.1.1. Formulation of Lateral Deflection Function.

Consider the equilibrium of an element of length dx from Fig.2.2.



Rotational equilibrium of the element gives;

$$S = - \frac{dM}{dx} \dots\dots\dots(2.1)$$

and since for vertical equilibrium, S is constant;

$$\frac{d^2M}{dx^2} = \frac{dS}{dx} = 0 \dots\dots\dots(2.2)$$

Thus on application of the equation of simple bending,

$$M = EI \frac{d^2v}{dx^2} \dots\dots\dots(2.3)$$

and assuming EI to be constant, equation (2.2) may be expressed as;

$$\frac{d^2M}{dx^2} = EI \frac{d^4v}{dx^4} = 0$$

ie

$$\frac{d^4 v}{dx^4} = 0 \quad \dots\dots\dots(2.4)$$

Successive integration of (2.4) yields the deflection profile of the beam as;

$$v = a_1 + a_2x + a_3x^2 + a_4x^3 \quad \dots\dots\dots(2.5)$$

Hence the lateral deflection function is a cubic polynomial in which a_1, a_2, a_3, a_4 are the constants of integration, and from this function the flexural stiffness matrix can be formed (It should be noted from the derivation above that any contribution to bending from the axial loads is ignored and thus the treatment appertains to linear behaviour, that is where the displacements are considered to tend to zero).

2.1.1.2. Calculation of Nodal Displacements from the Arbitrary Constants $\{a_b\}$.

In order that the displacements can be uniquely determined in terms of the nodal displacements, the four arbitrary constants $\{a_b\}$ must be written in terms of the four end displacements namely $v_1, \theta_1, v_2, \theta_2$ where θ is the slope of the member and is given by;

$$\theta = \frac{dv}{dx} = a_2 + 2a_3x + 3a_4x^2 \quad \dots\dots\dots(2.6)$$

or in matrix form as

$$\theta = [0 \quad 1 \quad 2x \quad 3x^2] \begin{matrix} a_1 \\ a_2 \\ a_3 \\ a_4 \end{matrix}$$

On substituting the boundary conditions at both nodes, the following matrix ensues;

$$\begin{Bmatrix} v_1 \\ \theta_1 \\ v_2 \\ \theta_2 \end{Bmatrix} = \begin{bmatrix} 1 & 0 & 0 & 0 \\ 0 & 1 & 0 & 0 \\ 1 & L & L^2 & L^3 \\ 0 & 1 & 2L & 3L^2 \end{bmatrix} \begin{Bmatrix} a_1 \\ a_2 \\ a_3 \\ a_4 \end{Bmatrix} \quad \dots\dots\dots(2.7)$$

$$\text{ie } \{\Delta_b\} = [C_b]\{a_b\}$$

which upon inversion gives;

$$\begin{Bmatrix} a_1 \\ a_2 \\ a_3 \\ a_4 \end{Bmatrix} = \begin{bmatrix} 1 & 0 & 0 & 0 \\ 0 & 1 & 0 & 0 \\ -\frac{3}{L^2} & -\frac{2}{L} & \frac{3}{L^2} & -\frac{1}{L} \\ \frac{2}{L^3} & \frac{1}{L^2} & -\frac{2}{L^3} & \frac{1}{L^2} \end{bmatrix} \begin{Bmatrix} v_1 \\ \theta_1 \\ v_2 \\ \theta_2 \end{Bmatrix} \quad \dots\dots\dots(2.8)$$

$$\text{ie } \{a_b\} = [C_b]^{-1}\{\Delta_b\}$$

Thus the four arbitrary constants are expressed in terms of the four nodal displacements.

2.1.1.3. Relationship Between Stress Resultants and Nodal Displacements $\{\Delta_b\}$.

From the equation (2.3)

$$M = EI \frac{d^2 v}{dx^2}$$

and from equation (2.1) it follows that

$$S = -EI \frac{d^3 v}{dx^3} \dots\dots\dots(2.9)$$

Then on differentiating the displacement function and substituting the result into (2.3) and (2.9), the stress resultants M and S can be obtained in terms of the nodal displacements thus:-

$$\begin{Bmatrix} S \\ M \end{Bmatrix} = EI \begin{bmatrix} 0 & 0 & 0 & -6 \\ 0 & 0 & 2 & -6x \end{bmatrix} \begin{Bmatrix} a_1 \\ a_2 \\ a_3 \\ a_4 \end{Bmatrix}$$

However since the arbitrary constants can be expressed in terms of the nodal displacements (2.8) the above can be written as;

$$\begin{Bmatrix} S \\ M \end{Bmatrix} = EI \begin{bmatrix} \frac{-12}{L^3} & \frac{-6}{L^2} & \frac{12}{L^3} & \frac{-6}{L^2} \\ \frac{-6 + 12x}{L^2} & \frac{-4 + 6x}{L} & \frac{6 - 12x}{L^2} & \frac{-2 + 6x}{L} \end{bmatrix} \begin{Bmatrix} v_1 \\ \theta_1 \\ v_2 \\ \theta_2 \end{Bmatrix} \dots\dots\dots(2.10)$$

ie $\{P_b\} = [H]\{\Delta_b\}$

2.1.1.4. Formulation of Stiffness Matrix $[K_b]$.

Since equilibrium is satisfied at all sections of the beam, the values of the nodal stress resultants must be numerically equal to the nodal external forces. At node 2 these values are of the same sign whereas at node 1 they are of opposite sign as shown in Fig. 2.3.

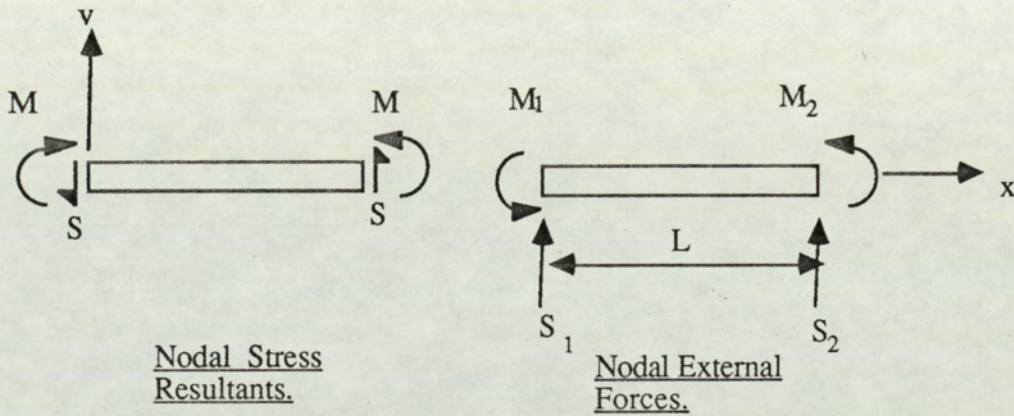


Fig 2.3. Diagram Showing Stress Resultants and External Forces for Beam in Flexure.

Thus applying this reasoning to equation (2.10), and substituting $x=0$ and $x=L$ at nodes 1 and 2 respectively, the relationship between the nodal forces and nodal displacements is given by:-

$$\begin{Bmatrix} S_1 \\ M_1 \\ S_2 \\ M_2 \end{Bmatrix} = \begin{bmatrix} \frac{12EI}{L^3} & \frac{6EI}{L^2} & -\frac{12EI}{L^3} & \frac{6EI}{L^2} \\ \frac{6EI}{L^2} & \frac{4EI}{L} & -\frac{6EI}{L^2} & \frac{2EI}{L} \\ -\frac{12EI}{L^3} & -\frac{6EI}{L^2} & \frac{12EI}{L^3} & -\frac{6EI}{L^2} \\ \frac{6EI}{L^2} & \frac{2EI}{L} & -\frac{6EI}{L^2} & \frac{4EI}{L} \end{bmatrix} \begin{Bmatrix} v_1 \\ \theta_1 \\ v_2 \\ \theta_2 \end{Bmatrix} \quad \dots\dots\dots(2.11)$$

$$\text{ie } \{P_b\} = [K_b]\{\Delta_b\}$$

where $[K_b]$ is the flexural stiffness matrix of the member, this matrix being symmetrical about the leading diagonal.

2.1.2. Construction of the Axial Stiffness Matrix $[K_a]$ for a Prismatic Bar.

The axial stiffness matrix can be formed in the same way as the bending stiffness matrix.

Consider the equilibrium of a length δx of the beam as shown in Fig. 2.4.

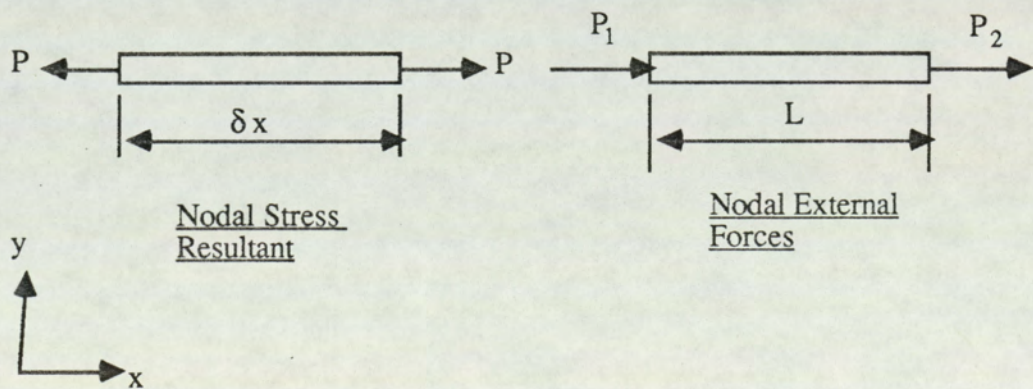


Fig 2.4. Diagram Showing Stress Resultants and External Forces for Axially-loaded Bar.

Horizontal equilibrium requires that;

$$\frac{dP}{dx} = 0 \quad \dots\dots\dots(2.12)$$

Ignoring any moment effect from the axial force, Hooke's Law gives;

$$P = EA \frac{du}{dx} \quad \dots\dots\dots(2.13)$$

Hence from (2.12) and (2.13) ;

$$\frac{d^2u}{dx^2} = 0 \quad \dots\dots\dots(2.14)$$

which upon integration gives the axial displacement function:-

$$u = a_5 + a_6x \quad \dots\dots\dots(2.15)$$

Hence following steps similar to those described in sections (2.1.2) and (2.1.4) and referring to the sign convention shown in Fig. 2.4 yields

$$\begin{Bmatrix} P_1 \\ P_2 \end{Bmatrix} = \begin{bmatrix} \frac{EA}{L} & -\frac{EA}{L} \\ -\frac{EA}{L} & \frac{EA}{L} \end{bmatrix} \begin{Bmatrix} u_1 \\ u_2 \end{Bmatrix} \quad \dots\dots\dots(2.16)$$

$$\text{ie } \{P_a\} = [K_a]\{\Delta_a\}$$

Again the symmetry of the matrix should be noted.

2.1.3. Combined Stiffness Matrix for Flexural and Axial Behavior.

Combining the two matrices for axial and bending effects produces;

$$\begin{Bmatrix} P_1 \\ P_2 \\ S_1 \\ M_1 \\ S_2 \\ M_2 \end{Bmatrix} = \begin{bmatrix} \frac{EA}{L} & & & & & & & \\ & -\frac{EA}{L} & \frac{EA}{L} & & & & & \\ & & & \frac{12EI}{L^3} & & & & \\ & & & & \frac{6EI}{L^2} & \frac{4EI}{L} & & \\ & & & & -\frac{12EI}{L^3} & -\frac{6EI}{L^2} & \frac{12EI}{L^3} & \\ & & & & \frac{6EI}{L^2} & \frac{2EI}{L} & \frac{6EI}{L^2} & \frac{4EI}{L} \end{bmatrix} \begin{Bmatrix} u_1 \\ u_2 \\ v_1 \\ \theta_1 \\ v_2 \\ \theta_2 \end{Bmatrix} \quad \dots\dots\dots(2.17)$$

S
Y
M

ie $\{P\} = [K]\{\Delta\}$

in which it can be noted that the axial and flexural matrices are independent. The co-efficients in the matrix [K] are the same as those in the well known Slope Deflection equations showing that the exact solution, within the confines of simple bending theory, is obtained using the finite element procedure provided the deflection function is a true representation of the behaviour of the element.

2.2. Work Method.

In many cases it is impossible or impracticable to obtain the precise mode of deformation of an element, and in such cases it is necessary to resort to the use of an approximation to the displacement profile.

The use of such approximations naturally implies that equilibrium will not be satisfied at every point of the structure and hence equality of nodal forces and stress resultants is not obtained. The equilibrium method of the previous section thus cannot be used and recourse must be made to a work process in which only overall equilibrium of the element is obtained.

Such a process is the Rayleigh-Ritz ⁽⁴⁶⁾ method in which the result that at equilibrium the total potential energy in the element is a minimum is used or alternatively the equivalent result that at equilibrium the total virtual work done by the system is zero.

The application of work-based procedures entails more calculations than the equilibrium method, but this is often offset by the simpler functions involved.

Once approximate displacement functions are used, the resulting stiffness matrices are also approximate and hence the accuracy of the solution will depend on the subdivision of the structure.

The process may be demonstrated by considering the formulation of the flexural stiffness matrix for a tapered rectangular beam (Fig 2.5) using the function for a prismatic member, ie;

$$v = a_1 + a_2x + a_3x^2 + a_4x^3$$

This function is an approximation to the true form and hence a stiffness matrix based on this function must be obtained by work methods.

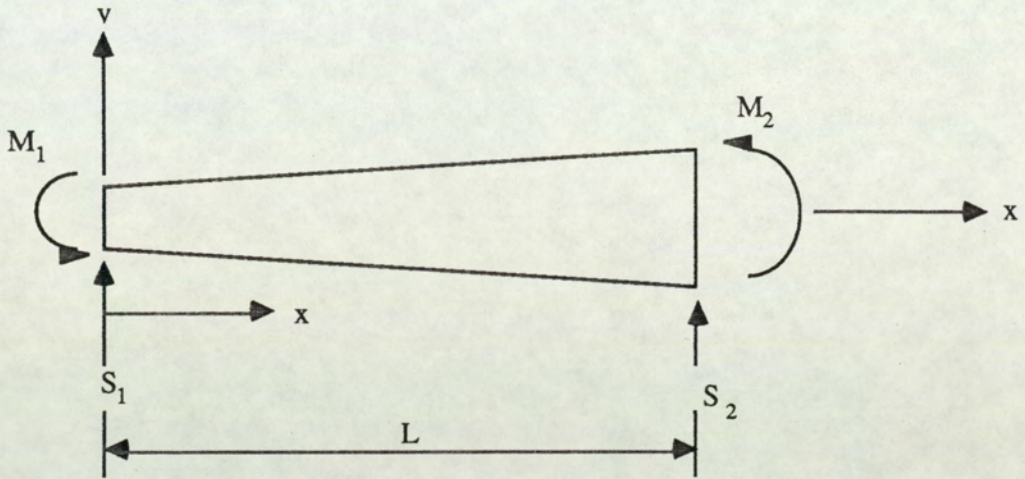


Fig 2.5. Tapered Beam Showing Positive Values of Nodal Forces.

2.2.1. Construction of Flexural Stiffness Matrix [K_b] for a Straight Tapered Rectangular Beam of Constant Breadth.

Since the deflection profile is assumed to take the form;

$$v = a_1 + a_2x + a_3x^2 + a_4x^3$$

the relationship between the nodal displacements and arbitrary constants is identical to that presented by equation (2.8).

2.2.1.1. Relationship Between Strains and Nodal Displacements.

Assuming that only bending strain occurs, ie, neglecting shear effects,

$$\{\epsilon_b\} = [0 \ 0 \ 2 \ 6x] \{a_b\} = [A] \{a_b\}$$

Thus upon substituting (2.8)

$$\{\epsilon_b\} = [A][C_b]^{-1} \{\Delta_b\} = [B] \{\Delta_b\} \quad \dots\dots\dots(2.18)$$

where, after performing the multiplication;

$$[B] = \left[\begin{array}{cc|cc} -\frac{6}{L^2} + \frac{12x}{L^3} & -\frac{4}{L} + \frac{6x}{L^2} & \frac{6}{L^2} - \frac{12x}{L^3} & -\frac{2}{L} + \frac{6x}{L^2} \end{array} \right]$$

2.2.1.2. Relationship Between Stress Resultants $\{\sigma\}$ and Strains $\{\epsilon\}$.

The relationship between the stresses and the strains at any point is given by;

$$\{\sigma_b\} = [D] \{\epsilon_b\} = [D] [B] \{\Delta_b\} \quad \dots\dots\dots(2.19)$$

where $\{\sigma_b\}$ is simply the bending moment M and [D] is the elasticity matrix, which for a beam is simply the flexural rigidity EI. For a prismatic beam this is a constant, whereas for a tapered member it is a function of x due to the variation of second moment of area I along the length.

Consider the rectangular beam of varying depth t_x and constant breadth b , as shown in Fig 2.6.

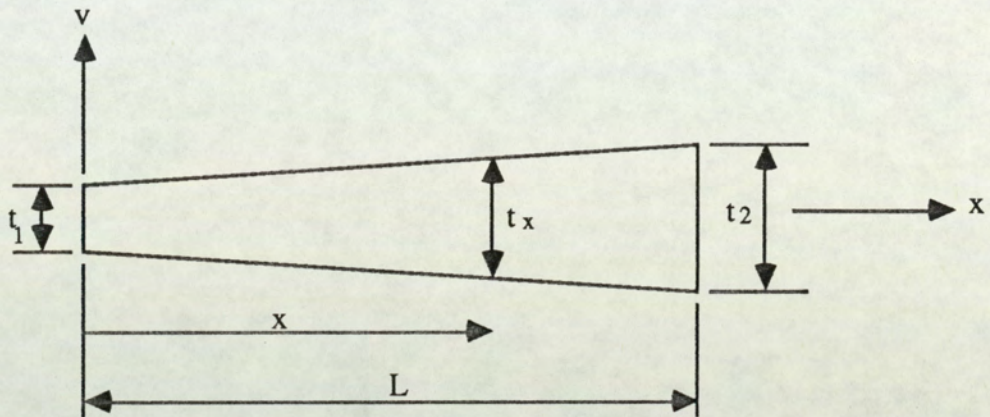


Fig 2.6. Tapered Beam Showing a General Depth at Distance x .

At a section distance x from end 1, the depth of the beam is

$$t_x = t_1 + \frac{(t_2 - t_1)x}{L} \dots\dots\dots(2.20)$$

and the second moment of area is given by;

$$I_x = \frac{b}{12} (t_1 + \phi x)^3 \dots\dots\dots(2.21)$$

where

$$\phi = \frac{t_2 - t_1}{L}$$

Hence it is seen that the elasticity matrix is a function of x of the form

$$[D] = \frac{Eb}{12} (t_1 + \phi x)^3 \quad \dots\dots\dots(2.22)$$

2.2.1.3. Formation of Stiffness Matrix [K_b].

At equilibrium the total virtual work done in the system is zero. By applying a virtual nodal displacement $\{\delta\Delta\}$ to the system and denoting the corresponding nodal forces by the vector $\{P\}$,

$$\text{External virtual work} = \{\delta\Delta\}^T \{P\} \quad \dots\dots\dots(2.23)$$

and

$$\text{Internal virtual work} = \int_0^L \{\delta\epsilon_b\}^T \{\sigma\} dx$$

Since $\{\delta\epsilon_b\} = [B] \{\delta\Delta_b\}$ then;

$$\text{Internal virtual work} = \int_0^L \{\delta\Delta_b\}^T [B]^T \{\sigma\} dx \quad \dots\dots\dots(2.24)$$

Thus equating equations (2.23) and (2.24) gives

$$\{P\} = \int_0^L [B]^T \{\sigma\} dx \quad \dots\dots\dots(2.25)$$

Substituting equation (2.19) into (2.25) gives,

$$\{P\} = \int_0^L [B]^T [D] [B] \{\Delta\} dx \quad \dots\dots\dots(2.26)$$

and hence the stiffness matrix is given by

$$[K] = \int_0^L [B]^T [D] [B] dx \quad \dots\dots\dots(2.27)$$

It should be noted that the above result is also the general result used for 2 and 3D finite element analysis. Hence the flexural stiffness matrix of the tapered beam will be given by substituting the respective values of [B] and [D] into expression (2.27).

2.2.1.4. Construction of Axial Stiffness Matrix [K_a] for a Tapered Rectangular Beam.

Assumption of the axial deflection profile,

$$u = a_5 + a_6 x$$

and following steps (2.2.2) to (2.2.3) gives for the axial case,

$$[B] = \begin{bmatrix} -\frac{1}{L} & \frac{1}{L} \end{bmatrix} \quad \dots\dots\dots(2.28)$$

In this case [D] becomes EA where the cross sectional area A is a linear function of x.

Thus

$$[D] = Eb (t_1 + \phi x) \quad \dots\dots\dots(2.29)$$

and hence substituting (2.28) and (2.29) into (2.27) and evaluating gives the axial stiffness matrix.

2.2.1.5. Combined Stiffness Matrix for Flexural and Axial Behaviour.

Combination of the flexural and axial matrices developed gives the equations:-

$$\begin{Bmatrix} P_1 \\ P_2 \\ S_1 \\ M_1 \\ S_2 \\ M_2 \end{Bmatrix} = \begin{bmatrix} K_{11} & & & & & \\ K_{21} & K_{22} & & & & \\ & & S & & & \\ & & & Y & & \\ & & & & M & \\ & & 0 & 0 & K_{33} & \\ & & 0 & 0 & K_{43} & K_{44} \\ & & 0 & 0 & K_{53} & K_{54} & K_{55} \\ & & 0 & 0 & K_{63} & K_{64} & K_{65} & K_{66} \end{bmatrix} \begin{Bmatrix} u_1 \\ u_2 \\ v_1 \\ \theta_1 \\ v_2 \\ \theta_2 \end{Bmatrix} \dots\dots\dots(2.30)$$

ie {P} = [K]{Δ}

where

$$K_{11} = K_{22} = -K_{21} = \frac{Eb}{2L} (2t_1 + \phi L)$$

$$K_{33} = \lambda (12t_1^3 + 18\phi t_1^2 L + 14.4\phi^2 t_1 L^2 + 4.2\phi^3 L^3)$$

$$K_{43} = \lambda (6t_1^3 L + 6\phi t_1^2 L^2 + 4.2\phi^2 t_1 L^3 + 1.2\phi^3 L^4)$$

$$K_{44} = \lambda(4t_1^3L^2 + 3\phi t_1^2L^3 + 1.6\phi^2t_1L^4 + 0.4\phi^3L^5)$$

$$K_{53} = -K_{33} \quad K_{54} = -K_{43} \quad K_{55} = K_{33}$$

$$K_{63} = \lambda(6t_1^3L^2 + 12\phi t_1^2L^3 + 10.2\phi^2t_1L^4 + 3\phi^3L^5)$$

$$K_{64} = \lambda(2t_1^3L^2 + 3\phi t_1^2L^3 + 2.6\phi^2t_1L^4 + 0.8\phi^3L^5)$$

$$K_{65} = -K_{63}$$

$$K_{66} = \lambda(4t_1^3L^2 + 9\phi t_1^2L^3 + 7.6\phi^2t_1L^4 + 2.2\phi^3L^5)$$

$$\phi = \frac{(t_2 - t_1)}{L}$$

$$\lambda = \frac{Eb}{12L^3}$$

Again it should be noted that the stiffness matrix is symmetrical about the leading diagonal. Also if $t_2 = t_1$, that is the beam is prismatic, then $\phi = 0$ and the stiffness matrix becomes the same as that in equation (2.17).

It should be noted that the stiffness matrix is an approximation of the tapered member, and the accuracy of solution converges to the exact result with increase in the number of elements employed. If the exact displacement function for a tapered beam is formulated, then the precise stiffness matrix is obtained where accuracy is independent of subdivisions.

Again it is seen that both the axial and flexural stiffness matrices are independent of each other and can be formulated individually.

2.3. Summary of the Two Methods.

2.3.1. Equilibrium Method.

- a) Formulation of the axial and lateral deflection function $u=u(x)$, $v=v(x)$.
- b) Calculation of the nodal displacements from the arbitrary constants $[C]^{-1}$.
- c) Relationship between stress resultants and nodal displacements $[H]$
- d) Formulation of Flexural Stiffness matrix $[K_b]$.
- e) Construction of Axial Stiffness matrix $[K_a]$.
- f) Combined Stiffness matrix for Flexural and Axial behaviour $[K]$.

2.3.2. Work Method.

- a) Assumption of the axial and lateral deflection function $u=u(x)$, $v=v(x)$.
- b) Calculation of the nodal displacements from the arbitrary constants $[C]^{-1}$.
- c) Relationship between strains and nodal displacements $[B]$.
- d) Relationship between Stress and Strain $[D]$.
- e) Formulation of Flexural Stiffness matrix $[K_b]$.
- f) Construction of Axial Stiffness matrix $[K_a]$.
- g) Combined Stiffness matrix for Flexural and Axial behaviour $[K]$.

PART A.

**Geometrically Non-Linear Analysis of
Prismatic Sections.**

Chapter 3.

Matrix Formulation.

In chapter 2 the finite element process as applied to beams was illustrated with reference to geometrically linear behaviour, that is the deflections were considered to tend to zero and hence the equilibrium equations could be legitimately written in the undeformed geometry of the structure. Such considerations lead to a proportional relationship between the applied forces and the deflections induced.

In reality the deflections, although usually small, have finite values and thus a more accurate assessment of behaviour will be attained if the equilibrium equations are set up in the deformed state of the structure. Thus if the member is subjected to both lateral and axial forces, the deflections will be dependent on both the lateral forces and on the axial forces, whereas in linear behaviour axial forces have no effect on the flexural action. Such considerations predict a non-linear relationship between loads and deflections.

Non-linear behaviour of this nature is known as geometrical non-linearity as distinct from material non-linearity in which the non-linear relationship occurs primarily between stress and strain.

Geometrically non-linear analysis is essential if the elastic stability of structures is to be investigated, a simple example of this being the prediction of the elastic critical, or Euler, load of a strut.

The development of the finite element process to examine geometrically non-linear behaviour has been investigated by a number of authors (9,10,11,12,17,18,20,21) and this chapter is concerned with the description of these, together with the further developments made to this topic by the author, as applied to prismatic members.

As in the case of linear analysis, formulation of the stiffness matrices for the examination of non-linear behaviour can be divided into;

- a) equilibrium methods, in which the derivation is obtained via derived displacement functions, and
- b) work methods in which assumed functions are utilized.

Throughout this thesis it is assumed that the material possesses a linear relationship between stress and strain during the structural behavior, that is that Young's modulus is constant, and also that deflections are sufficiently small to allow the simple theory of bending to be invoked.

3.1. Equilibrium Method.

As described in Chapter 2 these methods, although shorter than the work procedures, depend upon the formulation of the precise mode of deformation of the member. Two stiffness matrices will be developed, each having the same flexural portion but differing in the treatment of the axial force component. The assumptions and limitations imposed in each of these formulations will be discussed during the development. It should be noted that the axial force can be either in compression or tension and hence the derivation will be carried out separately for each case.

3.1.1. Non-linear Stiffness Matrix with Mutually Independent Flexural and Axial Components for Member in Compression.

With reference to a prismatic beam subjected to nodal axial and shearing forces and to nodal bending moments, as shown in Fig 3.1, consider the equilibrium

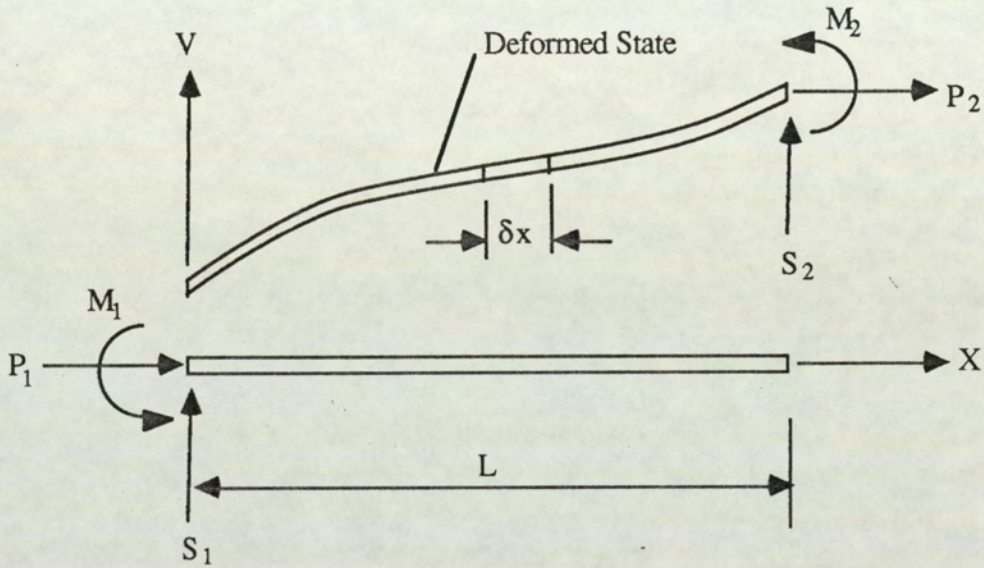


Fig 3.1. Diagram Showing The Nodal Forces on the Deformed Member.

of an element of this member in its deformed state as shown in Fig 3.2.

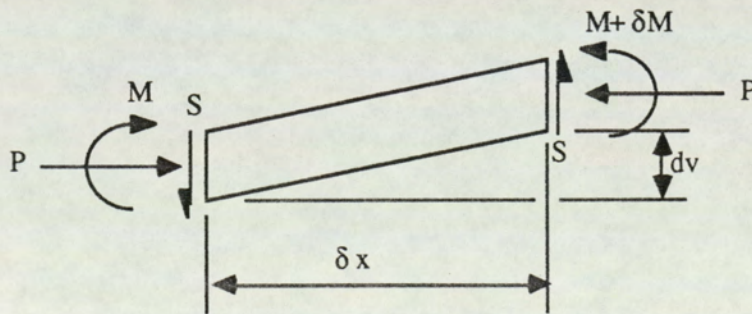


Fig 3.2. Diagram Showing the Element in its Deformed State in Compression.

It is assumed that the displacements are small enough to allow the approximations $\cos(dv/dx) = 1$ and $\sin (dv/dx) = (dv/dx)$ to be validly made. Hence the axial and shearing forces with respect to the deformed member axis may be considered to take the values of those forces with respect to the undeformed member axis as depicted in Fig 3.2.

Consideration of rotational equilibrium of this element gives;

$$S = - \frac{dM}{dx} - P \frac{dv}{dx} \dots\dots\dots(3.1)$$

Substituting the relationship $M = EI \frac{d^2v}{dx^2}$, ie equation (2.3), gives

$$S = - EI \frac{d^3v}{dx^3} - P \frac{dv}{dx} \dots\dots\dots(3.2)$$

and since for vertical equilibrium, S is constant;

$$\frac{dS}{dx} = - EI \frac{d^4v}{dx^4} - P \frac{d^2v}{dx^2} = 0$$

that is

$$\frac{d^4v}{dx^4} + \frac{P}{EI} \frac{d^2v}{dx^2} = 0$$

which upon successive integration yields the lateral deflection profile of the beam as;

$$v = a_1 + a_2x + a_3 \sin \alpha x + a_4 \cos \alpha x \dots\dots\dots(3.3)$$

where

$$\alpha = \sqrt{P/EI}$$

Differentiation of the deflection equation gives the slope, θ , of the member as;

$$\theta = \frac{dv}{dx} = a_2 + a_3 \alpha \cos \alpha x - a_4 \alpha \sin \alpha x \quad \dots\dots\dots(3.4)$$

Following the procedure explained in Chapter 2 for the equilibrium method, the flexural stiffness matrix of the non-linear member can be formulated.

The square matrix relating the nodal displacements to the arbitrary constants is first obtained as;

$$\begin{Bmatrix} v_1 \\ \theta_1 \\ v_2 \\ \theta_2 \end{Bmatrix} = \begin{bmatrix} 1 & 0 & 0 & 0 \\ 0 & 1 & \alpha & 0 \\ 1 & L & \sin \alpha L & \cos \alpha L \\ 0 & 1 & \alpha \cos \alpha L & -\alpha \sin \alpha L \end{bmatrix} \begin{Bmatrix} a_1 \\ a_2 \\ a_3 \\ a_4 \end{Bmatrix}$$

ie $\{\Delta_b\} = [C_b]\{a_b\}$

which upon inversion gives,

$$\begin{Bmatrix} a_1 \\ a_2 \\ a_3 \\ a_4 \end{Bmatrix} = \begin{bmatrix} C_{11} & C_{12} & C_{13} & C_{14} \\ C_{21} & C_{22} & C_{23} & C_{24} \\ C_{31} & C_{32} & C_{33} & C_{34} \\ C_{41} & C_{42} & C_{43} & C_{44} \end{bmatrix} \begin{Bmatrix} v_1 \\ \theta_1 \\ v_2 \\ \theta_2 \end{Bmatrix}$$

$$\text{ie } \{a_b\} = [C_b]^{-1} \{\Delta_b\}$$

where

$$C_{11} = \alpha C_{32} = \frac{\alpha - \alpha^2 L \cos \alpha L - \sin \alpha L}{\lambda}$$

$$C_{11} = -C_{42} = \frac{\alpha L \cos \alpha L - \sin \alpha L}{\lambda}$$

$$C_{13} = C_{22} = C_{24} = C_{41} = -C_{43} = -\alpha C_{34} = \frac{\alpha (1 - \cos \alpha L)}{\lambda}$$

$$C_{14} = C_{44} = \frac{\sin \alpha L - \alpha L}{\lambda}$$

$$C_{21} = -C_{23} = \alpha C_{33} - \alpha C_{31} = \frac{\alpha^2 \sin \alpha L}{\lambda}$$

and

$$\lambda = 2\alpha (1 - \cos \alpha L) - \alpha^2 L \sin \alpha L$$

Following the derivation given in section (2.1.3) and using the relationships;

$$M = EI \frac{d^2 v}{dx^2} \text{ and } S = -EI \frac{d^3 v}{dx^3} - P \frac{dv}{dx} \text{ gives;}$$

$$\begin{Bmatrix} S \\ M \end{Bmatrix} = \begin{bmatrix} 0 & -P & 0 & 0 \\ 0 & 0 & -P \sin \alpha x & -P \cos \alpha x \end{bmatrix} \{a_b\}$$

$$= \begin{bmatrix} -P C_{21} & -P C_{22} & -P C_{23} & -P C_{24} \\ -P \sin \alpha x C_{31} & -P \sin \alpha x C_{32} & -P \sin \alpha x C_{33} & -P \sin \alpha x C_{34} \\ -P \cos \alpha x C_{41} & -P \cos \alpha x C_{42} & -P \cos \alpha x C_{43} & -P \cos \alpha x C_{44} \end{bmatrix} \begin{Bmatrix} v_1 \\ \theta_1 \\ v_2 \\ \theta_2 \end{Bmatrix}$$

since $\{a_b\} = [C_b]^{-1} \{\Delta_b\}$. The flexural stiffness matrix can now be written directly

following the arguments presented in 2.1.4 giving the non-linear flexural matrix $[K_b]$ as;

$$\begin{Bmatrix} S_1 \\ M_1 \\ S_2 \\ M_2 \end{Bmatrix} = \begin{bmatrix} K_{33} & & & \\ K_{43} & K_{44} & & \\ K_{53} & K_{54} & K_{55} & \\ K_{63} & K_{64} & K_{65} & K_{66} \end{bmatrix} \begin{Bmatrix} v_1 \\ \theta_1 \\ v_2 \\ \theta_2 \end{Bmatrix} \dots\dots\dots(3.5)$$

ie $\{P_b\} = [K_b] \{\Delta_b\}$

where

$$K_{33} = K_{55} = -K_{53} = \frac{P\alpha^2 \sin \alpha L}{\lambda}$$

$$K_{43} = K_{63} = -K_{54} = -K_{65} = \frac{P\alpha (1 - \cos \alpha L)}{\lambda}$$

$$K_{44} = K_{66} = \frac{P (\sin \alpha L - \alpha L \cos \alpha L)}{\lambda}$$

$$K_{64} = \frac{P (\alpha L - \sin \alpha L)}{\lambda}$$

and

$$\lambda = 2\alpha (1 - \cos \alpha L) - \alpha^2 L \sin \alpha L$$

It should be noted that this matrix is symmetrical about the leading diagonal as in the linear case but now is also dependent on the axial force P.

If it is assumed that the axial force depends only on the displacements, u, then the axial force/displacement relationship may be obtained from $P = EA (du/dx)$, as in the linear case, and the complete stiffness matrix containing both flexural and axial components will become;

$$\begin{Bmatrix} P_1 \\ P_2 \\ S_1 \\ M_1 \\ S_2 \\ M_2 \end{Bmatrix} = \begin{bmatrix} K_{11} & & & & & & & \\ K_{21} & K_{22} & & & & & & \\ 0 & 0 & K_{33} & & & & & \\ 0 & 0 & K_{43} & K_{44} & & & & \\ 0 & 0 & K_{53} & K_{54} & K_{55} & & & \\ 0 & 0 & K_{63} & K_{64} & K_{65} & K_{66} & & \end{bmatrix} \begin{Bmatrix} u_1 \\ u_2 \\ v_1 \\ \theta_1 \\ v_2 \\ \theta_2 \end{Bmatrix}$$

S Y M M

ie $\{P\} = [K]\{\Delta\}$

or more compactly

$$\begin{Bmatrix} P_a \\ P_b \end{Bmatrix} = \begin{bmatrix} [K_a] & 0 \\ 0 & [K_b] \end{bmatrix} \begin{Bmatrix} \Delta_a \\ \Delta_b \end{Bmatrix} \dots\dots\dots(3.6)$$

where

$$K_{11} = K_{22} = -K_{21} = \frac{EA}{L}$$

This matrix, produced in a different manner, has been described in the subject literature (47,48,22,12).

If the axial force is tensile rather than compressive, the bending displacement profile will be slightly different. Apart from this, the derivation of the stiffness matrix is similar to that for the compressive case and is described in the following section.

3.1.2. Non-linear Stiffness Matrix with Mutually Independent Flexural and Axial Components for Member in Tension.

Consider the equilibrium of a deformed element of a member in flexure and in tension as shown in Fig 3.3.

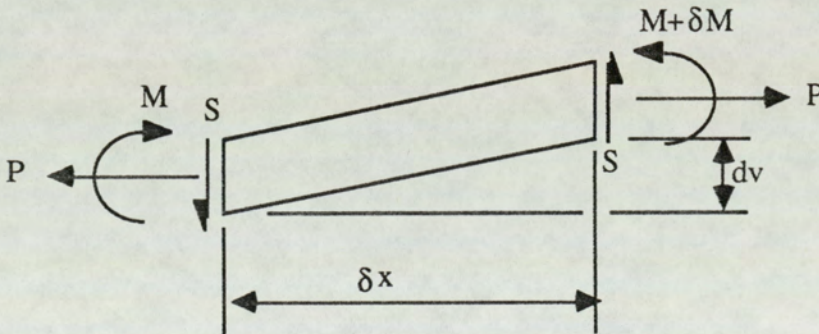


Fig 3.3. Diagram Showing the Element in its Deformed State in Tension.

Consideration of rotational equilibrium of this element gives;

$$S = -\frac{dM}{dx} + P \frac{dv}{dx} \dots\dots\dots(3.7)$$

Substituting equation (2.3) into (3.7) gives;

$$S = -EI \frac{d^3v}{dx^3} + P \frac{dv}{dx} \dots\dots\dots(3.8)$$

Since vertical equilibrium requires that S be constant;

$$\frac{dS}{dx} = -EI \frac{d^4v}{dx^4} + P \frac{d^2v}{dx^2} = 0$$

that is

$$\frac{d^4v}{dx^4} - \frac{P}{EI} \frac{d^2v}{dx^2} = 0$$

which upon successive integration gives the deflection profile of the beam as;

$$v = a_1 + a_2x + a_3 \sinh \alpha x + a_4 \cosh \alpha x \dots\dots\dots(3.9)$$

where

$$\alpha = \sqrt{(P/EI)}$$

Thus

$$\theta = \frac{dv}{dx} = a_2 + a_3 \alpha \cosh \alpha x + a_4 \alpha \sinh \alpha x$$

The matrix $[C_b]$ relating the nodal displacements to the arbitrary constants is thus;

$$[C_b] = \begin{bmatrix} 1 & 0 & 0 & 0 \\ 0 & 1 & \alpha & 0 \\ 1 & L & \sinh \alpha L & \cosh \alpha L \\ 0 & 1 & \alpha \cosh \alpha L & \alpha \sinh \alpha L \end{bmatrix}$$

and its inverse is;

$$[C_b]^{-1} = \begin{bmatrix} C_{11} & C_{12} & C_{13} & C_{14} \\ C_{21} & C_{22} & C_{23} & C_{24} \\ C_{31} & C_{32} & C_{33} & C_{34} \\ C_{41} & C_{42} & C_{43} & C_{44} \end{bmatrix}$$

where

$$C_{11} = \alpha C_{32} = \frac{\alpha^2 L \sinh \alpha L - \alpha \cosh \alpha L + \alpha}{\lambda}$$

$$C_{12} = -C_{42} = \frac{\alpha L \cosh \alpha L - \sinh \alpha L}{\lambda}$$

$$C_{13} = C_{24} = C_{41} = C_{22} = -C_{43} = -\alpha C_{34} = \frac{\alpha (1 - \cosh \alpha L)}{\lambda}$$

$$C_{14} = -C_{44} = \frac{\sinh \alpha L - \alpha L}{\lambda}$$

$$C_{21} = \alpha C_{33} = -C_{23} = -\alpha C_{31} = -\frac{\alpha^2 \sinh \alpha L}{\lambda}$$

and

$$\lambda = 2\alpha (1 - \cosh \alpha L) + \alpha L \sinh \alpha L$$

Following the steps given in section 3.1.1 produces the combined flexural and axial stiffness matrix as;

$$\begin{Bmatrix} P_1 \\ P_2 \\ S_1 \\ M_1 \\ S_2 \\ M_2 \end{Bmatrix} = \begin{bmatrix} K_{11} & & & & & \\ K_{21} & K_{22} & & & & \\ 0 & 0 & K_{33} & & & \\ 0 & 0 & K_{43} & K_{44} & & \\ 0 & 0 & K_{53} & K_{54} & K_{55} & \\ 0 & 0 & K_{63} & K_{64} & K_{65} & K_{66} \end{bmatrix} \begin{Bmatrix} u_1 \\ u_2 \\ v_1 \\ \theta_1 \\ v_2 \\ \theta_2 \end{Bmatrix} \quad \text{SYMM} \quad (3.10)$$

$$\{P\} = [K]\{\Delta\}$$

where

$$K_{11} = K_{22} = -K_{21} = \frac{EA}{L}$$

$$K_{33} = K_{55} = -K_{53} = \frac{P \alpha^2 \sinh \alpha L}{\lambda}$$

$$K_{43} = K_{63} = -K_{54} = -K_{65} = \frac{P \alpha (1 - \cosh \alpha L)}{\lambda}$$

$$K_{44} = K_{66} = \frac{P (\sinh \alpha L - \alpha L \cosh \alpha L)}{\lambda}$$

$$K_{64} = \frac{P (\alpha L - \sinh \alpha L)}{\lambda}$$

and

$$\lambda = 2\alpha (1 - \cosh \alpha L) + \alpha^2 L \sinh \alpha L$$

Again the matrix is symmetrical about the leading diagonal and is dependent on the axial force P.

3.1.3. Limitations of the Linear Matrices so far Described.

A close examination of the nature of these matrices reveals that, since the axial and flexural components are mutually independent, their use is strictly limited to situations in which the axial force and deflections remain independent of any flexural behaviour.

In reality very few situations of this nature occur. Usually, the finite lateral deflections cause a modification to the axial forces and displacements so that the flexural and axial effects are not independent.

This can be demonstrated very simply by considering a pin-ended member under a lateral load as depicted in Fig 3.4.

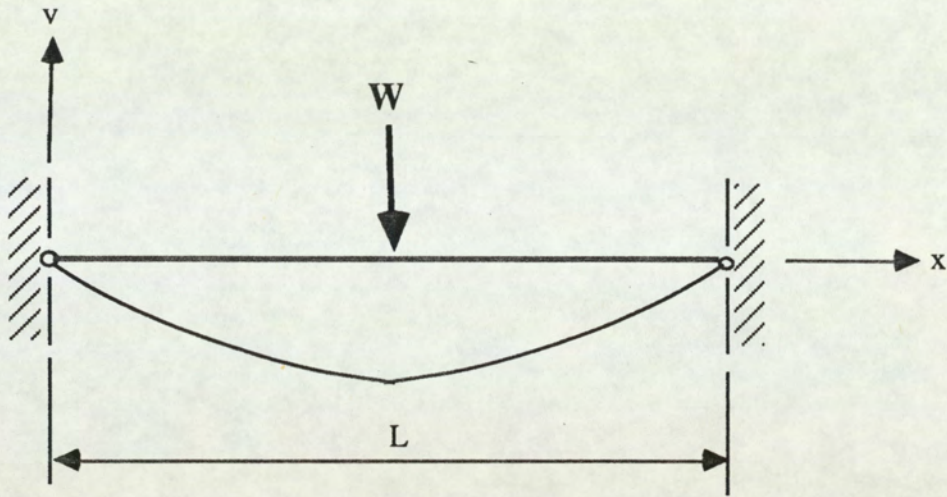


Fig 3.4 Diagram Showing Member under Lateral Loading.

Since the pins are fixed positionally, the lateral displacement of the member causes the member to lengthen, thus inducing axial strain and hence a tensile force. Since there are no displacements, u , along the x axis, the axial effects must be a function of the lateral displacement, v .

Generally the nodes of the members of a frame are not fixed in position and hence u displacements do occur. Thus in general the axial strain is composed of two components, one due to u displacements, as already discussed, and the other due to lateral displacements, v .

3.1.4. Modification of Axial Strain Expression due to Finite Lateral Displacements.

To effect the calculation of a more precise axial strain expression, consider an element dx

of a member displaced and deformed to a new length ds as shown in Fig 3.5.

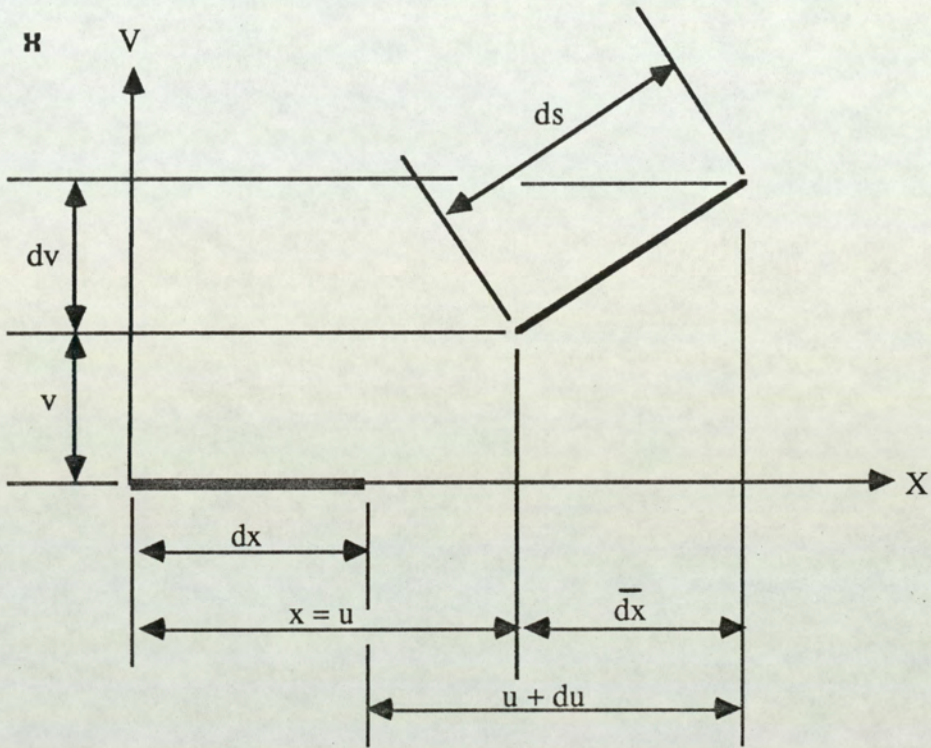


Fig 3.5. Diagram Showing Element Deformation Due to Axial and Lateral Displacements.

By Pythagorus' Theorem;

$$ds^2 = \bar{dx}^2 + dv^2 \quad \dots\dots\dots(3.11)$$

and from the figure above;

$$du = \bar{dx} - dx \quad \dots\dots\dots(3.12)$$

ie $\bar{dx} = du + dx$



Squaring (3.12) gives;

$$\overline{dx}^2 = du^2 + 2 du dx + dx^2$$

and thus from (3.11)

$$ds^2 = du^2 + 2 du dx + dx^2 + dv^2$$

Hence

$$ds^2 - dx^2 = 2 du dx + du^2 + dv^2 \quad \dots\dots\dots(3.13)$$

ie

$$ds^2 - dx^2 = 2 \left[\frac{du}{dx} + \frac{1}{2} \left\{ \left(\frac{du}{dx} \right)^2 + \left(\frac{dv}{dx} \right)^2 \right\} \right] dx^2$$

The term in the square bracket is known as the strain component and hence

$$ds^2 - dx^2 = 2 \epsilon_x dx^2 \quad \dots\dots\dots(3.14)$$

where

$$\epsilon_x = \frac{du}{dx} + \frac{1}{2} \left\{ \left(\frac{du}{dx} \right)^2 + \left(\frac{dv}{dx} \right)^2 \right\}$$

which upon neglecting terms in (du/dx) as very small in comparison with the other terms becomes;

$$\epsilon_x = \frac{du}{dx} + \frac{1}{2} \left(\frac{dv}{dx} \right)^2 \dots\dots\dots(3.15)$$

It should be noted that when the lateral deflections tend to zero then the strain simply tends to the expression

$$\epsilon_x = \frac{du}{dx}$$

3.1.5. Non-Linear Stiffness Matrix with Coupled Flexural and Axial Components.

Use of the strain expression, 3.15 together with the equilibrium process, enables a more precise non-linear stiffness matrix, applicable to general frame problems, to be formulated. The difference between this new matrix and that described in 3.1.1 lies in the modification to the axial force equations which will now include effects due to lateral displacements. The flexural stiffness matrix already obtained remains unaltered.

Applying Hooke's Law to equation (3.15) gives;

$$P = EA \left[\frac{du}{dx} + \frac{1}{2} \left(\frac{dv}{dx} \right)^2 \right] \dots\dots\dots(3.16)$$

Since P is constant along the element, integration of equation (3.16) gives;

$$\int_0^L P \, dx = EA \int_0^L \frac{du}{dx} \, dx + \frac{EA}{2} \int_0^L \left(\frac{dv}{dx} \right)^2 dx \quad \dots\dots\dots(3.17)$$

ie

$$P = \frac{EA}{L} (u_2 - u_1) + \frac{EA}{2L} \int_0^L \left(\frac{dv}{dx} \right)^2 dx \quad \dots\dots\dots(3.18)$$

Noting from Fig 3.1 that $P_1 = -P$ and $P_2 = P$;

$$P_1 = -\frac{EA}{2L} \int_0^L \left(\frac{dv}{dx} \right)^2 dx + \frac{EA}{L} (u_1 - u_2) \quad \dots\dots\dots(3.19)$$

and

$$P_2 = \frac{EA}{2L} \int_0^L \left(\frac{dv}{dx} \right)^2 dx + \frac{EA}{L} (u_2 - u_1) \quad \dots\dots\dots(3.20)$$

The first terms in equations (3.19) and (3.20) represent the modification to the axial force due to lateral deflections and can be calculated in terms of the four lateral nodal displacements as described below.

3.1.6. Formulation of Lateral Deflection Effects on Axial Force for Member in Compression.

The term

$$\frac{EA}{2L} \int_0^L \left(\frac{dv}{dx} \right)^2 dx$$

in equations (3.18), (3.19) and (3.20) can be formulated as follows in terms of the lateral nodal displacements.

Equation (3.4) can be expressed in matrix form as;

$$\theta = \frac{dv}{dx} = [0 \quad 1 \quad \alpha \cos \alpha x \quad -\alpha \sin \alpha x] \{ a_b \}$$

which, since $\{ a_b \} = [C_b]^{-1} \{ \Delta_b \}$, can be written

$$\left(\frac{dv}{dx} \right) = [C_{21} + C_{31} \alpha \cos \alpha x - C_{41} \alpha \sin \alpha x \quad | \quad C_{22} + C_{32} \alpha \cos \alpha x - C_{42} \alpha \sin \alpha x \quad | \\ | C_{23} + C_{33} \alpha \cos \alpha x - C_{43} \alpha \sin \alpha x \quad | \quad C_{24} + C_{34} \alpha \cos \alpha x - C_{44} \alpha \sin \alpha x] \left\{ \begin{array}{c} v_1 \\ \theta_1 \\ v_2 \\ \theta_2 \end{array} \right\}$$

Writing G_N for $(C_{2N} + C_{3N} \alpha \cos \alpha x - C_{4N} \alpha \sin \alpha x)$ this may be expressed as;

$$\frac{dy}{dx} = [G_1 \ G_2 \ G_3 \ G_4] \begin{Bmatrix} v_1 \\ \theta_1 \\ v_2 \\ \theta_2 \end{Bmatrix} \dots\dots\dots(3.21)$$

ie $\frac{dy}{dx} = G_1 v_1 + G_2 \theta_1 + G_3 v_2 + G_4 \theta_2$

which upon squaring gives;

$$\begin{aligned} \left(\frac{dy}{dx}\right)^2 = & G_1 (G_1 v_1 + G_2 \theta_1 + G_3 v_2 + G_4 \theta_2) v_1 \\ & + G_2 (G_1 v_1 + G_2 \theta_1 + G_3 v_2 + G_4 \theta_2) \theta_1 \\ & + G_3 (G_1 v_1 + G_2 \theta_1 + G_3 v_2 + G_4 \theta_2) v_2 \\ & + G_4 (G_1 v_1 + G_2 \theta_1 + G_3 v_2 + G_4 \theta_2) \theta_2 \end{aligned}$$

It is thus necessary to evaluate $G_M G_N$ giving

$$\begin{aligned} G_M G_N = & C_{2M} C_{2N} + (C_{2M} C_{3N} + C_{3M} C_{2N}) \alpha \cos \alpha x \\ & - (C_{2M} C_{4N} + C_{4M} C_{2N}) \alpha \sin \alpha x + C_{3M} C_{3N} \alpha^2 \cos^2 \alpha x \\ & - (C_{3M} C_{4N} + C_{4M} C_{3N}) \alpha^2 \sin \alpha x \cos \alpha x + C_{4M} C_{4N} \alpha^2 \sin^2 \alpha x \end{aligned} \dots\dots\dots(3.22)$$

Integration of $G_M G_N$ and subsequent multiplication by $EA/2L$ gives;

$$Q_M Q_N = \frac{EA}{2L} \int_0^L G_M G_N dx$$

where

$$\begin{aligned}
 Q_M Q_N = EA \left\{ \frac{C_{2M} C_{2N}}{2} + \frac{(C_{2M} C_{3N} + C_{3M} C_{2N}) \sin \alpha L}{2L} \right. \\
 + \frac{(C_{2M} C_{4N} + C_{4M} C_{2N}) (\cos \alpha L - 1)}{2L} + C_{3M} C_{3N} \left(\frac{\alpha^2}{4} + \frac{\alpha \sin 2\alpha L}{8L} \right) \\
 \left. + \alpha \frac{(C_{3M} C_{4N} + C_{4M} C_{3N}) (\cos 2\alpha L - 1)}{8L} + C_{4M} C_{4N} \left(\frac{\alpha^2}{4} - \frac{\alpha \sin 2\alpha L}{8L} \right) \right\} \\
 \dots\dots\dots(3.23)
 \end{aligned}$$

Thus the term $Q_M Q_N$ may be expressed in terms of the nodal displacements as;

$$\begin{aligned}
 & [Q_1 (Q_1 v_1 + Q_2 \theta_1 + Q_3 v_2 + Q_4 \theta_2)] v_1 \\
 & + [Q_2 (Q_1 v_1 + Q_2 \theta_1 + Q_3 v_2 + Q_4 \theta_2)] \theta_1 \\
 & + [Q_3 (Q_1 v_1 + Q_2 \theta_1 + Q_3 v_2 + Q_4 \theta_2)] v_2 \\
 & + [Q_4 (Q_1 v_1 + Q_2 \theta_1 + Q_3 v_2 + Q_4 \theta_2)] \theta_2
 \end{aligned}$$

or in matrix form

$$[A_1 \ A_2 \ A_3 \ A_4] \begin{Bmatrix} v_1 \\ \theta_1 \\ v_2 \\ \theta_1 \end{Bmatrix} \dots\dots\dots(3.24)$$

Hence from equations (3.19) and (3.20) the relationship between the axial force and the axial and lateral displacements becomes;

$$\begin{Bmatrix} P_1 \\ P_2 \end{Bmatrix} = \begin{bmatrix} \frac{EA}{L} & -\frac{EA}{L} & -A_1 & -A_2 & -A_3 & -A_4 \\ -\frac{EA}{L} & \frac{EA}{L} & A_1 & A_2 & A_3 & A_4 \end{bmatrix} \begin{Bmatrix} u_1 \\ u_2 \\ v_1 \\ \theta_1 \\ v_2 \\ \theta_2 \end{Bmatrix} \quad \dots\dots\dots(3.25)$$

The complete force/displacement relationships may then be written as;

$$\begin{Bmatrix} P_1 \\ P_2 \\ S_1 \\ M_1 \\ S_2 \\ M_2 \end{Bmatrix} = \begin{bmatrix} \text{AXIAL} & \text{COUPLING} \\ 0 & \text{FLEXURAL} \end{bmatrix} \begin{Bmatrix} u_1 \\ u_2 \\ v_1 \\ \theta_1 \\ v_2 \\ \theta_2 \end{Bmatrix} \quad \dots\dots\dots(3.26)$$

where the flexural matrix is that given in equation (3.5).

It can be seen that the combined stiffness matrix is no longer symmetrical and that the axial force in the member is dependent on the lateral as well as the axial displacements. It will be seen later in Chapter 4 that a special solution routine can be developed in which symmetry is restored by a modification to the left hand force vector.

3.1.7. Formulation of Lateral Deflection Effects on Axial Force for Member in Tension.

Following steps similar to those presented in the previous section but using the deflection profile for a deformed member in tension, the following result analogous to equation (3.23) is obtained.

$$\begin{aligned}
 Q_M Q_N = EA \left\{ \frac{C_{2M} C_{2N}}{2} + \frac{(C_{2M} C_{3N} + C_{3M} C_{2N})}{2L} \sinh \alpha L \right. \\
 + \frac{(C_{2M} C_{4N} + C_{4M} C_{2N})}{2L} (\cosh \alpha L - 1) + C_{3M} C_{3N} \left(\frac{\alpha^2}{4} + \frac{\alpha \sinh 2\alpha L}{8L} \right) \\
 \left. + \alpha \frac{(C_{3M} C_{4N} + C_{4M} C_{3N})}{8L} (\cosh 2\alpha L - 1) + C_{4M} C_{4N} \left(\frac{\alpha \sinh 2\alpha L}{8L} + \frac{\alpha^2}{4} \right) \right\} \\
 \dots\dots\dots(3.27)
 \end{aligned}$$

from which the coupling portion of the stiffness matrix can be obtained.

3.2. Work Methods.

As discussed in chapter 2 derived deflection profiles may be impossible to obtain or may contain complexities which cause intractability in their use. Thus it is often either necessary or convenient to use approximate displacement functions and formulate the stiffness matrix using a work process.

In this section two work-based stiffness matrices will be developed based on the polynomial displacement functions for a linear prismatic beam namely;

$$v = a_1 + a_2x + a_3x^2 + a_4x^3$$

and

$$u = a_5 + a_6x$$

The first of these is a matrix in which flexural and axial components are considered independent, this being the basis of the derivation of the matrices described in section 3.1.1, while the second is a more realistic matrix in which the effect of finite lateral displacements on axial behaviour is taken into account.

3.2.1. Non-linear Stiffness Matrix with Mutually Independent Flexural and Axial Components.

If, as is inherent in the derivations presented in section 3.1.1 and 3.1.2, it is assumed that the axial force in the member is not significantly affected by the lateral displacements, then this force may be considered to be dependent only on the displacements u along the x -axis, and to remain unchanged during lateral displacements.

Consider again the increment of the axially loaded beam under flexure depicted in Fig 3.2 (or Fig 3.3) and reproduced again below in Fig 3.6.

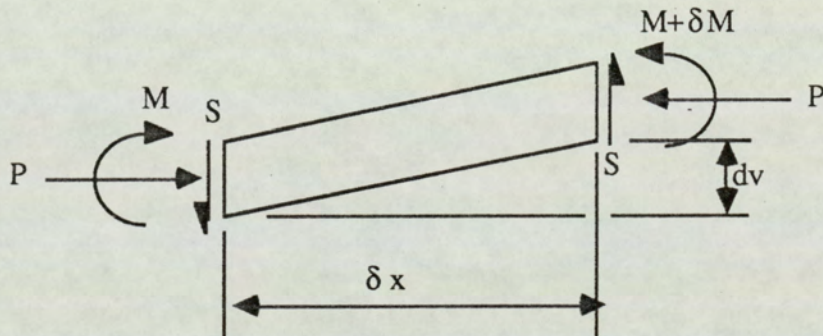


Fig 3.6. Diagram Showing the Element in its Deformed State in Compression.

If virtual nodal flexural displacements $\{\delta\Delta_b\}$ are applied to the beam, then the internal virtual work is composed of that done by the bending moment distribution during virtual rotation of the beam together with the virtual work done by the axial force P during the extension of the beam caused solely by the virtual lateral displacements.

Consideration of the virtual work done by the bending moment will, by following the derivation given in section 2.2.5, yield the flexural stiffness matrix, $[K_b]$, of a linear prismatic beam, relating nodal lateral forces to the corresponding displacements, ie;

$$\begin{Bmatrix} S_1 \\ M_1 \\ S_2 \\ M_2 \end{Bmatrix} = \begin{bmatrix} \frac{12EI}{L^3} & & & \\ & \frac{6EI}{L^2} & \frac{4EI}{L} & \\ & \frac{-12EI}{L^3} & \frac{-6EI}{L^2} & \frac{12EI}{L^3} \\ & \frac{6EI}{L^2} & \frac{2EI}{L} & \frac{-6EI}{L^2} & \frac{4EI}{L} \end{bmatrix} \begin{Bmatrix} v_1 \\ \theta_1 \\ v_2 \\ \theta_2 \end{Bmatrix}$$

$S \quad Y \quad M$

$$\{P_b\} = [K_b]\{\Delta_b\}$$

while the virtual work done by the constant axial force P leads to an additional flexural stiffness matrix dependent on P , and known as the 'initial stress matrix', which can be formulated in the following manner.

Noting that the axial strain due to lateral displacement is;

$$\frac{1}{2} \left(\frac{dv}{dx} \right)^2$$

the internal virtual work done by P during virtual lateral displacements is;

$$P \int_0^L \delta \left[\frac{1}{2} \left(\frac{dv}{dx} \right)^2 \right] dx$$

while the external virtual work is given by equation (2.23), that is

$$\{\delta \Delta_b\}^T \{P\}$$

Thus

$$\begin{aligned} \{\delta \Delta_b\}^T \{P\} &= P \int_0^L \delta \left[\frac{1}{2} \left(\frac{dv}{dx} \right)^2 \right] dx \\ &= P \int_0^L \frac{dv}{dx} \delta \left(\frac{dv}{dx} \right) dx \end{aligned} \quad \dots\dots\dots(3.25)$$

Since $\delta Q = \frac{dQ}{dq} \delta q$.

Now since the lateral displacement function is assumed to be;

$$v = a_1 + a_2x + a_3x^2 + a_4x^3$$

the value of (dv/dx) can be obtained in terms of the nodal displacements $\{\Delta_b\}$ by substitution of equation (2.8) into equation (2.6) giving;

$$\frac{dv}{dx} = \begin{bmatrix} -\underline{6}x + \underline{6}x^2 & | & 1 - \underline{4}x + \underline{3}x^2 & | & \underline{6}x - \underline{6}x^2 & | & -\underline{2}x + \underline{3}x^2 \\ L^2 & L^3 & L & L^2 & L^2 & L^3 & L & L^2 \end{bmatrix} \begin{Bmatrix} v_1 \\ \theta_1 \\ v_2 \\ \theta_2 \end{Bmatrix}$$

which may be expressed more shortly as;

$$\frac{dv}{dx} = [G_1 \ G_2 \ G_3 \ G_4] \{ \Delta_b \} = [G] \{ \Delta_b \} \quad \dots\dots\dots(3.26)$$

Thus equation (3.25) becomes, on reordering of terms;

$$\{ \delta \Delta_b \}^T \{ P \} = P \int_0^L \{ \delta \Delta_b \}^T [G]^T [G] \{ \Delta_b \} dx$$

from which

$$\begin{aligned} \{ P \} &= \int_0^L [G]^T P [G] \{ \Delta_b \} dx \\ &= [K_\sigma] \{ \Delta_b \} \quad \dots\dots\dots(3.27) \end{aligned}$$

where $[K_\sigma]$ is the initial stress matrix.

Calculation of expression (3.27) yields this additional relationship between {P} and {Δ} as;

$$\begin{Bmatrix} S_1 \\ M_1 \\ S_2 \\ M_2 \end{Bmatrix} = \begin{bmatrix} \frac{6P}{5L} & & & \\ & \frac{2PL}{15} & & \\ & & \frac{6P}{5L} & \\ & & & \frac{2PL}{15} \end{bmatrix} \begin{Bmatrix} v_1 \\ \theta_1 \\ v_2 \\ \theta_2 \end{Bmatrix} \quad \dots\dots\dots(3.28)$$

S Y M

ie {P_b} = [K_σ]{Δ_b}

Hence the total stiffness matrix, including both flexural and axial effects, becomes

$$\begin{Bmatrix} P_a \\ P_b \end{Bmatrix} = \begin{bmatrix} K_a & 0 \\ 0 & K_b + K_\sigma \end{bmatrix} \begin{Bmatrix} \Delta_a \\ \Delta_b \end{Bmatrix} \quad \dots\dots\dots(3.29)$$

or {P} = [K₀ + K_σ]{Δ}

where [K_a] is the axial stiffness matrix described in Chapter 2.

Hence the flexural component of the total stiffness matrix is dependent on the axial force in a similar manner to that in the matrix presented in equation (3.6).

While here applied to the solution of beam problems, this form of derivation was first introduced by (45,47) for the non-linear behaviour of plates and shells.

3.2.2. Non-linear Stiffness Matrix with Coupled Flexural and Axial Components (Tangential Stiffness Matrix).

The development of the previous section contains assumptions which, as discussed in section 3.1.3, do not describe the actual nature of the axial strain. As already shown a more accurate expression for this is;

$$\epsilon_x = \frac{du}{dx} + \frac{1}{2} \left(\frac{dv}{dx} \right)^2$$

and hence this extra second term effect should be considered if a more realistic assessment of non-linear behaviour is to be made. The development contained in this section allows for this extra term and, as will be shown, leads to an extension of the matrix developed in the previous section. This method produces a symmetrical matrix known as the Tangential Stiffness Matrix, which does not explicitly relate forces to displacements but from which such relationships can be obtained.

3.2.2.1. Relationship Between Strains and Nodal Displacements.

Again letting the displacement functions be assumed as;

$$v = a_1 + a_2x + a_3x^2 + a_4x^3$$

$$u = a_5 + a_6x$$

the values of the axial and flexural strains;

$$\epsilon_a = \frac{du}{dx} + \frac{1}{2} \left(\frac{dv}{dx} \right)^2$$

$$\epsilon_b = \frac{d^2 v}{dx^2}$$

can be obtained by differentiation in terms of the arbitrary constants and then via equation (2.8) in terms of the nodal displacements. Thus, noting from equation (3.26), that

$$\frac{dv}{dx} = [G] \{ \Delta_b \} \quad \dots\dots\dots(3.30)$$

and that hence

$$\frac{1}{2} \left(\frac{dv}{dx} \right)^2 = \frac{1}{2} \frac{dv}{dx} [G] \{ \Delta_b \} \quad \dots\dots\dots(3.31)$$

the expression for the strains may be written

$$\left\{ \begin{array}{l} \epsilon_a \\ \epsilon_b \end{array} \right\} = \left[\begin{array}{cccc|cc} \frac{1}{2} \frac{dv}{dx} G_1 & \frac{1}{2} \frac{dv}{dx} G_2 & \frac{1}{2} \frac{dv}{dx} G_3 & \frac{1}{2} \frac{dv}{dx} G_4 & -\frac{1}{L} & \frac{1}{L} \\ \hline -\frac{6}{L^2} + \frac{12x}{L^3} & -\frac{4}{L} + \frac{6x}{L^2} & \frac{6}{L^2} - \frac{12x}{L^3} & -\frac{2}{L} + \frac{6x}{L^2} & 0 & 0 \end{array} \right] \left\{ \begin{array}{l} v_1 \\ \theta_1 \\ v_2 \\ \theta_2 \\ u_1 \\ u_2 \end{array} \right\}$$

that is

$$\{\epsilon\} = [B(\Delta)]\{\Delta\} \dots\dots\dots(3.32)$$

where $[B(\Delta)]$, the matrix relating the strains to the nodal displacements, is dependent on the nodal displacements themselves due to the inclusion of the term (dv/dx) .

3.2.2.2. Relationship Between Stress Resultants and Strains.

Since the stresses and hence the stress resultants are linearly related to the strains, the relationship between these quantities is given by;

$$\begin{Bmatrix} P \\ M \end{Bmatrix} = \begin{bmatrix} EA & 0 \\ 0 & EI \end{bmatrix} \begin{Bmatrix} \epsilon_a \\ \epsilon_b \end{Bmatrix}$$

that is

$$\{\sigma\} = [D]\{\epsilon\}$$

or, from equation (3.32);

$$\{\sigma\} = [D][B(\Delta)]\{\Delta\} \dots\dots\dots(3.33)$$

3.2.2.3. Formulation of Tangential Stiffness Matrix.

Consideration of external and internal virtual work yields;

$$\text{External virtual work} = \{\delta\Delta\}^T \{P\}$$

$$\text{Internal virtual work} = \int_0^L \{\delta\epsilon\}^T \{\sigma\} dx$$

Hence by the principle of virtual work (see section 2.2.)

$$\{\delta\Delta\}^T \{P\} = \int_0^L \{\delta\epsilon\}^T \{\sigma\} dx \quad \dots\dots\dots(3.34)$$

Thus in order to obtain the relationship between $\{P\}$ and $\{\Delta\}$ it is necessary to express $\{\delta\epsilon\}$ in terms of $\{\delta\Delta\}$ thus allowing the virtual displacements to be eliminated from both sides of equation (3.34).

From equation (3.32) since $[B(\Delta)]$ is a function of $\{\Delta\}$, application of virtual displacements will cause virtual strains

$$\{\delta\epsilon\} = [B(\Delta)]\{\delta\Delta\} + [\delta B(\Delta)]\{\Delta\} \quad \dots\dots\dots(3.35)$$

by virtue of the product rule for differentiation.

Hence in order to obtain a relationship between $\{\delta\epsilon\}$ and $\{\delta\Delta\}$ it is necessary to equate the second term of equation (3.35) to a term in which the vector $\{\Delta\}$ is replaced by $\{\delta\Delta\}$, and this may be accomplished in the following manner.

Writing equation (3.32) as;

$$\{\epsilon\} = \begin{bmatrix} B_L^b & B_0^a \\ B_0^b & 0 \end{bmatrix} \begin{Bmatrix} \Delta_b \\ \Delta_a \end{Bmatrix}$$

where

$$[B_L^b] = \begin{bmatrix} \frac{1}{2} \frac{dv}{dx} G_1 & \frac{1}{2} \frac{dv}{dx} G_2 & \frac{1}{2} \frac{dv}{dx} G_3 & \frac{1}{2} \frac{dv}{dx} G_4 \end{bmatrix}$$

$$[B_0^a] = \begin{bmatrix} -\frac{1}{L} & \frac{1}{L} \end{bmatrix}$$

$$[B_0^b] = \begin{bmatrix} \frac{-6 + 12x}{L^2} & \frac{4 + 6x}{L^3} & \frac{6 - 12x}{L^2} & \frac{-2 + 6x}{L^3} \end{bmatrix}$$

it is seen that

$$[\delta B(\Delta)] \{\Delta\} = \begin{bmatrix} \delta B_L^b & 0 \\ 0 & 0 \end{bmatrix} \begin{Bmatrix} \Delta_b \\ \Delta_a \end{Bmatrix} = [\delta B_L^b] \{\Delta_b\}$$

by virtue of the constancy of the coefficients in $[B_0^a]$ and $[B_0^b]$.

Now from the expression for $[B_L^b]$ above, it can be seen that;

$$[\delta B_L^b] \{\Delta_b\} = [B_L^b] \{\delta \Delta_b\}$$

and hence equation (3.35) can be written

$$\begin{aligned} \{\delta \epsilon\} &= \begin{bmatrix} B_L^b & B_0^a \\ B_0^b & 0 \end{bmatrix} \begin{Bmatrix} \delta \Delta_b \\ \delta \Delta_a \end{Bmatrix} + \begin{bmatrix} B_L^b & 0 \\ 0 & 0 \end{bmatrix} \begin{Bmatrix} \delta \Delta_b \\ \delta \Delta_a \end{Bmatrix} \\ &= \begin{bmatrix} 2 B_L^b & B_0^a \\ B_0^b & 0 \end{bmatrix} \begin{Bmatrix} \delta \Delta_b \\ \delta \Delta_a \end{Bmatrix} = [\bar{B}] \{\delta \Delta\} \dots\dots\dots(3.36) \end{aligned}$$

Thus on substituting equation (3.33) and (3.36) into equation (3.34) and eliminating the vector $\{\delta \Delta\}^T$ the relationship between the external forces $\{P\}$ and the nodal displacements $\{\Delta\}$ is

$$\{P\} = \int_0^L [\bar{B}]^T [D] [B(\Delta)] \{\Delta\} dx$$

$$\text{ie } \{P\} = [K] \{\Delta\} \dots\dots\dots(3.37)$$

On performing the various matrix operations, the stiffness matrix [K] in equation (3.37) can be seen to be non-symmetric and hence equations (3.37) are not amenable to solution by standard procedures based on matrix symmetry.

However it can be shown (26,45,47) that a matrix [K_T] such that

$$\{dP\} = [K_T] \{d\Delta\} \dots\dots\dots(3.38)$$

is symmetrical, and this matrix, for reasons that will become apparant in Chapter 4, is known as the tangential stiffness matrix.

The symmetrical properties of the matrix [K_T] means that its use enables standard symmetrical solution routines to be utilised, rather than the more cumbersome non-symmetrical procedures that would be required for the treatment of matrix [K].

The matrix [K_T] will now be derived and a description of its use left until Chapter 4.

From equation (3.33) and (3.37) the nodal forces may be expressed as

$$\{P\} = \int_0^L [\bar{B}]^T \{ \sigma \} dx \dots\dots\dots(3.38a)$$

Since both $[\bar{B}]$ and $\{\sigma\}$ are functions of the nodal displacements

$$\begin{aligned} \{dP\} &= \int_0^L [d\bar{B}]^T \{\sigma\} dx + \int_0^L [\bar{B}]^T \{d\sigma\} dx \\ &= [K_T] \{d\Delta\} \end{aligned} \quad \dots\dots\dots(3.39)$$

Now

$$\{d\sigma\} = [D]\{d\epsilon\} = [D][B]\{d\Delta\} \quad \dots\dots\dots(3.40)$$

and hence

$$\{dP\} = \int_0^L [d\bar{B}]^T \{\sigma\} dx + \int_0^L [\bar{B}]^T [D] [\bar{B}] \{d\Delta\} dx \quad \dots\dots\dots(3.41)$$

Noting from equation (3.36) that $[\bar{B}]$ may be written as

$$[B] = \begin{bmatrix} 0 & B_0^a \\ B_0^b & 0 \end{bmatrix} + \begin{bmatrix} 2B_L^b & 0 \\ 0 & 0 \end{bmatrix} = [B_0] + [B_L] \quad \dots\dots\dots(3.42)$$

and hence that $[d\bar{B}] = [dB_L]$

$$\int_0^L [\bar{B}]^T [D] [\bar{B}] dx = \int_0^L ([B_0] + [B_L])^T [D] ([B_0] + [B_L]) dx$$

$$= [K_0] + [K_L] \quad \dots\dots\dots(3.43)$$

where

$$[K_0] = \int_0^L [B_0]^T [D] [B_0] dx$$

and

$$[K_L] = \int_0^L \left([B_0]^T [D] [B_L] + [B_L]^T [D] [B_0] + [B_L]^T [D] [B_L] \right) dx$$

The first term in equation (3.41) can be written, through equation (3.42), as

$$2 \int_0^L [dB_L^b]^T \{ \sigma \} dx$$

which can in turn be expressed through equation (3.30) and (3.32) as;

$$\int_0^L [G]^T P [G] \{ \delta \Delta_b \} dx$$

where P is the axial force in the member.

This expression may thus be written as

$$[K_{\sigma}]\{\delta\Delta_b\}$$

where

$$[K_{\sigma}] = \int_0^L [G]^T P [G] dx \quad \dots\dots\dots(3.44)$$

Hence equation (3.39) may be written;

$$\{dP\} = [K_T]\{d\Delta\}$$

where

$$[K_T] = [K_0 + K_{\sigma} + K_L] \quad \dots\dots\dots(3.45)$$

It can be noted that $[K_0]$ is the linear stiffness matrix for a prismatic member while $[K_{\sigma}]$ is the initial stress matrix derived in the previous section and given explicitly by equation (3.28).

Thus to form the complete tangential stiffness matrix $[K_T]$ it is only necessary to evaluate $[K_L]$ and to superimpose this on the stiffness matrix $[K_0 + K_{\sigma}]$ given in equation (3.29).

3.2.2.3.1. Evaluation of $[K_L]$.

The matrix $[K_L]$, known as the initial displacement matrix, is composed of three portions as shown in equation (3.43). Thus $[K_L]$ may be written

$$[K_L] = [K_1] + [K_2] + [K_3]$$

where

$$[K_1] = \int_0^L [B_0]^T [D] [B_L] dx$$

$$[K_2] = \int_0^L [B_L]^T [D] [B_L] dx$$

$$[K_3] = \int_0^L [B_L]^T [D] [B_0] dx$$

Inspection of $[K_1]$ and $[K_3]$ shows that;

$$[K_1]^T = [K_3]$$

and thus the composition of $[K_L]$ may be reduced to two matrices so that;

$$[K_L] = [K_1] + [K_1]^T + [K_2]$$

Substitution of the constituent matrices [B₀], [D] and [B_L] and subsequent integration yields the matrices [K₁] and [K₂] as;

$$[K_1] = \begin{bmatrix} 0 & 0 & | & -A1 & -A2 & -A3 & -A4 \\ 0 & 0 & | & A1 & A2 & A3 & A4 \\ \hline 0 & 0 & | & 0 & 0 & 0 & 0 \\ 0 & 0 & | & 0 & 0 & 0 & 0 \\ 0 & 0 & | & 0 & 0 & 0 & 0 \\ 0 & 0 & | & 0 & 0 & 0 & 0 \end{bmatrix} \quad \dots\dots\dots(3.46)$$

where

$$A1 = \frac{EA}{L} \left(\frac{6}{5L} v_1 + \frac{1}{10} \theta_1 - \frac{6}{5L} v_2 + \frac{1}{10} \theta_2 \right)$$

$$A2 = \frac{EA}{L} \left(\frac{1}{10} v_1 + \frac{2L}{15} \theta_1 - \frac{1}{10} v_2 - \frac{L}{30} \theta_2 \right)$$

$$A3 = - A1$$

$$A4 = \frac{EA}{L} \left(\frac{1}{10} v_1 - \frac{L}{30} \theta_1 - \frac{1}{10} v_2 - \frac{2L}{15} \theta_2 \right)$$

and

$$[K_2] = \begin{bmatrix} 0 & & & & & & & \\ 0 & 0 & & & & & & \\ \hline 0 & 0 & B_{11} & & & & & \\ 0 & 0 & B_{21} & B_{22} & & & & \\ 0 & 0 & B_{31} & B_{32} & B_{33} & & & \\ 0 & 0 & B_{41} & B_{42} & B_{43} & B_{44} & & \end{bmatrix} \quad \text{SYMM} \quad \dots\dots\dots(3.47)$$

where

$$B_{11} = EA \left(\frac{6}{5L} a_2^2 + \frac{12}{5} a_2 a_3 + \frac{72L}{35} a_2 a_4 + \frac{48L}{35} a_3^2 + \frac{18L^2}{7} a_3 a_4 + \frac{9L^3}{7} a_4^2 \right)$$

$$B_{21} = EA \left(\frac{1}{10} a_2^2 + \frac{2L}{5} a_2 a_3 + \frac{3L^2}{7} a_2 a_4 + \frac{2L^2}{7} a_3^2 + \frac{3L^3}{5} a_3 a_4 + \frac{9L^4}{28} a_4^2 \right)$$

$$B_{22} = EA \left(\frac{2L}{15} a_2^2 + \frac{2L^2}{15} a_2 a_3 + \frac{4L^3}{35} a_2 a_4 + \frac{8L^3}{105} a_3^2 + \frac{11L^4}{70} a_3 a_4 + \frac{3L^5}{35} a_4^2 \right)$$

$$B_{31} = -B_{11}, \quad B_{32} = -B_{21}, \quad B_{33} = B_{11}$$

$$B_{41} = EA \left(-\frac{11}{10} a_2^2 - \frac{6L^2}{35} a_2 a_4 - \frac{4L^2}{35} a_3^2 - \frac{3L^2}{7} a_3 a_4 - \frac{9L^4}{28} a_4^2 \right)$$

It should be noted that the complete tangential stiffness matrix $[K_T]$ is dependent on the deflections of the joints of the structure and also that it exhibits symmetry about the leading diagonal.

3.3. The Displacement Transformation Matrix.

Up till now the displacements at the ends of each member have been written in terms of their components with respect to the local member axes. Generally, because of the arbitrary orientation of the constituent members of a frame, it is necessary to express these local displacements in terms of displacements relative to a common global coordinate system, thereby enabling displacement compatibility between adjacent members to be achieved. Thus the displacements must be 'transformed' from the local system into the global system (5,49).

Consider a member (i - j) of a rigid-jointed plane frame with local axes x, y in which the displacements are u, v, respectively and to a global coordinate system in which the displacements are X, Y as shown in fig 3.7.

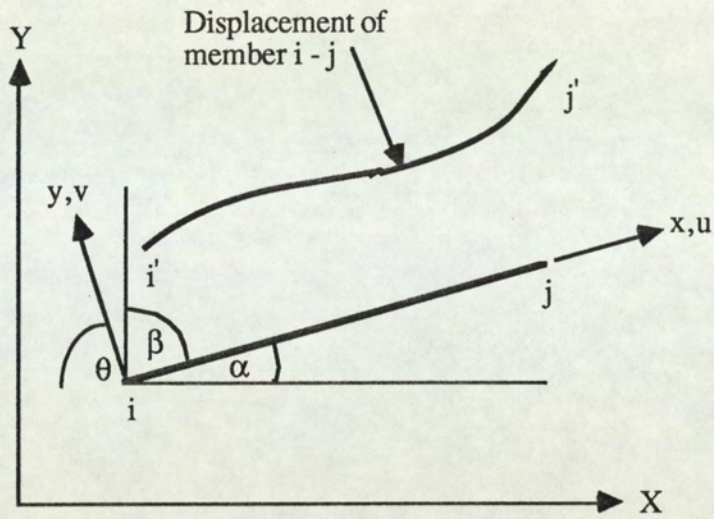


Fig. 3.7. General Deformation of Member.

After deformation joint i moves to a new position, i' , this displacement having components u_i, v_i in the local axis and X_i, Y_i in the global axis, as shown in fig 3.8.

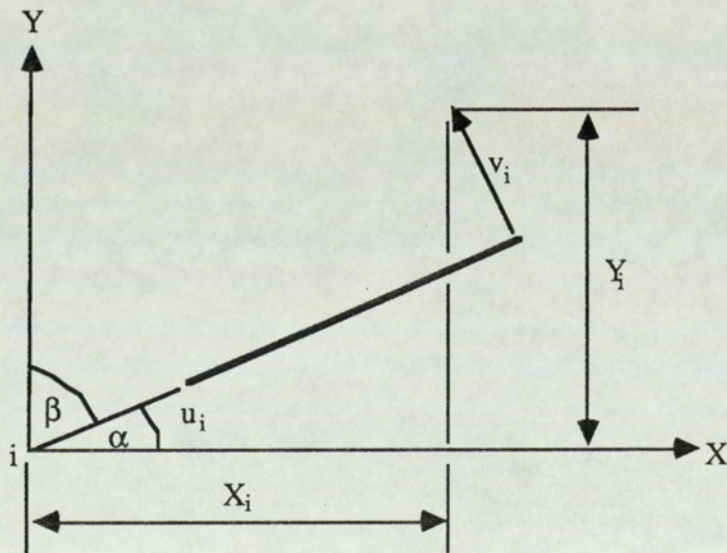


Fig. 3.8. Displacement Components.

By a standard transformation of axis, u_i, v_i can be expressed in terms of X_i and Y_i thus;

$$u_i = X_i \cos \alpha + Y_i \cos \beta$$

$$v_i = -X_i \cos \beta + Y_i \cos \alpha$$

or, in terms of directional cosine notation;

$$u_i = X_i l_p + Y_i m_p$$

$$v_i = X_i l_q + Y_i m_q$$

The rotation θ_i is invariant under the transformation. The similar transformation at joint j is of exactly the same form as that at i . Hence the displacement transformation for member $(i - j)$ can be written as;

$$\begin{Bmatrix} u_i \\ v_i \\ \theta_i \\ u_j \\ v_j \\ \theta_j \end{Bmatrix} = \begin{bmatrix} l_p & m_p & 0 & & & \\ l_q & m_q & 0 & & & \\ 0 & 0 & 1 & & & \\ \hline & & & l_p & m_p & 0 \\ & & & l_q & m_q & 0 \\ & & & 0 & 0 & 1 \end{bmatrix} \begin{Bmatrix} X_i \\ Y_i \\ \theta_i \\ X_j \\ Y_j \\ \theta_j \end{Bmatrix}$$

or, on writing the local displacements in the order used in the development of the stiffness matrices;

$$\begin{Bmatrix} u_i \\ u_j \\ v_i \\ \theta_i \\ v_j \\ \theta_j \end{Bmatrix} = \begin{bmatrix} l_p & m_p & 0 & 0 & 0 & 0 \\ 0 & 0 & 0 & l_p & m_p & 0 \\ l_q & m_q & 0 & 0 & 0 & 0 \\ 0 & 0 & 1 & 0 & 0 & 0 \\ 0 & 0 & 0 & l_q & m_q & 0 \\ 0 & 0 & 0 & 0 & 0 & 1 \end{bmatrix} \begin{Bmatrix} X_i \\ Y_i \\ \theta_i \\ X_j \\ Y_j \\ \theta_j \end{Bmatrix} \quad \dots\dots\dots(3.49)$$

ie $\{\Delta\} = [A]\{X\}$

where [A] is the displacement transformation matrix and {X} is the global displacement vector.

3.4. Formulation of the Global Stiffness Matrix.

Just as the joint displacements must be expressed in terms of displacement components in a global set of axes so that compatibility may be attained, it is necessary to transform similarly the nodal forces into global components to facilitate joint equilibrium requirements.

Consider again a member (i - j) subjected to nodal forces in both the local and global system as shown in fig 3.9.

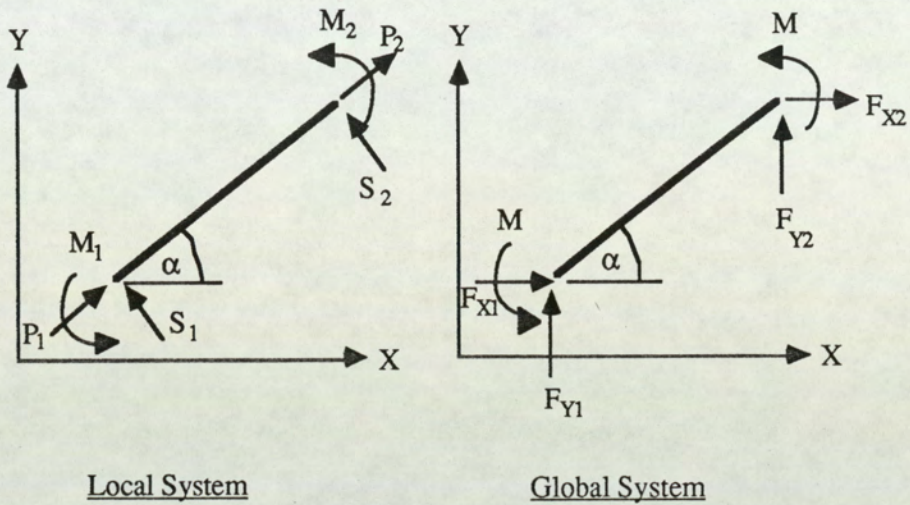


Fig 3.9. Forces in Local and Global Coordinate System.

Because the force and displacement systems are formally identical, the transformation of the force components in the local system to those in the global system must be of the form;

$$\{P\} = [A]\{L\} \dots\dots\dots(3.50)$$

where [A] is the displacement transformation matrix and {P} and {L} are the vectors of the nodal force components in the local and global system respectively. On writing these vectors in full, equation (3.50) becomes;

$$\begin{Bmatrix} P_1 \\ P_2 \\ S_1 \\ M_1 \\ S_2 \\ M_2 \end{Bmatrix} = [A] \begin{Bmatrix} F_{X1} \\ F_{Y1} \\ M_1 \\ F_{X2} \\ F_{Y2} \\ M_2 \end{Bmatrix}$$

The relationship between the nodal force and displacement components in the global coordinate system can now be constructed to give the global stiffness matrix.

From the relationship

$$\{P\} = [K]\{\Delta\}$$

which relates the nodal forces and the displacements in the local system, using equation (3.49) and (3.50) one may write

$$\begin{aligned}
 \{L\} &= [A]^{-1}\{P\} = [A]^{-1}[K]\{\Delta\} \\
 &= [A]^{-1}[K][A]\{X\} \dots\dots\dots(3.51)
 \end{aligned}$$

Now it is easily shown that;

$$[A]^{-1} = [A]^T$$

and hence equation (3.51) may be expressed as;

$$\{L\} = [A]^T [K] [A] \{X\}$$

or

$$\{L\} = [S] \{X\} \dots\dots\dots(3.52)$$

where [S] is the global stiffness matrix relating the force and displacement components in the global coordinate system.

Chapter 4.

Construction of Stiffness Matrices and Methods of Solution.

This chapter will discuss in detail, the sub-routines employed in the computer programs to construct the stiffness matrices and to solve the resulting equations. Firstly the routines for setting up the overall stiffness matrix will be described and secondly an insight into the solution techniques employed will be presented.

4.1. Construction of the Global Equations for the Structure.

4.1.1. Linear Element.

It is convenient to begin a discussion of the construction of the overall equations of the system by illustrating such construction with reference to the prismatic element undergoing linear behaviour, the local stiffness matrix of which is given in equation (2.17).

On performing the triple multiplication $[A^T][K][A]$, equation (3.52), and systematically reordering the elements of the vectors, the global stiffness matrix $[S]$ is obtained. This matrix relating the nodal external forces on a member in the global system to their corresponding displacements is, for the member shown in fig 4.1.

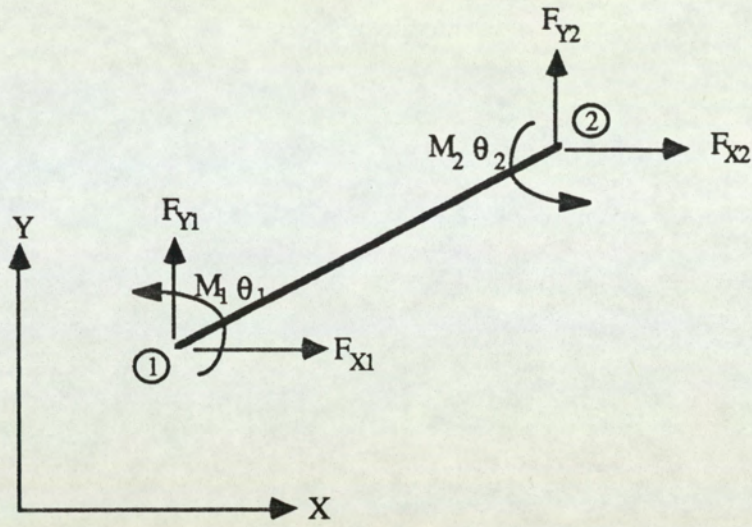


Fig 4.1. Diagram showing Nodal External Forces to Their corresponding displacements.

where;

$$\begin{Bmatrix} F_{X1} \\ F_{Y1} \\ M_1 \\ F_{X2} \\ F_{Y2} \\ M_2 \end{Bmatrix} = \begin{bmatrix} a & & & & & \\ c & b & & & & \\ d & e & f & & & \\ -a & -c & -d & a & & \\ -c & -b & -e & c & b & \\ d & e & g & -d & -e & -f \end{bmatrix} \begin{Bmatrix} x_1 \\ y_1 \\ \theta_1 \\ x_2 \\ y_2 \\ \theta_2 \end{Bmatrix} \dots\dots\dots(4.1)$$

$$\{L\} = [S]\{X\}$$

in which the elements are;

$$a = \frac{EA}{L} l_p^2 + \frac{12EI}{L^3} l_q^2$$

$$b = \frac{EA}{L} m_p^2 + \frac{12EI}{L^3} m_q^2$$

$$c = \frac{EA}{L} l_p l_q + \frac{12EI}{L^3} m_p m_q$$

$$d = \frac{6EI}{L^2} l_q$$

$$e = \frac{6EI}{L^2} m_q$$

$$f = \frac{4EI}{L}$$

$$g = \frac{2EI}{L}$$

It can be noted that the global stiffness matrix [S] is symmetrical about the leading diagonal and hence only the lower triangle needs to be considered. This symmetry is an extremely useful property as it enables storage to be reduced and allows for relatively simple solution routines.

The equations presented in expression (4.1) can be more generally and compactly expressed in terms of their nodal i and j components for every member of the frame as;

$$\begin{Bmatrix} L_i \\ L_j \end{Bmatrix} = \begin{bmatrix} S_{ii} & S_{ij} \\ S_{ji} & S_{jj} \end{bmatrix} \begin{Bmatrix} X_i \\ X_j \end{Bmatrix}$$

where the sub-matrices S_{ii} , S_{ij} , S_{ji} , S_{jj} are the contributions of each end of the member to the overall stiffness matrix of the structure. The location of these sub-matrices for each element in the overall stiffness matrix of the structure is governed by the values of the subscripts i and j respectively.

To clarify this construction procedure consider two elements a and b , with nodes $(i-j)$ and $(j-k)$ respectively, of a framework structure as shown in fig 4.2.

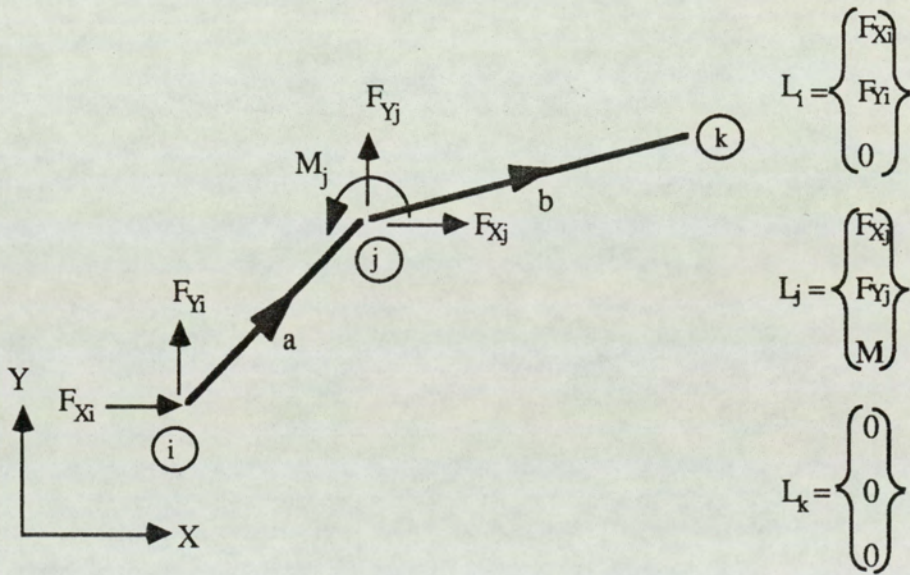


Fig 4.2. Diagram Showing Joint External Nodal Loadings.

in which typical external nodal forces are applied at joints i, j, k respectively.

On construction of the overall structural stiffness matrix, it is seen that the locations of the various components of the two members in the matrix will be as shown in fig 4.3 in

which the subscripts a and b refer to the members a and b respectively.

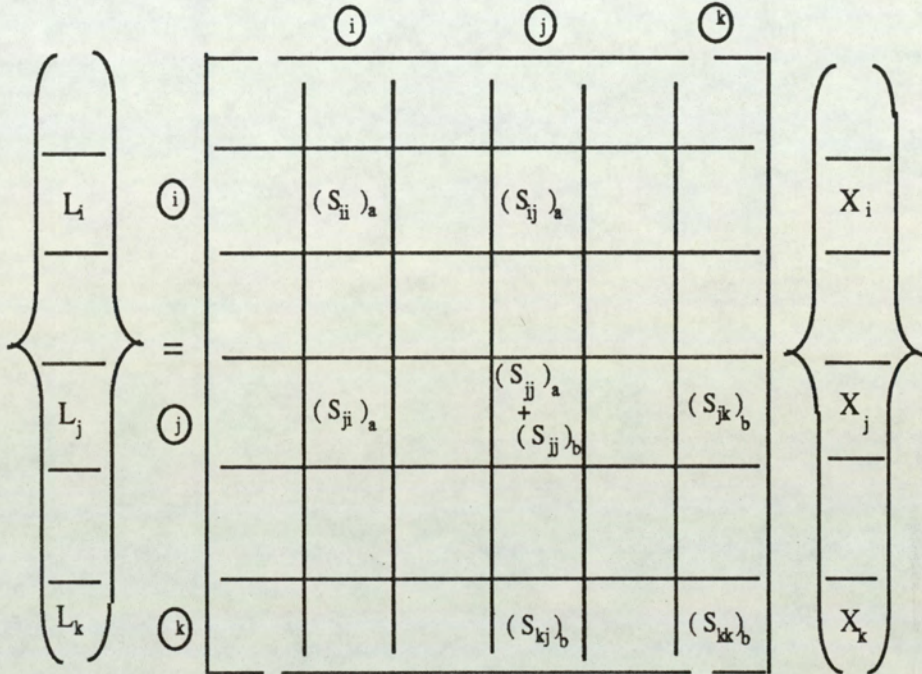


Fig 4.3. Construction of Overall Stiffness Matrix and Formation of Global Equations.

Continued similar systematic superposition of the stiffness contributions for every other member of the frame results in the formation of the complete set of global equations, which can be expressed briefly as

$$\{L_T\} = [S_T]\{X_T\} \dots\dots\dots(4.2)$$

where the suffix T implies that the matrices apply to the complete structure.

Further details of this construction procedure may be found in the various standard text on matrix analysis (5,49,58).

4.1.2. Non-linear Element.

Of the four non-linear elements presented, three, namely those described in section (3.1.1), (3.1.2) and (3.2.2.3), contain stiffness matrices that are symmetrical about the leading diagonal. Hence the construction of the equations pertaining to those elements follows the same procedure as that described in section (4.1.1) above.

The stiffness matrix for the non-linear element obtained from the derived exact function and including interactions between the flexural and axial effects is, however non-symmetrical. Since every other element produces symmetry in the stiffness matrix, it is convenient to rearrange the equations of this fourth non-linear element so that it too exhibits symmetry, thus allowing the same solution routine to be employed for matrices constructed from any element form.

The symmetry of this derived 'interactive' element can be carried out in the following manner. Consideration of the local element given in equation (3.22) shows that the stiffness matrix is composed of two portions, a symmetrical component comprising independent flexural and axial matrices and a non-symmetrical 'coupling' component.

Transformation into global coordinates is achieved by firstly rewriting the local nodal displacements, occurring within the unsymmetrical component of the matrix, in terms of the global nodal displacements and then performing the triple multiplication $[A]^T[K][A]$. The resulting global stiffness matrix can now itself be separated into symmetrical and non-symmetrical components producing the global equations:-

$$\begin{Bmatrix} F_{X1} \\ F_{Y1} \\ M_1 \\ F_{X2} \\ F_{Y2} \\ M_2 \end{Bmatrix} = \begin{bmatrix} a & & & & & \\ c & b & & & & \\ d & e & f & & & \\ -a & -c & -d & a & & \\ -c & -b & -e & c & b & \\ d & e & g & -d & -e & -f \end{bmatrix} + \begin{bmatrix} -ZN1 & -ZN2 & -ZN3 & -ZN7 & -ZN10 & -ZN8 \\ -ZN5 & -ZN6 & -ZN4 & -ZN11 & -ZN12 & -ZN7 \\ 0 & 0 & 0 & 0 & 0 & 0 \\ ZN1 & ZN2 & ZN3 & ZN9 & ZN10 & ZN8 \\ ZN5 & ZN6 & ZN4 & ZN11 & ZN12 & ZN7 \\ 0 & 0 & 0 & 0 & 0 & 0 \end{bmatrix} \begin{Bmatrix} X_1 \\ Y_1 \\ \theta_1 \\ X_2 \\ Y_2 \\ \theta_2 \end{Bmatrix}$$

Symmetrical
Non-symmetrical

where for the prismatic member exhibiting non-linear behaviour under compression;

$$a = \frac{EA}{L} l_p^2 + \frac{P\alpha^2 \sin^2 \alpha L}{\lambda} l_q^2$$

$$b = \frac{EA}{L} m_p^2 + \frac{P\alpha^2 \sin^2 \alpha L}{\lambda} m_q^2$$

$$c = \frac{EA}{L} l_p m_p + \frac{P\alpha^2 \sin^2 \alpha L}{\lambda} l_q m_q$$

$$d = \frac{P\alpha (1 - \cos \alpha L)}{\lambda} l_q$$

$$e = \frac{P\alpha (1 - \cos \alpha L)}{\lambda} m_q$$

$$f = \frac{P (\sin \alpha L - \alpha L \cos \alpha L)}{\lambda}$$

$$g = \frac{P (\alpha L - \sin \alpha L)}{\lambda}$$

where

$$\lambda = 2\alpha (1 - \cos \alpha L) - \alpha^2 L \sin \alpha L \quad \alpha = \sqrt{P/EI}$$

and

$$\begin{aligned} ZN1 &= A1 l_p l_q & ZN2 &= A1 l_p m_p \\ ZN3 &= A2 l_p & ZN4 &= A2 m_p \\ ZN5 &= A1 m_p l_q & ZN6 &= A1 m_p m_q \\ ZN7 &= A4 m_p & ZN8 &= A4 l_p \\ ZN9 &= A3 l_p l_q & ZN10 &= A3 l_p m_q \\ ZN11 &= A3 m_p l_q & ZN12 &= A3 m_p m_q \end{aligned}$$

where it should be noted that the coefficients A1, A2, A3, A4 are here described in terms of displacements in the local coordinate system.

Hence by transferring the un-symmetrical components to the left hand side, symmetry of the stiffness matrix is restored, the equations taking the form;

$$\begin{Bmatrix} F_{X1} \\ F_{Y1} \\ M_1 \\ F_{X2} \\ F_{Y2} \\ M_2 \end{Bmatrix} - \begin{bmatrix} -ZN1 & -ZN2 & -ZN3 & -ZN7 & -ZN10 & -ZN8 \\ -ZN5 & -ZN6 & -ZN4 & -ZN11 & -ZN12 & -ZN7 \\ 0 & 0 & 0 & 0 & 0 & 0 \\ ZN1 & ZN2 & ZN3 & ZN9 & ZN10 & ZN8 \\ ZN5 & ZN6 & ZN4 & ZN11 & ZN12 & ZN7 \\ 0 & 0 & 0 & 0 & 0 & 0 \end{bmatrix} \begin{Bmatrix} x_1 \\ y_1 \\ \theta_1 \\ x_2 \\ y_2 \\ \theta_2 \end{Bmatrix} = \begin{bmatrix} a & & & & & \\ c & b & & & & \\ d & e & f & & & \\ -a & -c & -d & a & & \\ -c & -b & -e & c & b & \\ d & e & g & -d & -e & -f \end{bmatrix} \begin{Bmatrix} x_1 \\ y_1 \\ \theta_1 \\ x_2 \\ y_2 \\ \theta_2 \end{Bmatrix} \dots\dots(4.3)$$

This process obviously requires a modification of the left hand vector which will be dependent on the nodal displacements.

It can be noted that the symmetrical portion of this matrix is the complete stiffness matrix obtained for the non-linear element, which was formulated from derived functions, but in which the interactions between the flexural and axial matrices were excluded (sections 3.1.1 and 3.1.2).

4.2. Imposition of Known Displacements.

The solution of a structural problem cannot proceed until sufficient boundary conditions have been imposed to define a datum from which the displacements can be measured. These boundary conditions consist of prescribed displacements at selected nodes, and although the values of these displacements are usually zero, corresponding to complete restraint, non-zero values can also be prescribed, these corresponding to perhaps known settlements.

The manner in which a prescribed zero displacement can be applied is by simply replacing the elements of the row and column corresponding to the displacement by zeros, leaving however the leading diagonal term unchanged. The corresponding load term is also made equal to zero. This process is illustrated in fig 4.4 where the displacements θ_1 and x_k are prescribed as zero, and where it can be noted that symmetry of the stiffness matrix is still preserved.

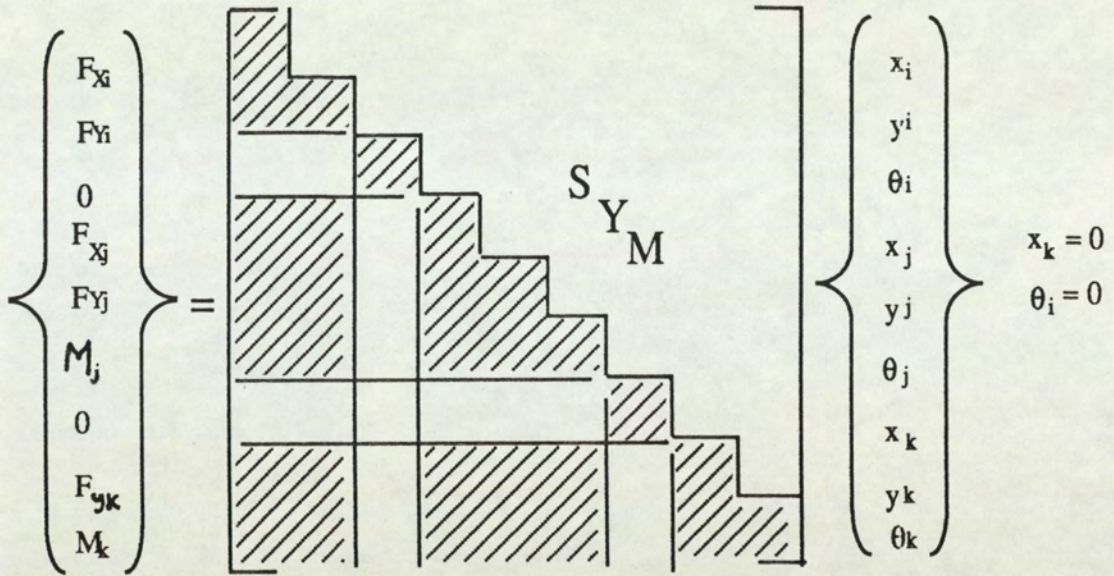


Fig 4.4. Method of Imposing Zero Displacements.

This technique can only be used to impose zero displacements and hence if non-zero values are prescribed a separate procedure must be followed. While precise insertion of prescribed values can be implemented, an approximate but very satisfactory method consists of multiplying the leading diagonal corresponding to the prescribed displacement by a large number, eg 10^{20} . Similarly it is necessary to replace the corresponding load by the product of the modified leading diagonal and the prescribed displacement. Thus considering an original equation;

$$F_i = K_{1i}\phi_1 + K_{2i}\phi_2 + \dots + K_{ii}\phi_i + \dots + K_{ik}\phi_k$$

in which the ϕ values represent the displacement, and $\phi_i = \psi$ is prescribed, the

modification described above will alter the equation to;

$$K_{ii} * 10^{20} \psi = K_{1i} \phi_1 + K_{2i} \phi_2 + \dots + K_{ii} * 10^{20} \phi_i + \dots + K_{ik} \phi_k$$

Since all the terms on the right hand side except $K_{ii} * 10^{20} \phi_i$ are small, it can be seen that ϕ_i must be approximately equal to ψ . Again the preservation of symmetry in the stiffness matrix may be noted.

4.3. Solution of Linear Equations.

Once the structural equations have been constructed and the boundary conditions imposed, the displacement vector can be obtained directly via inversion of the stiffness matrix as long as the elements of the matrix are constants. Thus from equation (4.2);

$$\{L_T\} = [S_T]\{X_T\}$$

the vector $\{X_T\}$ is obtained from;

$$\{X_T\} = [S_T]^{-1}\{L_T\}$$

A number of techniques both direct and iterative are available for performing this inversion (5,50,51,52), the most popular of these being perhaps the direct methods of Gaussian elimination (50,51) and Cholesky decomposition (52). Gaussian elimination may be applied to both symmetrical and non-symmetrical matrices, while the Cholesky procedure only applies to matrices of symmetrical form. With matrices which are symmetrical and positive definite the Cholesky method is more economical in storage than the Gauss procedure and thus, since only such matrices are encountered in the thesis, this method of solution was chosen.

Once the nodal displacements have been determined, the nodal forces in each member can be found by back substitution of the deflections into the member equations.

4.3.1. Cholesky Decomposition Method.

This method consists of rewriting the equations set

$$\{L_T\} = [S_T]\{X_T\}$$

into the form

$$\{L_T\} = [U]^T[U]\{X_T\}$$

where $[U]$ is an upper triangular matrix and $[U]^T$, its transpose, is a lower triangular matrix.

Thus letting

$$[U]\{X_T\} = \{Y\} \quad \dots\dots\dots(4.4)$$

the vector $\{Y\}$ can be found from

$$\{L_T\} = [U]^T\{Y\}$$

and hence $\{X_T\}$ obtained from equation (4.4) that is

$$\{X_T\} = [U]^{-1}\{Y\}$$

The inverse of the matrix $[U]$ or $[U]^T$ is obtained via a simple systematic procedure due to the triangular characteristics of $[U]$. The algebraic details of the procedure are well documented (52), providing a comprehensive description.

4.4. Solution of Non-linear Equations.

In the treatment of geometrical non-linearity the coefficients of the stiffness matrix have been shown to depend on the axial force in the element and also on the nodal displacements themselves. Hence in order to obtain solutions to non-linear problems, clearly iterative techniques must be employed. The nature of these procedures will depend on the form of element used to model the non-linear behaviour and thus it is necessary to describe the solution techniques for each element separately.

4.4.1. Elements obtained from Equilibrium and Work Processes in which Axial and Flexural Effects are Independent (Section 3.1.1, 3.1.2 and 3.2.1)

The solution of frames using these elements entails performing an initial linear analysis using the element described in section 2.1 through which the axial forces in each element are obtained. These axial forces are then used to obtain the non-linear flexural stiffness matrices described in sections (3.1.1), (3.1.2) and (3.2.1) which are functions of the axial force in the member. Thus a second analysis may be performed which includes the effects of the axial forces. It would appear that further iterations are illogical since the axial forces are considered to be independent of the lateral displacements as explained in section (3.1.4). Hence the solution process using these elements should be considered complete after one iteration.

4.4.2. Element obtained from Equilibrium in which Axial and Flexural Effects are Coupled (Section 3.1.5 and 3.1.6).

Analysis using this element is expected to produce the most accurate results. In this case the non-linear equations contain both the axial force in the member and the nodal flexural displacements. A first approximation to these forces and displacements can again be found by performing a linear analysis. If these results are substituted into the non-linear equations, a process which involves modification of the load vector (equation 4.3), and a second analysis carried out, a closer approximation will be obtained. Such iteration can then be continued until the difference between two successive sets of displacements is acceptably small. Hence solution using this element should be considered one of continued iterations.

4.4.3. Element Formulated Through a Tangential Stiffness Matrix (Section 3.2.2).

As shown in equation (3.38a), at equilibrium the relationship between external and internal forces is given by

$$\{P\} = \int_0^L [\bar{B}]^T \{\sigma\} dx$$

which may be expressed as

$$\psi(\delta) = \int_0^L [\bar{B}]^T \{\sigma\} dx - \{P\} = 0$$

since the internal force term is a function of the nodal displacements $\{\delta\}$.

If an approximate displacement vector $\{\delta_n\}$ is obtained, then $\psi(\delta_n)$ will not be equal to

zero but may be related to $\psi(\delta_{n+1}) = 0$ by the equation

$$\psi(\delta_{n+1}) = \psi(\delta_n) + \left(\frac{d\psi}{d\delta} \right)_n \Delta\delta_n = 0$$

ie

$$\psi(\delta_{n+1}) = \psi(\delta_n) + [K_T]_n \{\Delta\delta_n\} = 0$$

where

$$\delta_{n+1} = \delta_n + \Delta\delta_n \dots\dots\dots(4.5)$$

and $[K_T]$ is the tangential stiffness matrix.

Thus

$$\Delta\delta_n = - [K_T]_n^{-1} \psi(\delta_n) \dots\dots\dots(4.6)$$

The solution process thus becomes (4.5);

- a) Perform a linear analysis to obtain $\{\delta_0\}$.
- b) Hence determine $\psi(\delta_0)$.
- c) Calculate $[K_T]_0$ using $\{\delta_0\}$ and the axial force in the member.
- d) Calculate $\Delta\delta_0$ from equation (4.6).
- e) Determine $\delta_1 = \delta_0 + \Delta\delta_0$ from equation (4.5)

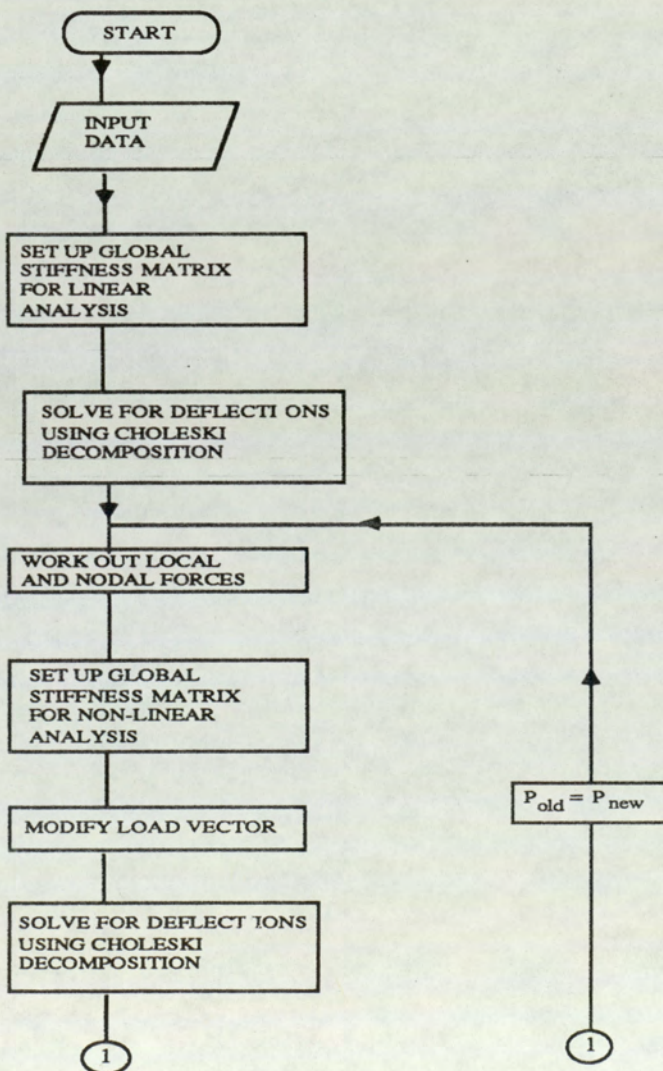
Repeat steps b) to e), using the next δ_n for each cycle, until $\Delta\delta_n$ becomes acceptably small.

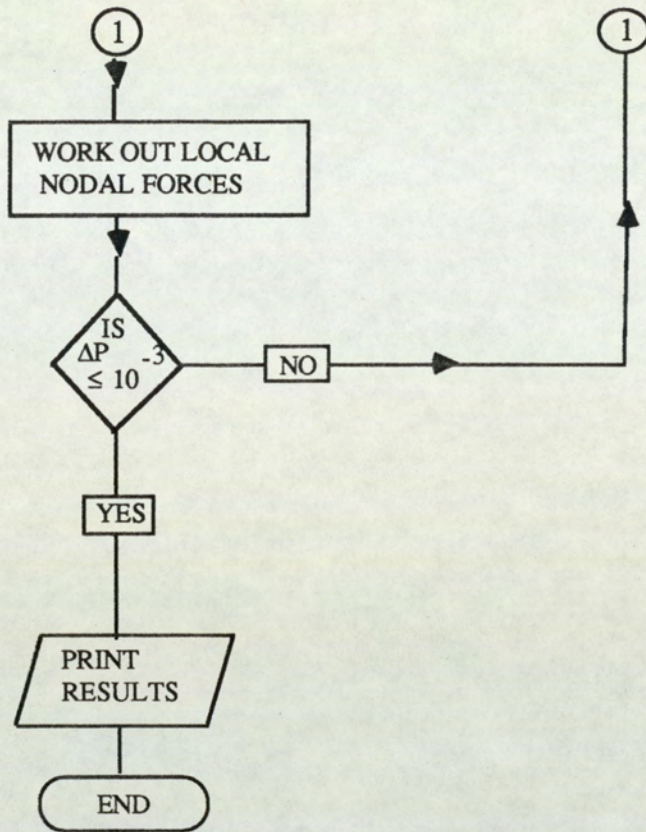
This process is thus again one of continual iteration. It can be noted that in essence the procedure is that of the Newton-Raphson method (50). The formulation of the internal forces, ie $\int_0^L [\bar{B}]^T \{\sigma\} dx$, is given in Appendix 2

4.5. Flow Charts for Programs.

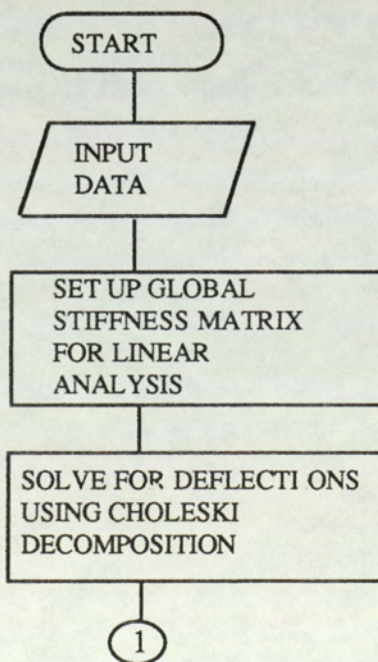
The descriptions of the solution processes given in the last section may be conveniently summarised through the medium of flow charts. Two flow charts are presented, these being for the two methods involving continual iterations. The corresponding flow charts for the simpler one-step iteration procedure can easily be deduced from those given. The programs were written in FORTRAN (53,54) and is listed in Appendix 3.

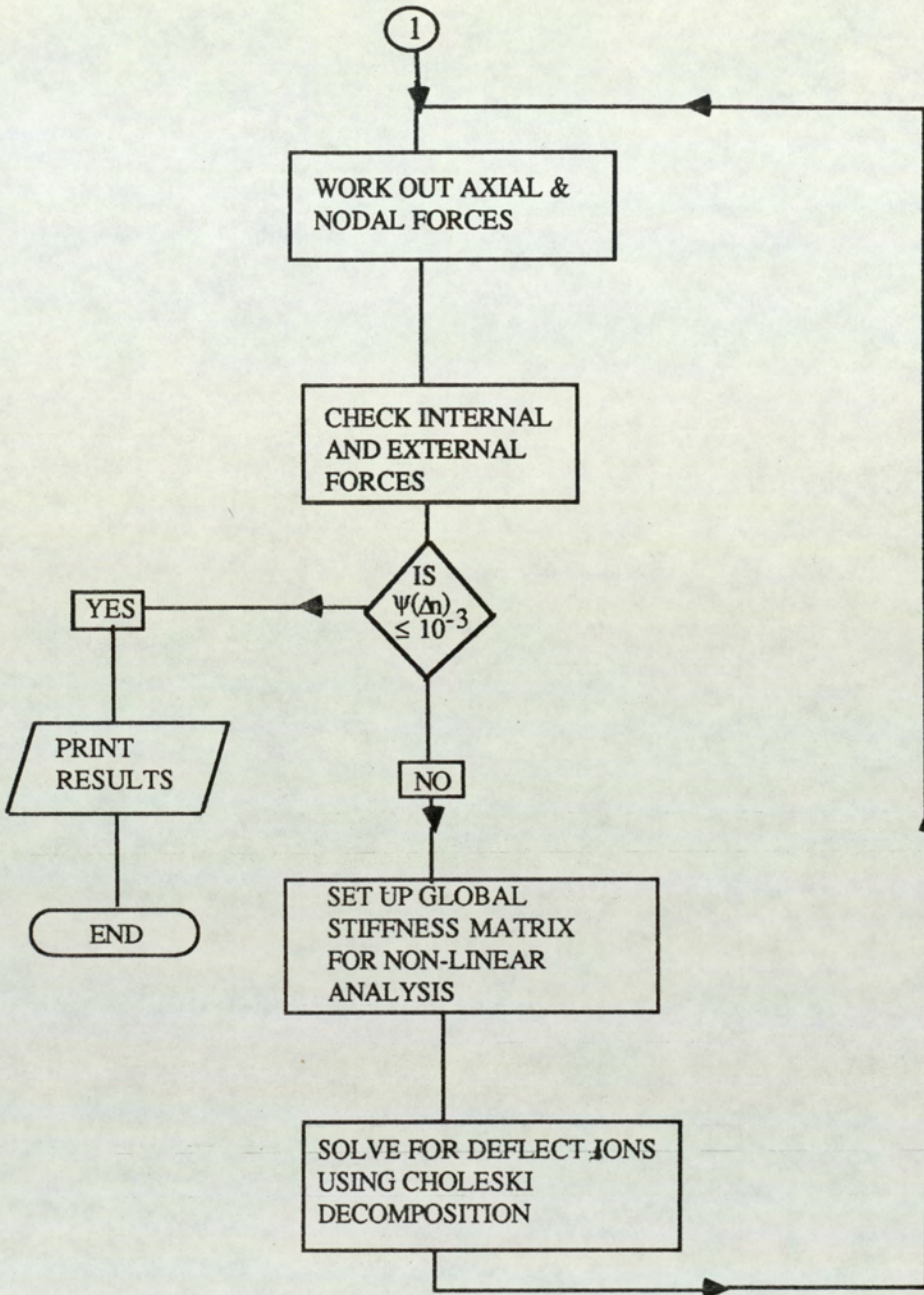
4.5.1. Exact Solution using Coupling Factors.





4.5.2. Tangential Stiffness Matrix.





Chapter 5.

**Treatment of Non-Nodal and
Distributed Loading.**

In the developments presented so far the external loading has been considered to consist of point loads applied at the nodes of the structure. In many practical instances the external loading may be of non-nodal or distributed form and hence, in order to be able to apply the processes so far developed, such loadings must be presented in the form of equivalent nodal loads.

The procedure for obtaining this equivalent loading will firstly be developed for the case of a non-nodal point load and the result obtained then used to determine the equivalent nodal forces due to distributed loading.

5.1. Non-nodal Point Load.

To find the nodal forces equivalent to a unit lateral point load, consider such a load applied to a beam in a structure a distance x from node 1 as shown in fig 5.1(a). The effect of this load may be considered equivalent to the sum of two components as shown in fig 5.1 (b) (c) where it is seen that the nodal forces producing the same nodal displacements as the unit load are numerically equal to the fixed end forces produced by the load.

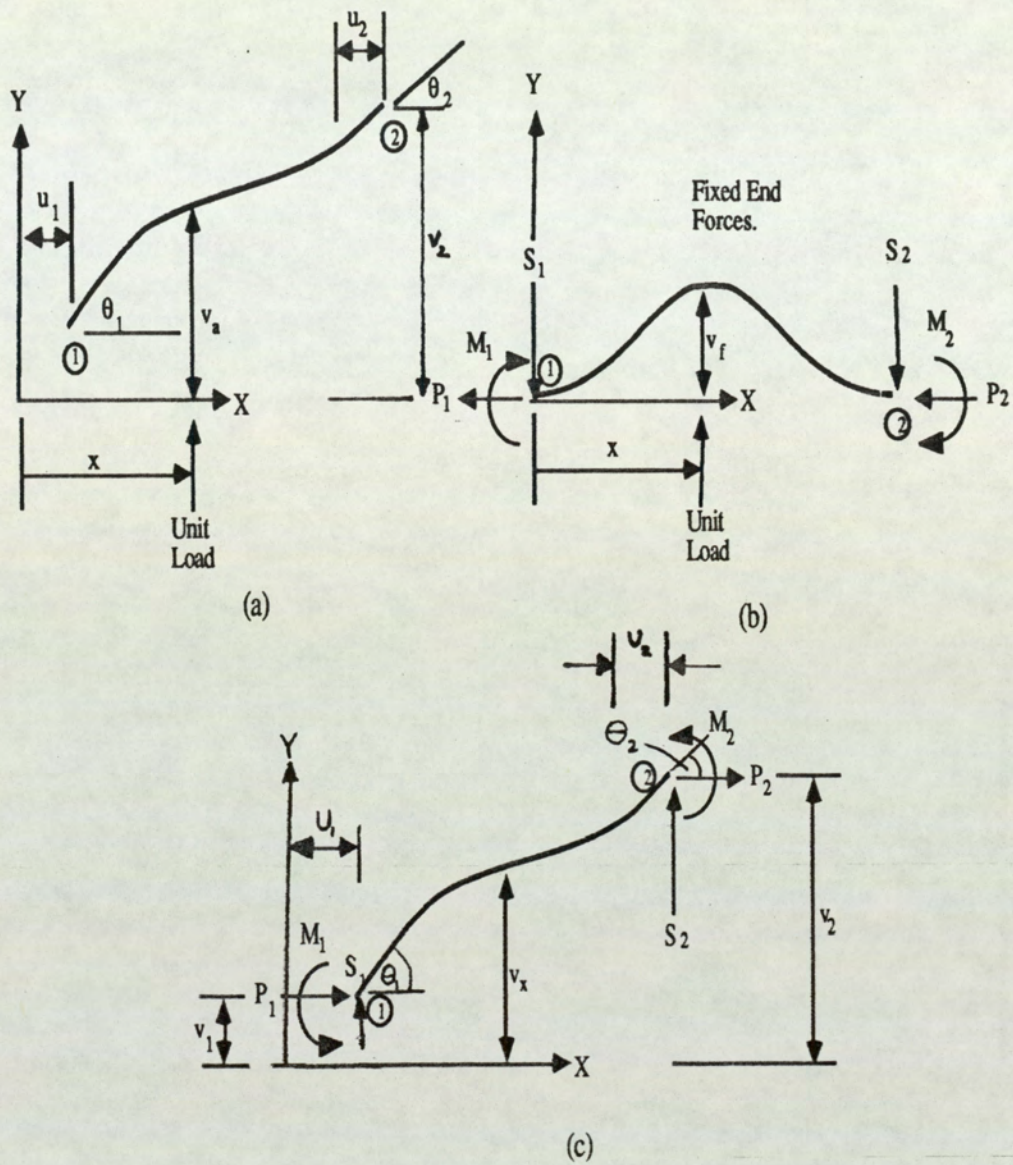


Fig 5.1. Decomposition of Effect of Non-nodal Point Load.

Considering the application of virtual displacements and equating the virtual work done by the external forces gives

$$1.\delta v_a = 1.\delta v_f + P_1\delta u_1 + P_2\delta u_2 + S_1\delta v_1 + M_1\delta\theta_1 + S_2\delta v_2 + M_2\delta\theta_2$$

Hence

$$\delta v_a - \delta v_f = \delta v_x = [P_1 \ P_2 \ S_1 \ M_1 \ S_2 \ M_2] \begin{Bmatrix} \delta u_1 \\ \delta u_2 \\ \delta v_1 \\ \delta \theta_1 \\ \delta v_2 \\ \delta \theta_2 \end{Bmatrix}$$

$$\text{ie } \delta v_x = \{P\}^T \{\delta \Delta\}$$

or

$$\delta v_x = \{\delta \Delta\}^T \{P\} \dots\dots\dots(5.1)$$

where it should be noted that v_x is the displacement profile produced by the nodal loadings.

Now using a general form of lateral displacement function

$$v_x = [1 \ x \ F_1(x) \ F_2(x) \ 0 \ 0] \begin{Bmatrix} a_1 \\ a_2 \\ a_3 \\ a_4 \\ a_5 \\ a_6 \end{Bmatrix}$$

$$\text{ie } v_x = [N]\{a\} = [N][C]^{-1}\{\Delta\}$$

it is seen that

$$\delta v_x = \{[N][C]^{-1}\} \{\delta\Delta\}$$

or

$$\delta v_x = \{\delta\Delta\}^T \{[N][C]^{-1}\}^T \dots\dots\dots(5.2)$$

Thus on comparison of equations (5.1) and (5.2) the equivalent nodal forces are given by

$$\{P\} = \{[N][C]^{-1}\}^T \dots\dots\dots(5.3)$$

Application of this result to the lateral displacement function

$$v_x = a_1 + a_2x + a_3x^2 + a_4x^3 \dots\dots\dots(5.4)$$

yields the values of the equivalent nodal forces {P} as

$$\{P\} = \begin{Bmatrix} S_1 \\ M_1 \\ S_2 \\ M_2 \end{Bmatrix} = \begin{Bmatrix} 1 - \frac{3}{L^2}x^2 + \frac{2}{L^3}x^3 \\ x - \frac{2}{L}x^2 + \frac{1}{L^2}x^3 \\ \frac{3}{L^2}x^2 - \frac{2}{L^3}x^3 \\ -\frac{1}{L}x^2 + \frac{1}{L^2}x^3 \end{Bmatrix} \dots\dots\dots(5.5)$$

while for the functions

$$v_x = a_1 + a_2x + a_3 \sin \alpha x + a_4 \cos \alpha x \quad \dots\dots\dots(5.6)$$

and

$$v_x = a_1 + a_2x + a_3 \sinh \alpha x + a_4 \cosh \alpha x \quad \dots\dots\dots(5.7)$$

the equivalent nodal forces are given by

$$\{P\} = \begin{Bmatrix} S_1 \\ M_1 \\ S_2 \\ M_2 \end{Bmatrix} = \begin{Bmatrix} C_{11} + C_{21}x + C_{31} \sin \alpha x + C_{41} \cos \alpha x \\ C_{12} + C_{22}x + C_{32} \sin \alpha x + C_{42} \cos \alpha x \\ C_{13} + C_{23}x + C_{33} \sin \alpha x + C_{43} \cos \alpha x \\ C_{14} + C_{24}x + C_{34} \sin \alpha x + C_{44} \cos \alpha x \end{Bmatrix} \quad \dots\dots\dots(5.8)$$

and

$$\{P\} = \begin{Bmatrix} S_1 \\ M_1 \\ S_2 \\ M_2 \end{Bmatrix} = \begin{Bmatrix} C_{11} + C_{21}x + C_{31} \sinh \alpha x + C_{41} \cosh \alpha x \\ C_{12} + C_{22}x + C_{32} \sinh \alpha x + C_{42} \cosh \alpha x \\ C_{13} + C_{23}x + C_{33} \sinh \alpha x + C_{43} \cosh \alpha x \\ C_{14} + C_{24}x + C_{34} \sinh \alpha x + C_{44} \cosh \alpha x \end{Bmatrix} \quad \dots\dots\dots(5.9)$$

respectively.

The equivalent nodal forces due to a unit axial point load applied within the length of the beam can be formed by an analogous procedure using the appropriate axial displacement function.

5.2. Distributed Loading.

The equivalent nodal forces due to distributed loading can be found from the previous result by considering the distributed loading p per unit run to be equivalent to a succession of point loads each of magnitude $p \cdot dx$.

Thus the equivalent nodal forces due to a uniformly distributed lateral load covering the whole span, L , can be written, from equation (5.3) as;

$$\{P\} = p \int_0^L \{[N][C]^{-1}\}^T dx \quad \dots\dots\dots(5.10)$$

Applying this result to the cubic displacement function given by equation (5.4) gives the result;

$$\{P\} = \begin{Bmatrix} S_1 \\ M_1 \\ S_2 \\ M_2 \end{Bmatrix} = p \int_0^L \begin{Bmatrix} 1 - \frac{3}{L^2} x^2 + \frac{2}{L^3} x^3 \\ x - \frac{2}{L} x^2 + \frac{1}{L^2} x^3 \\ \frac{3}{L^2} x^2 - \frac{2}{L^3} x^3 \\ -\frac{1}{L} x^2 + \frac{1}{L^2} x^3 \end{Bmatrix} dx = \begin{Bmatrix} \frac{pL}{2} \\ \frac{pL^2}{12} \\ \frac{pL}{2} \\ -\frac{pL^2}{12} \end{Bmatrix} \dots\dots\dots(5.11)$$

while for the functions given in equation (5.6) and (5,7) the equivalent nodal forces are;

$$\{P\} = \begin{Bmatrix} S_1 \\ M_1 \\ S_2 \\ M_2 \end{Bmatrix} = P \begin{Bmatrix} \frac{L C_{11} + L^2 C_{21} - \frac{C_{31}(\cos \alpha L - 1)}{\alpha} + \frac{\sin \alpha L}{\alpha} C_{41}}{2} \\ \frac{L C_{12} + L^2 C_{22} - \frac{C_{32}(\cos \alpha L - 1)}{\alpha} + \frac{\sin \alpha L}{\alpha} C_{42}}{2} \\ \frac{L C_{13} + L^2 C_{23} - \frac{C_{33}(\cos \alpha L - 1)}{\alpha} + \frac{\sin \alpha L}{\alpha} C_{43}}{2} \\ \frac{L C_{14} + L^2 C_{24} - \frac{C_{34}(\cos \alpha L - 1)}{\alpha} + \frac{\sin \alpha L}{\alpha} C_{44}}{2} \end{Bmatrix} \dots\dots\dots(5.12)$$

and

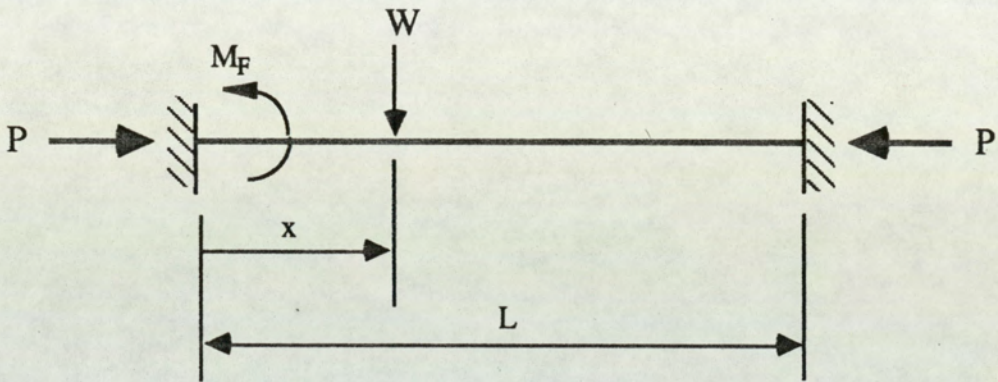
$$\{P\} = \begin{Bmatrix} S_1 \\ M_1 \\ S_2 \\ M_2 \end{Bmatrix} = P \begin{Bmatrix} \frac{L}{2} C_{11} + \frac{L^2}{2} C_{21} - \frac{C_{31}(\cosh \alpha L - 1)}{\alpha} + \frac{\sinh \alpha L}{\alpha} C_{41} \\ \frac{L}{2} C_{12} + \frac{L^2}{2} C_{22} - \frac{C_{32}(\cosh \alpha L - 1)}{\alpha} + \frac{\sinh \alpha L}{\alpha} C_{42} \\ \frac{L}{2} C_{13} + \frac{L^2}{2} C_{23} - \frac{C_{33}(\cosh \alpha L - 1)}{\alpha} + \frac{\sinh \alpha L}{\alpha} C_{43} \\ \frac{L}{2} C_{14} + \frac{L^2}{2} C_{24} - \frac{C_{34}(\cosh \alpha L - 1)}{\alpha} + \frac{\sinh \alpha L}{\alpha} C_{44} \end{Bmatrix} \dots(5.13)$$

respectively.

Again the equivalent nodal forces for a uniformly axially distributed load covering the span may be found similarly, as can those for other forms of uniform or non-uniform loadings.

5.3. Example of the Effect of Axial load on Fixed End Moments.

Consider the fixed ended beam below with a variable axial force and a moving lateral non-nodal point load.



Letting

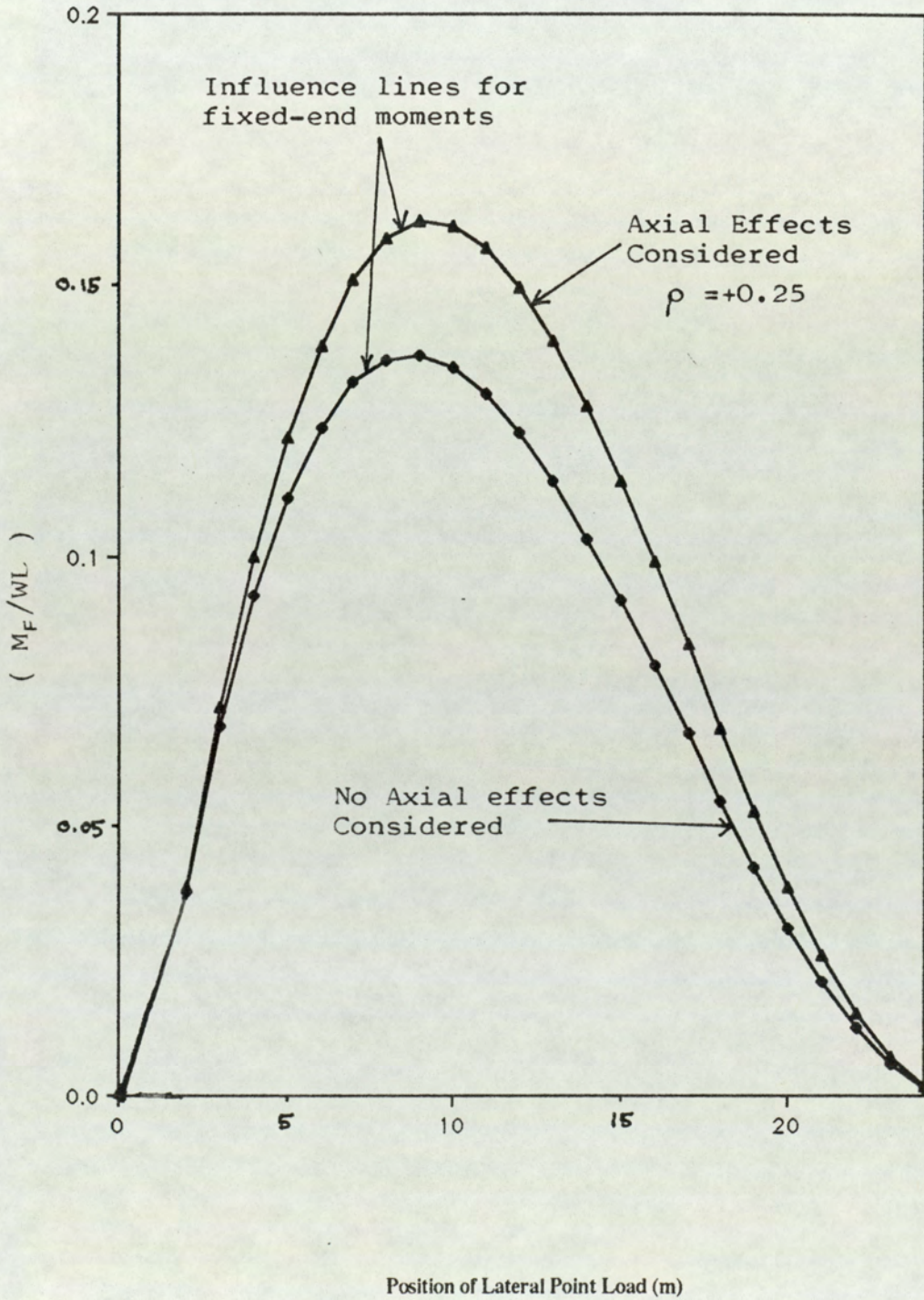
$$\rho = \frac{P}{P_e}$$

where

$$P_e = \frac{4 \pi^2 E I}{L^2} \quad (\text{Euler's buckling load for a fixed ended beam})$$

then plotting (M_F / WL) against x gives the following graph.

Variation in FEM for Member with Axial and Moving Lateral Loading



5.4. Modification to the Program.

As the non-nodal forces can be expressed in equivalent nodal form, all that is required in the program is an additional sub-routine in which these equivalent nodal forces are transformed from local coordinates to global coordinates, and added on to the existing load vector of the structure.

PART B.

**Gometrically Non-Linear Analysis of
Non-Prismatic Sections.**

Chapter 6.

Matrix Formulation.

The increasing performance required of modern frameworks, especially with regard to increase in span, has produced the impetus to seek greater efficiency in the use of shape and material in the design of structures.

The use of prismatic members automatically means that if a variation of bending moment exists in a member, then a proportion of the length of the element may be substantially understressed and hence not used efficiently. In order to attain greater efficiency, therefore, such elements could be tapered so that a more uniform distribution of stress occurs along the length of the member. This method of producing greater material efficiency is now becoming quite popular although manufacturing costs are higher when compared with those for prismatic sections.

In this chapter, therefore, attention is concentrated on the development of stiffness matrices for both linear and non-linear behaviour as applied to tapered sections. Firstly the exact linear stiffness matrix for a generally non-prismatic member obtained from derived displacement functions is presented, and then developed for specific cross-sectional shapes, and secondly the intractability of applying derived functions to the solution of non-linear tapered structures is demonstrated.

The development of approximate stiffness matrices based on work methods is then presented for the non-linear behaviour of non-prismatic sections, similar to those described in chapter 3 for prismatic sections.

6.1. Formation of the Exact Stiffness Matrix for Geometrically Linear Behaviour of a Prismatic Beam.

As presented previously for the linear prismatic beam (section 2.2), the complete stiffness matrix relating nodal forces to nodal displacements is composed of independent axial and flexural portions, and these components will be developed separately.

6.1.1. Development of the Flexural Stiffness Matrix.

Consider a general non-prismatic section member depicted in Fig 6.1 with the nodal forces shown.

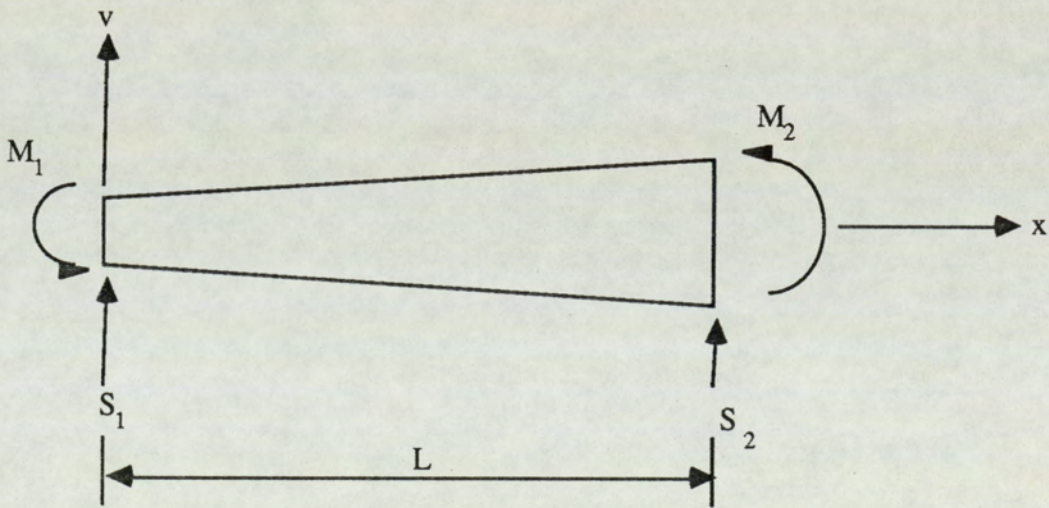


Fig. 6.1. Tapered Beam Showing Positive Values of Nodal forces.

The stress resultants on an element of length δx of this beam is shown in Fig 6.2 below.

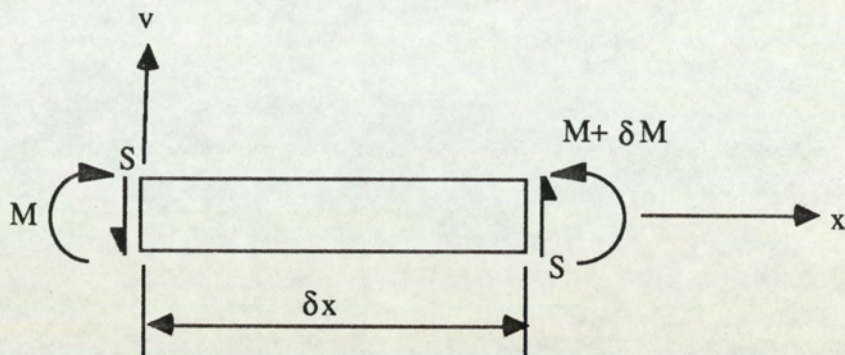


Fig 6.2. Stress Resultants on Element.

6.1.1.1. Formulation of Lateral Deflection Function.

As for the prismatic beam, rotational equilibrium of the element gives;

$$S = - \frac{dM}{dx} \dots\dots\dots(6.1)$$

and since for vertical equilibrium, S is constant;

$$\frac{dS}{dx} = - \frac{d^2M}{dx^2} = 0 \dots\dots\dots(6.2)$$

Intergrating (6.2) with respect to x gives;

$$M = b_1 + b_2x \dots\dots\dots(6.3)$$

where b_1 and b_2 are the constants of integration.

From the simple theory of bending

$$M = E I(x) \frac{d^2 v}{dx^2} \dots\dots\dots(6.4)$$

where I, the second moment of area of the section, is a function of x.

Thus substituting (6.3) into (6.4) and rearranging gives;

$$\frac{d^2 v}{dx^2} = \frac{M}{E I(x)} = \frac{b_1}{E I(x)} + \frac{b_2 x}{E I(x)}$$

or, assuming E to be constant;

$$\frac{d^2 v}{dx^2} = \frac{a_3}{I(x)} + \frac{a_4 x}{I(x)} \dots\dots\dots(6.5)$$

where $a_3 = \frac{b_1}{E}$ and $a_4 = \frac{b_2}{E}$.

Further integration gives;

$$\frac{dv}{dx} = \theta = a_2 + a_3 \int \frac{1}{I(x)} dx + a_4 \int \frac{x}{I(x)} dx \dots\dots\dots(6.6)$$

and

$$v = a_1 + a_2 x + a_3 \int \int \frac{1}{I(x)} dx dx + a_4 \int \int \frac{x}{I(x)} dx dx \dots\dots\dots(6.7)$$

thus giving the exact description of the beam displacement within the confines of the simple theory of bending.

6.1.1.2. Calculation of Nodal Displacements from the Arbitrary Constants $\{a_b\}$.

As the procedure is similar to that described in chapter 2, only the results will be presented. Substituting the nodal conditions into equations (6.6) and (6.7), the following matrix relationship ensues;

$$\begin{Bmatrix} v_1 \\ \theta_1 \\ v_2 \\ \theta_2 \end{Bmatrix} = \begin{bmatrix} 1 & 0 & G_1 & H_1 \\ 0 & 1 & g_1 & h_1 \\ 1 & L & G_2 & H_2 \\ 0 & 1 & g_2 & h_2 \end{bmatrix} \begin{Bmatrix} a_1 \\ a_2 \\ a_3 \\ a_4 \end{Bmatrix} \quad \dots\dots\dots(6.8)$$

$$\{\Delta_b\} = [C_b]\{a_b\}$$

in which;

$$\begin{aligned} g_1 &= \int_0^L \left(\frac{1}{I(x)} \right) dx & g_2 &= \int_L^L \left(\frac{1}{I(x)} \right) dx \\ h_1 &= \int_0^L \left(\frac{x}{I(x)} \right) dx & h_2 &= \int_L^L \left(\frac{x}{I(x)} \right) dx \\ G_1 &= \int_0^L \int_0^L \left(\frac{1}{I(x)} \right) dx dx & G_2 &= \int_L^L \int_L^L \left(\frac{1}{I(x)} \right) dx dx \\ H_1 &= \int_0^L \int_0^L \left(\frac{x}{I(x)} \right) dx dx & H_2 &= \int_L^L \int_L^L \left(\frac{x}{I(x)} \right) dx dx \end{aligned} \quad \dots\dots\dots(6.9)$$

Inversion of (6.8) produces;

$$\begin{Bmatrix} a_1 \\ a_2 \\ a_3 \\ a_4 \end{Bmatrix} = \begin{bmatrix} C_{11} & C_{12} & C_{13} & C_{14} \\ C_{21} & C_{22} & C_{23} & C_{24} \\ C_{31} & C_{32} & C_{33} & C_{34} \\ C_{41} & C_{42} & C_{43} & C_{44} \end{bmatrix} \begin{Bmatrix} v_1 \\ \theta_1 \\ v_2 \\ \theta_2 \end{Bmatrix} \quad \dots\dots\dots(6.10)$$

$$\{a_b\} = [C_b]^{-1}\{\Delta_b\}$$

where the elements of $[C_b]^{-1}$ are given in appendix 1 and reference 40.

6.1.1.3. Relationship Between Stress Resultants and Nodal Displacements.

From equation (6.5)

$$M = E I(x) \frac{d^2 v}{dx^2} = E [a_3 + a_4 x] \quad \dots\dots\dots(6.11)$$

and from equation (6.1) it follows that

$$S = - E I(x) \frac{d^3 v}{dx^3} \quad \dots\dots\dots(6.12)$$

or

$$S = - E a_4 \quad \dots\dots\dots(6.13)$$

Combining (6.11) and (6.13) gives

$$\begin{Bmatrix} S \\ M \end{Bmatrix} = E \begin{bmatrix} 0 & 0 & 0 & -1 \\ 0 & 0 & 1 & x \end{bmatrix} \begin{Bmatrix} a_1 \\ a_2 \\ a_3 \\ a_4 \end{Bmatrix} \dots\dots\dots(6.14)$$

But $\{a_b\} = [C_b]^{-1}\{\Delta_b\}$ and hence

$$\begin{Bmatrix} S \\ M \end{Bmatrix} = E \begin{bmatrix} -C_{41} & -C_{42} & -C_{43} & -C_{44} \\ C_{31} + x C_{41} & C_{32} + x C_{42} & C_{33} + x C_{43} & C_{34} + x C_{44} \end{bmatrix} \begin{Bmatrix} v_1 \\ \theta_1 \\ v_2 \\ \theta_2 \end{Bmatrix} \dots\dots\dots(6.15)$$

ie $\{P_b\} = [H]\{\Delta_b\}$

6.1.1.4. Formulation of Stiffness Matrix $[K_b]$.

Since equilibrium is satisfied at all sections of the beam, the values of the nodal stress resultants must be numerically equal to the nodal external forces as described in section (2.1.2). Thus considering equilibrium of the external and internal nodal forces and noting that they are of the same sign at node 2 and of opposite sign at node 1 the relationship between the external nodal forces and the displacements is given by;

$$\begin{Bmatrix} S_1 \\ M_1 \\ S_2 \\ M_2 \end{Bmatrix} = E \begin{bmatrix} C_{41} & C_{42} & C_{43} & C_{44} \\ -C_{31} & -C_{32} & -C_{33} & -C_{34} \\ -C_{41} & -C_{42} & -C_{43} & -C_{44} \\ C_{31} + LC_{41} & C_{32} + LC_{42} & C_{33} + LC_{43} & C_{34} + LC_{44} \end{bmatrix} \begin{Bmatrix} v_1 \\ \theta_1 \\ v_2 \\ \theta_2 \end{Bmatrix} \quad \dots(6.16)$$

$$\text{ie } \begin{Bmatrix} S_1 \\ M_1 \\ S_2 \\ M_2 \end{Bmatrix} = \begin{bmatrix} K_{33} & & & \\ K_{43} & K_{44} & & \\ K_{53} & K_{54} & \text{SYM} & \\ K_{63} & K_{64} & K_{65} & K_{66} \end{bmatrix} \begin{Bmatrix} v_1 \\ \theta_1 \\ v_2 \\ \theta_2 \end{Bmatrix}$$

$$\text{ie } \{P_b\} = [K_b]\{\Delta_b\}$$

After some manipulation it can be shown that

$$K_{33} = -K_{33} = K_{55} = C_{41} = -C_{41} = -C_{43} = \frac{E}{D} \int_0^L x \, dx$$

$$K_{43} = -C_{31} = -C_{33} = -C_{42} = \frac{E}{D} \int_0^L x X \, dx$$

$$K_{44} = -C_{32} = \frac{E}{D} \int_0^L x^2 X \, dx$$

$$K_{54} = K_{43}$$

$$K_{63} = -K_{65} = C_{44} = \frac{E}{D} \int_0^L (L-x) X \, dx$$

$$K_{64} = C_{34} = \frac{E}{D} \int_0^L x (L-x) X \, dx$$

$$K_{66} = C_{34} + LC_{44} = \frac{E}{D} \int_0^L (L-x)^2 X dx$$

where

$$X = \frac{1}{I(x)}$$

and

$$D = \int_0^L X dx \int_0^L x^2 X dx - \left(\int_0^L x X dx \right)^2$$

$[K_b]$ is the flexural stiffness matrix and is symmetrical about the leading diagonal.

6.1.2. Construction of the Axial Stiffness Matrix $[K_a]$ for a Non-prismatic Bar.

The axial stiffness matrix can be formed in a similar manner to that for the bending stiffness matrix. Considering the equilibrium of a length δx of the beam as shown in Fig 6.3.

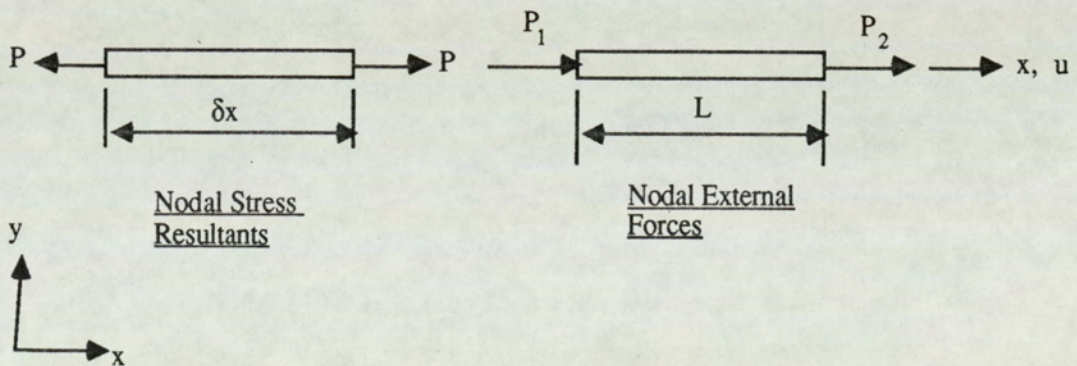


Fig 6.3. Diagram Showing Stress Resultants and Nodal Forces.

it is seen that;

$$\frac{dP}{dx} = 0 \quad \dots\dots\dots(6.17)$$

Ignoring any moment effects from the axial force, and noting that the cross-sectional area is a function of x , Hooke's Law gives;

$$P = EA(x) \frac{du}{dx} \dots\dots\dots(6.18)$$

where u is the axial displacement.

Hence differentiating (6.18) with respect to x and substituting in (6.17) gives;

$$\frac{dP}{dx} = E \left[A(x) \frac{d^2u}{dx^2} + \left(\frac{dA(x)}{dx} \right) \frac{du}{dx} \right] = 0$$

or

$$A(x) \frac{d^2u}{dx^2} + \left(\frac{dA(x)}{dx} \right) \frac{du}{dx} = 0 \dots\dots\dots(6.19)$$

Integration of (6.19) with respect to x gives the axial displacement function as;

$$u = a_5 + a_6 \int \frac{1}{A(x)} dx \dots\dots\dots(6.20)$$

Hence following steps (6.1.1.2) to (6.1.1.4) and referring to the sign convention shown in Fig 6.3 the following result is given:-

$$\begin{Bmatrix} P_1 \\ P_2 \end{Bmatrix} = \frac{E}{\phi} \begin{bmatrix} 1 & -1 \\ -1 & 1 \end{bmatrix} \begin{Bmatrix} u_1 \\ u_2 \end{Bmatrix} \dots\dots\dots(6.21)$$

$$\text{ie } \{P_a\} = [K_a]\{\Delta_a\}$$

where

$$\phi = \int_0^L \frac{1}{A(x)} dx$$

Again the symmetry of the matrix should be noted.

6.1.3. Combined Stiffness Matrix for Flexural and Axial Behaviour.

Combination of the flexural and axial equations yields the complete stiffness matrix relating the six nodal forces to the corresponding displacements, thus:-

$$\begin{Bmatrix} P_1 \\ P_2 \\ S_1 \\ M_1 \\ S_2 \\ M_2 \end{Bmatrix} = \begin{bmatrix} K_{11} & & & & & \\ K_{21} & K_{22} & & & & \\ \hline 0 & 0 & K_{33} & & & \\ 0 & 0 & K_{43} & K_{44} & & \\ 0 & 0 & K_{53} & K_{54} & K_{55} & \\ 0 & 0 & K_{63} & K_{64} & K_{65} & K_{66} \end{bmatrix} \begin{Bmatrix} u_1 \\ u_2 \\ v_1 \\ \theta_1 \\ v_2 \\ \theta_2 \end{Bmatrix} \quad \text{SYMM} \quad \dots\dots(6.23)$$

$$\text{or } \{P\} = [K]\{\Delta\}$$

The above relationships represent linear behaviour of a general non-prismatic section, the individual elements being evaluated from $I(x)$ and $A(x)$ of the beam under consideration. It should also be noted that the stiffness matrix is symmetrical about the leading diagonal and that the flexural and axial sub-matrices are mutually independent of each other.

A close study of the above stiffness matrix shows that the elements can be calculated from four simple integral evaluations. From sections 6.1.1.4 and 6.2 and letting

$$\int_0^L \frac{1}{A(x)} dx = \bar{A}_0 \quad \int_0^L \frac{1}{I(x)} dx = \bar{I}_0$$

$$\int_0^L \frac{x}{I(x)} dx = \bar{I}_1 \quad \int_0^L \frac{x^2}{I(x)} dx = \bar{I}_2$$

where $A(x)$ and $I(x)$ represent the variation of the cross-sectional area and second moment of area along the section respectively, the combined stiffness matrix may be written as;

$$K_{11} = -K_{21} = K_{22} = \frac{E}{\bar{A}_0}$$

$$K_{33} = -K_{53} = K_{55} = \frac{E}{D} (\bar{I}_0)$$

$$K_{43} = -K_{54} = \frac{E}{D} (\bar{I}_1)$$

$$K_{44} = \frac{E}{D} (\bar{I}_2)$$

$$K_{63} = -K_{65} = \frac{E}{D} [L(\bar{I}_0) - \bar{I}_1]$$

$$K_{64} = \frac{E}{D} [L(\bar{I}_1) - \bar{I}_2]$$

$$K_{66} = \frac{E}{D} [L^2(\bar{I}_0) - 2L(\bar{I}_1) + \bar{I}_2]$$

where E = Young's Modulus and

$$D = (\bar{I}_0 \bar{I}_2) - (\bar{I}_1)^2$$

6.1.4. Formulation of 'Exact' Flexural Stiffness Matrices for Rectangular and I-sections.

The general results derived in the previous sections will now be applied to the specific cases of tapering rectangular and I-section beams.

6.1.4.1. Rectangular Section.

Consider a rectangular beam with constant breadth b and varying depth as shown in Fig 6.4;

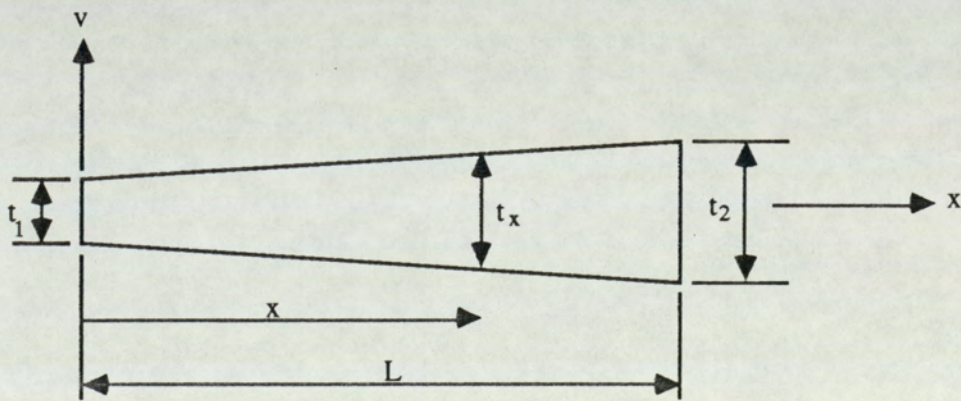


Fig 6.4. Tapered Beam Showing a General Depth at Distance x .

From the geometry of the tapered section, at a distance x from the origin;

$$\begin{aligned}
 t_x &= t_1 + \left(\frac{t_2 - t_1}{L} \right) x \\
 &= t_1 + \gamma x \qquad \dots\dots\dots(6.24)
 \end{aligned}$$

where

$$\gamma = \left(\frac{t_2 - t_1}{L} \right)$$

Now it is possible to express the second moment of area and the cross-sectional area in terms of the depth at distance x as

$$I_x = \frac{b}{12} (t_1 + \gamma x)^3$$

$$A_x = b (t_1 + \gamma x)$$

Hence using the two expressions, the four integrals presented in section (6.1.3) can be evaluated, giving

$$\bar{A}_0 = \frac{L \left[\ln \left(\frac{t_2}{t_1} \right) \right]}{b (t_2 - t_1)}$$

$$\bar{I}_0 = \frac{6L (t_2 - t_1)}{b t_1^2 t_2^2}$$

$$\bar{I}_1 = \frac{6L^2}{b t_1 t_2^2}$$

$$I_2 = \frac{12}{b (t_2 - t_1)^2} \left[\frac{\ln \left(\frac{t_2}{t_1} \right)}{(t_2 - t_1)} - \frac{(3t_2 - t_1)}{2t_2^2} \right]$$

which can be substituted into the standard results given in the previous section to obtain the stiffness matrix coefficients.

6.1.4.2. I-section.

Consider a beam with constant breadth b and the section shown below in Fig 6.5;

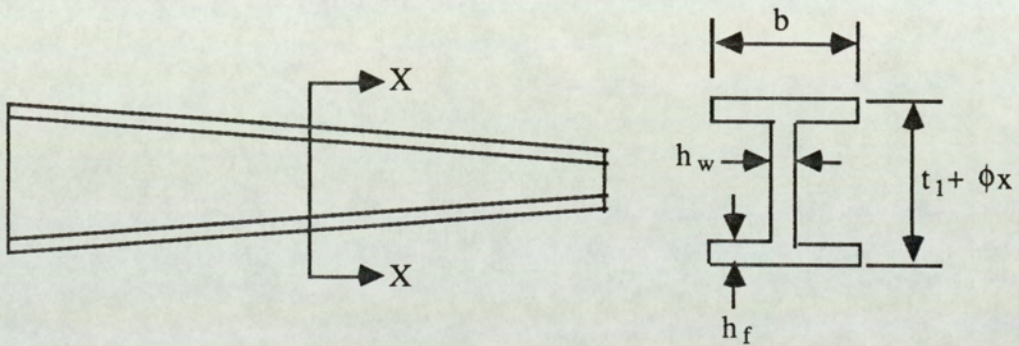


Fig 6.5. Showing typical I-section.

From the figure above it can be seen that the second moment of area can be expressed as;

$$I(x) = \frac{1}{12} \left[bt_x^3 - (b - h_w)(t_x - 2h_f)^3 \right]$$

where

$$t_x = t_1 + \phi x$$

Rearranging the above expression gives

$$I(x) = \frac{b}{12} \left\{ t_x^3 - \left[\left(\frac{b - h_w}{b} \right)^{1/3} (t_x - 2h_f) \right]^3 \right\}$$

Letting $\xi = \left(\frac{b - h_w}{b}\right)^{1/3}$

$$I(x) = \left[t_x - \xi (t_x - 2h_f) \right]^3$$

and expanding and evaluating the general integrals (59) gives;

$$\bar{I}_0 = \int_0^L \frac{1}{I(x)} dx = \frac{2}{b K^2 k^2} \left(\frac{L}{t_2 - t_1} \right) \left[2\sqrt{3} (1 + K) \mu - (1 - K) \rho \right]$$

$$\bar{I}_1 = \int_0^L \frac{x}{I(x)} dx = \frac{2}{b K k} \left(\frac{L}{t_2 - t_1} \right)^2 \left[2\sqrt{3} \mu - \rho \right] - \left(\frac{t_1 L}{t_2 - t_1} \right) \bar{I}_0$$

$$\begin{aligned} \bar{I}_2 = \int_0^L \frac{x^2}{I(x)} dx = & \frac{2}{b(1-K)(1+K+K^2)} \left(\frac{L}{t_2 - t_1} \right)^3 \left[3\tau + 2\sqrt{3} K (1-K) \mu - (1+K+K^2) \rho \right] \\ & - 2 \left(\frac{t_1 L}{t_2 - t_1} \right) \bar{I}_1 - \left(\frac{t_1 L}{t_2 - t_1} \right)^2 \bar{I}_0 \end{aligned}$$

where

$$\tau = \log \frac{at_2^2 + bt_2 + c}{at_1^2 + bt_1 + c}$$

$$\rho = \log \left(\frac{at_2^2 + bt_2 + c \left[(1-K)t_1 + Kk \right]^2}{at_1^2 + bt_1 + c \left[(1-K)t_2 + Kk \right]^2} \right)$$

$$\mu = \tan^{-1} \left(\frac{2at_2 + b}{\sqrt{3} Kk} \right) - \tan^{-1} \left(\frac{2at_1 + b}{\sqrt{3} Kk} \right)$$

and

$$a = 1 + K + K^2 \quad b = - Kk (1 + 2K) \quad c = K^2k^2$$

k = total flange depth

$$K = \left(\frac{g}{b} \right)^{1/3} \text{ where } g = b - \text{total web thickness}$$

The axial stiffness matrix may be calculated similarly by noting that the cross sectional area may be written as;

$$A_x = 2bh_f + h_w (t_1 + \phi x - 2h_f)$$

which upon rearranging gives

$$A_x = \phi_1 + \phi_2 x \quad \dots\dots\dots(6.26)$$

where

$$\phi_1 = 2bh_f + h_w t_1 - 2h_f h_w$$

$$\phi_2 = h_w \phi$$

Hence performing integration as in previous section gives;

$$\bar{A}_0 = \frac{1}{\phi_2} \left[\ln \left(\frac{\phi_1 + \phi_2 L}{\phi_1} \right) \right]$$

It can be noted that this formulation applies also to the box section where h_w represents the combined thickness of the webs.

6.1.5. Formulation of Stiffness Matrix for a General Shape of Section.

The analysis given in (6.1.4) will now be developed to enable the stiffness matrix for any idealised section to be obtained. The construction of the values of \bar{A}_0 , \bar{I}_0 , \bar{I}_1 , and \bar{I}_2 for shapes other than those of the simplest geometrical form can become extremely tedious. Even the I-section as seen above, one of the most common of structural forms, exhibits a high complexity of analysis (41).

Because of this it is considered practical to use an approximation to the true form by assuming that the variation of the section properties (39) may be expressed as

$$A_x = A_1 (1 + \phi x)^m \dots\dots\dots(6.25a)$$

$$I_x = I_1 (1 + \phi x)^n \dots\dots\dots(6.25b)$$

where A_1, I_1 are the cross-sectional and second moment of area at node 1 and;

$$\phi = \frac{(t_2 - t_1)}{t_1 L}$$

where t_1, t_2 are the section depths at nodes 1 and 2 respectively, assuming linear variation of depth.

The form of equation (6.25) is thus seen to be the same as that for the rectangular section. The exponents m and n can be found from the conditions at node 2 where x equals L . Thus

$$A_2 = A_1 \left(1 + \frac{t_2 - t_1}{t_1} \right)^m = A_1 \left(\frac{t_2}{t_1} \right)^m$$

$$I_2 = I_1 \left(1 + \frac{t_2 - t_1}{t_1} \right)^n = I_1 \left(\frac{t_2}{t_1} \right)^n$$

ie

$$\left(\frac{A_2}{A_1} \right) = \left(\frac{t_2}{t_1} \right)^m \quad \text{and} \quad \left(\frac{I_2}{I_1} \right) = \left(\frac{t_2}{t_1} \right)^n$$

Thus

$$m = \frac{\log \left(\frac{A_2}{A_1} \right)}{\log \left(\frac{t_2}{t_1} \right)} \quad \text{and} \quad n = \frac{\log \left(\frac{I_2}{I_1} \right)}{\log \left(\frac{t_2}{t_1} \right)}$$

Using equations (6.25) and performing the necessary integrations gives the values of

A_0, I_0, I_1, I_2 as;

$$A_0 = \frac{L}{A_1 r (1 - m)} \left[\left(\frac{t_2}{t_1} \right)^{1-m} - 1 \right]$$

$$I_0 = \frac{L}{I_1 r (1 - n)} \left[\left(\frac{t_2}{t_1} \right)^{1-n} - 1 \right]$$

$$I_1 = \frac{L^2}{I_1 r^2} \left[\frac{1}{(2-n)} \left(\frac{t_2}{t_1} \right)^{2-n} - \frac{1}{(1-n)} \left(\frac{t_2}{t_1} \right)^{1-n} + \frac{1}{(2-n)(1-n)} \right]$$

$$I_2 = \frac{L^3}{I_1 r^3} \left\{ \frac{1}{(3-n)} \left[\left(\frac{t_2}{t_1} \right)^{3-n} - 1 \right] - \frac{2}{(2-n)} \left[\left(\frac{t_2}{t_1} \right)^{2-n} - 1 \right] + \frac{1}{(1-n)} \left[\left(\frac{t_2}{t_1} \right)^{1-n} - 1 \right] \right\}$$

where

$$r = \phi/L$$

It can be observed that when m equals 1 and n equals 1, 2 or 3 this formulation is invalid due to the infinite nature of some of the terms. These values of exponents correspond to section properties which result in simpler formulations, eg, for m equals 1, n equals 3 the section is one of tapering rectangular form as discussed previously.

It should be noted that all the stiffness matrices developed so far in this chapter pertain to linear behaviour, ie where any axial effects on the flexural behaviour are ignored.

6.2. Formulation of Exact Deflection Function for Non-linear Behaviour.

As already shown in chapter 3, it is in principle possible to derive the exact deflection profiles for a beam from equilibrium considerations. In this section the exact flexural deflection profile for a geometrically non-linear, tapered rectangular section will be derived.

6.2.1. Formation of Lateral Deflection Function.

Consider a non-prismatic rectangular beam of constant breadth b and of depth varying linearly from t_1 to t_2 under an axial compressive force P at both ends.

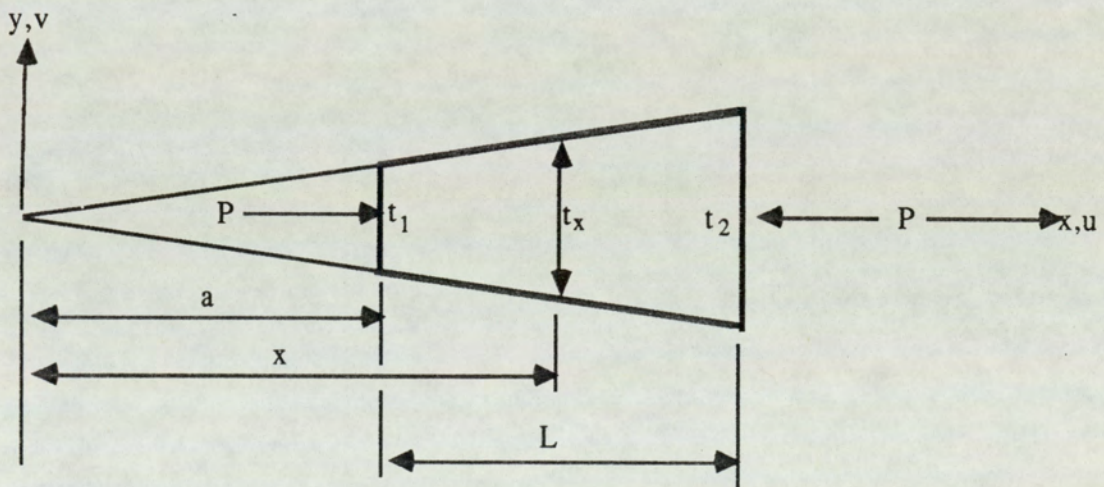


Fig 6.6. Non-prismatic Member Under Axial Loading.

Consider an element of length δx in its deformed state under this compressive load;

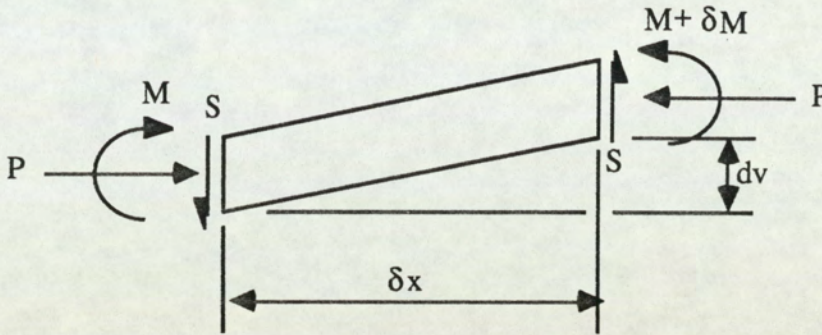


Fig 6.7. Diagram Showing the Element in its Deformed State in Compression.

Rotational equilibrium gives;

$$\frac{dM}{dx} + S + P \frac{dv}{dx} = 0$$

ie

$$S = -\frac{dM}{dx} - P \frac{dv}{dx} \dots\dots\dots(6.27)$$

But S is constant throughout the element and thus;

$$\frac{dS}{dx} = \frac{d^2M}{dx^2} + P \frac{d^2v}{dx^2} = 0$$

Substitution of equation (6.4) gives;

$$\frac{d^4v}{dx^4} + \frac{P}{EI(x)} \frac{d^2v}{dx^2} = 0 \dots\dots\dots(6.28)$$

where the second moment of area $I(x)$ is now a function of x whereas in chapter 3 it was taken as constant.

Letting $q = \frac{d^2v}{dx^2}$ then;

$$\frac{d^2q}{dx^2} + \frac{P}{EI(x)}q = 0 \quad \dots\dots\dots(6.29)$$

But $I(x)$ can be written as;

$$I(x) = \frac{bt_x^3}{12} \quad \dots\dots\dots(6.30)$$

where from fig. 6.6,

$$t_x = t_1 \left(\frac{x}{a} \right)$$

Hence substitution into (6.30) gives;

$$I(x) = \frac{bt_1^3}{12} \left(\frac{x}{a} \right)^3 = I_1 \left(\frac{x}{a} \right)^3$$

Substituting this result into equation (6.29) produces;

$$\frac{d^2q}{dx^2} + \frac{P}{EI_1} \frac{a^3}{x^3}q = 0$$

or

$$\frac{d^2q}{dx^2} + k^2 x^{-3}q = 0 \quad \dots\dots\dots(6.31)$$

where

$$k^2 = \frac{P a^3}{E I_1}$$

The solution of equation (6.31) can be written in terms of Bessel functions (55,56), thus;

$$q = a_3 x^{0.5} J_1(z) + a_4 x^{0.5} Y_1(z) \quad \dots\dots\dots(6.31a)$$

where $z = 2k x^{-0.5}$ and $J_1(z)$ and $Y_1(z)$ are Bessel functions of order one and of the first and second kind respectively which may be written (55,56) as;

$$J_1(z) = \frac{z}{2} \left[1 - \frac{1}{2} \left(\frac{z}{2}\right)^2 + \frac{1}{2!3!} \left(\frac{z}{2}\right)^4 - \frac{1}{3!4!} \left(\frac{z}{2}\right)^6 + \dots \right]$$

$$Y_1(z) = \frac{2}{\pi} \left[\gamma + \log\left(\frac{z}{2}\right) \right] J_1(z) - \frac{2}{\pi z} - \frac{1}{\pi} \left[\frac{z}{2} - \frac{1}{2} \left(\frac{z}{2}\right)^3 (1 + 1 + \frac{1}{2}) \right]$$

$$\left[+ \frac{1}{2!3!} \left(\frac{z}{2}\right)^5 (1 + \frac{1}{2} + 1 + \frac{1}{2} + \frac{1}{2}) - \frac{1}{3!4!} \left(\frac{z}{2}\right)^7 (1 + \frac{1}{2} + \frac{1}{2} + 1 + \frac{1}{2} + \frac{1}{2} + \frac{1}{4}) + \dots \right]$$

γ being Euler's constant (0.5772.....)

Double integration of equation (6.31a) will yield the lateral deflection profile as;

$$w = a_1 + a_2x + a_3F_1(x) + a_4F_2(x) \dots\dots\dots(6.32)$$

It is apparent that continuation of this process, although in principle able to produce a precise stiffness matrix, is practically not viable owing to the complexities involved and the approximations that would occur due to curtailment of the series.

A more fruitful avenue to pursue is thus one based on work processes in which approximate but simpler deflection functions are used. The relevant procedures have already been described in chapter 3 with regard to prismatic beams, the results there being obtained via the linear prismatic deflection functions. It would appear logical, therefore, when applying the work methods to non-prismatic beams, to base the derivations on the linear non-prismatic functions. As for the prismatic sections, two stiffness matrices will be developed, the first assuming that the axial force is independent of the flexural deformations, and the second taking the effects of flexural deformations on the axial forces into account, a procedure that leads to the tangential stiffness matrix.

6.3. Formulation of Non-linear Stiffness Matrix with Mutually Independent Flexural and Axial Components.

As described in Chapter 3 the effect of geometrical non-linearity assuming that the axial forces do not depend on the flexural deformations can be studied by simply adding the initial stress matrix $[K_\sigma]$ to the flexural stiffness matrix.

Using the flexural and axial deflection functions for a general non-prismatic beam, that is;

$$v = a_1 + a_2x + a_3 \int \int \frac{1}{I(x)} dx dx + a_4 \int \int \frac{x}{I(x)} dx dx \quad \dots\dots\dots(6.7)$$

$$u = a_5 + a_6 \int \frac{1}{A(x)} dx \quad \dots\dots\dots(6.20)$$

the flexural, axial, and initial stress matrices can be computed.

The flexural and axial matrices have already been presented in sections (6.1.1) and (6.1.2). It thus only remains to determine the initial stress matrix. Two sections will be considered, firstly the rectangular section and secondly the general section in which the section properties are represented by power functions.

6.3.1. Rectangular Section.

The form of the initial stress matrix $[K_\sigma]$ has already been given in chapter 3 as;

$$[K_\sigma] = \int_0^L [G]^T P [G] dx \quad \dots\dots\dots(6.33)$$

where $[G]$ is found from the lateral deflection function.

Differentiation of the deflection function for v (equation 6.7) gives the slope θ as

$$\theta = \frac{dv}{dx} = a_2 + a_3 \int \frac{1}{I(x)} dx + a_4 \int \frac{x}{I(x)} dx \quad \dots\dots\dots(6.34)$$

which can be written more compactly as

$$\theta = [0 \ 1 \ f(x) \ g(x)] \{a_b\} \quad \dots\dots\dots(6.35)$$

For a rectangular section

$$I(x) = \frac{b}{12} (t_1 + \phi x)^3$$

where here $\phi = \frac{t_2 - t_1}{L}$ and hence

$$f(x) = \int \frac{1}{I(x)} dx = \frac{-6}{b\phi (t_1 + \phi x)^2}$$

and

$$\begin{aligned} g(x) &= \int \frac{x}{I(x)} dx = \left(\frac{6 t_1}{b\phi^2 (t_1 + \phi x)^2} - \frac{12}{b\phi^2 (t_1 + \phi x)} \right) \\ &= \frac{-6 (t_1 + 2\phi x)}{b\phi^2 (t_1 + \phi x)^2} \quad \dots\dots\dots(6.36) \end{aligned}$$

Multiplication of (6.35) by $[C_b]^{-1}$ (equation 6.10) produces

$$\theta = \begin{bmatrix} \overline{G}_1 & G_2 & G_3 & \overline{G}_4 \end{bmatrix} \begin{Bmatrix} v_1 \\ \theta_1 \\ v_2 \\ \theta_2 \end{Bmatrix} \dots\dots\dots(6.37)$$

ie $[G]\{\Delta_b\}$

where the four elements of $[G]$ are of the form

$$G_m = C_{2m} + f(x) C_{3m} + g(x) C_{4m}$$

Thus an element of $[K_\sigma]$ which may be written as

$$K_{\sigma_{mn}} = P \int_0^L G_m G_n dx$$

becomes after substitution of G_m and G_n ;

$$K_{\sigma_{mn}} = P \int_0^L \left\{ C_{2m}C_{2n} + f(x) (C_{2m}C_{3n} + C_{2n}C_{3m}) + f(x)^2 C_{3m}C_{3n} \right. \\ \left. + g(x) (C_{3m}C_{4n} + C_{3n}C_{4m}) + f(x)g(x) (C_{3m}C_{4n} + C_{3n}C_{4m}) \right. \\ \left. + g(x)^2 C_{4m}C_{4n} \right\} dx \dots\dots\dots(6.38)$$

Hence $[K_\sigma]$ can be incorporated using a simple routine and the non-linear stiffness matrix $[K]$ formulated to produce the matrix equations

$$\{P\} = [K] \{\Delta\} = \begin{bmatrix} - & - & K_a & | & - & - & 0 & - & - \\ & & 0 & | & & & K_0 + K_\sigma & & \end{bmatrix} \begin{Bmatrix} \Delta_a \\ \Delta_b \end{Bmatrix} \dots\dots\dots(6.39)$$

It should be noted that as before this matrix is symmetrical about the leading diagonal. Also as before $[K_a]$ and $[K_0]$ are the matrices due to linear behaviour developed in section (6.1) above.

6.3.2. General Section (Power Function).

As shown in previous sections the second moment of area of any section may be conveniently expressed by the approximation;

$$I(x) = I_1 (1 + \phi x)^n$$

where n is dependent on the shape of the cross-section. Using this second moment of area in the derivation of $[K_\sigma]$, the same result is obtained as equation (6.38) above except that $f(x)$ and $g(x)$ are given as;

$$f(x) = \frac{(1 + \phi x)^{1-n}}{I_1 \phi (1-n)}$$

$$g(x) = \frac{(1 + \phi x)^{2n}}{I_1 \phi (2-n)} - \frac{(1 + \phi x)^{1-n}}{I_1 \phi (1-n)}$$

The results are valid for all values of n except for n = 1,2 and 3 as discussed previously.

6.4. Non-linear Stiffness Matrix with Coupled Flexural and Axial Components
(Tangential Stiffness Matrix).

As demonstrated for prismatic beams, a more accurate assessment of non-linear behaviour is attained by use of the expression for axial strain

$$\epsilon_a = \frac{du}{dx} + \frac{1}{2} \left(\frac{dv}{dx} \right)^2$$

where the second term is the component due to lateral deflections. This extra expression leads to further stiffness coefficients which will add on to the existing expressions shown in equation (6.39) above.

6.4.1. Relationship Between Strains and Nodal Displacements.

Again writing the lateral and axial displacement functions as;

$$v = a_1 + a_2 x + a_3 \int \int \frac{1}{I(x)} dx dx + a_4 \int \int \frac{x}{I(x)} dx dx \dots\dots\dots(6.7)$$

$$u = a_5 + a_6 \int \frac{1}{A(x)} dx \quad \dots\dots\dots(6.20)$$

and the values of the axial and flexural strains as;

$$\epsilon_a = \frac{du}{dx} + \frac{1}{2} \left(\frac{dv}{dx} \right)^2$$

$$\epsilon_b = \frac{d^2v}{dx^2}$$

and by following a similar procedure as before and formulating $[C]^{-1}$ the slope can again be written as

$$\frac{dv}{dx} = [G_1 \ G_2 \ G_3 \ G_4] \{ \Delta_b \} = [G] \{ \Delta_b \}$$

where

$$G_m = C_{2m} + f(x) C_{3m} + g(x) C_{4m}$$

and the strain/displacement relationships as;

$$\begin{Bmatrix} \epsilon_a \\ \epsilon_b \end{Bmatrix} = \begin{bmatrix} \frac{1}{2} \frac{dv}{dx} G_1 & \frac{1}{2} \frac{dv}{dx} G_2 & \frac{1}{2} \frac{dv}{dx} G_3 & \frac{1}{2} \frac{dv}{dx} G_4 & \frac{-1}{m A(x)} & \frac{1}{m A(x)} \\ \frac{C_{31} + xC_{41}}{I(x)} & \frac{C_{32} + xC_{42}}{I(x)} & \frac{C_{33} + xC_{43}}{I(x)} & \frac{C_{34} + xC_{44}}{I(x)} & 0 & 0 \end{bmatrix} \begin{Bmatrix} v_1 \\ \theta_1 \\ v_2 \\ \theta_2 \\ u_1 \\ u_2 \end{Bmatrix}$$

$$\{ \epsilon \} = [B(\Delta)] \{ \Delta \}$$

where

$$m = \frac{L \ln \left(\frac{t_2}{t_1} \right)}{b (t_2 - t_1)}$$

for a rectangular section.

6.4.2. Relationship Between Stress Resultants and Strains.

The relationship between the stresses and strains is given by the expression;

$$\{\sigma\} = [D]\{\epsilon\}$$

where

$$[D] = \begin{bmatrix} E A_x & 0 \\ 0 & E I_x \end{bmatrix}$$

It can be noted that $[D]$ is now a function of x and not constant as in chapter 3.

6.4.3. Formulation of Tangential Stiffness Matrix.

From section (3.2), and using the nomenclature described there,

$$[K_L] = [K_1] + [K_1]^T + [K_2]$$

where

$$[K_1] = \int_0^L [B_0]^T [D] [B_L] dx$$

$$[K_2] = \int_0^L [B_L]^T [D] [B_L] dx$$

and

$$[B_0] = \begin{bmatrix} 0 & 0 & 0 & 0 & \frac{-1}{m A(x)} & \frac{1}{m A(x)} \\ \frac{C_{31} + xC_{41}}{I(x)} & \frac{C_{32} + xC_{42}}{I(x)} & \frac{C_{33} + xC_{43}}{I(x)} & \frac{C_{34} + xC_{44}}{I(x)} & 0 & 0 \end{bmatrix}$$

$$[B_L] = \begin{bmatrix} \frac{1}{2} \frac{dv}{dx} G_1 & \frac{1}{2} \frac{dv}{dx} G_2 & \frac{1}{2} \frac{dv}{dx} G_3 & \frac{1}{2} \frac{dv}{dx} G_4 & 0 & 0 \\ 0 & 0 & 0 & 0 & 0 & 0 \end{bmatrix}$$

6.4.3.1. Evaluation of [K_L].

Substitution of the constituent matrices [B₀], [D] and [B_L] and subsequent integration yields the matrices [K₁] and [K₂] as;

$$[K_1] = \begin{array}{c} \left[\begin{array}{cc|cccc} 0 & 0 & -A1 & -A2 & -A3 & -A4 \\ 0 & 0 & A1 & A2 & A3 & A4 \\ \hline 0 & 0 & 0 & 0 & 0 & 0 \\ 0 & 0 & 0 & 0 & 0 & 0 \\ 0 & 0 & 0 & 0 & 0 & 0 \\ 0 & 0 & 0 & 0 & 0 & 0 \end{array} \right] \end{array} \quad \dots\dots\dots(6.40)$$

where

$$A_N = \frac{E}{m} \int_0^L \left\{ \begin{array}{l} (C_{2n} + g(x)C_{3n} + f(x)C_{4n}) a_2 \\ + (g(x)C_{2n} + g(x)^2 C_{3n} + f(x)g(x)C_{4n}) a_3 \\ + (f(x)C_{2n} + f(x)g(x)C_{3n} + f(x)^2 C_{4n}) a_4 \end{array} \right\} dx$$

and

$$[K_2] = \begin{bmatrix} 0 & & & & & & & \\ 0 & 0 & & & & & & \\ \hline 0 & 0 & B_{11} & & & & & \\ 0 & 0 & B_{21} & B_{22} & & & & \\ 0 & 0 & B_{31} & B_{32} & B_{33} & & & \\ 0 & 0 & B_{41} & B_{42} & B_{43} & B_{44} & & \end{bmatrix} \quad \text{.....(6.41)}$$

S Y M

where

$$B_{mn} = \int_0^L E A_x \theta^2 G_m G_n dx$$

which upon expansion yields;

$$B_{mn} = E \int_0^L \left\{ b t_x \left(\gamma_1 + f(x) \gamma_2 + g(x) \gamma_3 + f(x)^2 \gamma_4 + f(x) g(x) \gamma_5 + g(x)^2 \gamma_6 \right) a_2^2 \right. \\ + 2 f(x) b t_x \left(\gamma_1 + f(x) \gamma_2 + g(x) \gamma_3 + f(x)^2 \gamma_4 + f(x) g(x) \gamma_5 + g(x)^2 \gamma_6 \right) a_2 a_3 \\ + 2 g(x) b t_x \left(\gamma_1 + f(x) \gamma_2 + g(x) \gamma_3 + f(x)^2 \gamma_4 + f(x) g(x) \gamma_5 + g(x)^2 \gamma_6 \right) a_2 a_4 \\ + f(x)^2 b t_x \left(\gamma_1 + f(x) \gamma_2 + g(x) \gamma_3 + f(x)^2 \gamma_4 + f(x) g(x) \gamma_5 + g(x)^2 \gamma_6 \right) a_3^2 \\ \left. + g(x)^2 b t_x \left(\gamma_1 + f(x) \gamma_2 + g(x) \gamma_3 + f(x)^2 \gamma_4 + f(x) g(x) \gamma_5 + g(x)^2 \gamma_6 \right) a_4^2 \right\} dx$$

where

$$t_x = (t_1 + \phi x)$$

$$\gamma_1 = C_{2m} C_{2n}$$

$$\gamma_2 = (C_{2m} C_{3n} + C_{2n} C_{3m})$$

$$\gamma_3 = (C_{2m} C_{4n} + C_{2n} C_{4m})$$

$$\gamma_4 = C_{3m} C_{3n}$$

$$\gamma_5 = (C_{3m} C_{4n} + C_{3n} C_{4m})$$

$$\gamma_6 = C_{4m} C_{4n}$$

and $f(x)$ and $g(x)$ are given above.

As can be seen the expression is very complex in nature and further integration is tedious and intractable.

Chapter 7.

**Treatment of Non-Nodal and
Distributed Loading.**

To formulate the equivalent nodal loads for a non-prismatic section, a similar procedure is followed to that shown in Chapter 5. Again two common examples will be discussed, ie, the inter joint loading and the uniformly distributed load.

Although already presented in Chapter 5, the two results obtained for the point loading and the UDL are rewritten below, ie;

$$\{P\} = \{ [N][C]^{-1} \}^T \dots\dots\dots(7.1)$$

for a unit inter-joint point load and

$$\{P\} = p \int_0^L \{ [N][C]^{-1} \}^T dx \dots\dots\dots(7.2)$$

for a uniformly distributed load p per unit length.

Also as only the linear flexural deflection profile is being used it is this which is employed in the determination of the equivalent nodal loadings, ie;

$$v_x = a_1 + a_2x + a_3 \int \int \frac{1}{I(x)} dx dx + a_4 \int \int \frac{x}{I(x)} dx dx \dots\dots\dots(7.3)$$

or

$$v_x = \begin{bmatrix} 1 & x & f(x) & g(x) \end{bmatrix} \begin{Bmatrix} a_1 \\ a_2 \\ a_3 \\ a_4 \end{Bmatrix}$$

$$= [N]\{a_b\} = [N][C_b]^{-1}\{\Delta\}$$

7.1. Point load.

Evaluation of equation (7.1) produces;

$$\{P\} = \begin{Bmatrix} S_1 \\ M_1 \\ S_2 \\ M_2 \end{Bmatrix} = \begin{Bmatrix} C_{11} + C_{21}x + C_{31} R_1(x) + C_{41} R_2(x) \\ C_{12} + C_{22}x + C_{32} R_1(x) + C_{42} R_2(x) \\ C_{13} + C_{23}x + C_{33} R_1(x) + C_{43} R_2(x) \\ C_{14} + C_{24}x + C_{34} R_1(x) + C_{44} R_2(x) \end{Bmatrix} \dots\dots\dots(7.4)$$

where $R_1(x) = \int \int \frac{1}{I(x)} dx dx$, $R_2(x) = \int \int \frac{x}{I(x)} dx dx$

and $I(x) = \frac{b}{12} (t_1 + \phi x)^3$ for rectangular section and $I_1 (1 + \phi x)^n$ for the general

power series respectively, the values of ϕ taking on their respective values.

7.2. Uniformly Distributed Loading.

Evaluation of equation (7.2) gives;

$$\{P\} = \begin{Bmatrix} S_1 \\ M_1 \\ S_2 \\ M_2 \end{Bmatrix} = \begin{Bmatrix} x C_{11} + (x^2/2) C_{21} + C_{31} R_1'(x) + C_{41} R_2'(x) \\ x C_{12} + (x^2/2) C_{22} + C_{32} R_1'(x) + C_{42} R_2'(x) \\ x C_{13} + (x^2/2) C_{23} + C_{33} R_1'(x) + C_{43} R_2'(x) \\ x C_{14} + (x^2/2) C_{24} + C_{34} R_1'(x) + C_{44} R_2'(x) \end{Bmatrix} \begin{matrix} L \\ \\ \\ 0 \end{matrix} \dots\dots\dots(7.5)$$

where $R_1'(x) = \int \int \int R_1(x) dx$ and $R_2'(x) = \int \int \int R_2(x) dx$ and $I(x)$ is the same as in section (7.1) above.

PART C.

**Results, Discussions
and Conclusions.**

Chapter 8.

Experimental Verifications.

In this section the results obtained from the several stiffness matrices developed in previous chapters will be compared and the experimental work carried out to assess their veracity presented. Also, in the theoretical analyses, several examples will be given to show the versatility of the programs developed and their application to practice.

However before this, a brief discussion on experimental methodology and the objectives of the experimental work will be presented.

8.1. Description of Experimental Work.

8.1.1. Experimental Objectives.

In the literature survey, no detailed experimental work on the non-linear behaviour of frames was found, especially on those incorporating tapered elements. It was thus necessary to perform structural tests in order to assess the accuracy of the theoretical solutions obtained.

There were two objectives to be considered in the experimental techniques employed;

- a). Measurement of relatively large non-linear deflections with a minimum application of loading.
- b). Measurement of surface strains for calculating the moments and axial forces induced in the framework.

After some consideration a frame was designed which would fit the above objectives and produce a significant amount of deformation without excessive loading and also a reasonable difference between linear and non-linear behaviour. For consistency three frames of prismatic and three frames of non-prismatic members were constructed and the dimensions are given below in fig. 8.1.

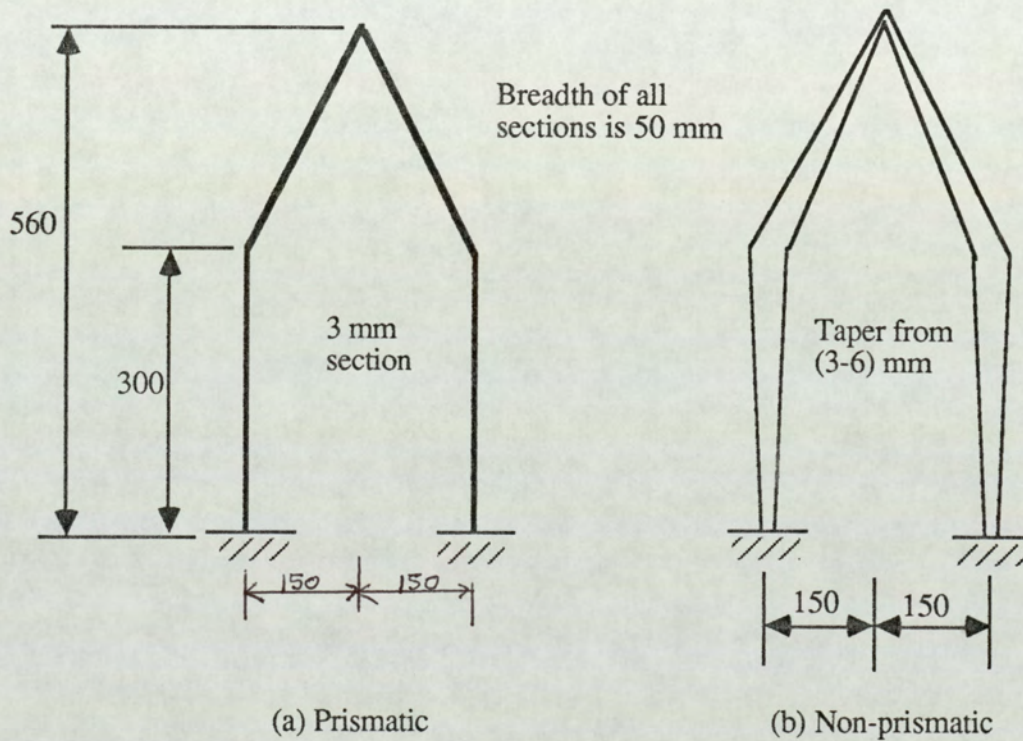


Fig. 8.1. Diagram of the two Experimental Frames Considered

The frames were constructed from (50 x 3) and (50 x 6) mild steel sections, the (50 x 6) being machined down linearly to 3mm to produce the taper. Both frameworks were welded using standard techniques and complete working drawings are presented in appendix 4. Mild steel was chosen as the material of the frames since it is linearly elastic over a wide loading range and also because of its negligible creep characteristics at ambient temperatures.

8.1.2. Determination of Elasticity Modulus (E).

To obtain a satisfactory correlation between the theoretical and experimental results it was necessary to measure the value of Young's Modulus for the material. This was done firstly by use of the arrangement shown in fig 8.2 and Plate 8.1 and secondly by the standard (57) tensile test. The first test, fig 8.2, consists of a specimen of mild steel from which the frames were constructed, of length 1m and of rectangular section (50 x 6), resting on knife edge supports and loaded by means of dead weights. The central deflections were recorded with a dial gauge of 100 divisions per mm.

Hence using the four point bending test, and by measuring the load against the central deflection of the beam, the modulus of elasticity can be evaluated.

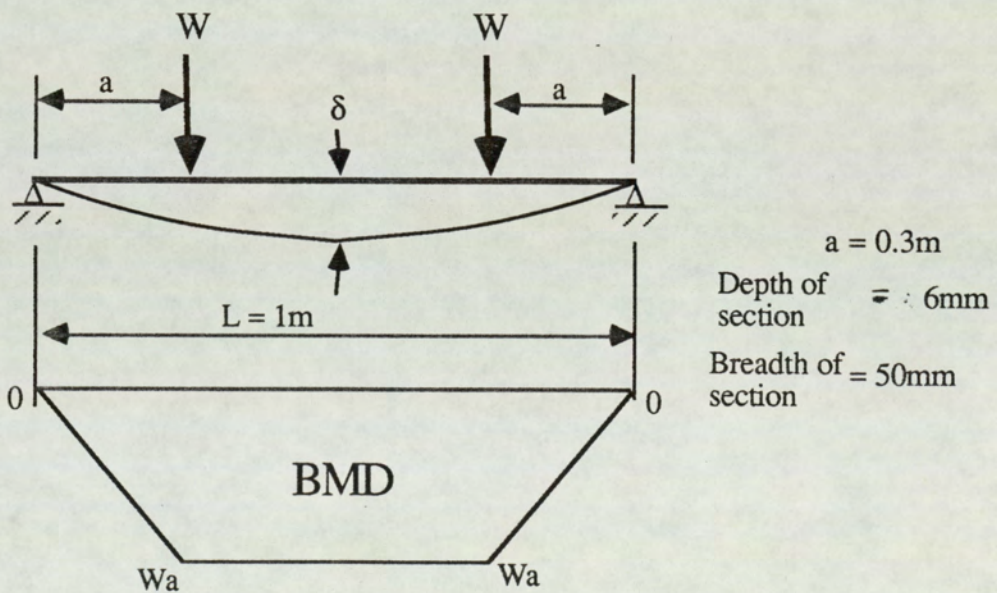


Fig 8.2. Four Point Bending Test for Determination of Young's Modulus.

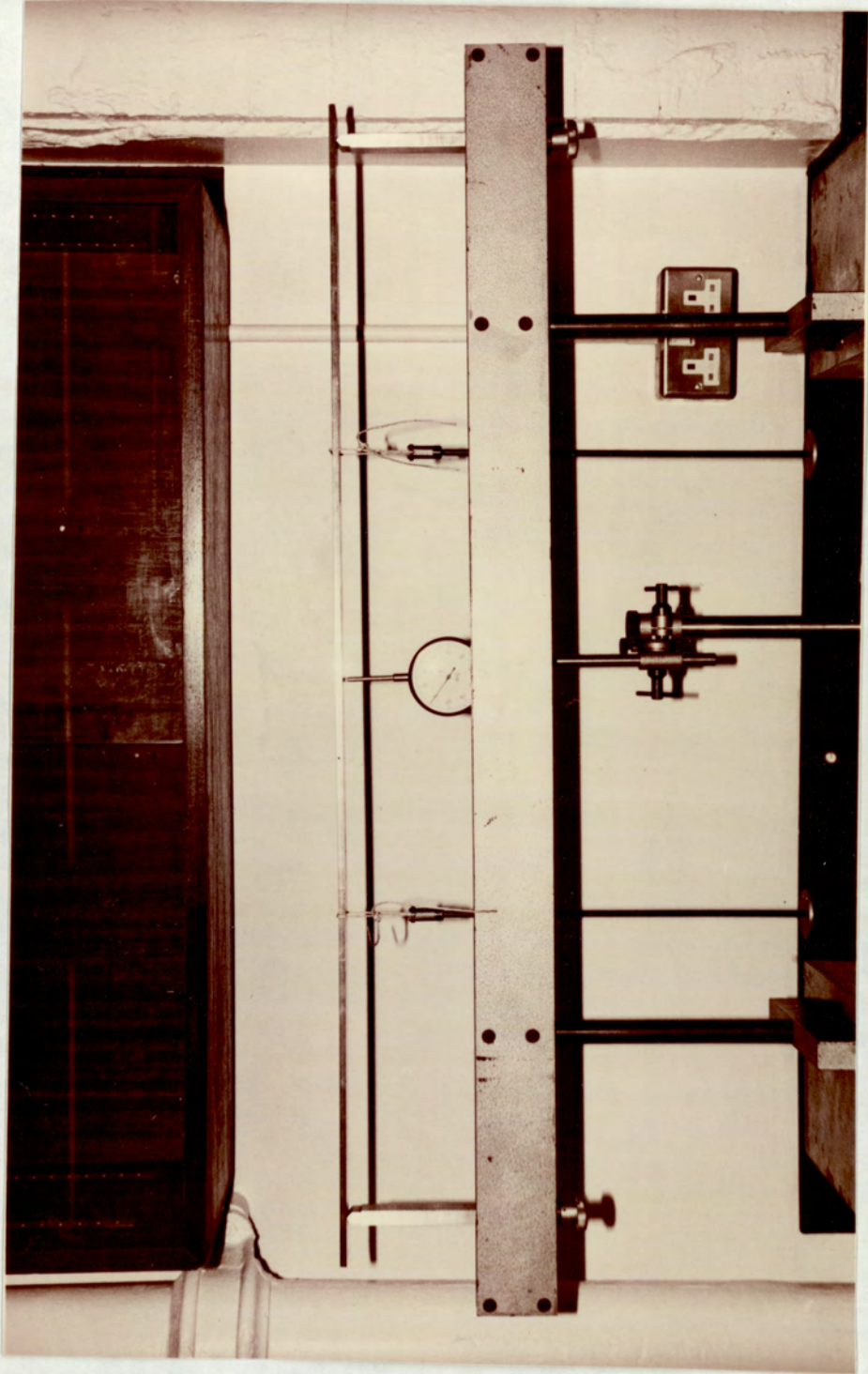


Plate. 8.1. The Four Point Bending test apparatus.

Application of Macauley's Method (2) gives the result;

$$\chi = \frac{W}{\delta} = \frac{8 EI}{a L^2}$$

where W is the magnitude of each of the point loads and δ is the central deflection.

Hence

$$E = \frac{\chi a L^2}{8 I} \dots\dots\dots(8.1)$$

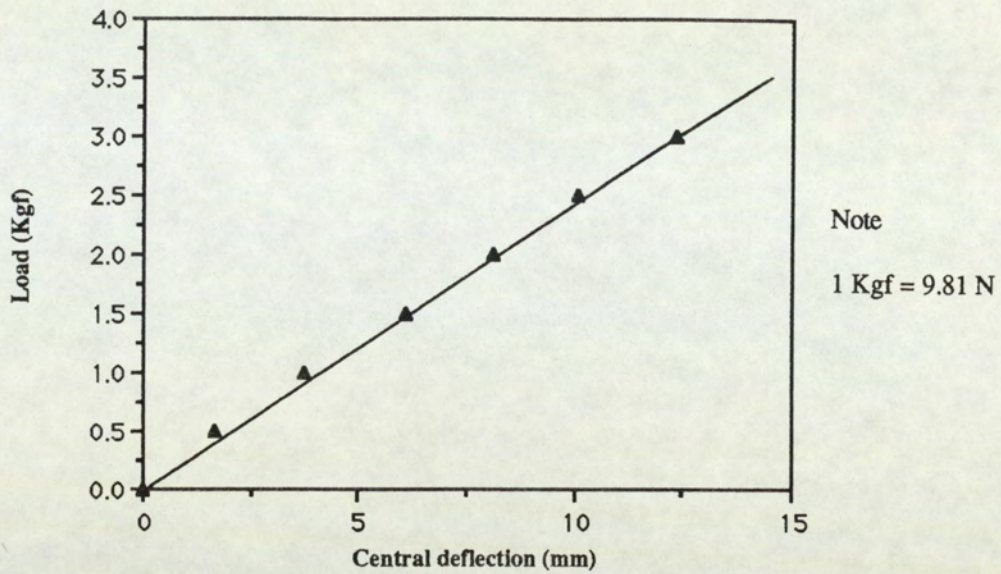
Thus the modulus of elasticity can be determined by evaluating the gradient (χ) of the load against deflection graph.

8.1.2.1. Flexural Results for material of Prismatic Section.

LOAD (Kgf) W	0.5	1.0	1.5	2.0	2.5	3.0
δ (mm)	1.648	3.73	6.064	8.126	10.11	12.38

NB To convert Kgf to N, multiply Kgf by 9.81

Table 8.1. Table of Load and Deflection for Prismatic Frame Material.



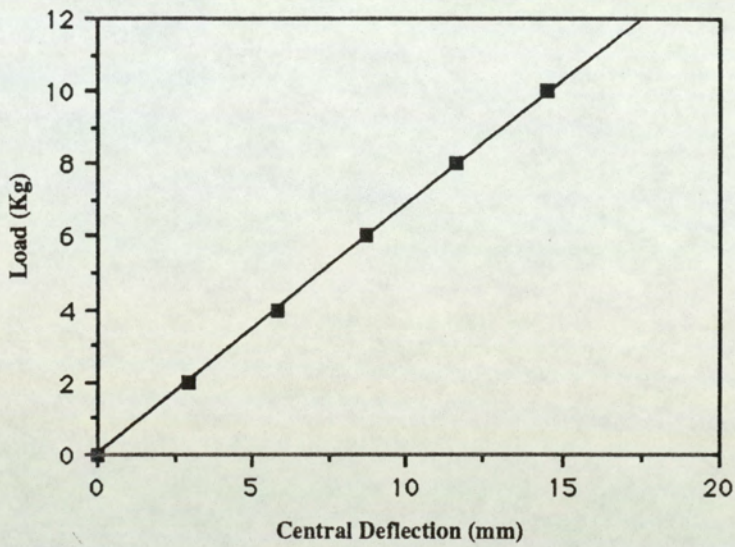
Graph 8.1. Load v Central Deflection for Prismatic Frame Material.

Use of equation (8.1) and the gradient of the straight line graph above gives
 $E = 223 \text{ KN/mm}^2$.

8.1.2.2. Flexural Results for material of non-prismatic Section.

LOAD (Kg) W	0	2.0	4.0	6.0	8.0	10.0
δ (mm)	0	2.90	5.85	8.76	11.63	14.52

Table 8.2. Table of Load and Deflection for Non-prismatic Beam Material.



Graph 8.2. Load v Central Deflection for Non-prismatic Frame Material.

Evaluation of equation (8.1) gives $E = 240 \text{ KN/mm}^2$.

8.1.2.3. Tensile Results for material Specimens.

Similarly the standard tensile test, to BS118, was carried out to evaluate the stress/strain characteristics of the material and to find the lower and upper yield stresses. The design and drawings of the specimens are presented in Appendix 4.

	PRISMATIC FRAME MATERIAL	NON-PRISMATIC FRAME MATERIAL
Upper yield Stress.N/mm ²	279.5	274.8
Lower yield Stress.N/mm ²	263.4	257.6
Modulus of Elasticity.KN/mm ²	232.3	245.7

Table 8.3. Results from the Tensile Tests of steel specimens.

Because of the very small difference between the values of Young's Modulus obtained from the tensile and flexural tests, the values obtained from the flexural tests were used in the theoretical analyses.

8.1.3. Method of Testing.

Before testing the frames several FLA-3-11, electrical resistance strain gauges of 3mm length were attached to both faces of salient members of the framework. Due to the symmetry of the frames, strain gauges were fixed on only one half of the framework and the layout of the gauges is shown in fig 8.3.

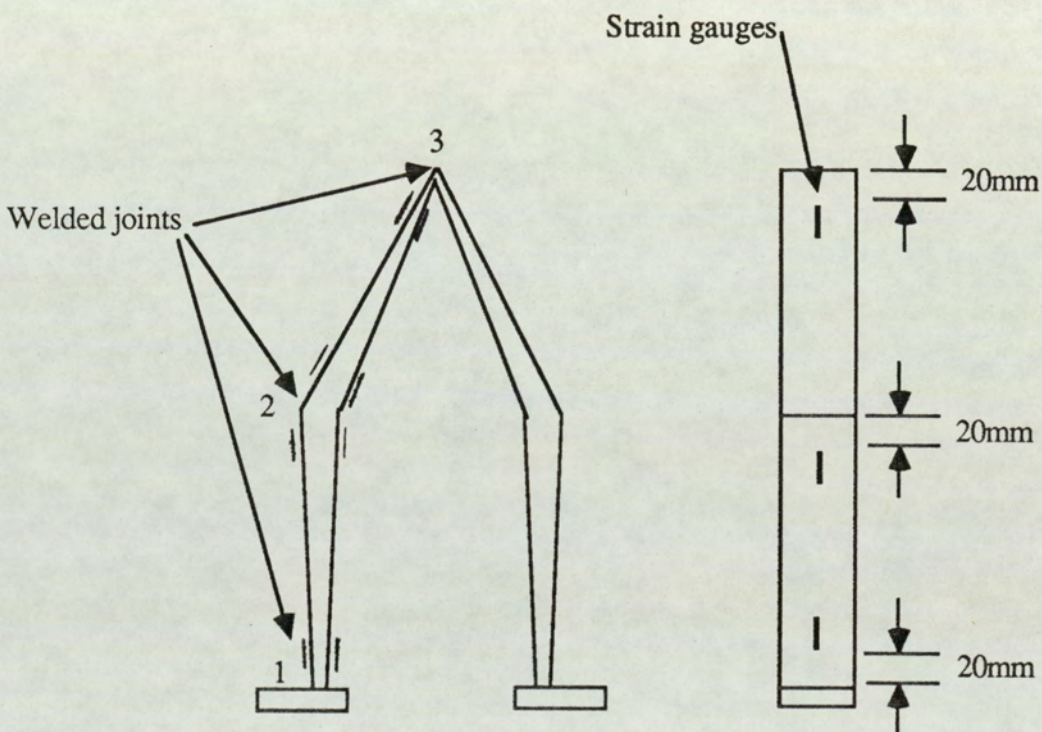


Fig. 8.3. Strain Gauge Positioning.

All strain gauges were fixed 20mm from the welded joints, a distance considered sufficient so that any effects caused by the welding could be assumed to be negligible.

A special rig was designed onto which the frameworks could be bolted at the base to prevent any movement whilst testing, as shown in fig 8.4.

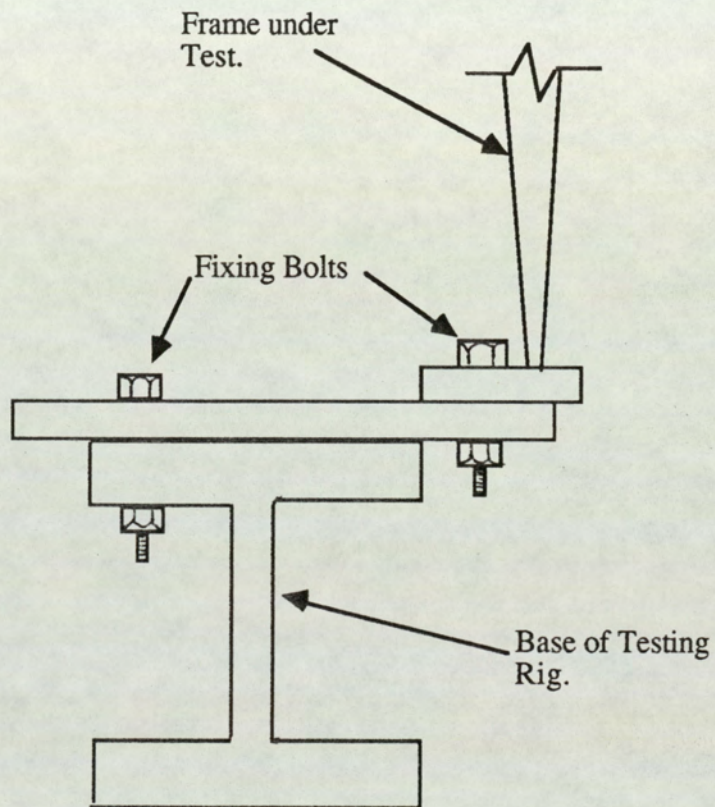


Fig. 8.4. Method of fixing of Test Frames to base of Rig.

This was considered to represent complete fixity of the supports.

The framework was loaded vertically downwards at the apex using a hydraulic ram. To ensure accurate load readings, a calibrated proving ring was employed and this was fixed to the ram to prevent movement during testing. Also, to enable the load to be applied along the apex, a steel capping piece was placed on the crown of the framework as shown in fig 8.5.

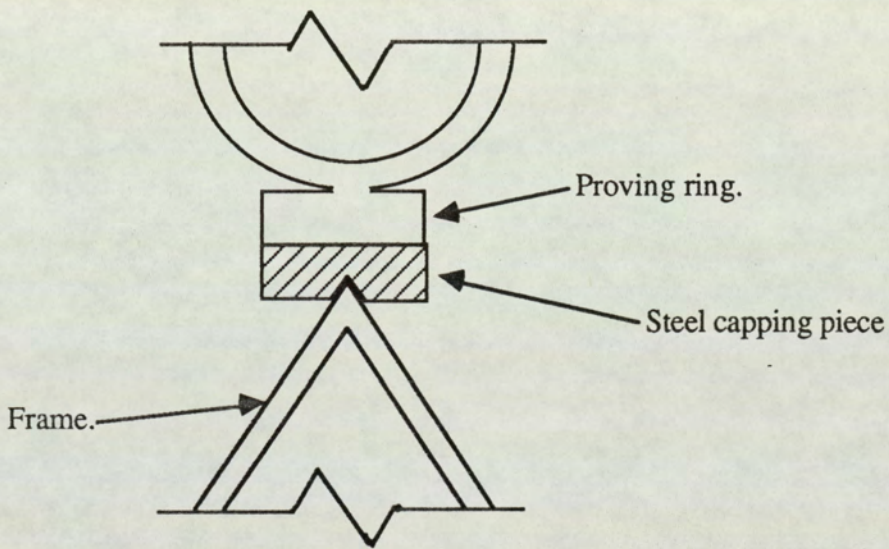


Fig 8.5. Diagram showing method of load application.

This prevented any movement of the hydraulic ram during loading and also enabled apex loading to be accurately attained (Plate 8.2).

The load was applied in 200N increments and deflections produced by the loading were measured using standard deflection dial gauges (100 divisions per mm), these being considered adequate for the accuracy required in the testing. The deflection gauges were

placed at the three joints as shown in Fig 8.6 below.

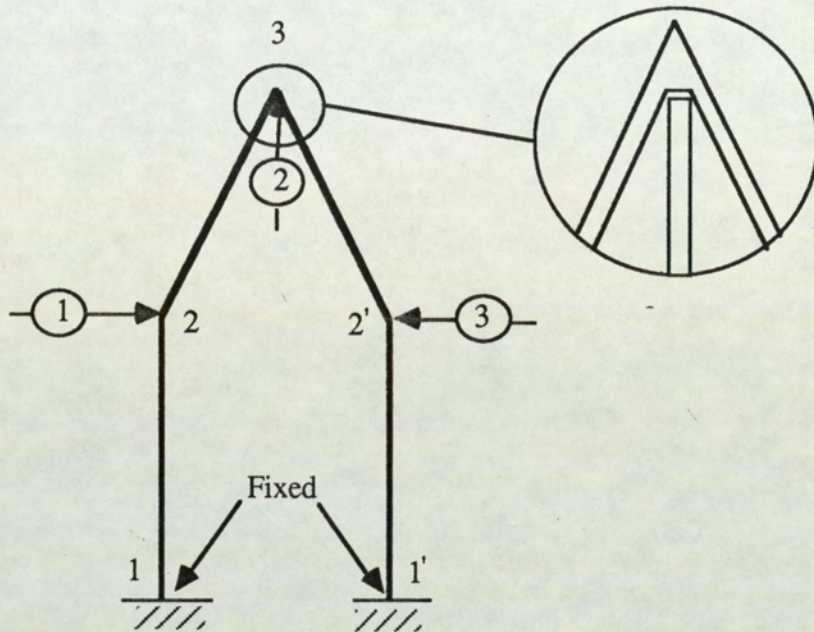


Fig. 8.6. Showing Positioning of Dial Gauges.

Plate 8.2 shows the complete arrangement of the apparatus with the strain recorder and extension box.

The bending moments at the points of application of the strain gauges were obtained from the strain gauge readings in the following manner.

Consider two gauges a, b, either side of a section of depth d. The strains, ϵ , in each of these gauges will be produced from a combination of axial strain and flexural strain and

hence the results can be expressed as

$$\epsilon_a = \epsilon_{axial} + \epsilon_{flexure}$$

$$\epsilon_b = \epsilon_{axial} - \epsilon_{flexure}$$

from which $\epsilon_{flexure}$ can be isolated.

Now using the results from the simple bending theory, namely

$$\epsilon_{flexure} = \frac{d}{2R} \quad \text{and} \quad \frac{M}{I} = \frac{E}{R}$$

it follows that the bending moment M can be expressed as;

$$M = \frac{2EI}{d} \epsilon_{flexure}$$

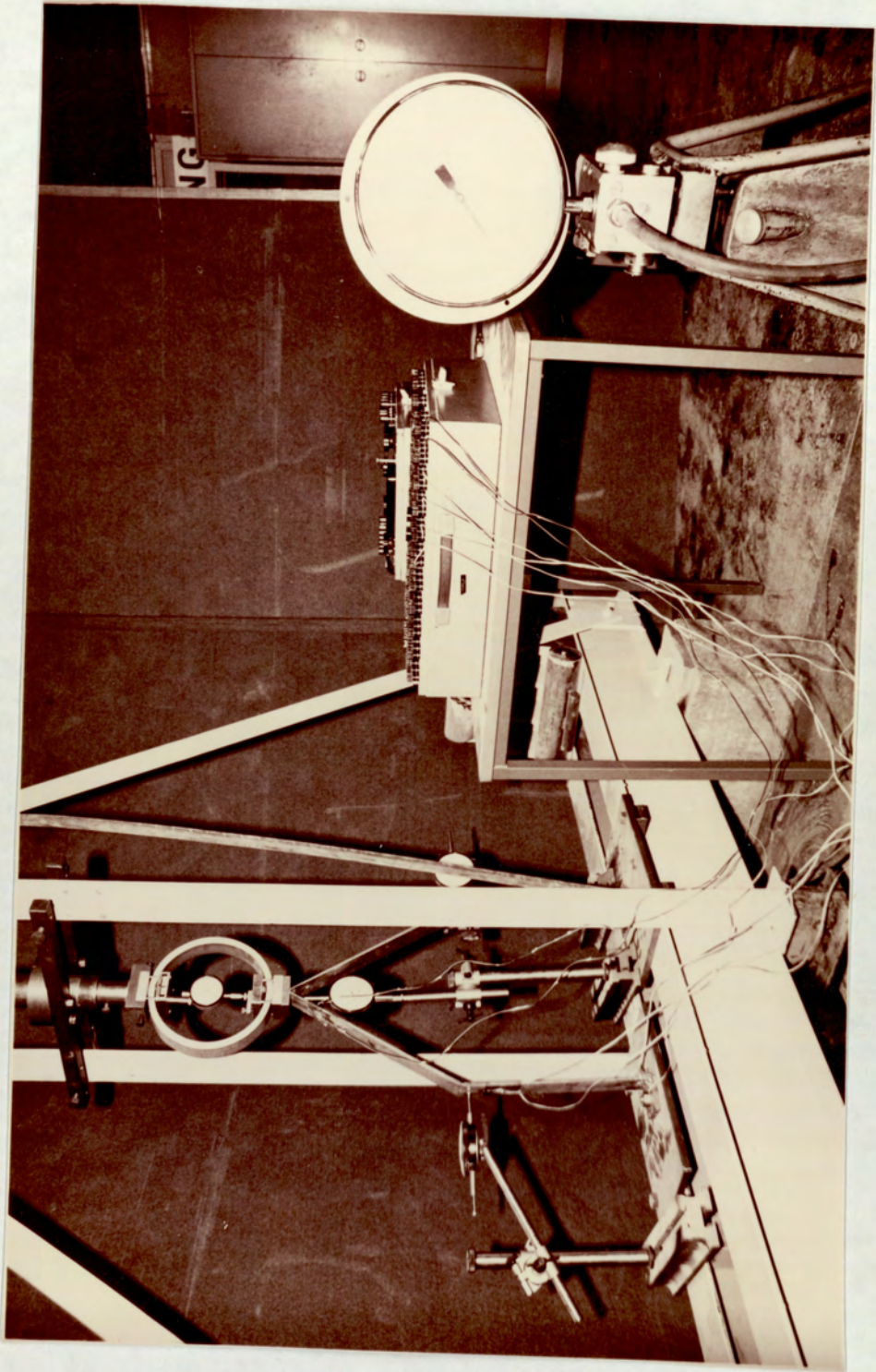


Plate 8.2. Arrangement of Apparatus with Strain Recorder.

The results obtained for deflections and bending moments will be presented separately for the prismatic and non-prismatic sections to facilitate ease of reading, the terminology used in previous chapters being simplified as follows for ease of understanding of the results:-

Linear (L) = the analysis where the effect of axial force on flexural action is ignored.

Constant Axial Force (CAF) = the analysis where the effects of the axial forces on the flexure are considered but where the axial & flexural matrices are independent of each other and are obtained from equilibrium considerations.

Tangential (T) = the tangential stiffness matrix in which the effects of axial forces and large deflections are incorporated in an approximate work process.

Coupled (C) = the refined stiffness matrix obtained from equilibrium considerations in which the axial effect is dependent on flexural action (coupled) due to large deflections.

$$\text{Axial strain given by } \varepsilon_a = \frac{du}{dx} + \frac{1}{2} \left(\frac{dv}{dx} \right)^2$$

Stepped = used for non-prismatic frame only. The non-prismatic member is Coupled (SC) represented by a number of prismatic portions. Analysis is by the 'coupling' (C) procedure above.

(E) = Experimental Results.

8.2. Prismatic Frame Results.

The results from the various theoretical analyses are compared with those obtained from experiment, these being shown in figs 8.8 to 8.12.

It can be noted that the results from the coupled (C) and Tangential (T) matrices are indistinguishable on the graph and hence for comparison the results are shown in Table 8.4 and 8.5.

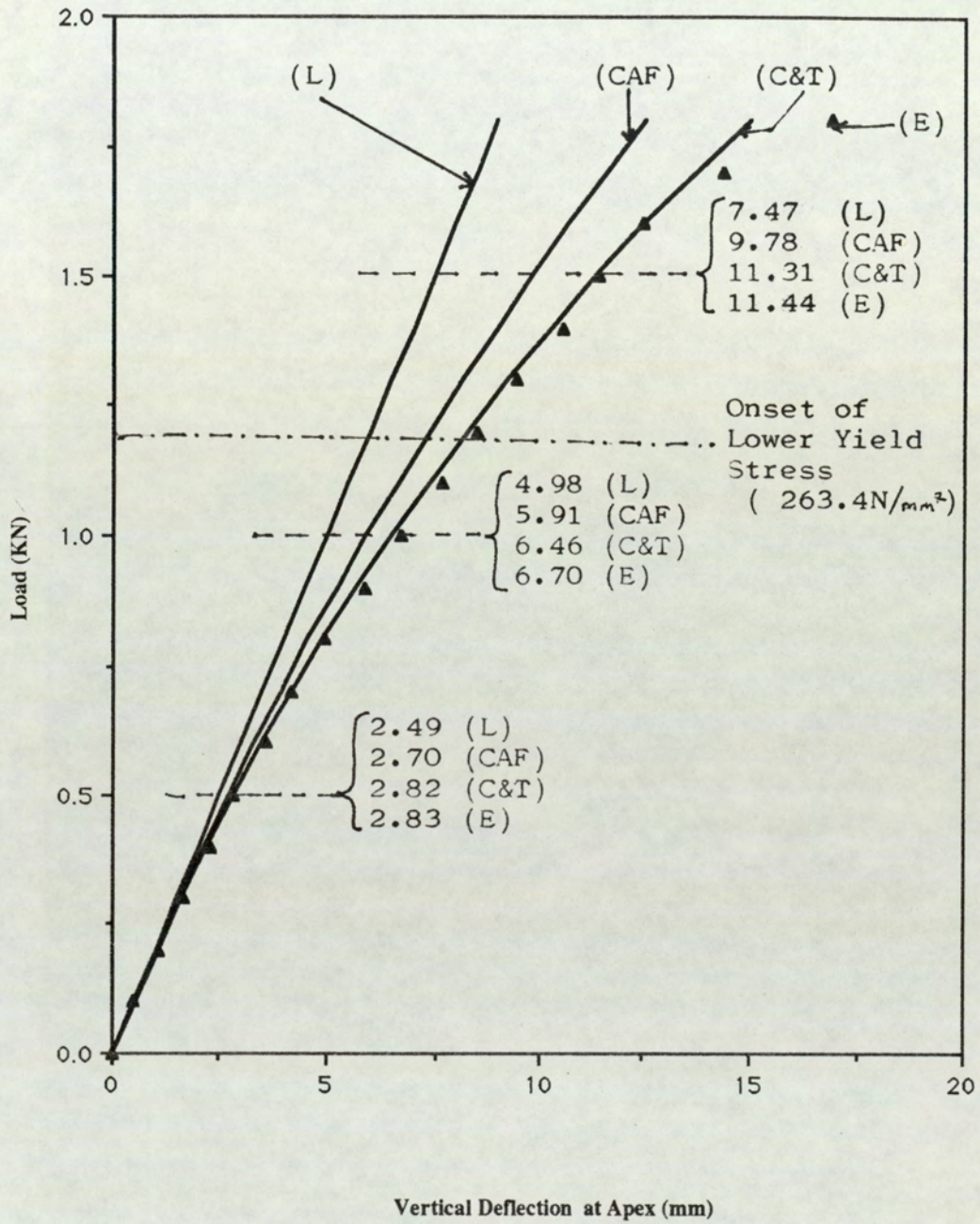
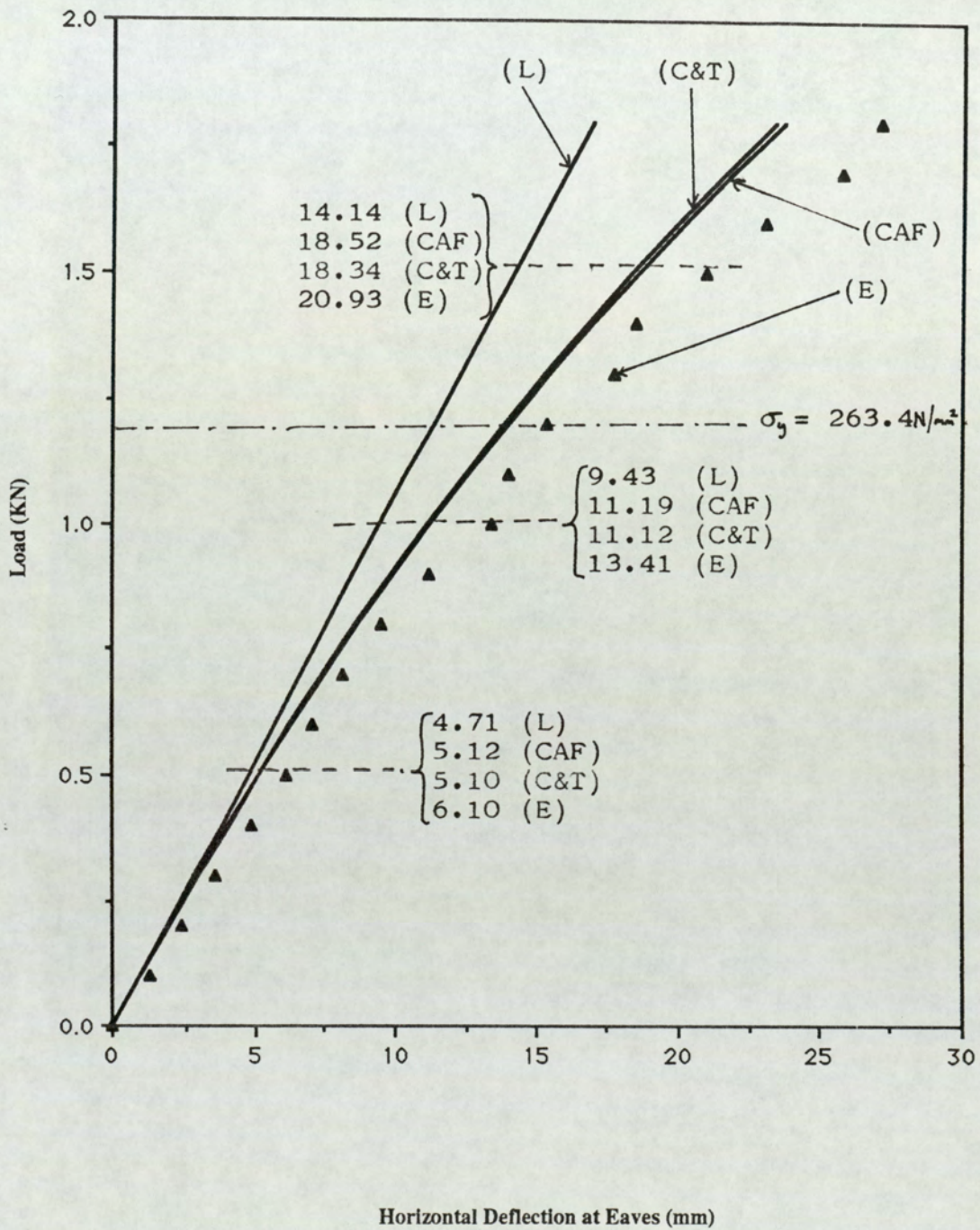


Fig 8.8. Load/Deflection for Frame composed of Prismatic Sections



(Experimental results presented are the average of readings of dial gauges 1 & 3)

Fig 8.9. Load/Deflection for Frame composed of Prismatic Sections

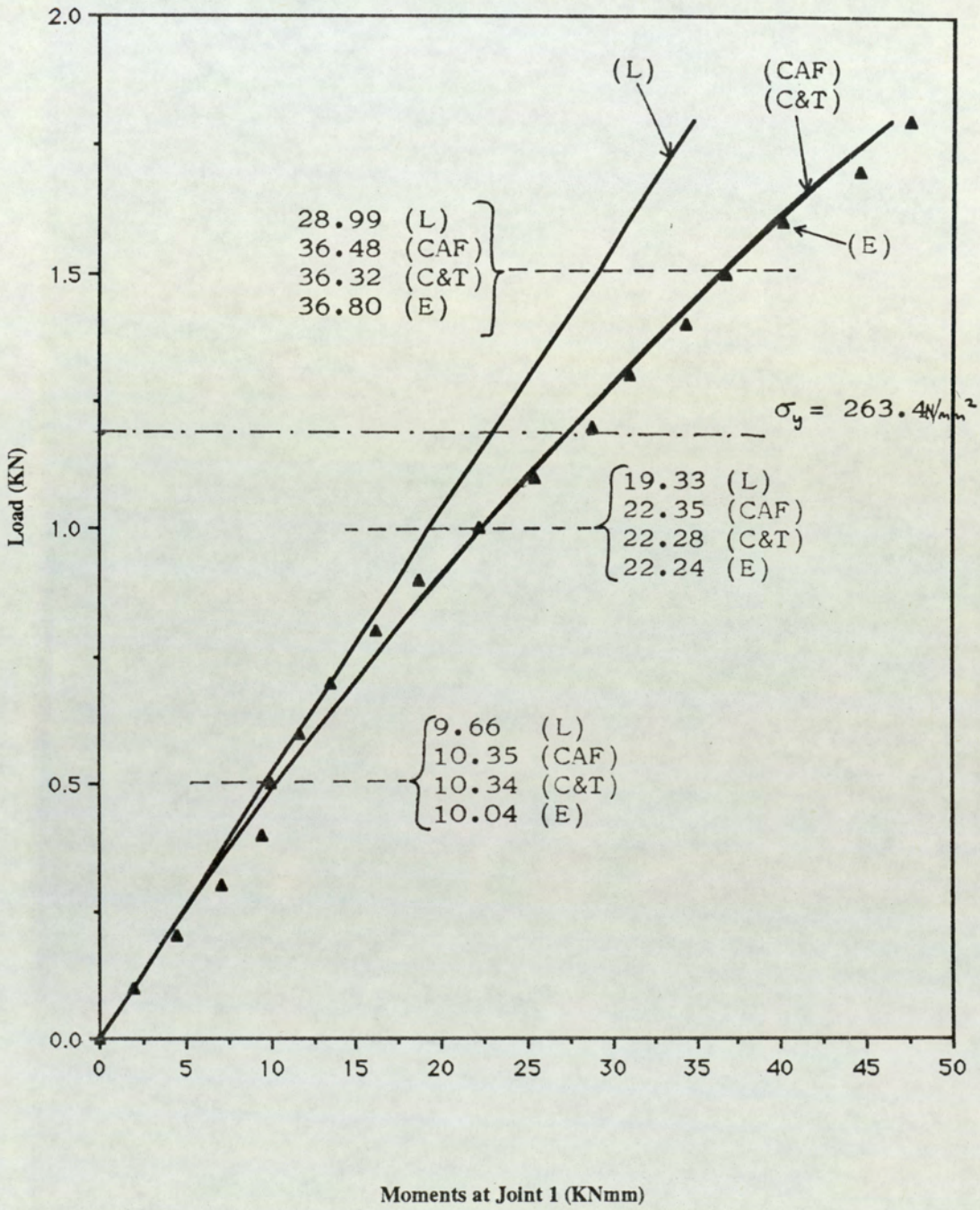


Fig 8.10. Load/Moment at Joint 1 for Prismatic Frame

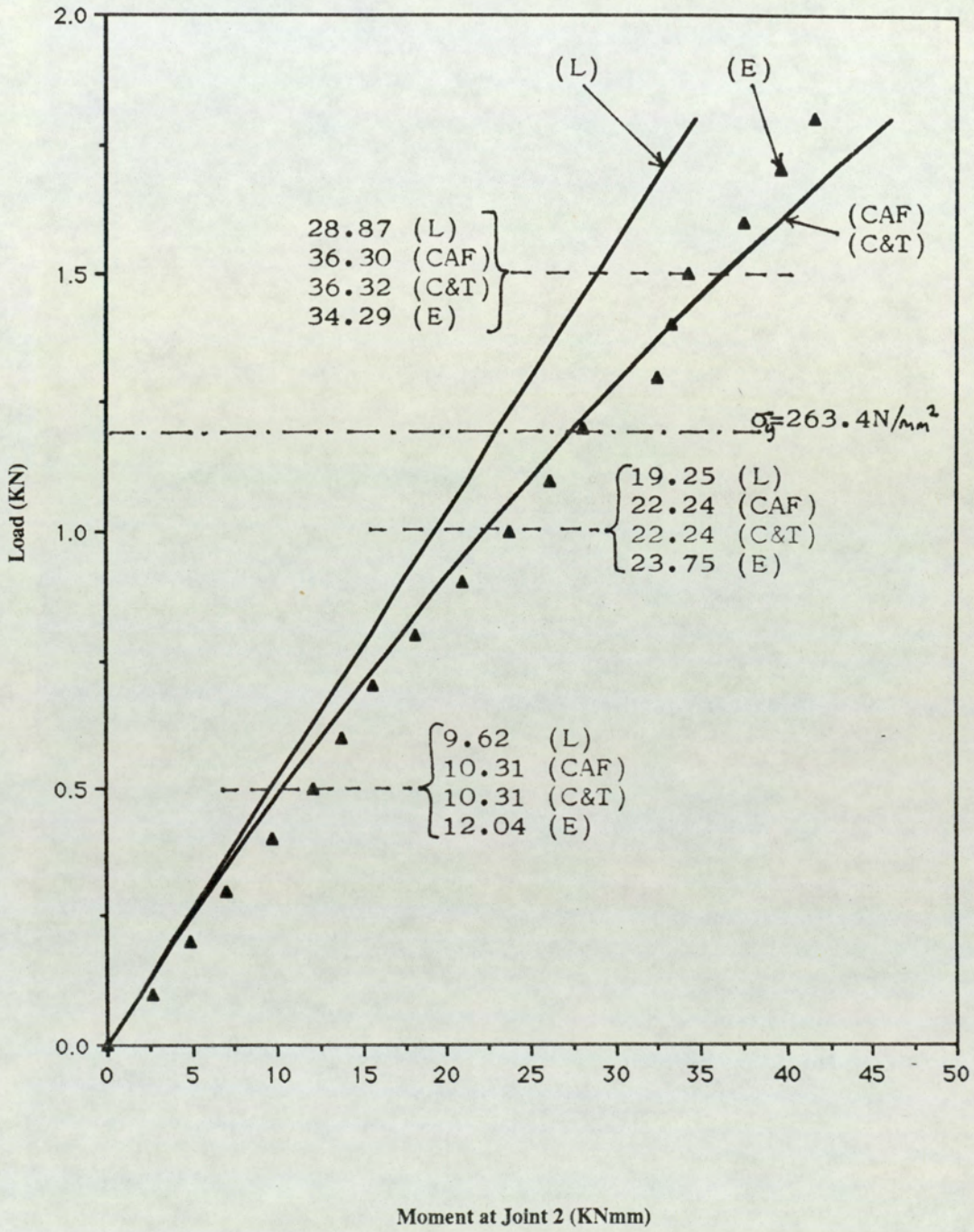


Fig 8.11. Load/Moment at Joint 2 for Prismatic Section

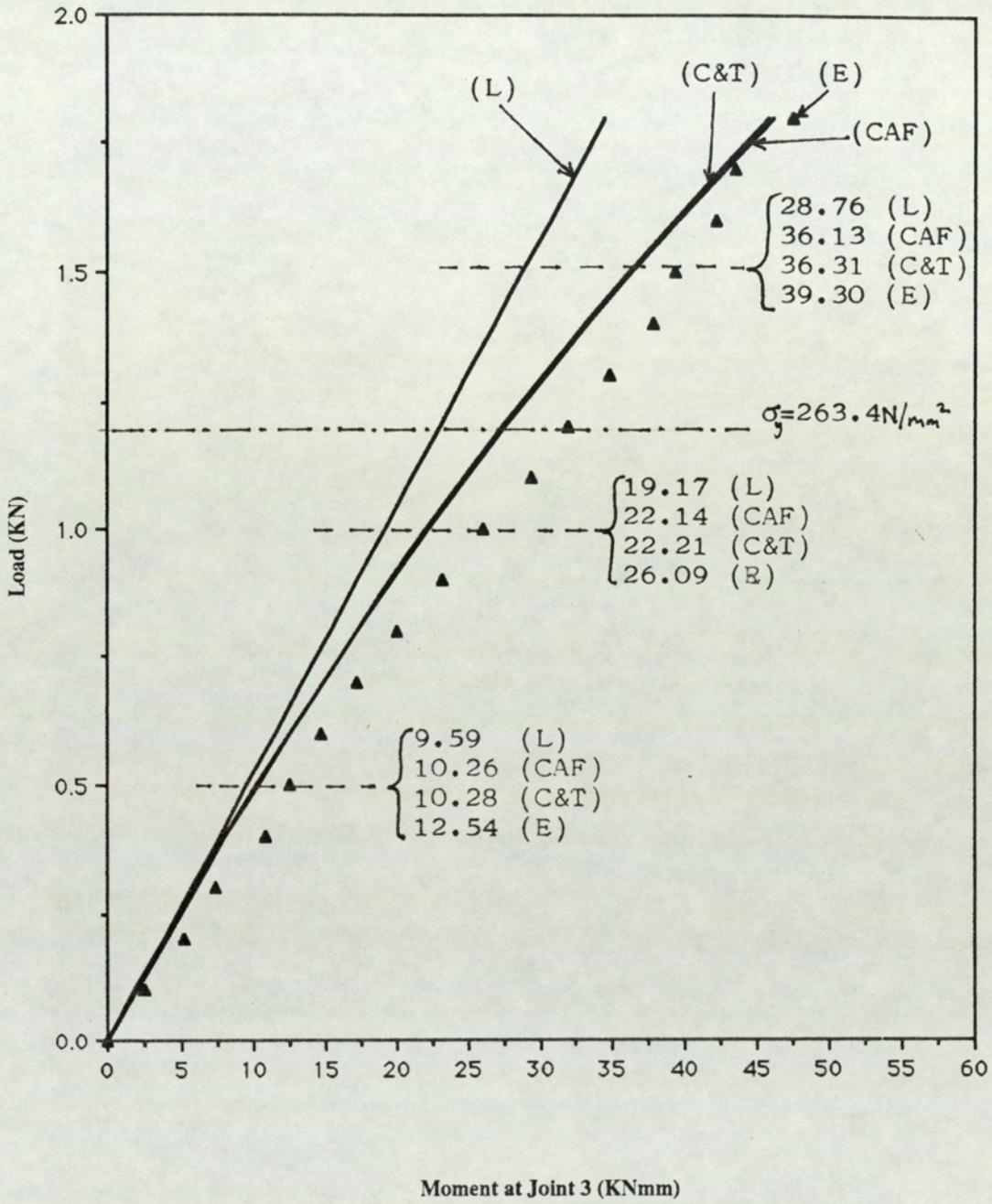


Fig 8.12. Load/Moment at Joint 3 for Prismatic Frame

LOAD (KN)	Vertical deflection (mm)	Horizontal deflection (mm)	Moment at joint 1 (KNmm)	Moment at joint 2 (KNmm)	Moment at joint 3 (KNmm)
0	0	0	0	0	0
0.2	1.0453	1.9452	3.97	3.95	3.94
0.4	2.1976	4.0166	8.16	8.13	8.10
0.6	3.4723	6.2255	12.59	12.55	12.52
0.8	4.8882	8.5911	17.29	17.25	17.21
1.0	6.4659	11.1246	22.28	22.24	22.21
1.2	8.2337	13.8437	27.62	27.59	27.55
1.4	10.2219	16.7821	33.32	33.30	33.28
1.6	12.4688	19.9511	39.45	39.45	39.45
1.8	15.0274	21.6441	46.30	46.10	46.13

Table 8.4 Tabulated Results for the Coupled Stiffness Matrix.

LOAD (KN)	Vertical deflection (mm)	Horizontal deflection (mm)	Moment at joint 1 (KNmm)	Moment at joint 2 (KNmm)	Moment at joint 3 (KNmm)
0	0	0	0	0	0
0.2	1.0450	1.9474	3.97	3.95	3.94
0.4	2.1969	4.0260	8.17	8.13	8.10
0.6	3.4715	6.2486	12.61	12.53	12.50
0.8	4.8862	8.6330	17.32	17.24	17.17
1.0	6.4645	11.1949	22.35	22.24	22.14
1.2	8.2310	13.9533	27.71	27.58	27.45
1.4	10.2182	16.9432	33.46	33.29	33.13
1.6	12.4642	20.1896	39.63	39.42	39.25
1.8	15.0220	23.4005	46.36	46.06	45.84

Table 8.5.Tabulated Results for the Tangential Stiffness Matrix.

8.2.1. Discussion.

In the simple geometrically - linear analyses in which the effect of axial force on lateral behaviour is ignored and the deflections may be considered to tend to zero, the load/deflection and load/bending moment relationships are represented by straight lines. The flexural displacement function describing such behaviour is given by the cubic polynomial.

$$v = a_1 + a_2x + a_3x^2 + a_4x^3$$

On considering the effect of axial force on lateral behaviour, equilibrium considerations produce the lateral deflection functions

$$v = a_1 + a_2x + a_3 \sin \alpha x + a_4 \cos \alpha x$$

for a member in compression and

$$v = a_1 + a_2x + a_3 \sinh \alpha x + a_4 \cosh \alpha x$$

for member in tension where

$$\alpha = \sqrt{(P/EI)}$$

The use of these deflection functions produces flexural stiffness matrices which are functions of the axial forces in the member. Examination of figures 8.8 and 8.9 show the deviation from the linear results that occurs on consideration of axial effects on flexure. It is seen, in particular from fig 8.8, that the use of the coupled (C) formulation agrees most closely with the experimental deflections and that the use of the simpler constant axial force (CAP) matrix can significantly underestimate the deflections produced.

Use of the tangential stiffness matrix (T) produced results comparable with the coupled (C) matrix without any member subdivision. However whereas the coupled (C) matrix required only one iteration to give acceptable results, the tangential stiffness matrix required about ten iterations for convergence, and hence the coupled (C) formulation appears to produce a more economical solution with respect to computer time.

Comparison of results for bending moment (Fig 8.10 to 8.12) showed very little difference between the various non-linear matrices used although there was substantial agreement with the experimental values. These results suggest that alteration of the axial strain produces little change in the curvature expression.

Although the elastic critical load can be computed this is probably only of theoretical interest. In reality the frame would have begun to exhibit plasticity at loads substantially below the elastic critical and thereafter would not be conforming to the assumption of material elastic behaviour. Based on the experimentally-determined value of the lower yield stress it was found that the first plastic hinge should form at a load of 0.85KN and that plastic collapse occurred at a load of 1.8KN, a value far below the elastic critical load of 2.9KN as computed from the coupled (C) matrix. It is seen that if indeed plasticity commenced at 0.85KN, the effect on deflections is small, although some limit to the moment capacity appears to be intimated at joint 2 and 3 (fig 8.11 and 8.12) in the region of this load.

8.3. Tapered Section Results.

It was shown in chapter 6, that the exact derivation of the non-linear deflection function involved Bessel functions and was hence discontinued. Similarly the tangential stiffness matrix for the tapered section, which should produce results similar to those for the coupled matrix, was unwieldy and considered capable of producing significant rounding errors. A simpler technique was to approximate the tapered beam by sub-division into several prismatic elemental steps. This will enable the use of the coupled (C) matrix already developed and hence the accurate investigation of the geometrically non-linear behaviour of non-prismatic sections.

To estimate the number of prismatic elements that would adequately represent a tapered section, a tapered cantilever was linearly analysed exactly and by using a stepped procedure. From figure 8.13 below, it can be seen that the accuracy increases with increase in the number of prismatic elements employed.

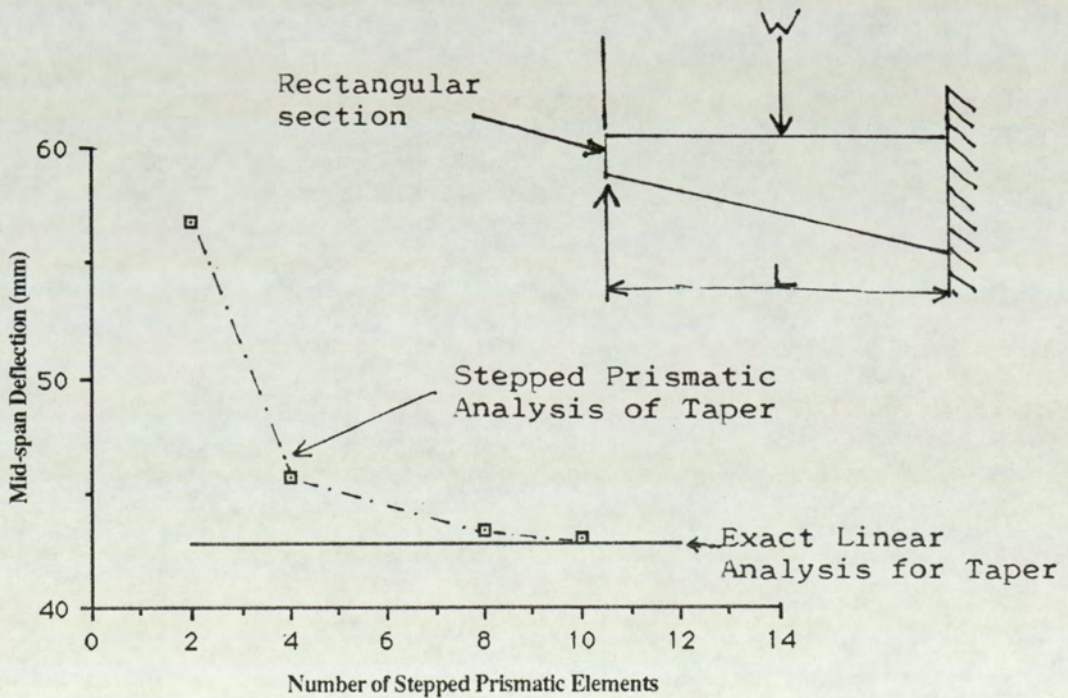


Fig 8.13. Showing Increasing Accuracy with Number of Elements Employed

It is seen that using ten elements per member will produce an adequate result.

The theoretical and experimental results obtained for the tapered frame are presented in figs 8.14 to 8.18, the theoretical results for non-linear behaviour being obtained from the constant axial force matrix derived from the linear deflection function for a tapered member and from the stepped prismatic technique discussed above.

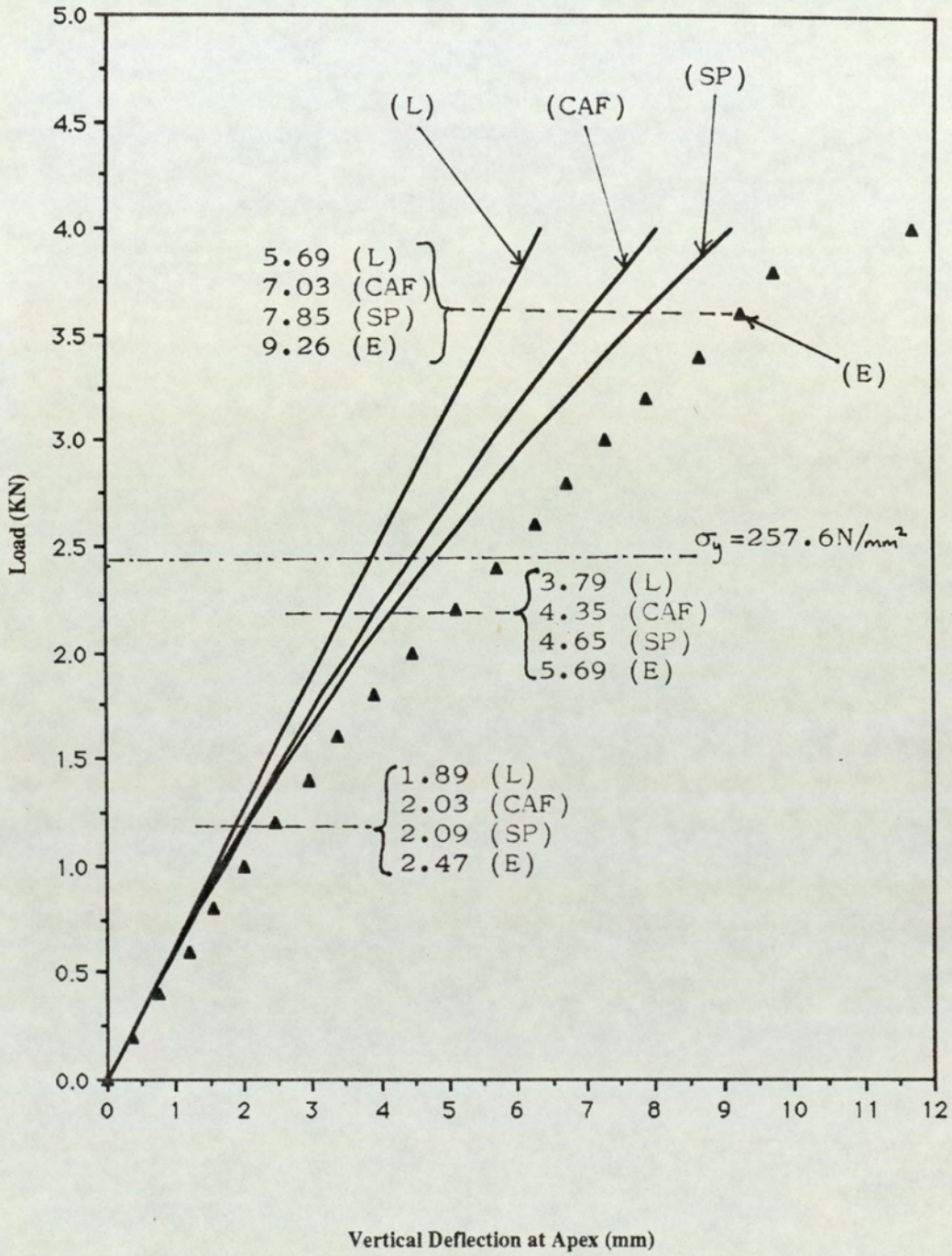
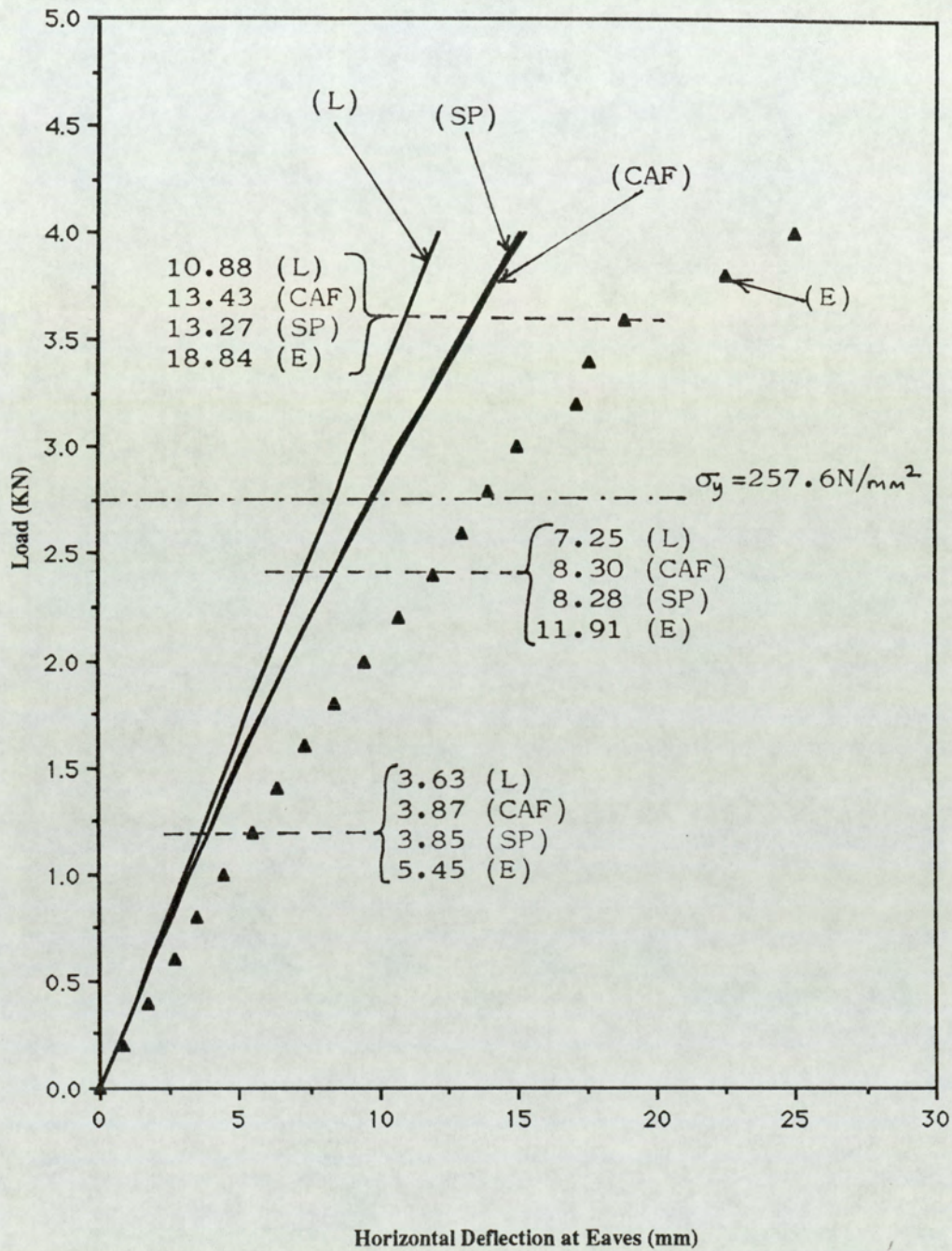


FIG 8.14. Load/Deflection for Frame composed of Tapered Sections



(Experimental results presented are the average of readings of dial gauges 1 & 3)

FIG 8.15. Load/Deflection for Frame composed of Tapered Sections

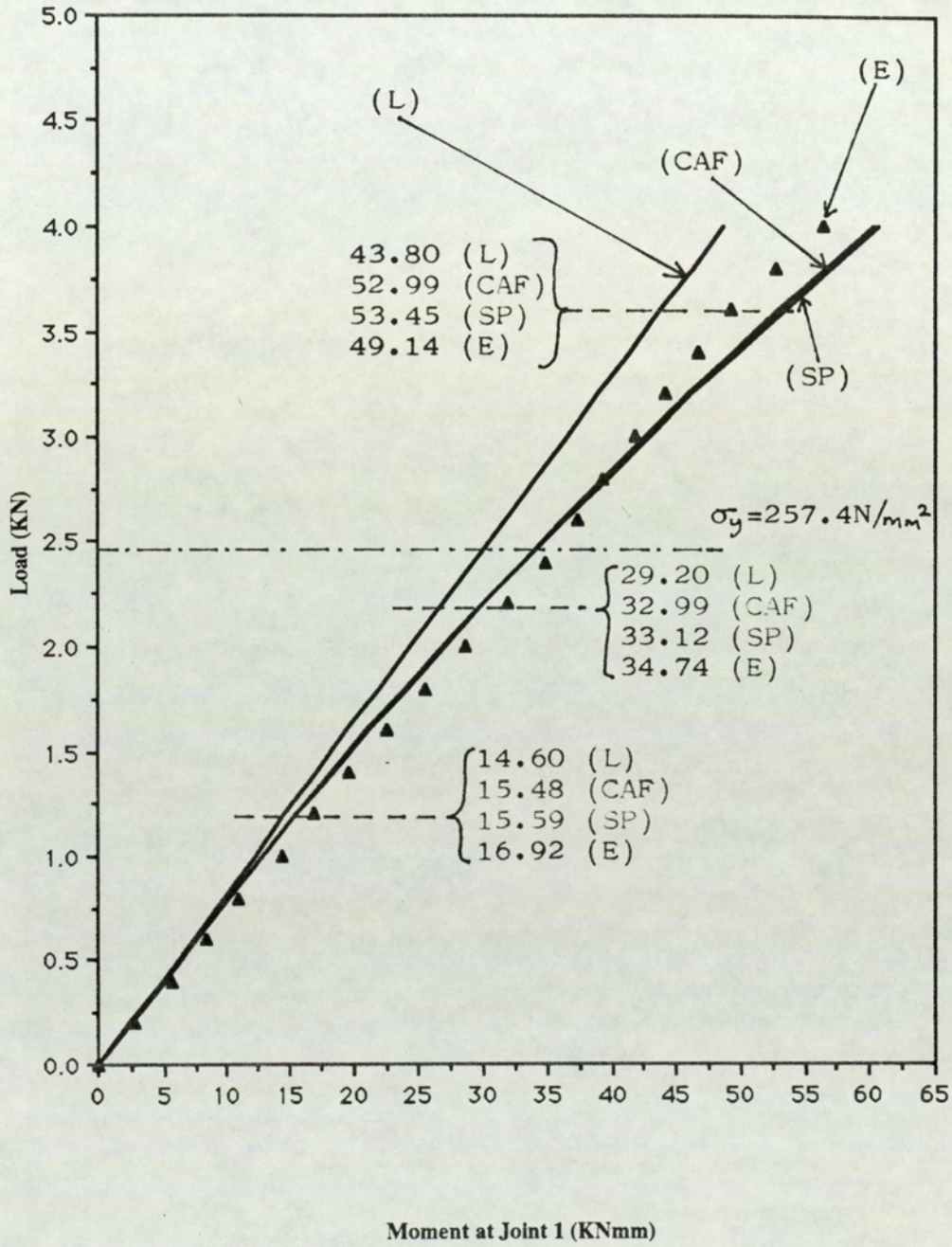


Fig 8.16. Load/Moment at joint 1 for Tapered Frame

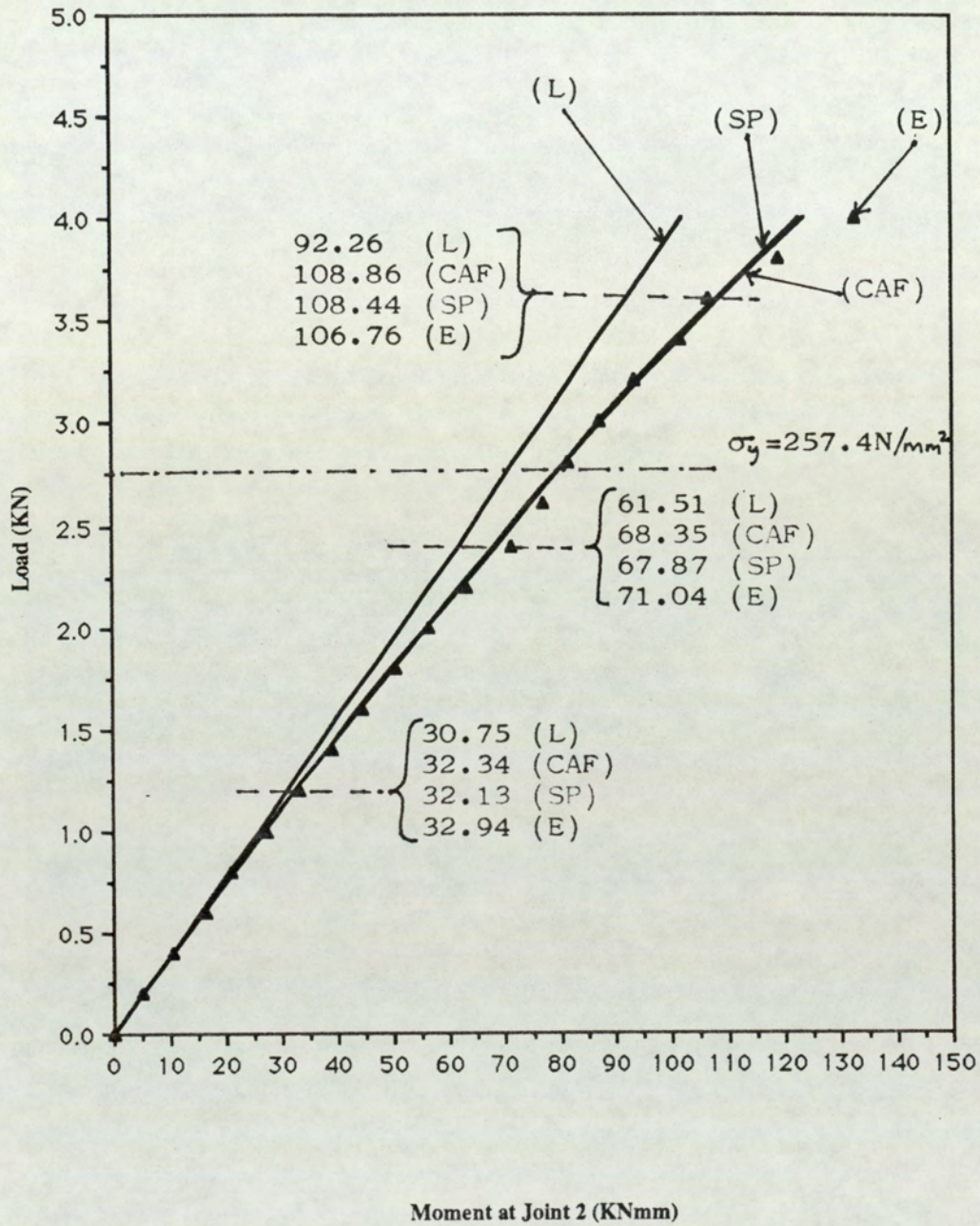


Fig 8.17. Load/Moment at Joint 2 for Tapered Frame

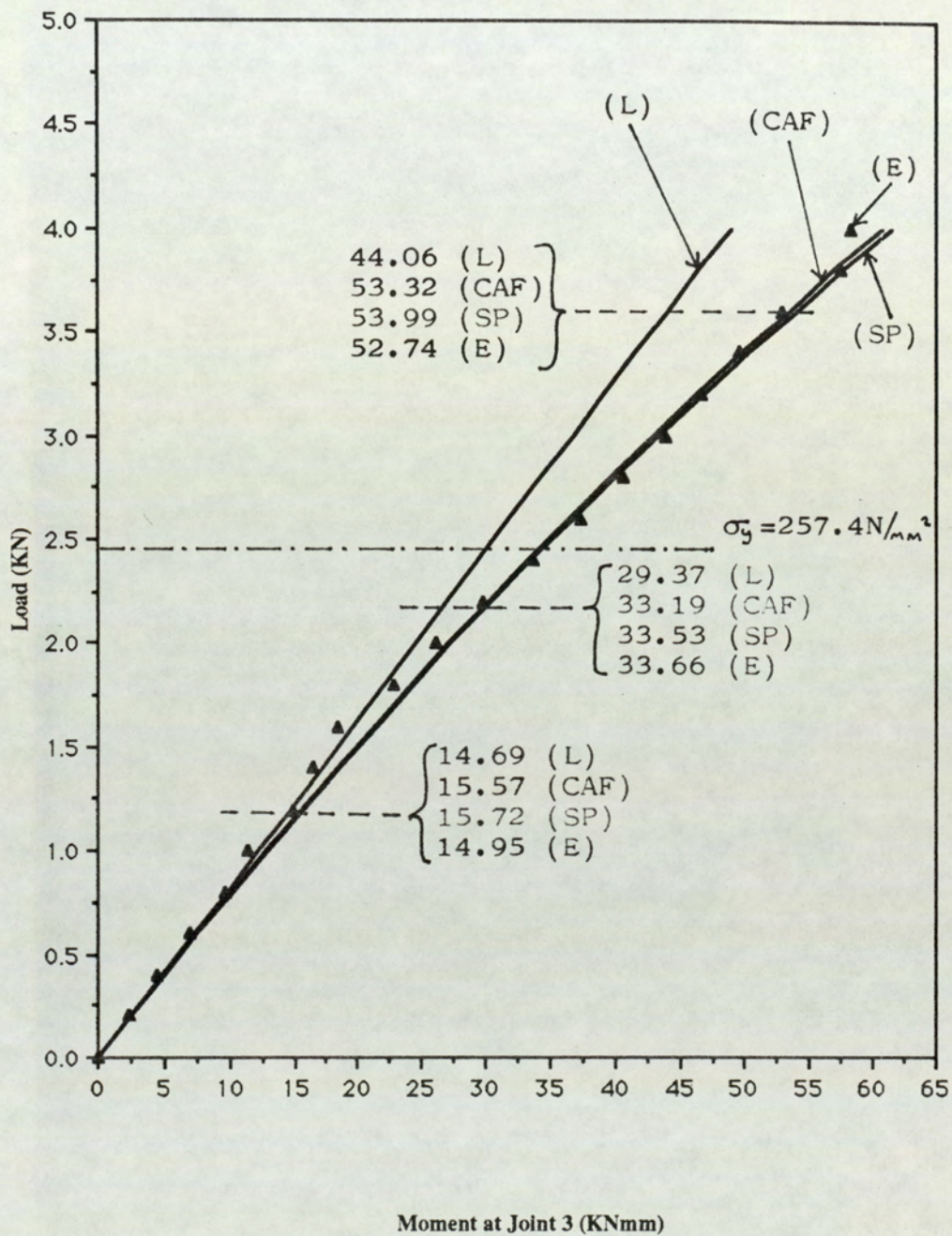


Fig 8.18. Load/Moment at Joint 3 for Tapered Frame

8.3.1. Discussion.

As seen in the case of the prismatic frames, the geometrically linear load/displacement and load/bending moment analyses obtained from the derived function

$$v = a_1 + a_2x + a_3 \int \int \frac{1}{I(x)} dx dx + a_4 \int \int \frac{x}{I(x)} dx dx$$

are represented by straight lines from which no information regarding elastic instability can be obtained.

Geometrically non-linear behaviour was examined using the constant axial force matrix and a stepped prismatic beam technique, the former being derived from the linear displacement function above via a work process and the latter using the refined coupled (C) matrix derived for prismatic sections via equilibrium considerations with each member subdivided into 10 components.

The theoretical results for the tapered frame show a similar pattern to those for the prismatic structure, namely that solutions using the axial strain expression

$$\epsilon_a = \frac{du}{dx} + \frac{1}{2} \left(\frac{dv}{dx} \right)^2$$

are preferred to those in which the flexural component in the expression is omitted.

It can be noted that the experimental deflections appear to be up to about 20% larger than the most refined of the theoretical analysis although the experimental bending moments show a far closer correlation. Such discrepancies may in part be due to the effects of the

machining in the manufacture of the tapered frames by which some curvature may have been introduced into the members.

Chapter 9.

**Applications to Framework
Behaviour.**

In the previous chapter, the veracity of the theoretical results was established by comparison with direct experiment. In this chapter a range of problems in which considerable non-linear effects can occur will be briefly investigated using the matrices previously developed in order to demonstrate the versatility of the approach and to illustrate the effects that geometrical non-linearity can produce. The examples that will be discussed are the behaviour of multi-storey frames loaded to the elastic critical load, the effect of a gantry crane load on the members of a prismatic and non-prismatic pitched portal, and the response of initial imperfections to increasing load in a plane frame.

9.1. Comparative Behaviour of Multi-storey Frames.

9.1.1. Load/Deflection Characteristics with Point Loads.

To examine the effect of storey behaviour in geometrical non-linear analysis, the two frames composed of prismatic members shown in fig 9.1 were solved under progressive increase of load using the refined coupled (C) matrix obtained from derived deflection functions.

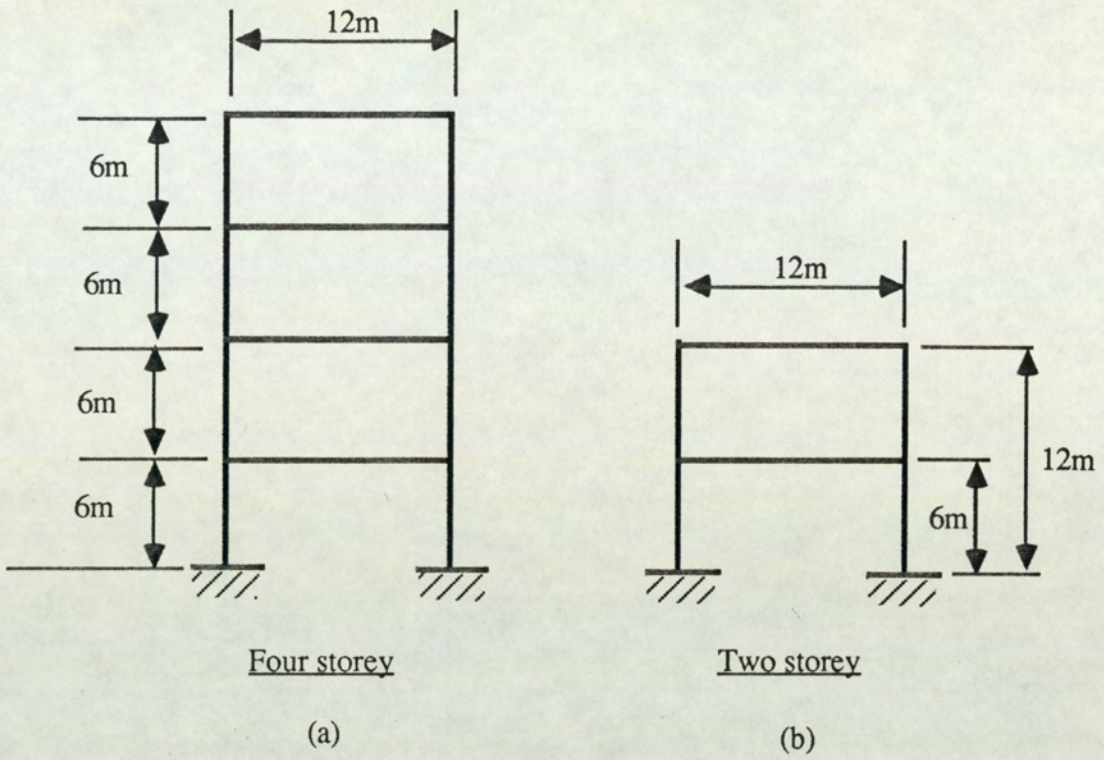
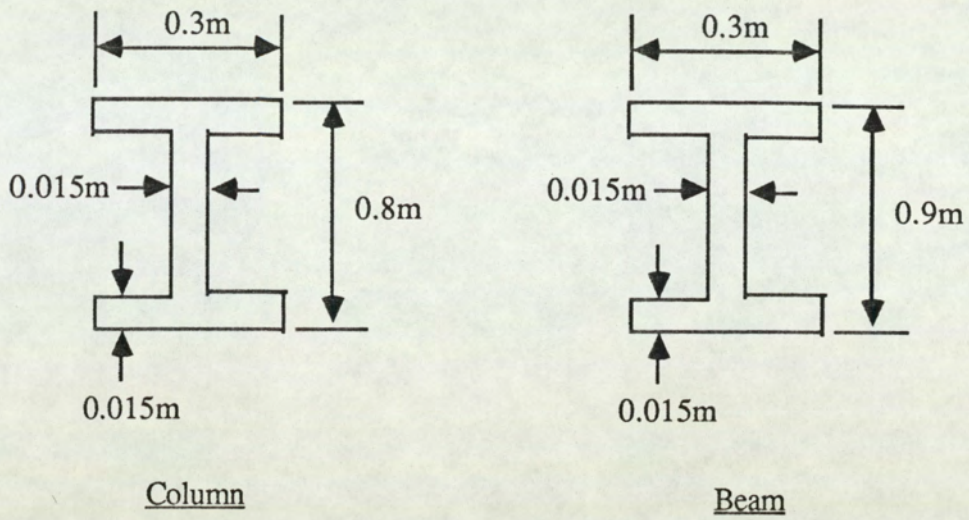


Fig 9.1. Multistorey Frames under Study.

The members of the frames were of I-section form with the dimensions and sectional properties as shown in fig 9.2, E , A , and I being Young's modulus, cross-sectional area and second moment of area respectively.



	COLUMN	BEAM
EI (KNm ²)	195734.13	258555.38
EA (KN)	2055000	2205000

Fig 9.2. Sectional Properties of Beams and Columns.

The loading applied to the frames is shown in fig 9.3 in which the horizontal load Q is maintained at a constant value and the vertical loads P increased up to the elastic critical value, ie when the determinant of the stiffness matrix becomes zero and the structure loses all its stiffness.

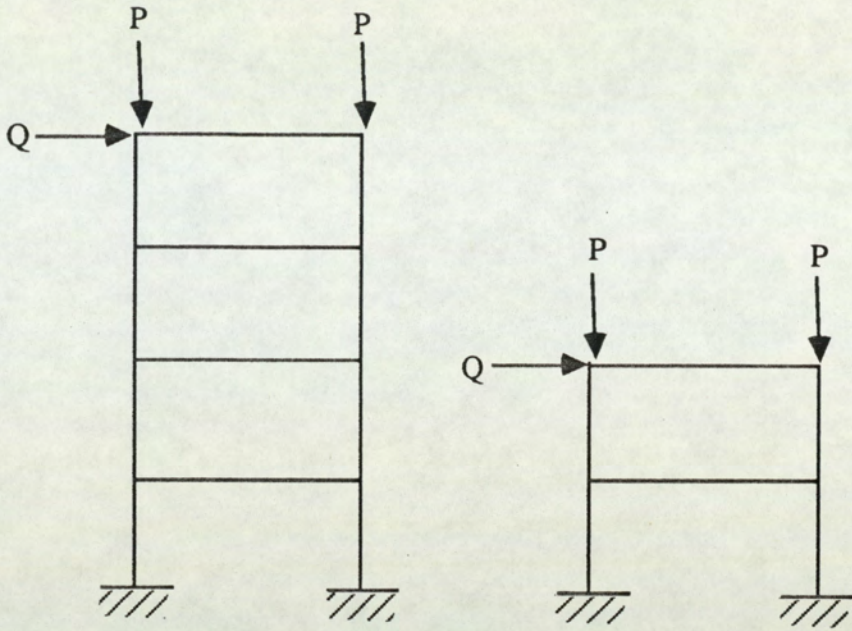
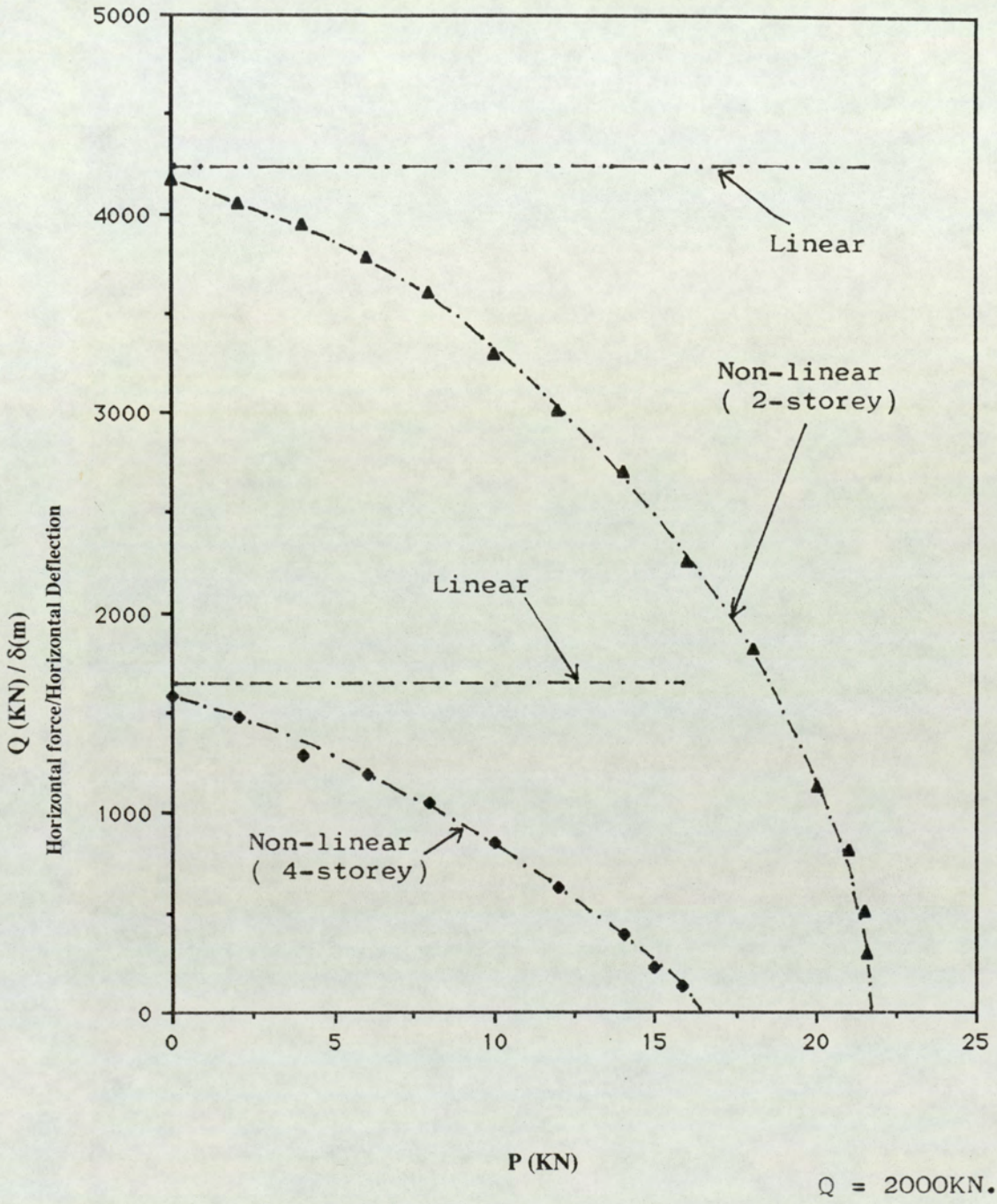


Fig 9.3. Frames showing System of Loadings.

The effect of increasing the vertical loads is assessed by plotting the ratio of the horizontal force Q to the horizontal deflection produced at its point of application δ , ie Q/δ , against the load P , as shown in fig 9.4.

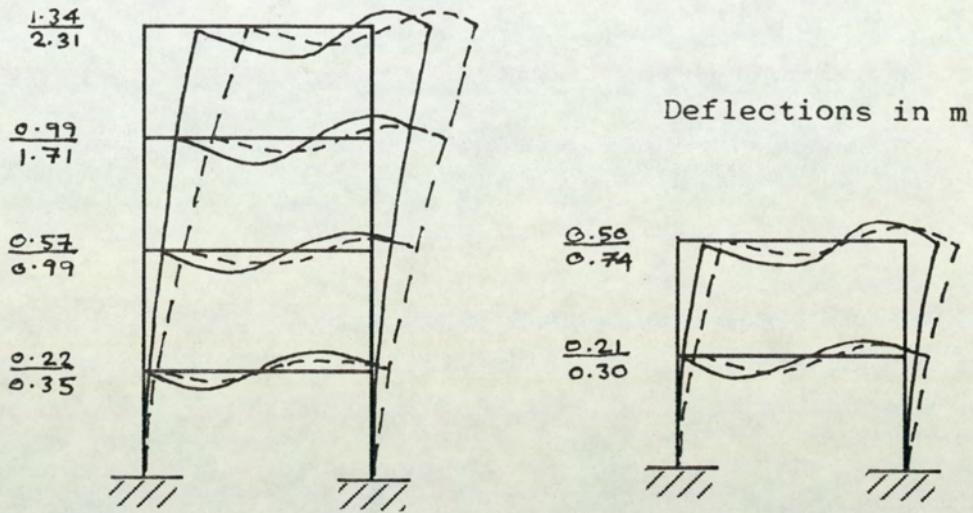


Horizontal force Q remains Constant throughout

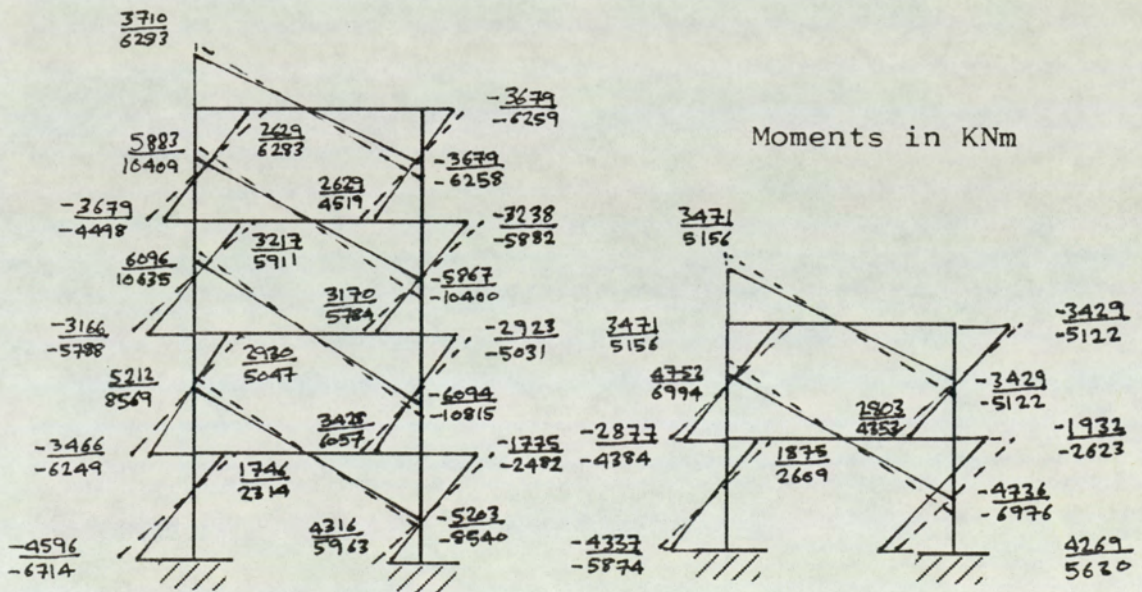
Fig 9.4. Reduction in Stiffness with increase of Load for two- and four-storey Frames.

It is seen that the elastic critical load for the two-storey frame is 22.0KN, obtained when δ is infinite or Q/δ is zero, whereas that for the four-storey frame is only 15.9KN. It can also be seen that the reduction of stiffness of the frames increases as the critical load is approached. For comparison similar results obtained from linear analyses are also given showing the importance of non-linear considerations in structures of this form.

The deflection and bending moment distributions for the frames at two levels of load P are presented in fig 9.5.



Deflection Profile



Bending Moment Diagram

Fig 9.5. Deflections and Moment Diagram.

9.1.2. Load/Deflection Characteristics with Uniformly Distributed Loading.

In addition to the analysis of the frames described above under point loads, the frames were also solved using the coupled (C) procedure when the uppermost beam was subjected to a progressively increasing u.d.l. as shown in fig 9.6.

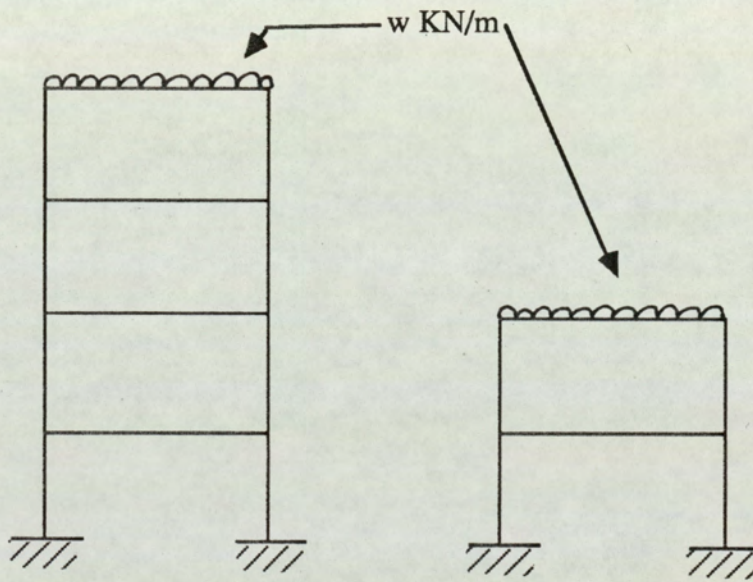


Fig 9.6. Frames Uniformly Distributed Loading.

The results from these analyses are presented in fig 9.7 as plots of the distributed load against the vertical deflection induced at the left uppermost corner.

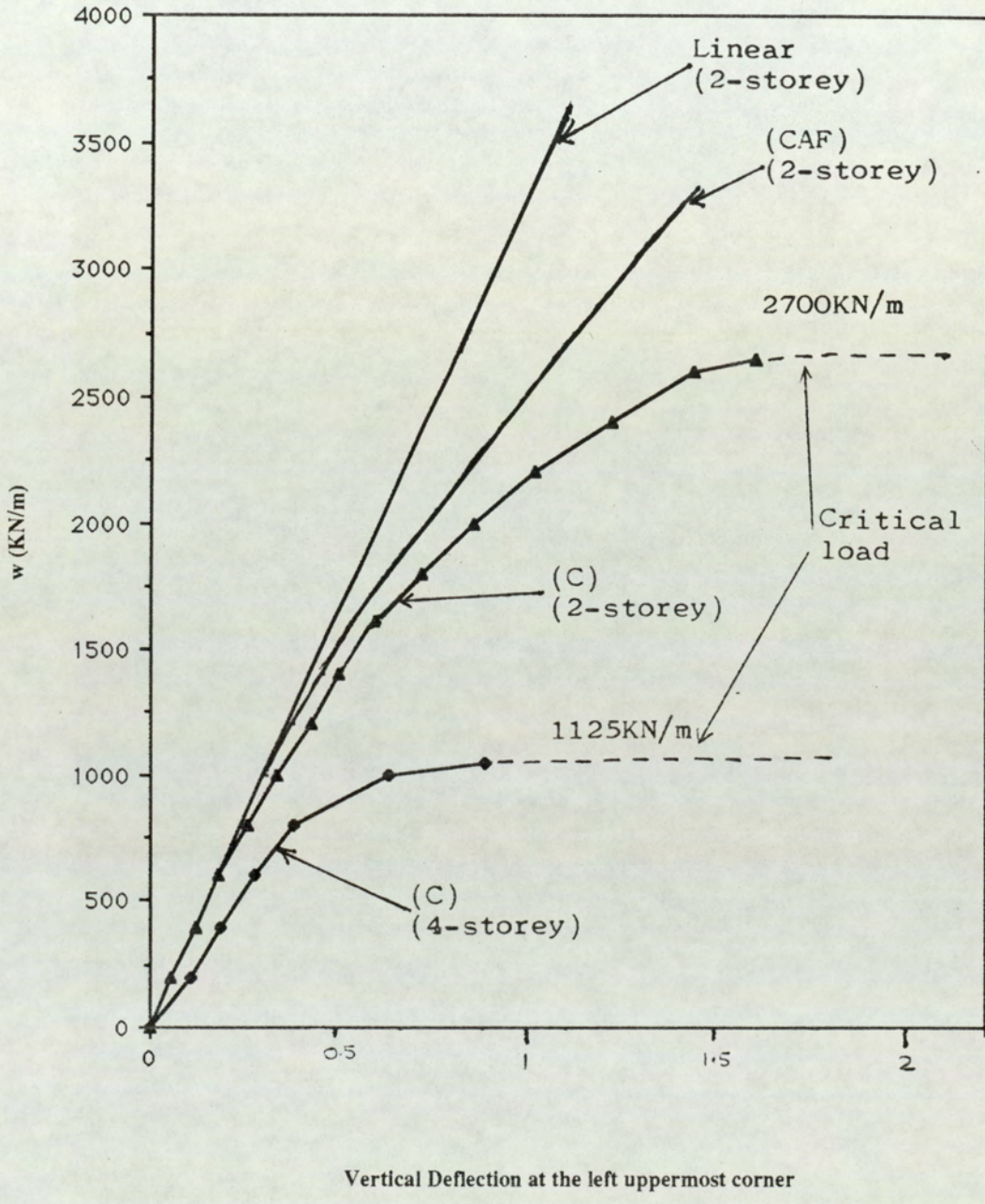
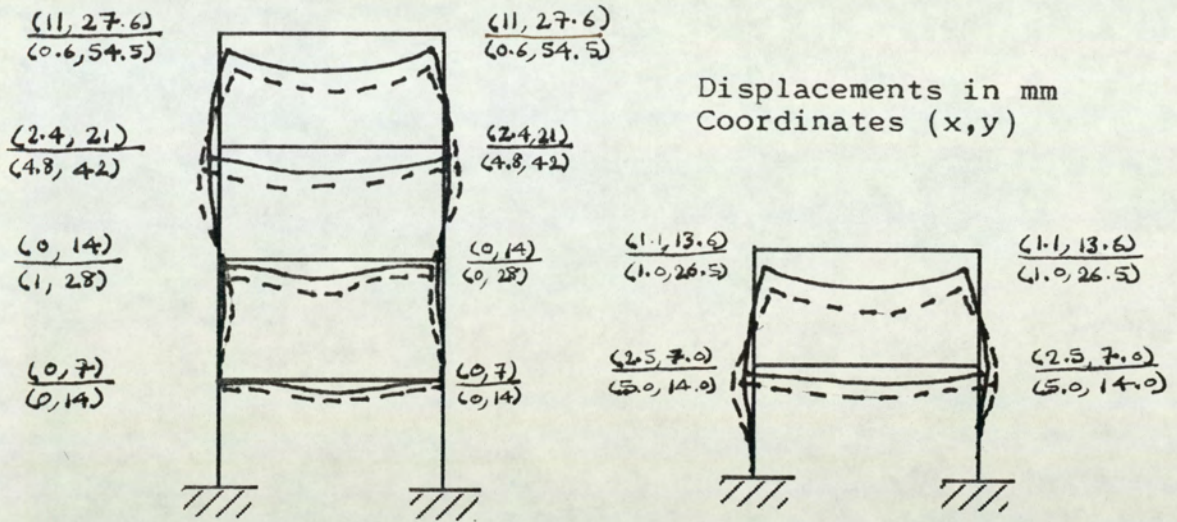


Fig 9.7. Load/Deflection Characteristics for 2 & 4 Storey Frames.

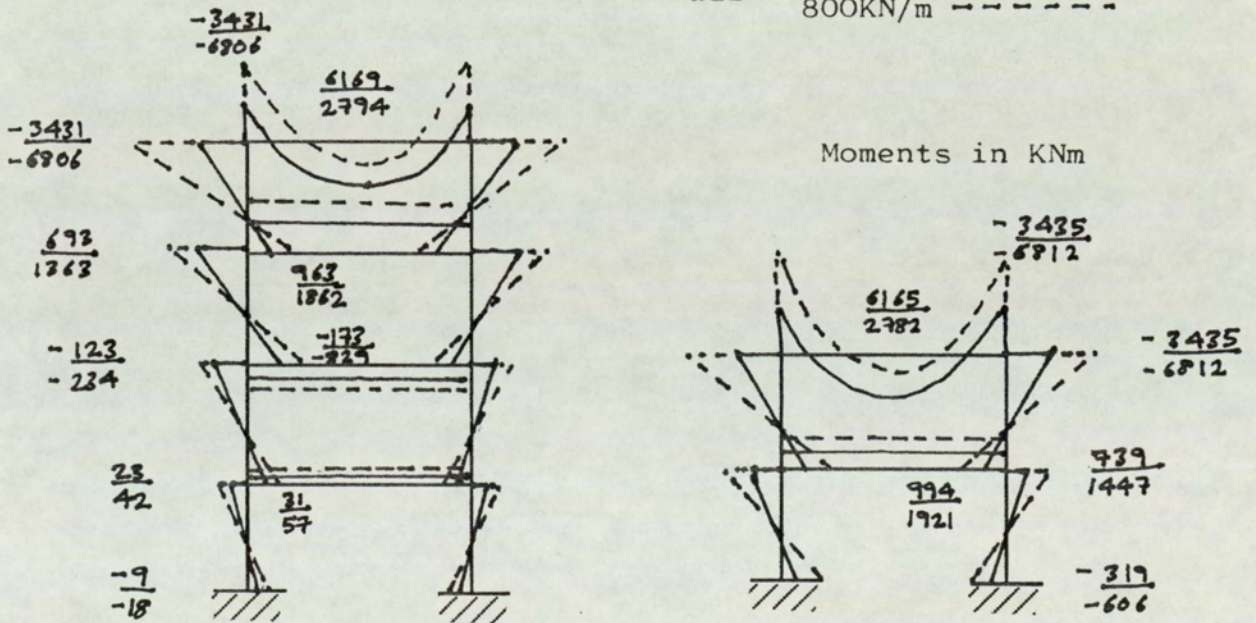
Again it can be seen that the elastic critical load for the four-storey frame is lower than that for the two-storey frame, these values being 2700KN/m and 1125KN/m respectively. For comparison a linear analysis and also an analysis based on the constant axial force (CAP) matrix for a prismatic member are presented for the two-storey frame showing the importance of the consideration of flexural effects on the axial forces in non-linear investigations.

Deflection and bending moment distributions for the two frames are presented in fig 9.8 for two levels of load.



Deflection Profile

$$udl = \frac{400\text{KN/m}}{800\text{KN/m}}$$



Bending Moment Diagram

Fig 9.8. Deflections and Moment Diagram.

9.2. Analysis of Pitched Portal Frames subjected to High Column loads via a Gantry Crane.

Two pitched portal frames were examined, one being composed of prismatic and the other of tapered I-section members. Both linear and non-linear behaviour was considered and the results compared.

9.2.1. Frame composed of Prismatic I-sections.

The geometry and loading of the frame is shown in fig 9.9 in which W represents a crane load that can move across the span of the portal thus subjecting the columns to variable axial forces at the eaves points.

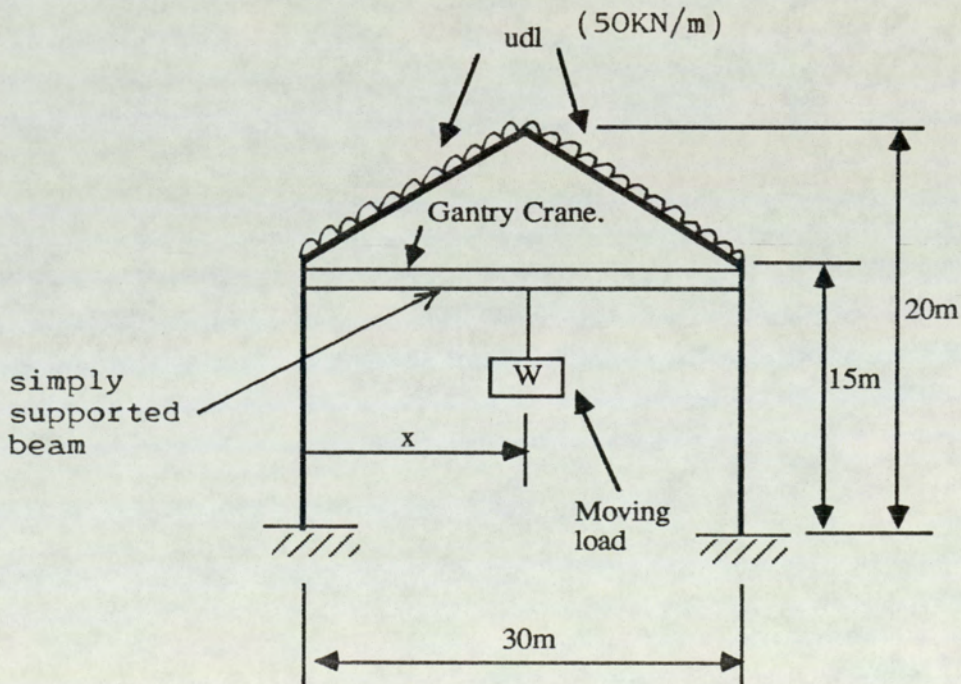


Fig 9.9. Typical Workshop Portal Frame with Column Loadings.

The material and sectional properties for the two columns and the two sloping beams are the same as those for the columns and beams in the examples of section 9.1.

Fig 9.10 shows the variation of the vertical and horizontal deflections at the apex with position of the crane load for both linear and non-linear behaviour, the latter being obtained by the refined coupling (C) matrix, while figs 9.11 and 9.12 depict the linear and non-linear deflections and bending moments in the frame for three positions of the load.

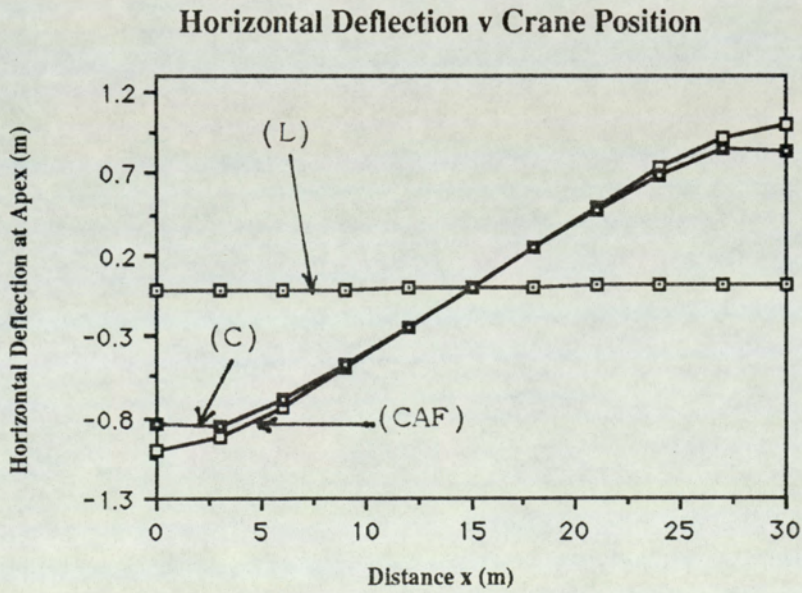
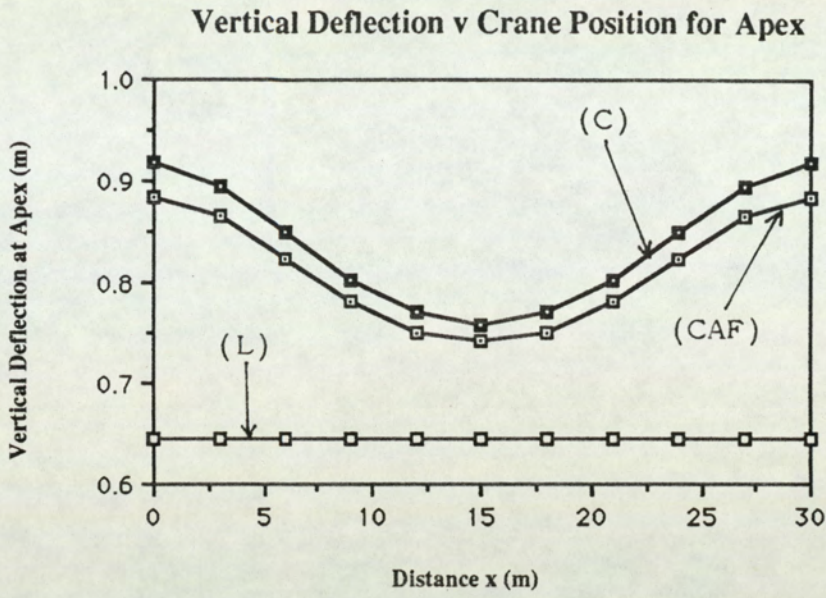
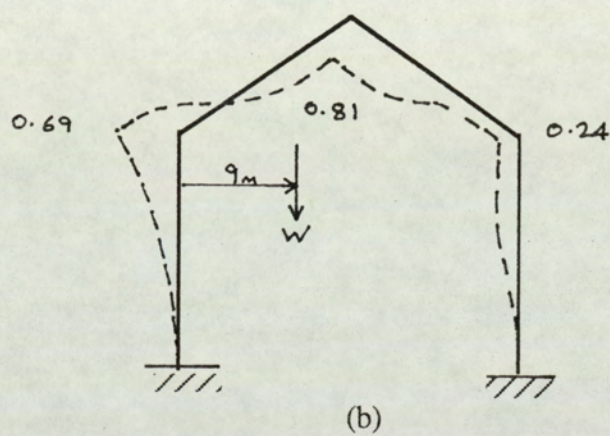
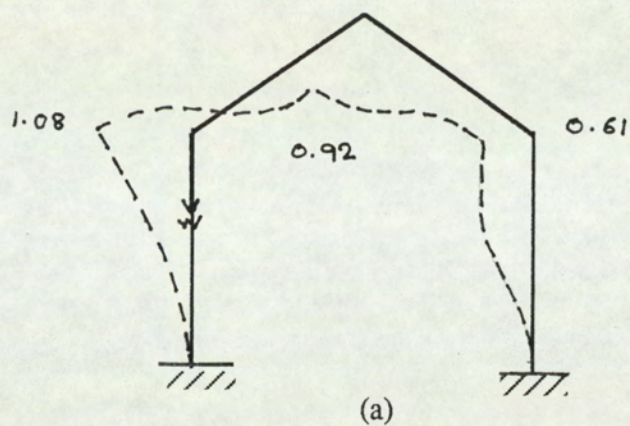


Fig 9.10. Showing Horizontal and Vertical Deflections at Apex as Crane moves across the Span.



Crane Load = 7490KN
 Deflections in m

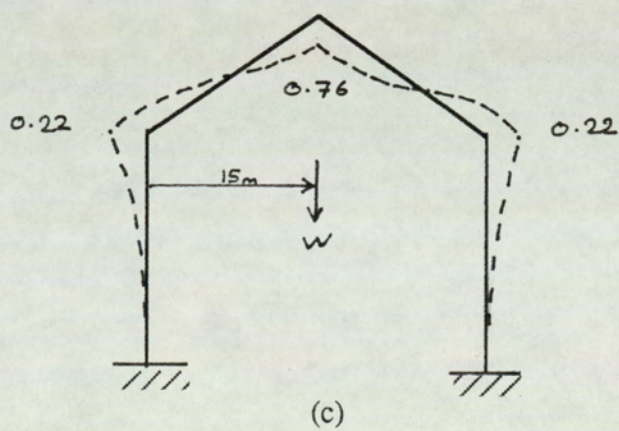
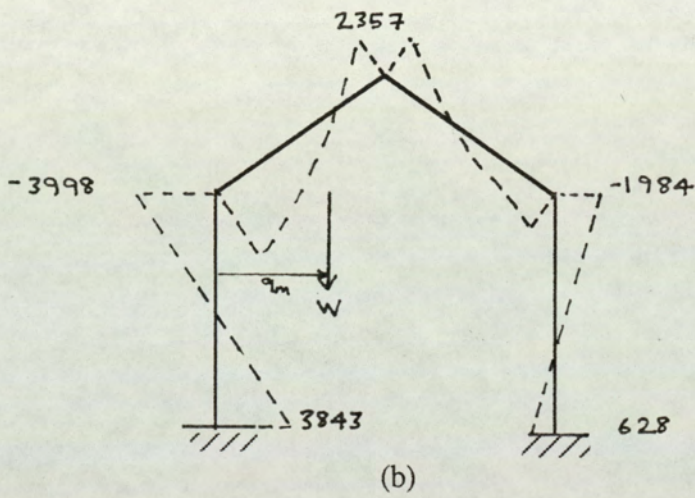
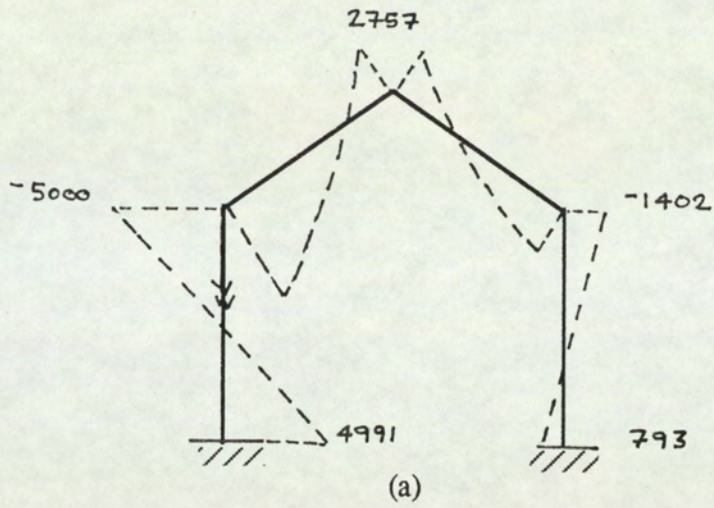


Fig 9.11. Frame Deflection as Crane Load moves from one Column to other.



Crane Load = 7490 kN
 Moments in kNm

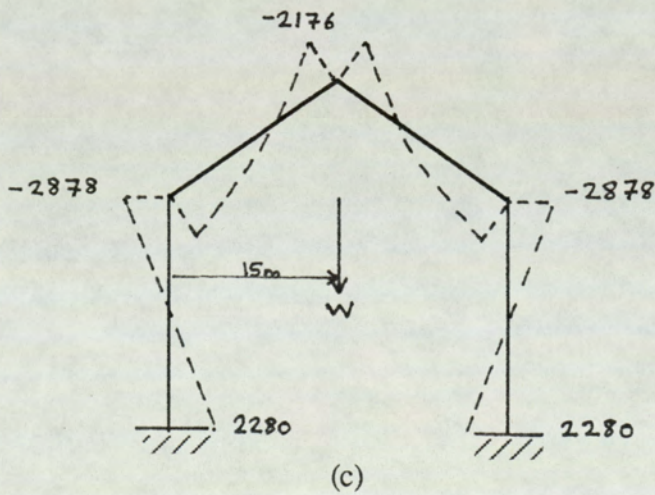


Fig 9.12. Frame Joint Moments as Crane Load moves from one Column to other.

9.2.2. Frame composed of Tapered I-sections.

The geometry and loading of the frame is as described in section 9.2.1 and is shown in fig 9.13. The sectional geometry of the members is shown in fig 9.14, the depth of each constituent member varying linearly from 0.4 to 0.8m.

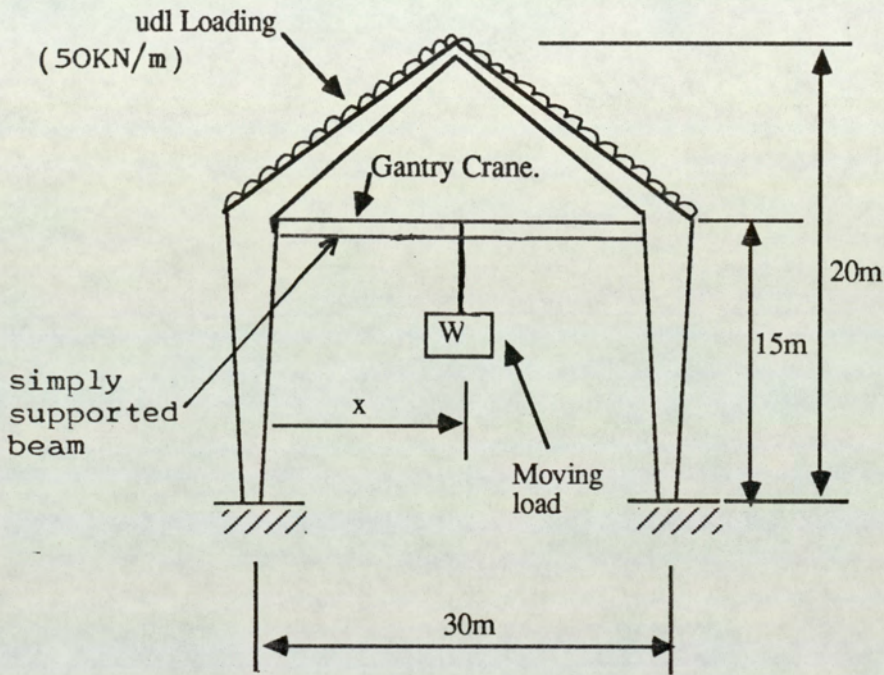


Fig 9.13. Typical Workshop Portal frame with Tapered members.

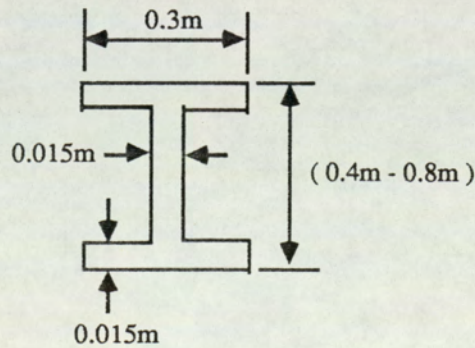


Fig 9.14. Dimensions of I-section.

The variation of apex deflection with load position is shown in fig 9.15 for both linear and non-linear behaviour, where the linear behaviour is obtained via the derived displacement function for an I-section and the non-linear behaviour from a stepped prismatic process using the coupled (C) matrix for prismatic members with each member divided into 10 increments.

Fig 9.16 and 9.17 show the linear and non-linear deflection and bending moment distributions throughout the frame for three load positions.

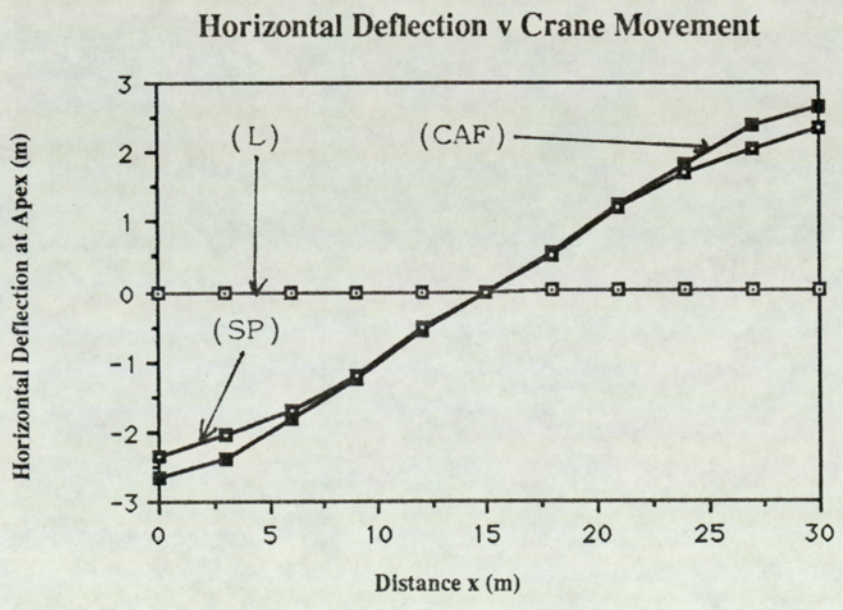
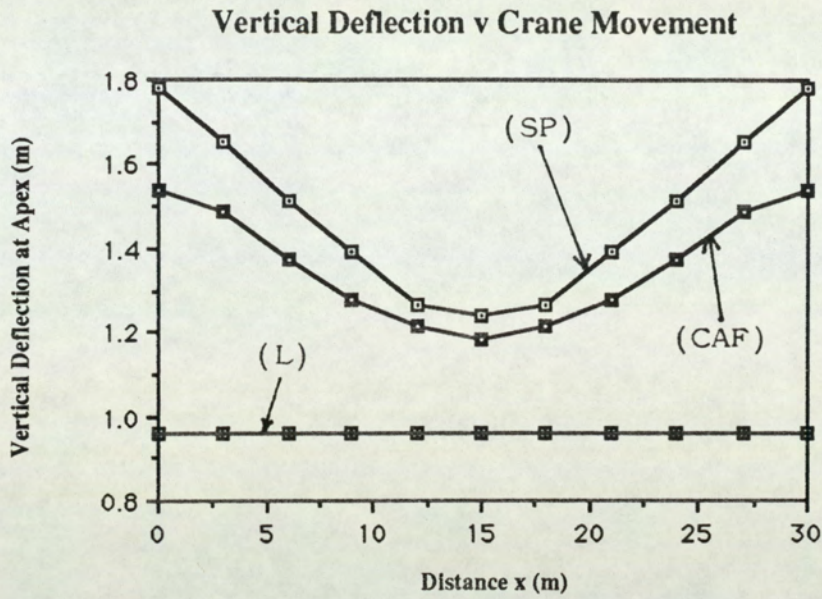
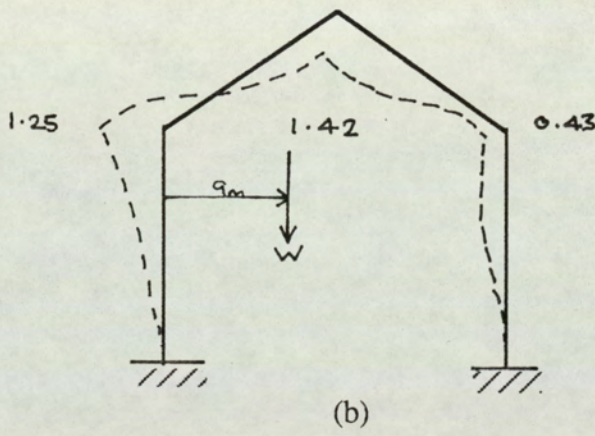
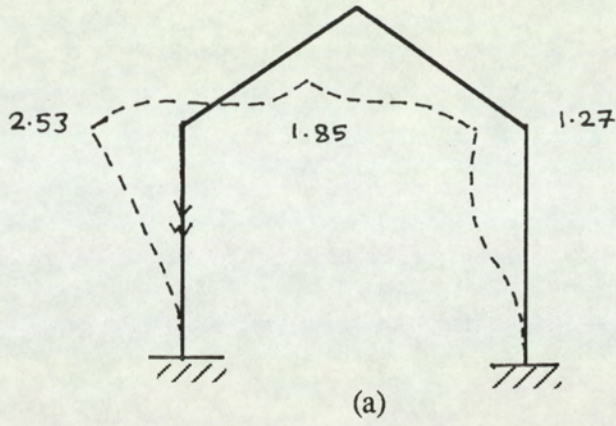


Fig 9.15. Showing Horizontal and Vertical Deflections at Apex as Crane moves across the Span.



Deflections in m

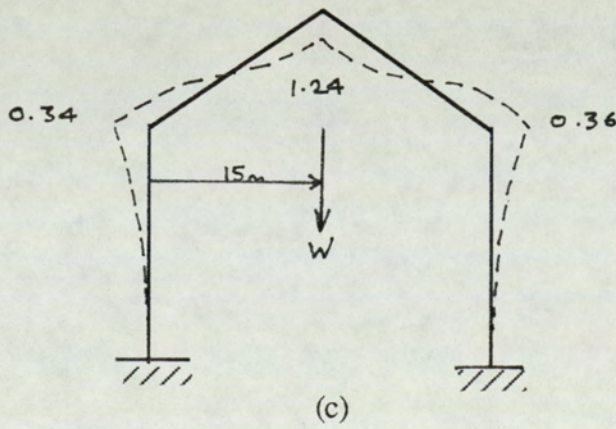
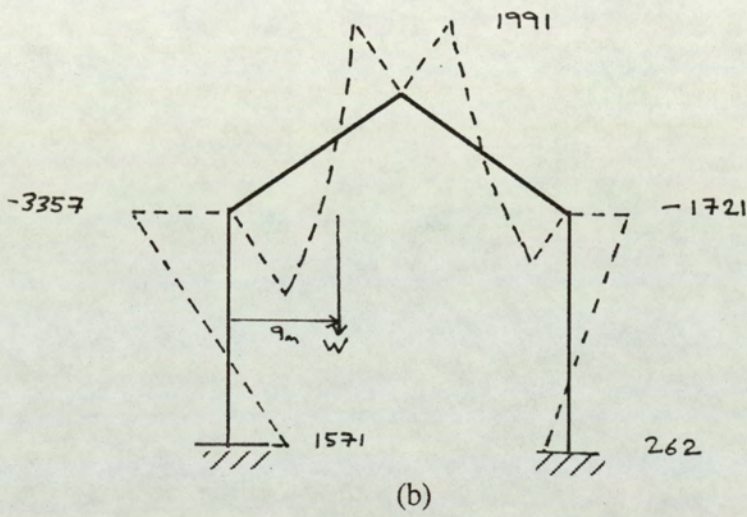
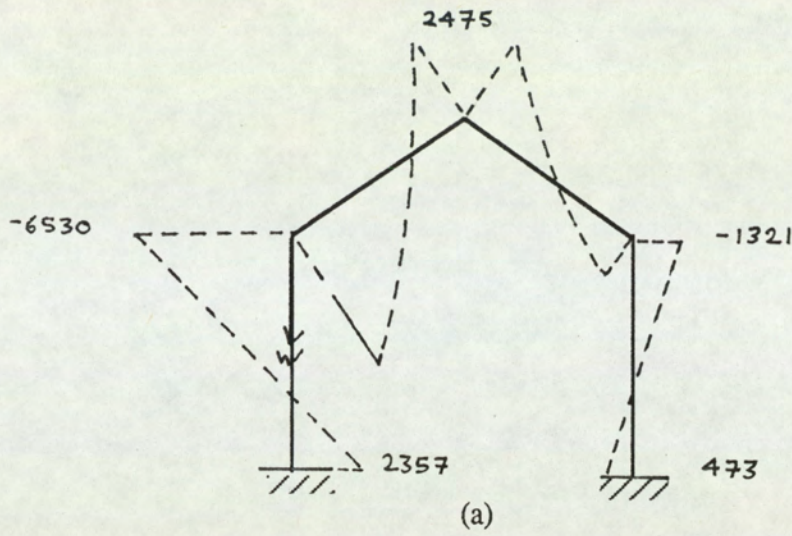


Fig 9.16. Frame Deflection as Crane Load moves from one Column to other.



Crane Load = 3790 kN
 Moments in kNm

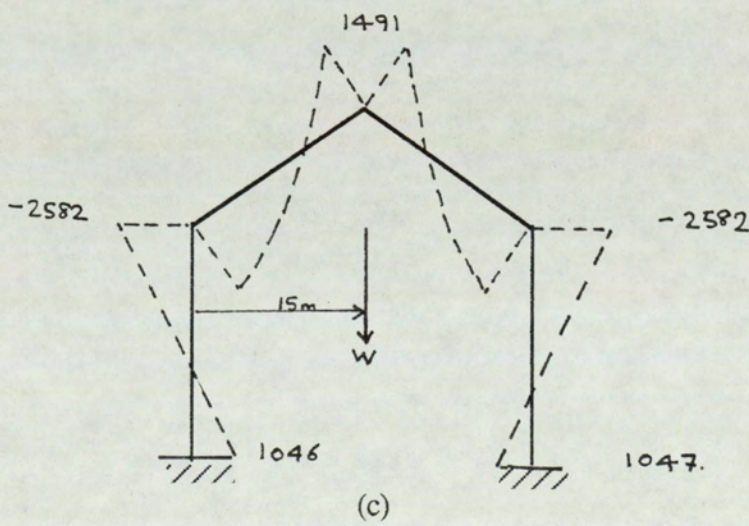


Fig 9.17. Frame Joint Moments as Crane Load moves from one Column to other.

9.3. Effects of Initial Imperfections on the Non-linear behaviour of Pitched Portal Frames.

The effect of lack of straightness or geometrical imperfections on the behaviour of slender structures is readily examined using the matrices in which the axial strain is expressed as;

$$\epsilon_a = \frac{du}{dx} + \frac{1}{2} \left(\frac{dv}{dx} \right)^2$$

In this section a brief introduction will be given to the effect of lack of straightness and to imperfections in constructional geometry.

9.3.1. Effect of Lack of Straightness in Prismatic Frame.

The effect of defects in the straightness of members will be illustrated by consideration of the prismatic frame used in the experimental work described in Chapter 8 in which one of the column members exhibits assumed initial deformations at the centre of 5mm and 10mm. The geometry of the structure together with the initial geometrical defects and the loading are shown in fig 9.18.

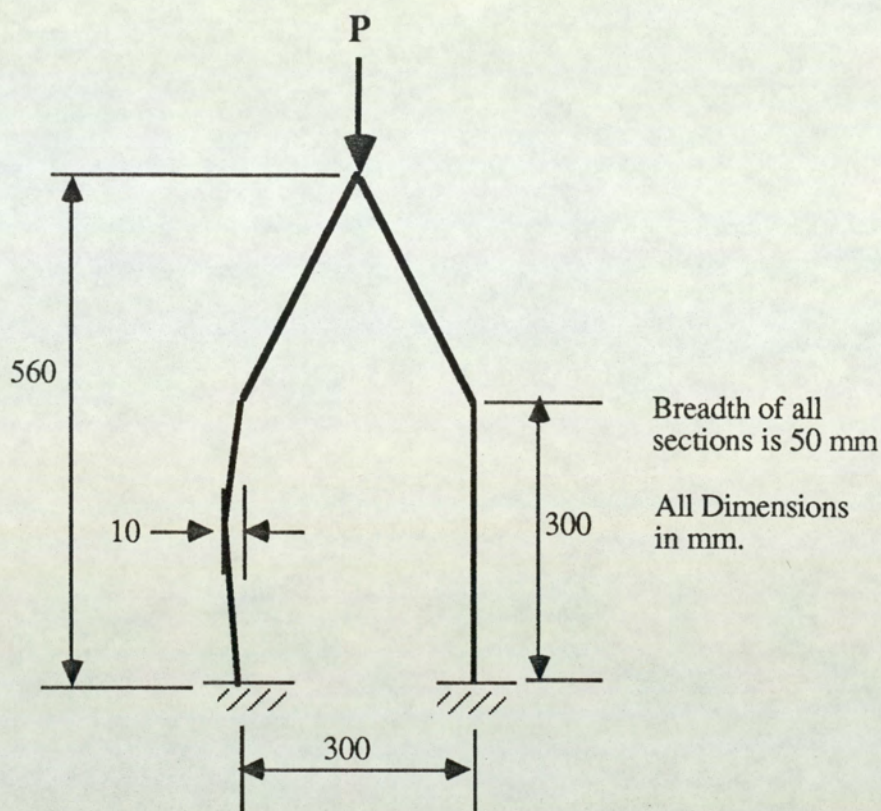


Fig. 9.18. Frame composed of Prismatic Sections with Imperfections in Column Members.

The frame was analysed both linearly and non-linearly using both the refined coupled (C) matrix and the constant axial force matrix (CAF) and the changes in the vertical deflections at the apex on increase of load are shown in fig 9.19. It is seen that relatively small defects of this nature produce a large decrease in the elastic critical load.

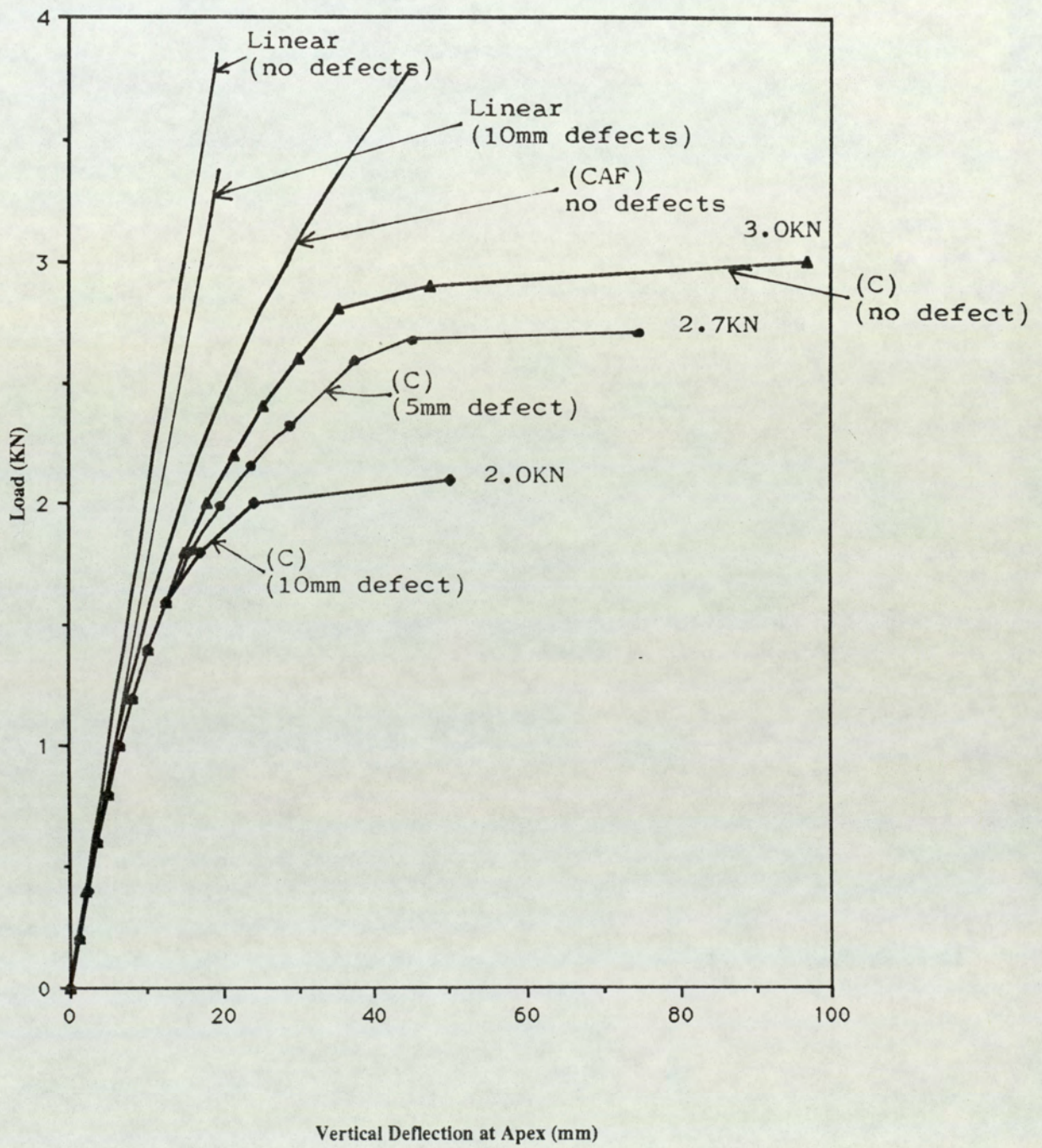


Fig 9.19. Graph of Load/Deflections due to Imperfections

Fig 9.20 shows the deflection and bending moment distribution in the frame at the level of load indicated for the defect-free frame and for the frame exhibiting the initial 10mm column deformation.

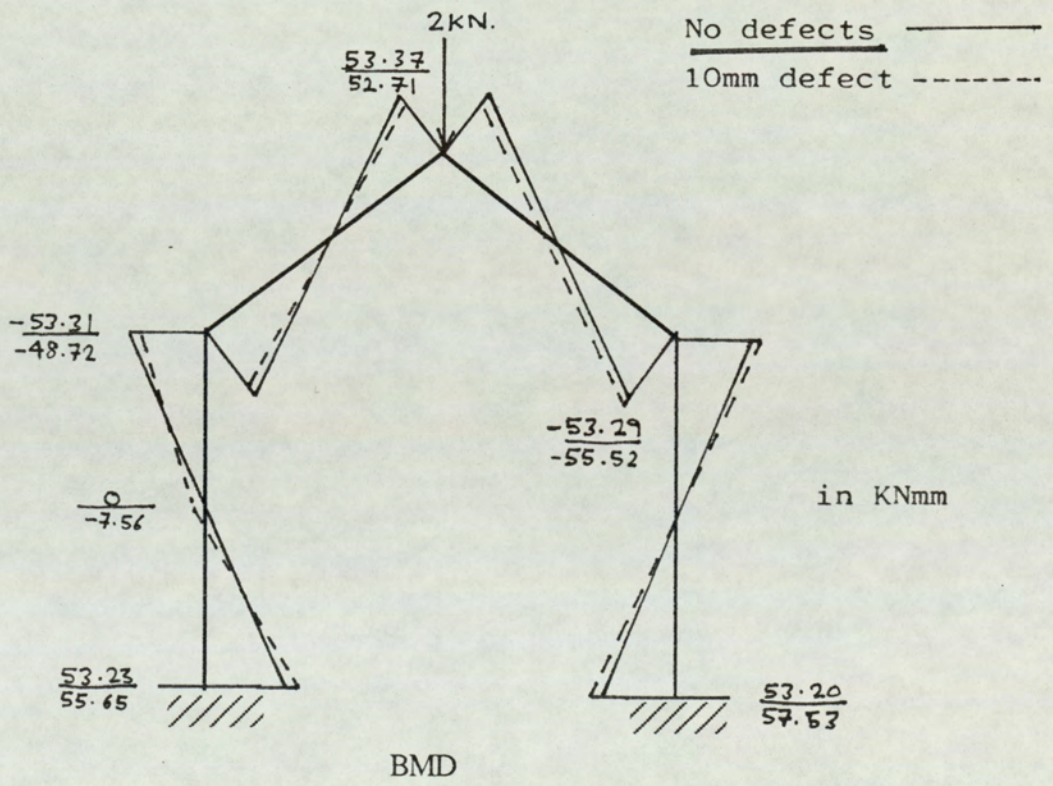
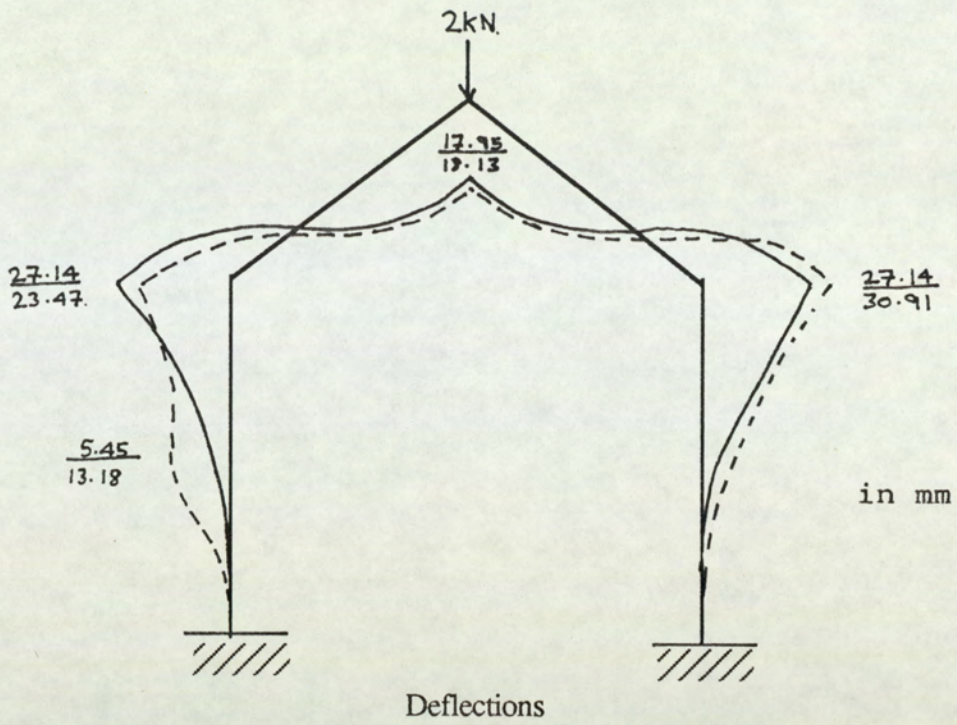


Fig 9.20. Deflections and Moments of Frame with Member Imperfections.

9.3.2. Effect of Constructional Tolerances.

Although not specifically stated in Chapter 8, it was noticed that the eaves nodes of the tapered framework used in the experimental work were slightly displaced outwards by about 10mm from their ideal positions. It was thus considered appropriate to analyse this frame with these initial constructional tolerances taken into account.

The frame together with its defects and loading is shown in fig 9.21 and the effect of these defects is shown in fig 9.22 where the change in vertical apex deflection with respect to increase of load is presented.

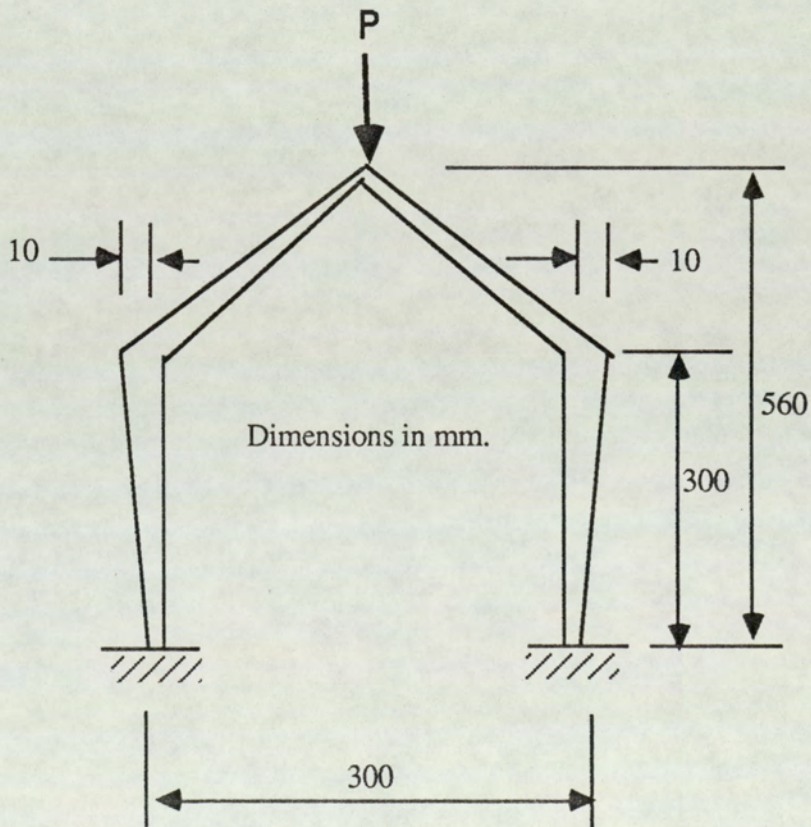


Fig 9.21. Frame Composed of tapered Members with initial Joint Displacement.

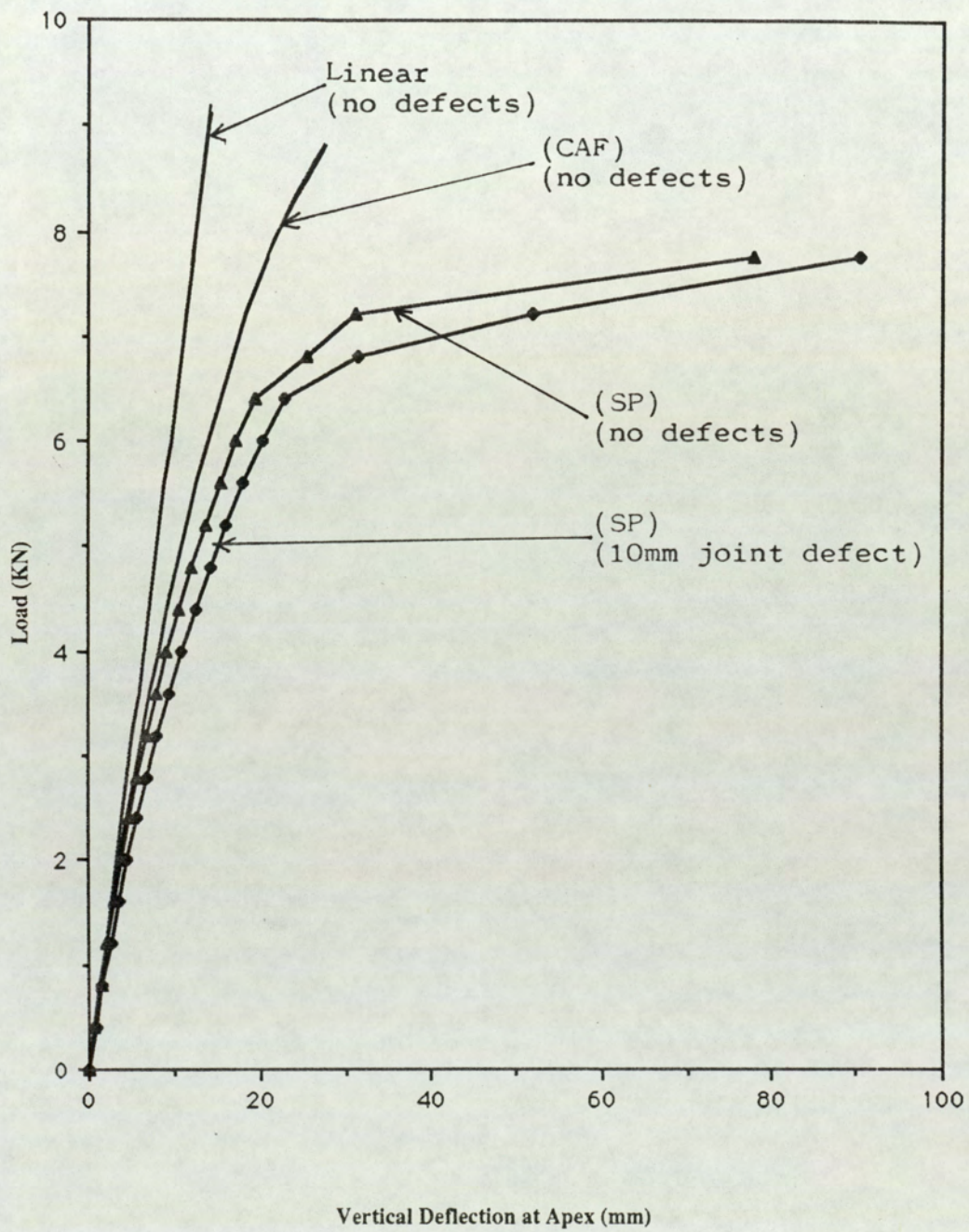


Fig 9.22. Graph of Load/Deflection due to Initial Joint Displacements

The non-linear analyses, performed using the stepped prismatic approach using the coupled (C) matrix with each member subdivided into ten prismatic elements, show that although the initial defects tend to reduce the elastic critical load, their effect is not as pronounced as the effect of lack of straightness of the members.

The deflection and bending moment distributions in the frame with and without defects are presented in fig 9.23 for the level of load indicated.

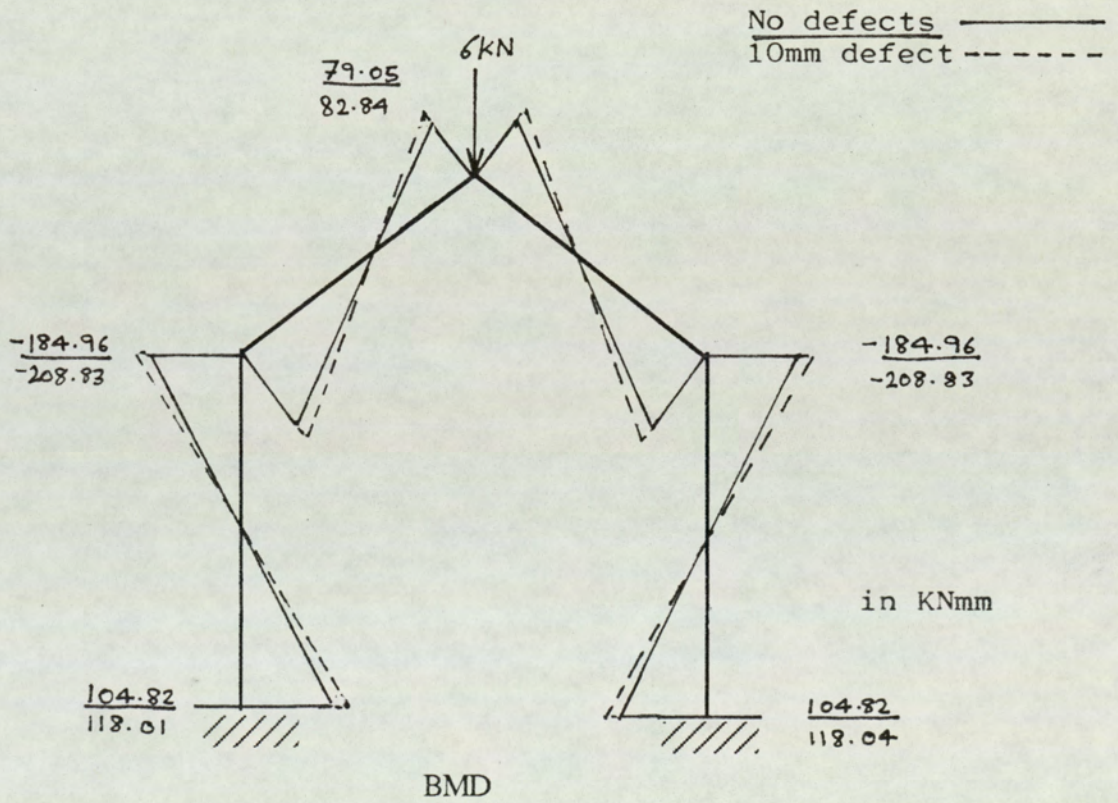
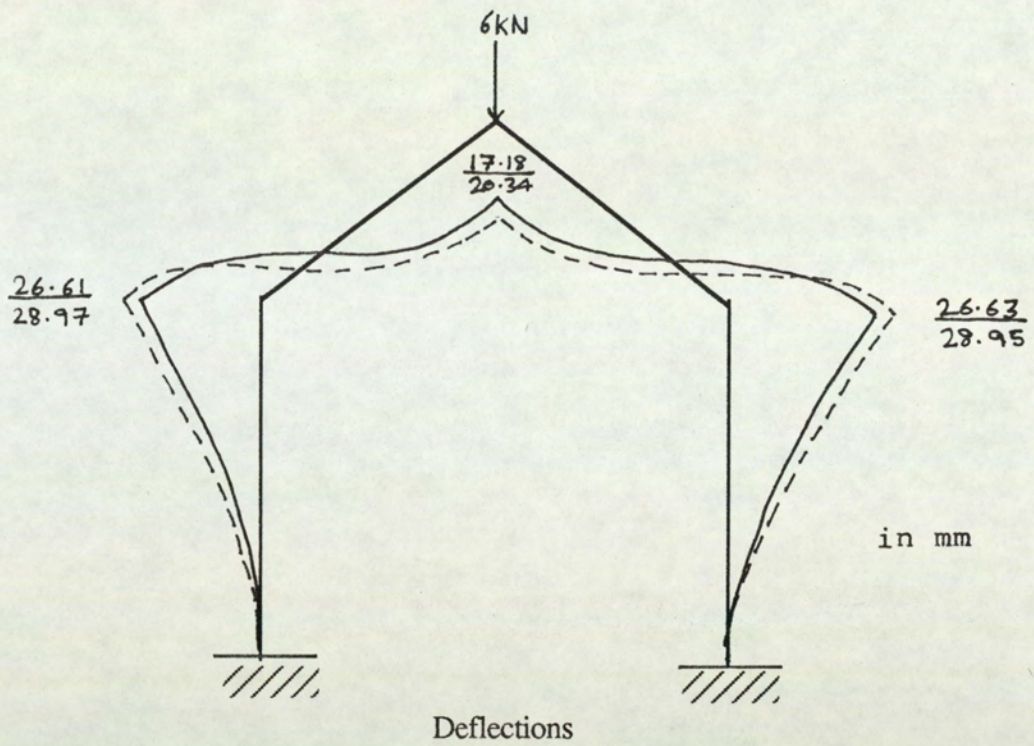


Fig 9.23. Deflections and Moments of Frame with Joint Imperfections.

In reality both initial imperfections and constructional tolerances are present in frameworks and their effect on structural behaviour is thought worthy of further research.

Chapter 10.

Summary, Conclusions and

Future Work.

10.1. Summary.

The displacement method of analysis has been applied extensively and with great success to the solution of geometrically linear frame problems and it was thus natural that this procedure should be attempted for the investigation of geometrically non-linear structures. However the effect of geometrical non-linearity appears largely to have been studied using the assumption of constant axial force, an assumption which does not strictly allow investigation of progressive non-linear behaviour.

In order to examine such effects, it was necessary to construct the relevant force/displacement relationships ie the stiffness matrices, for members exhibiting non-linear behaviour, and this was carried out using the finite element procedure.

Since the displacements of a one-dimensional member are given by the solution of an ordinary differential equation, it is shown that for such a structural element the exact displacement profile may be obtained, and the standard work-based finite element procedure curtailed due to the satisfaction of equilibrium at every point in the member. The resulting stiffness matrix is thus exact in the sense that there is no increase in accuracy upon subdivision of the member.

The first stage of this research was to employ this curtailed process using the derived displacement functions of an isolated member to produce firstly the exact non-linear stiffness matrix assuming constant axial force, and then to extend this to produce a more refined but more complex matrix capable of a more realistic assessment of geometrical non-linearity.

In addition to these exact formulations, approximate polynomial functions were also used to produce a tangential stiffness matrix for comparison purposes (the use of the

tangential stiffness matrix finds application in the geometrically non-linear behaviour of plates where exact displacement functions cannot in general be found).

10.2. Conclusions.

For easy presentation of the conclusions the prismatic and non-prismatic members will be discussed separately.

10.2.1. Frames with Prismatic Members.

The finite element method of analysis provides a systematic procedure for the development of the force/displacement relationships of structural elements, the final form of the stiffness matrix being dependent on the form of displacement function used.

Generally the displacement functions of the elements have to be assumed, but in the case of elements whose displacements are a function of only one variable, as in the case of beam-columns, the displacement function can in principle be determined exactly. The use of such derived functions has two fundamental advantages; firstly the resulting stiffness matrix is exact within the confines of the governing differential equations and hence no increase in accuracy ensues on subdivision of the element, and secondly the matrix may be formulated from simple equilibrium principles rather than the more lengthy work-based procedure which must be used with assumed functions.

The investigation of frames composed of prismatic elements showed that by assuming that the axial forces in the members were only dependent on the axial displacements, ie

by assuming that the axial strain was given by

$$\epsilon_a = \frac{du}{dx}$$

the loss of stiffness on increase of load was underestimated, implying an overestimate of the elastic critical load. This is shown by comparison with results obtained using the more refined expression for axial strain, ie;

$$\epsilon_a = \frac{du}{dx} + \frac{1}{2} \left(\frac{dv}{dx} \right)^2$$

and with the experimental results for deflections, which may be favourably compared.

Comparison of the results using the refined derived function formulation and the tangential stiffness matrix approach using the approximate polynomial functions showed that very similar results were obtained from both matrices. However it was found that whereas the formulation using the derived functions required only one or two iterations to obtain an acceptable deflection estimate, that using the tangential stiffness matrix required many more. This may be due to the fact that the derived function formulation operates using direct iteration whereas the Newton- Raphson technique is used with the tangential stiffness matrix method.

It is noted that although the deflection results obtained using the two expressions for axial strain showed a distinct difference, very little variation was shown in the bending moment results, implying little variation in the curvature of the members. This observation appears surprising and it is suggested that further work should be carried out on different frame configurations in order ascertain whether or not such results occur generally.

10.2.2. Frames with Non-prismatic Members.

The investigations undertaken for prismatic frames were further extended to the analysis of frames composed of non-prismatic sections.

Firstly it was envisaged that the development of exact equilibrium-based matrices formulated using derived functions could be both intractable and impracticable and indeed this was found to be the case, the exact formulations being expressed in terms of Bessel functions which involved the calculation of series with associated rounding errors.

Thus examination of the behaviour of non-prismatic frames was undertaken using work-based methods with approximate displacement functions. In the work on prismatic frames, the work-based stiffness matrices for geometrically non-linear behaviour were obtained using the polynomial displacement functions which represent linear prismatic behaviour exactly. It was thus considered logical to use for the non-linear investigations of non-prismatic members the derived displacement functions for linear non-prismatic members. These derived functions were used to construct both the non-linear stiffness matrix in which the axial force is assumed to be dependent only on the axial displacement and also the tangential stiffness matrix. Although the former matrix was formulated successfully, development of areas of the tangential stiffness matrix were found to be unwieldy and intractable regarding practical implementation.

Thus in addition to results obtained using the approximate constant axial force element referred to above, non-prismatic behaviour was also investigated using a stepped prismatic element approach in which the non-prismatic members of the frame were subdivided into a number of prismatic elements of differing section properties. The resulting model was solved using the derived function prismatic stiffness matrix using

the refined axial strain expression,ie;

$$\epsilon_a = \frac{du}{dx} + \frac{1}{2} \left(\frac{dv}{dx} \right)^2$$

This stepped prismatic element technique produced, on adequate subdivision, results which compared favourably with experimental results and as expected represented a more accurate model than the matrix based on the assumption of constant axial force. However because of the necessity for subdivision the amount of data preparation and computer storage may become large and the economy of such a procedure must be balanced against the nature of the results required.

10.2.3. Practical examples of Geometrically Non-linear Behaviour.

The effect of geometrical non-linearity was examined for a number of common practical examples in which both point and distributed loading was considered.

Firstly the effect of overall slenderness was considered with reference to two- and four-storey prismatic frames subjected to point and uniformly distributed loads showing how the critical load is reduced with increase in the number of storeys.

Secondly a pitched roof portal frame was described in which a gantry crane could move from one side to the other, thus inducing high column loads at the ends of the travel. Both prismatic and tapered sections were considered in this example which is typical of those in which the effects of stability should be considered in design.

Thirdly the important practical situation of lack of straightness was considered with reference to a pitched portal frame where it was seen that the load-carrying capacity of

the frame was reduced dramatically by virtue of a relatively small amount of initial straightness. In the examples presented it is seen that an initial lack of straightness of 10mm in the centre of one of the 300mm vertical legs of a 560mm high portal produced a reduction in the critical load of the order of 30%. In contrast initial joint displacements at the eaves of the portal causing the legs of the portal to be slightly inclined to the vertical produced only a small reduction in the collapse load.

10.3. Recomendations for Future Research.

- 1) The small amount of work carried out in this thesis into the effect of initial imperfections is sufficient to show that this important practical topic may now be investigated in depth using the sophisticated non-linear matrix with coupled axial and flexural components developed in this thesis.
- 2) Further the use of connected straight elements may be used to examine the geometrically non-linear behaviour of arches or structures comprising curved members. Such an idealisation is shown in Fig 10.1.

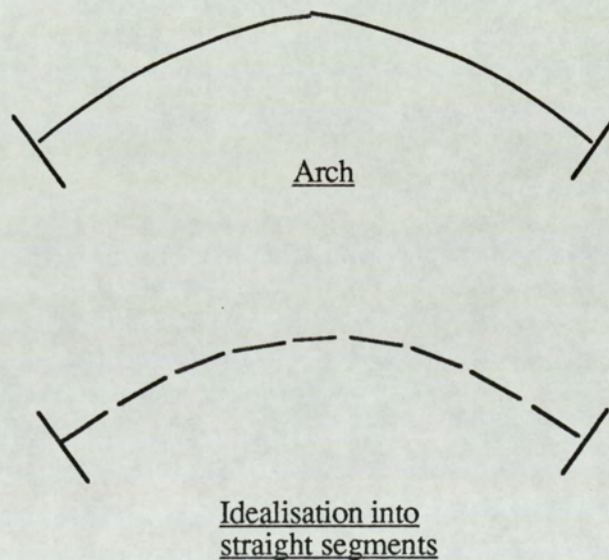


Fig 10.1. Showing idealisation of curved members.

Indeed this may be the only viable finite element method to treat arch behaviour as it is most probable that solutions attempted using curved elements may be either intractable or impossible to obtain.

3) In this thesis all the frames considered have been rigid jointed. In practice situations can occur where some nodes are in fact hinges. Perhaps the most important of these situations are those occurring in the elastic-plastic behaviour of frames constructed from ductile materials, for example mild steel. On loading of such a frame beyond the elastic limit the progressive formation of plastic hinges occurs and thus a rigid jointed frame is transformed into a frame containing an increasing number of hinges until plastic collapse occurs. Such behaviour cannot be studied using the matrices developed here as they stand, but they could be developed to take into account such hinge conditions.

Consider the simple frame shown in Fig 10.2.

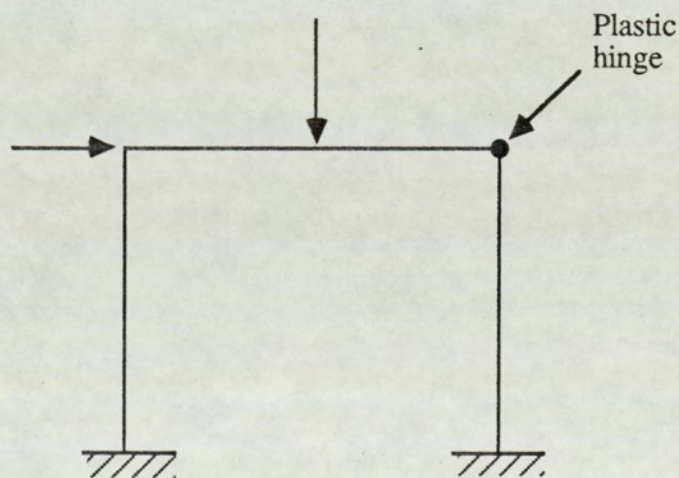


Fig 10.2. Showing frame with plastic hinge.

Upon formation of the hinge shown both the right hand leg and the beam contain a hinge at one end. The modified flexural stiffness matrix for such a member does not now contain four nodal displacements but only three since the moment at the hinge is

known. This modification can be shown by considering a member (1-2) of a linear frame, the standard force/displacement relationship being

$$\begin{Bmatrix} S_1 \\ M_1 \\ S_2 \\ M_2 \end{Bmatrix} = \begin{bmatrix} K_{11} & & & \\ K_{12} & K_{22} & & \\ K_{13} & K_{23} & K_{33} & \\ K_{14} & K_{24} & K_{34} & K_{44} \end{bmatrix} \begin{Bmatrix} v_1 \\ \theta_1 \\ v_2 \\ \theta_2 \end{Bmatrix}$$

S Y M

If end 1 is pinned, then M_1 is zero and the second equation becomes;

$$0 = K_{12} v_1 + K_{22} \theta_1 + K_{23} v_2 + K_{24} \theta_2$$

ie

$$\theta_1 = -\frac{1}{K_{22}} (K_{12} v_1 + K_{23} v_2 + K_{24} \theta_2)$$

Substituting θ_1 into the above matrix and rearranging gives

$$S_1 = \left(K_{11} - \frac{K_{12}^2}{K_{22}} \right) v_1 + \left(K_{13} - \frac{K_{12} K_{23}}{K_{22}} \right) v_2 + \left(K_{14} - \frac{K_{12} K_{24}}{K_{22}} \right) \theta_2$$

$$S_2 = \left(K_{13} - \frac{K_{12} K_{23}}{K_{22}} \right) v_1 + \left(K_{33} - \frac{K_{23}^2}{K_{22}} \right) v_2 + \left(K_{34} - \frac{K_{23} K_{24}}{K_{22}} \right) \theta_2$$

$$M_2 = \left(K_{14} - \frac{K_{12}K_{24}}{K_{22}} \right) v_1 + \left(K_{34} - \frac{K_{23}K_{24}}{K_{22}} \right) v_2 + \left(K_{44} - \frac{K_{24}^2}{K_{22}} \right) \theta_2$$

or in matrix form

$$\begin{Bmatrix} S_1 \\ 0 \\ S_2 \\ M_2 \end{Bmatrix} = \begin{bmatrix} N_{11} & & & \\ 0 & 0 & & \\ N_{13} & 0 & N_{33} & \\ N_{14} & 0 & N_{34} & N_{44} \end{bmatrix} \begin{Bmatrix} v_1 \\ 0 \\ v_2 \\ \theta_2 \end{Bmatrix}$$

SYMM

ie the (4 x 4) matrix is reduced to a (3 x 3). Similar results can be obtained if the hinge is at end 2. The fixed end moments and forces can also be modified by the presence of a hinge if it is desired to treat distributed loading.

Although this brief description has been illustrated by means of a linear member, it is possible that the geometrically non-linear behaviour of frames containing hinges may be similarly developed.

- 4) Although only plane frames have been considered in this thesis, the possibilities of extending this work for the treatment of space frames is obvious. Such an extension will mean investigation of the additional aspects of geometrical non-linearity, namely lateral and torsional instability effects.
- 5) The combination of the beam elements developed in this thesis with geometrically non-linear plate elements would enable the non-linear behaviour of stiffened plate

structures to be investigated.

- 6) It is hoped that the geometrically non-linear analysis of frames composed of both prismatic and non-prismatic elements which has been developed in this thesis and incorporated in a computer package will be a useful addition to structural engineering knowledge.

References

- 1) John Case & A.H.Chilver "Strength of Materials & Structures".
Arnold Books. Second Edition.
- 2) W.T.Marshall & H.M.Nelson "Structures" (Second Edition).
Pitman Publishing Ltd. 1977.
- 3) J.H.Argyris & S.Kelsey "Energy Theorems & Structural Analysis"
Butterworth Books. 1960.
- 4) M.J.Turner, R.W.Clough,
H.C.Martin & L.J.Topp. "Stiffness & Deflection Analysis of
Complex Structures.
J.Aero. Sci. Page 805-23. 1956.
- 5) K.H.M.Bray, P.C.L.Croxton & L.H.Martin. "Matrix Analysis of Structures".
Arnold Books. 1976.
- 6) W.M.Jenkins. "Matrix & Digital Computer Methods
in Structural Analysis"
McGraw-Hill Book Co. 1969

- 7) Y.K.Cheung & M.F.Yeo. "A Practical Introduction to Finite Element Analysis". Pitman Books. 1979.
- 8) H.B.Harrison. "Computer Methods in Structural Analysis". Arnold Books. 1973.
- 9) S.P.Timoshenko & J.M.Gere. "Theory of Elastic Stability". McGraw-Hill Books. 1961.
- 10) M.R.Horne & W.Merchant. "The Stability of Frames". Pergamon Press. 1965.
- 11) P.A.Kirby & D.A.Nethercot. "Design for Structural Stability". Constrado (Publishing) Ltd. 1979.
- 12) K.I.Majid. "Matrix Methods of Analysis & Design by Computers (Non-linear Structures)". Butterworth Books. 1972.
- 13) F.W.Williams. "An approach to the Non-linear behaviour of the members of a Framework with Finite Deflections". J.Mech. & App. Mech. Vol. 17. 1964.

- 14) J.M.Daviss. "Collapse & Shakedown Loads of Plane Frames".
J.of Struct Div. ASCE. June 1967.
- 15) F.Mazzolani, A.Di.Carlo & M.Pignataro "Post Buckling Behaviour of Multistorey steel Frames".
University of Naples, Italy. 1977.
- 16) M.Eisenberger & V.gorbanos. "Stability of Plane Frames omitting axial Strains".
J.of Struct Div. ASCE. Nov. 1984.
- 17) R.H.Gallagher, Y. Yamada & J.T.Oden. "Recent Advances in Matrix Method of Structural Analysis & Design".
USA-Japan Seminar on Matrix Methods Part 1. 1971.
- 18) J.T.Oden, Y. Yamamoto & R.W.Clough. "Recent Advances in Matrix Method of Structural Analysis & Design".
USA-Japan Seminar on Matrix Methods Part 2. 1972.
- 19) J.G.Myoung. "Post-buckling Behaviour of Elastic Frame Structures".
Ph.D Univ. of Arizona. USA.1981.

- 20) J.R.Hanachi. "Non-linear Elastic Frame Analysis by Finite Elements".
Ph.D Michigan State Univ.USA. 1981.
- 21) P.A.Mendis & P.L.Darvall. "Computer Method for Stability Analysis of Plane Frames".
Research Report, Monash Univ. USA. 1985.
- 22) B.J.Hartz. "Matrix Formulation of Structural Stability Problems".
J.of Struct Div. ASCE. Dec. 1965.
- 23) R.K.Liversley & D.B.Chandler. "Stability Functions for Structural Frameworks".
Manchester University Press.1956.
- 24) J.W.Bunce & E.H.Brown. "The Finite Deflection of Plane Frames".
J.of Struct Div. ASCE. July. 1972.
- 25) H.S.Harung & M.A.Millar. "General Failure Analysis of Skeletal Plane Frames".
J.of Struct Div. ASCE. June. 1973.

- 26) R.D.Wood & O.C.Zienkiewicz. "Geometrically Nonlinear Finite Element Analysis of Beams, Frames, Arches & Axisymmetric Shells".
Computers & Structures, Vol. 7. 1977.
- 27) A.Chajes & J.E.Churchill. "Nonlinear Frame Analysis by Finite Element Methods".
J.of Struct Div. ASCE. June. 1987.
- 28) S.Z.Al-Sarraf. "Elastic Stability of Frameworks".
PhD. Univ. of Liverpool. UK. 1964.
- 29) J.M.Gere & W.O.Carter. "Critical Buckling Loads for Tapered Columns".
J.of Struct Div. ASCE. Feb. 1962.
- 30) C.G.Culver & S.M.Preg. "Elastic Stability of Tapered Beam-Columns".
J.of Struct Div. ASCE. Feb. 1968.
- 31) C.V.Girijavallabhan. "Buckling Loads of Non-uniform Columns".
J.of Struct Div. ASCE. Nov. 1969.
- 32) S.Kitiporchai & N.S.Trahair. "Elastic Stability of Tapered I-beams".
J.of Struct Div. ASCE. March. 1972.

- 33) Fogel & Ketter. "Elastic Strength of Tapered Columns".
J.of Struct Div. ASCE. Oct. 1962.
- 34) Butler & Anderson. "The Elastic Buckling of
Beam-Columns".
Welding Journal. June. 1963.
- 35) Prawel & Lee. "Bending & Buckling Strength of Tapered
Structural Members".
Experimental Mechanics. May 1969.
- 36) E.J.Krynicky & Z.E.Mazurkiewicz. "Frames of Solid Bars of varying
Cross-sections".
J.of Struct Div. ASCE. Aug. 1964.
- 37) S.Wang & S.Z.Al-Sarraf. "Frames of Solid Bars of varying
Cross-sections".
J.of Struct Div. ASCE. Feb. 1965.
- 38) C.K.Wang. "Stability of Rigid Frames with
Non-uniform Members".
J.of Struct Div. ASCE. Feb. 1967.
- 39) J.M.Gere. "Moment Distribution".
Van Nostrand Books.New York. 1962.

- 40) D.J.Just. "Analysis of Plane Frames of Linearly varying Rectangular Sections". Synopsis. The Structural Engineer. 1975.
- 41) D.J.Just. "Plane Frameworks of Tapered Box and I-sections. J.of Struct Div. ASCE. Jan. 1977.
- 42) C.J.Brown. "Approximate Stiffness Matrix for Tapered Beams". J.of Struct Div. ASCE. Dec. 1984.
- 43) D.L.Karabalis. "Approximate Stiffness Matrix for Tapered Beams (Discussions)". J.of Struct Div. ASCE. Dec. 1984.
- 44) D.L.Karabalis & D.E.Beskos. "Static, Dynamic & Stability Analysis of Structures Composed of Tapered Beams". Computers & Structures Vol 16. 1983.
- 45) O.C.Zienkiewicz. "The Finite Element Method". McGraw-Hill Books. 1977.

- 46) E.Hinton & D.R.J.Owen. "An Introduction to Finite Element Computations". Pineridge Press. 1979.
- 47) O.C.Zienkiewicz. "The Finite Element Method in Structural & Continuum Mechanics". McGraw-Hill Books. 1967.
- 48) J.M.Gere & W.Weaver. "Analysis of Framed Structures". Van Nostrand Books.New York. 1965.
- 49) B.Nath. "Fundamentals of Finite Elements for Engineers". Pitman Press. 1974.
- 50) C.F.Gerald. "Applied Numerical Analysis". Addison-Wesley Publishing Co. 1978.
- 51) M.F.Rubinstein. "Matrix Computer Analysis of Structures". Prentice Hall Inc. 1966.
- 52) R.C.Coates, M.G.Coutie, F.K.Kong. "Structural Analysis". Nelson Press. 1972.
- 53) D.M.Monro "Fortran 77" Arnold Books. 1982.

- 54) Digital "VAX User Manual"
Digital Publishings. 1985.
- 55) C.J.Tranter. "Bessel Functions with some Physical
Applications".
Pitman Press. 1968.
- 56) K.A.Stroud. "Engineering Mathematics Part 2".
Longman Press. 1984.
- 57) British Standard Institution. "Tensile Testing of Metals (including
aerospace materials) BS118".
1987.
- 58) R.K.Livesley. "Matrix Methods of Structural Analysis"
Pergamon Press. 1969.
- 59) D.J.Just. private correspondance

Appendix 1.

Inversion of $[C]_B$ for Taper.

For Tapered Section.

$$[C]^{-1} = \begin{bmatrix} C_{11} & C_{12} & C_{13} & C_{14} \\ C_{21} & C_{22} & C_{23} & C_{24} \\ C_{31} & C_{32} & C_{33} & C_{34} \\ C_{41} & C_{42} & C_{43} & C_{44} \end{bmatrix}$$

where

$$C_{11} = \frac{(G_2 h_2 - H_2 g_2) + (H_2 g_1 - G_2 h_1) + L(g_2 h_1 - g_1 h_2)}{D}$$

$$C_{12} = \frac{(G_2 H_1 - G_1 H_2) + L(G_1 h_2 - H_1 g_2)}{D}$$

$$C_{13} = \frac{G_1(h_1 - h_2) - H_1(g_1 - g_2)}{D}$$

$$C_{14} = \frac{(G_1 H_2 - G_2 H_1) + L(H_1 g_1 - G_1 h_1)}{D}; \quad C_{21} = \frac{g_1 h_2 - g_2 h_1}{D}$$

$$C_{22} = \frac{g_2(H_1 - H_2) - h_2(G_1 - G_2)}{D}; \quad C_{23} = -C_{21}$$

$$C_{24} = \frac{g_1(H_2 - H_1) - h_1(G_2 - G_1)}{D}; \quad C_{31} = \frac{h_1 - h_2}{D}$$

$$C_{32} = \frac{H_2 - H_1 - L h_2}{D}; \quad C_{33} = -C_{31}; \quad C_{34} = \frac{H_1 - H_2 + L h_1}{D}$$

$$C_{41} = \frac{g_2 - g_1}{D}; \quad C_{42} = \frac{G_1 - G_2 + L g_2}{D}; \quad C_{43} = -C_{41}$$

$$C_{44} = \frac{G_2 - G_1 + L g_1}{D}$$

and

$$D = (G_1 h_1 - H_1 g_1) + (H_1 g_2 - G_1 h_2) + (G_2 h_2 - H_2 g_2) \\ + (H_2 g_1 - G_2 h_1) + L(g_2 h_1 - g_1 h_2)$$

Appendix 2.

Calculation of Internal forces
for Tangential Stiffness
Matrix.

$$P = \int_0^L [\bar{B}]^T \{\sigma\} dx.$$

On evaluation gives;

$$S_1 = \frac{EA}{70} \left\{ \frac{9}{L^3} (v_1 - v_2) [8(v_1 - v_2)^2 + 3L(v_1 - v_2)(\theta_1 + \theta_2) + L^2(\theta_1^2 + \theta_2^2)] \right. \\ \left. + \frac{1}{4} [3\theta_1\theta_2(\theta_1 + \theta_2) - (\theta_1^3 + \theta_2^3)] \right\} \\ - \frac{EA}{10L^2} (u_1 - u_2) [12(v_1 - v_2) + L(\theta_1 + \theta_2)] \\ + \frac{EI}{L^2} [12(v_1 - v_2) + 6L(\theta_1 + \theta_2)].$$

$$M_1 = \frac{EA}{280} \left\{ \frac{3}{L^2} (v_1 - v_2) [12(v_1 - v_2)(v_1 - v_2 + L\theta_1) + L^2(\theta_2^2 + 2\theta_1\theta_2 - \theta_1^2)] \right. \\ \left. + L[\theta_1^2(8\theta_1 - 3\theta_2) + \theta_2^2(2\theta_1 - \theta_2)] \right\} \\ - \frac{EA}{30L} (u_1 - u_2) [3(v_1 - v_2) + L(4\theta_1 - \theta_2)] \\ + \frac{EI}{L^2} [6(v_1 - v_2) + 2L(2\theta_1 + \theta_2)]$$

$$S_2 = -S_1.$$

$$\begin{aligned}
 M_2 = \frac{EA}{280} & \left\{ \frac{3}{L^2} (v_1 - v_2) [12(v_1 - v_2)(v_1 - v_2 + L\theta_2) + L^2(\theta_1^2 + 2\theta_1\theta_2 - \theta_2^2)] \right. \\
 & \left. + L[\theta_2^2(8\theta_2 - 3\theta_1) + \theta_1^2(2\theta_2 - \theta_1)] \right\} \\
 & - \frac{EA}{30L} (u_1 - u_2) [3(v_1 - v_2) + L(\theta_2 - \theta_1)] \\
 & + \frac{EI}{L^2} [6(v_1 - v_2) + 2L(\theta_1 + 2\theta_2)].
 \end{aligned}$$

$$\begin{aligned}
 P_1 = -\frac{EA}{30L^2} & [18(v_1 - v_2)^2 + 3L(v_1 - v_2)(\theta_1 + \theta_2) + L^2(2\theta_1^2 - \theta_1\theta_2 + 2\theta_2^2)] \\
 & + \frac{EA}{L} (u_1 - u_2).
 \end{aligned}$$

$$P_2 = -P_1.$$

Appendix 3.

Listing of Computer Program
in FORTRAN.

29-Jul-1988 19:55:12#1#DUA3:[BAWAGS]NONPRIS.FOR;60

0001 PROGRAM COUPLING FACTORS

0002 C

0003 C

0004 C

0005 C

0006 C THIS PROGRAM IS TO ANALYSE LARGE CIVIL ENGINEERING

0007 C =====

0008 C PLAIN FRAMES WITH THE USE OF FINITE

0009 C =====

0010 C ELEMENT TECHNIQUES

0011 C =====

0012 C

0013 C

0014 C

BY

0015 C

==

0016 C

0017 C

0018 C

G. S. BAWA VERSION 1.1

0019 C

=====

0020 C

0021 C

0022 C

0023 C

0024 DOUBLE PRECISION X(100),Y(100),XX(100),YY(100),L(100),CA(100)

0025 * CB(100),CL(100),CM(100),EI(100),EA(100),TT(100),

0026 * A(100),B(100),C(100),D(100),E(100),F(100),G(100),

0027 * S(300,300),LL(300),P(100),GG(100),W(100),V(100),

0028 * SS(100),MA(100),MB(100),U(100),BB(300),CW(100),

0029 * SW(100),MEM(4,4),FDR(4),CC(4,4),Q(4,4),W1(300),

0030 * W2(300),R1(300),R2(300),ZZ(300),A1(100),A2(100),

0031 * AMDA(100),WKS2(300),A3(100),A4(100),P1(100),P2(100),

0032 * CT11(100),CT22(100),CT32(100),CT33(100),CT42(100),

0033 * CT43(100),CT44(100),LX(300),UDL(100),XL(300),XLX(300),

0034 * XM1(100),XM2(100)

0035

0036 INTEGER KR(100),JR(100),IDDF(300)

0037

0038 WRITE(6,4000)

0039 PRINT*, '-----'

0040 PRINT*, ' '

0041 PRINT*, 'THIS PROGRAM IS FOR THE ANALYSIS OF PLANE FRAMEWORK

0042 PRINT*, 'WITH THE USE OF FINITE ELEMENT TECHNIQUES. '

0043 PRINT*, ' '

0044 PRINT*, 'THE FINAL PRINTOUT GIVING THE JOINT DEFLECTIONS, MEM

0045 PRINT*, 'DIRCETIONAL COSINES AND FORCES. '

0046 PRINT*, ' '

0047 PRINT*, '-----'

0048 PRINT*, ' '

0049 PRINT*, 'ENTER 1 TO CONTINUE'

0050 READ*, Z

0051 WRITE(6,4000)

0052 OPEN(6, FILE='PRISRES', STATUS='NEW', ERR=10000)

0053 OPEN(5, FILE='PRISINPUT', STATUS='OLD', ERR=10000)

0054 WRITE(6,2000)

0055 READ(5,*), NJ

0056 WRITE(6,2100)NJ

0057


```

0058      I=1
0059      10      READ(5,*)X(I),Y(I),IDOF(3*I-2),IDOF(3*I-1),IDOF(3*I),
0060      *          XLX(3*I-2),XLX(3*I-1),XLX(3*I)
0061      IF (I.LT.NJ) GOTO 15
0062      IF (I.EQ.NJ) GOTO 20
0063      15      I=I+1
0064      GOTO 10
0065      20      CONTINUE
0066
0067      I=1
0068      22      XL(I)=XLX(I)
0069      IF (I.LT.(3*NJ)) GOTO 25
0070      IF (I.EQ.(3*NJ)) GOTO 27
0071      25      I=I+1
0072      GOTO 22
0073      27      CONTINUE
0074
0075      I=1
0076      31      WRITE(6,2200)I,X(I),Y(I)
0077      IF (I.LT.NJ) GOTO 32
0078      IF (I.EQ.NJ) GOTO 33
0079      32      I=I+1
0080      GOTO 31
0081      33      CONTINUE
0082
0083      WRITE(6,2300)
0084
0085      I=1
0086      34      WRITE(6,2400)I,IDOF(3*I-2),IDOF(3*I-1),IDOF(3*I)
0087      IF (I.LT.NJ) GOTO 35
0088      IF (I.EQ.NJ) GOTO 36
0089      35      I=I+1
0090      GOTO 34
0091      36      CONTINUE
0092
0093      WRITE(6,2500)
0094
0095      I=1
0096      37      WRITE(6,2600)I,XLX(3*I-2),XLX(3*I-1),XLX(3*I)
0097      IF (I.LT.NJ) GOTO 38
0098      IF (I.EQ.NJ) GOTO 39
0099      38      I=I+1
0100      GOTO 37
0101      39      CONTINUE
0102
0103      READ(5,*)NM
0104      WRITE(6,2700)NM
0105
0106      I=1
0107      40      READ(5,*)KR(I),JR(I),EI(I),EA(I),UDL(I)
0108      C
0109      C      CALCULATION OF MEMBER LENGTH L(I)
0110      C
0111      L(I)=(((X(JR(I))-X(KR(I)))**2)+((Y(JR(I))-Y(KR(I)))**2))**0.5
0112      WRITE(6,2800)I,KR(I),JR(I),L(I)
0113
0114      C

```



```

0115      C      CALCULATION FOR DIRECTIONAL COSINES FOR MEMBER I
0116      C
0117          IF (Y(JR(I)).GT.Y(KR(I))) GOTO 50
0118          IF (Y(JR(I)).LT.Y(KR(I))) GOTO 60
0119          IF (Y(JR(I)).EQ.Y(KR(I))) GOTO 70
0120          IF (X(JR(I)).EQ.X(KR(I))) GOTO 80
0121          IF (X(JR(I)).EQ.X(KR(I)).AND.Y(JR(I)).LT.Y(KR(I))) GOTO 85
0122      50      AA=(X(JR(I))-X(KR(I)))
0123             O=(Y(JR(I))-Y(KR(I)))
0124             CA(I)=AA/L(I)
0125             CB(I)=O/L(I)
0126             GOTO 90
0127      60      AA=(X(JR(I))-X(KR(I)))
0128             O=(Y(KR(I))-Y(JR(I)))
0129             CA(I)=AA/L(I)
0130             CB(I)=-O/L(I)
0131             GOTO 90
0132      70      CA(I)=1
0133             CB(I)=0
0134             GOTO 90
0135      80      CA(I)=0
0136             CB(I)=1
0137             GOTO 90
0138      85      CA(I)=0
0139             CB(I)=-1
0140             GOTO 90
0141      90      CL(I)=-CB(I)
0142             CM(I)=CA(I)
0143      C
0144      C      NON-NODAL FORCES
0145      C
0146             S1=UDL(I)*L(I)/2
0147             XM1(I)=UDL(I)*L(I)*L(I)/12
0148             S2=S1
0149             XM2(I)=-XM1(I)
0150
0151             FX1=S1*CB(I)
0152             FY1=S1*CM(I)
0153             XM1(I)=XM1(I)
0154             FX2=S2*CB(I)
0155             FY2=S2*CM(I)
0156             XM2(I)=XM2(I)
0157
0158             XL(3*KR(I)-2)=XL(3*KR(I)-2)+FX1
0159             XL(3*KR(I)-1)=XL(3*KR(I)-1)+FY1
0160             XL(3*KR(I))=XL(3*KR(I))+XM1(I)
0161             XL(3*JR(I)-2)=XL(3*JR(I)-2)+FX2
0162             XL(3*JR(I)-1)=XL(3*JR(I)-1)+FY2
0163             XL(3*JR(I))=XL(3*JR(I))+XM2(I)
0164      C
0165      C      CALCULATION OF THE GLOBAL STIFFNESS MATRIX FOR MEMBER I
0166      C
0167             A(I)=((EA(I)/L(I))*(CA(I)**2))+((12*EI(I)/(L(I)**3))*(CL(I)
0168             B(I)=((EA(I)/L(I))*(CB(I)**2))+((12*EI(I)/(L(I)**3))*(CM(I)
0169             UU=((EA(I)/L(I))*CA(I)*CB(I))
0170             VV=((12*EI(I)/(L(I)**3))*(CL(I))*(CM(I)))
0171             C(I)=UU+VV

```


29-Jul-1988 19:55:12#1#DUA3:[BAWAGS]NONPRIS.FOR;60

```

0172      D(I)=(6*EI(I)/(L(I)**2))*CL(I)
0173      E(I)=(6*EI(I)/(L(I)**2))*CM(I)
0174      F(I)=(4*EI(I)/L(I))
0175      G(I)=(F(I)/2)
0176      C
0177      C      CALCULATION OF THE OVERALL STIFFNESS MATRIX FOR
0178      C      MEMBER
0179      C
0180      S((3*KR(I)-2),(3*KR(I)-2))=S((3*KR(I)-2),(3*KR(I)-2))+A(I)
0181      S((3*KR(I)-1),(3*KR(I)-1))=S((3*KR(I)-1),(3*KR(I)-1))+B(I)
0182      S((3*KR(I)-1),(3*KR(I)-2))=S((3*KR(I)-1),(3*KR(I)-2))+C(I)
0183      S((3*KR(I)),(3*KR(I)))=S((3*KR(I)),(3*KR(I)))+F(I)
0184      S((3*KR(I)),(3*KR(I)-1))=S((3*KR(I)),(3*KR(I)-1))+E(I)
0185      S((3*KR(I)),(3*KR(I)-2))=S((3*KR(I)),(3*KR(I)-2))+D(I)
0186      S((3*JR(I)-2),(3*JR(I)-2))=S((3*JR(I)-2),(3*JR(I)-2))+A(I)
0187      S((3*JR(I)-1),(3*JR(I)-1))=S((3*JR(I)-1),(3*JR(I)-1))+B(I)
0188      S((3*JR(I)-1),(3*JR(I)-2))=S((3*JR(I)-1),(3*JR(I)-2))+C(I)
0189      S((3*JR(I)),(3*JR(I)))=S((3*JR(I)),(3*JR(I)))+F(I)
0190      S((3*JR(I)),(3*JR(I)-1))=S((3*JR(I)),(3*JR(I)-1))-E(I)
0191      S((3*JR(I)),(3*JR(I)-2))=S((3*JR(I)),(3*JR(I)-2))-D(I)
0192      S((3*JR(I)-2),(3*KR(I)-2))=S((3*JR(I)-2),(3*KR(I)-2))-A(I)
0193      S((3*JR(I)-2),(3*KR(I)-1))=S((3*JR(I)-2),(3*KR(I)-1))-C(I)
0194      S((3*JR(I)-2),(3*KR(I)))=S((3*JR(I)-2),(3*KR(I)))-D(I)
0195      S((3*JR(I)-1),(3*KR(I)-2))=S((3*JR(I)-1),(3*KR(I)-2))-C(I)
0196      S((3*JR(I)-1),(3*KR(I)-1))=S((3*JR(I)-1),(3*KR(I)-1))-B(I)
0197      S((3*JR(I)-1),(3*KR(I)))=S((3*JR(I)-1),(3*KR(I)))-E(I)
0198      S((3*JR(I)),(3*KR(I)-2))=S((3*JR(I)),(3*KR(I)-2))+D(I)
0199      S((3*JR(I)),(3*KR(I)-1))=S((3*JR(I)),(3*KR(I)-1))+E(I)
0200      S((3*JR(I)),(3*KR(I)))=S((3*JR(I)),(3*KR(I)))+G(I)
0201      IF (I.LT.NM) GOTO 100
0202      IF (I.EQ.NM) GOTO 110
0203      100      I=I+1
0204      GOTO 40
0205      110      CONTINUE
0206
0207      WRITE(6,2900)
0208
0209      I=1
0210      111      WRITE(6,3000)I,EI(I),EA(I)
0211      IF (I.LT.NM) GOTO 112
0212      IF (I.EQ.NM) GOTO 113
0213      112      I=I+1
0214      GOTO 111
0215      113      CONTINUE
0216
0217      READ(5,*)ICON
0218      PRINT*, '
0219      PRINT*, '
0220      PRINT*, '
0221      PRINT*, '
0222      PRINT*, '
0223      PRINT*, '
0224      PRINT*, '
0225      PRINT*, '
0226      PRINT*, '
0227      PRINT*, '
0228      PRINT*, '

```

PROGRAM RUNNING

```
0229          PRINT*, '      '  
0230          PRINT*, '      '  
0231          PRINT*, '      '  
0232          C  
0233          C      RESTRAINT BOUNDARY CONDITIONS FOR MATRIX  
0234          C  
0235          I=1  
0236          114      LL(I)=XL(I)  
0237          IF (I.LT.(3*NJ)) GOTO 115  
0238          IF (I.EQ.(3*NJ)) GOTO 116  
0239          115      I=I+1  
0240          GOTO 114  
0241          116      CONTINUE  
0242  
0243          I=1  
0244          121      IF (IDOF(I).EQ.0) GOTO 122  
0245          IF (IDOF(I).EQ.1) GOTO 123  
0246          122      S(I,I)=S(I,I)*1.0E20  
0247          LL(I)=S(I,I)*IDOF(I)  
0248          123      IF (I.EQ.3*NJ) GOTO 124  
0249          I=I+1  
0250          GOTO 121  
0251          124      CONTINUE  
0252  
0253  
0254          C  
0255          C      DECOMPOSITION  
0256          C  
0257  
0258          J=0  
0259          160      J=J+1  
0260          I=J-1  
0261          170      I=I+1  
0262          IF (I.EQ.J) GOTO 210  
0263          K=0  
0264          SUM=0  
0265          180      K=K+1  
0266          IF (K.NE.J) GOTO 190  
0267          IF (K.EQ.J) GOTO 200  
0268          190      SUM=SUM+(S(I,K)*S(J,K))  
0269          GOTO 180  
0270          200      S(I,J)=(S(I,J)-SUM)/S(J,J)  
0271          GOTO 245  
0272          210      K=0  
0273          SUM=0  
0274          220      K=K+1  
0275          IF (K.NE.J) GOTO 230  
0276          IF (K.EQ.J) GOTO 240  
0277          230      SUM=SUM+(S(I,K)**2)  
0278          GOTO 220  
0279          240      S(I,I)=((S(I,I)-SUM)**0.5)  
0280          245      IF (I.NE.(3*NJ)) GOTO 170  
0281          IF (I.EQ.(3*NJ)) GOTO 250  
0282          250      IF (J.NE.(3*NJ)) GOTO 160  
0283          IF (J.EQ.(3*NJ)) GOTO 260  
0284          260      CONTINUE  
0285
```



```
0286 C
0287 C FORWARD SUBSTITUTION
0288
0289 C
0290 I=1
0291 263 BB(I)=LL(I)
0292 IF (I.LT.(3*NJ)) GOTO 264
0293 IF (I.EQ.(3*NJ)) GOTO 267
0294 264 I=I+1
0295 GOTO 263
0296 267 CONTINUE
0297 I=0
0298 270 I=I+1
0299 J=0
0300 SUM=0
0301 280 J=J+1
0302 IF (I.EQ.J) GOTO 290
0303 SUM=SUM+BB(J)*S(I,J)
0304 GOTO 280
0305 290 BB(I)=(BB(I)-SUM)/S(I,I)
0306 IF (I.NE.(3*NJ)) GOTO 270
0307 IF (I.EQ.(3*NJ)) GOTO 300
0308 300 CONTINUE
0309
0310 C
0311 C BACK SUBSTITUTION
0312 C
0313
0314 I=(3*NJ)+1
0315 310 I=I-1
0316 J=(3*NJ)+1
0317 SUM=0
0318 320 J=J-1
0319 IF (I.EQ.J) GOTO 330
0320 SUM=SUM+S(J,I)*BB(J)
0321 GOTO 320
0322 330 BB(I)=(BB(I)-SUM)/S(I,I)
0323 IF (I.NE.1) GOTO 310
0324 IF (I.EQ.1) GOTO 340
0325 340 CONTINUE
0326
0327 C
0328 C MEMBER FORCES P, S, M1, M2.
0329 C
0330
0331 I=1
0332 380 FN1=-((EA(I)/L(I))*CA(I)*BB(3*KR(I)-2))
0333 FN2=-((EA(I)/L(I))*CB(I)*BB(3*KR(I)-1))
0334 FN3=((EA(I)/L(I))*CA(I)*BB(3*JR(I)-2))
0335 FN4=((EA(I)/L(I))*CB(I)*BB(3*JR(I)-1))
0336 P1(I)=FN1+FN2+FN3+FN4
0337 FN5=-((12*EI(I)/(L(I)**3))*CL(I)*BB(3*KR(I)-2))
0338 FN6=-((12*EI(I)/(L(I)**3))*CM(I)*BB(3*KR(I)-1))
0339 FN7=-((6*EI(I)/(L(I)**2))*BB(3*KR(I)))
0340 FN8=((12*EI(I)/(L(I)**3))*CL(I)*BB(3*JR(I)-2))
0341 FN9=((12*EI(I)/(L(I)**3))*CM(I)*BB(3*JR(I)-1))
0342 FN10=-((6*EI(I)/(L(I)**2))*BB(3*JR(I)))
```



```
0343      SS(I)=FN5+FN6+FN7+FN8+FN9+FN10
0344      FN11=((6*EI(I)/(L(I)**2))*CL(I)*BB(3*KR(I)-2))
0345      FN12=((6*EI(I)/(L(I)**2))*CM(I)*BB(3*KR(I)-1))
0346      FN13=((4*EI(I)/L(I))*BB(3*KR(I)))
0347      FN14=-((6*EI(I)/(L(I)**2))*CL(I)*BB(3*JR(I)-2))
0348      FN15=-((6*EI(I)/(L(I)**2))*CM(I)*BB(3*JR(I)-1))
0349      FN16=((2*EI(I)/L(I))*BB(3*JR(I)))
0350      MA(I)=-((FN11+FN12+FN13+FN14+FN15+FN16)+(UDL(I)*L(I)*L(I)/12)
0351      FN17=((6*EI(I)/(L(I)**2))*CL(I)*BB(3*KR(I)-2))
0352      FN18=((6*EI(I)/(L(I)**2))*CM(I)*BB(3*KR(I)-1))
0353      FN19=((2*EI(I)/L(I))*BB(3*KR(I)))
0354      FN20=-((6*EI(I)/(L(I)**2))*CL(I)*BB(3*JR(I)-2))
0355      FN21=-((6*EI(I)/(L(I)**2))*CM(I)*BB(3*JR(I)-1))
0356      FN22=((4*EI(I)/L(I))*BB(3*JR(I)))
0357      MB(I)=FN17+FN18+FN19+FN20+FN21+FN22-((-UDL(I)*L(I)*L(I)/12)
0358      IF (I.LT.NM) GOTO 390
0359      IF (I.EQ.NM) GOTO 400
0360      390      I=I+1
0361              GOTO 380
0362      400      CONTINUE
0363
0364      WRITE(6,3100)
0365      WRITE(6,3150)
0366      WRITE(6,3175)
0367      WRITE(6,3180)
0368
0369      I=1
0370      410      WRITE(6,3200)I,CA(I),CB(I),CL(I),CM(I)
0371              IF (I.LT.NM) GOTO 420
0372              IF (I.EQ.NM) GOTO 430
0373      420      I=I+1
0374              GOTO 410
0375      430      CONTINUE
0376
0377      WRITE(6,3300)
0378
0379      I=1
0380      440      WRITE(6,3400)I,BB(3*I-2),BB(3*I-1),BB(3*I)
0381              IF (I.LT.NJ) GOTO 450
0382              IF (I.EQ.NJ) GOTO 460
0383      450      I=I+1
0384              GOTO 440
0385      460      CONTINUE
0386
0387      WRITE(6,3500)
0388
0389      I=1
0390      470      WRITE(6,3600)I,SS(I),P1(I),MA(I),MB(I)
0391              IF (I.LT.NM) GOTO 480
0392              IF (I.EQ.NM) GOTO 490
0393      480      I=I+1
0394              GOTO 470
0395      490      CONTINUE
0396
0397      WRITE(6,3700)
0398
0399      C
```



```

0400      C
0401      C          NON-LINEAR ANALYSIS STARTS HERE (CONSTANT AXIAL FORCE)
0402      C
0403      C
0404
0405          J=0
0406      500      J=J+1
0407          I=J-1
0408      510      I=I+1
0409          IF (I.EQ.J) GOTO 520
0410          S(I,J)=0
0411          GOTO 530
0412      520      S(I,I)=0
0413      530      IF (I.NE.(3*NJ)) GOTO 510
0414          IF (I.EQ.(3*NJ)) GOTO 540
0415      540      IF (J.NE.(3*NJ)) GOTO 500
0416          IF (J.EQ.(3*NJ)) GOTO 550
0417      550      CONTINUE
0418
0419          I=1
0420      552      XL(I)=XLX(I)
0421          IF (I.LT.(3*NJ)) GOTO 555
0422          IF (I.EQ.(3*NJ)) GOTO 557
0423      555      I=I+1
0424          GOTO 552
0425      557      CONTINUE
0426
0427      C
0428      C          CALCULATION OF THE LOCAL STIFFNESS MATRIX
0429      C          FOR A NON-LINEAR MEMBER
0430      C
0431
0432
0433          I=1
0434      560      IF (P1(I).EQ.0) GOTO 570
0435          IF (P1(I).LT.0) GOTO 564
0436          IF (P1(I).GT.0) GOTO 566
0437
0438      564      P1(I)=-P1(I)
0439          W(I)=((P1(I)/EI(I))*0.5)
0440          QQ(I)=W(I)*L(I)
0441          CW(I)=COS(QQ(I))
0442          SW(I)=SIN(QQ(I))
0443          V(I)=-W(I)*((QQ(I)*SW(I))+(2*CW(I))-2)
0444          CT11(I)=EA(I)/L(I)
0445          CT22(I)=(P1(I)*W(I)*W(I)*SW(I)/V(I))
0446          CT32(I)=(P1(I)*W(I)*(1-CW(I))/V(I))
0447          CT33(I)=(P1(I)*(SW(I)-(QQ(I)*CW(I)))/V(I))
0448          CT42(I)=CT32(I)
0449          CT43(I)=(P1(I)*(QQ(I)-SW(I))/V(I))
0450          CT44(I)=CT33(I)
0451
0452      C
0453      C          NON-NODAL LOADING SUBROUTINE
0454      C
0455
0456          VN=(2*W(I)*(1-CW(I)))-(W(I)*W(I)*L(I)*SW(I))

```



```

0457      CN11=(W(I)-(W(I)*W(I)*L(I)*SW(I))-(W(I)*CW(I)))/VN
0458      CN12=((W(I)*L(I)*CW(I))-SW(I))/VN
0459      CN13=(W(I)*(1-CW(I)))/VN
0460      CN14=(SW(I)-(W(I)*L(I)))/VN
0461      CN21=W(I)*W(I)*SW(I)/VN
0462      CN22=CN13
0463      CN23=-CN21
0464      CN24=CN13
0465      CN31=-CN21/W(I)
0466      CN32=CN11/W(I)
0467      CN33=CN21/W(I)
0468      CN34=-CN13/W(I)
0469      CN41=CN13
0470      CN42=-CN12
0471      CN43=-CN13
0472      CN44=-CN14
0473
0474      SNN1=(L(I)*CN11)+(CN21*L(I)*L(I)/2)
0475      SNN2=(CN31*(1-CW(I))/W(I)+(CN41*SW(I)/W(I))
0476      S1=UDL(I)*(SNN1+SNN2)
0477      SNN3=(L(I)*CN12)+(CN22*L(I)*L(I)/2)
0478      SNN4=(CN32*(1-CW(I))/W(I)+(CN42*SW(I)/W(I))
0479      XM1(I)=UDL(I)*(SNN3+SNN4)
0480      SNN5=(L(I)*CN13)+(CN23*L(I)*L(I)/2)
0481      SNN6=(CN33*(1-CW(I))/W(I)+(CN43*SW(I)/W(I))
0482      S2=UDL(I)*(SNN5+SNN6)
0483      SNN7=(L(I)*CN14)+(CN24*L(I)*L(I)/2)
0484      SNN8=(CN34*(1-CW(I))/W(I)+(CN44*SW(I)/W(I))
0485      XM2(I)=UDL(I)*(SNN7+SNN8)
0486      C
0487      C      CONVERSION TO GLOBAL COORDINATES
0488      C
0489      FX1=S1*CB(I)
0490      FY1=S1*CM(I)
0491      XM1(I)=XM1(I)
0492      FX2=S2*CB(I)
0493      FY2=S2*CM(I)
0494      XM2(I)=XM2(I)
0495      XL(3*KR(I)-2)=XL(3*KR(I)-2)+FX1
0496      XL(3*KR(I)-1)=XL(3*KR(I)-1)+FY1
0497      XL(3*KR(I))=XL(3*KR(I))+XM1(I)
0498      XL(3*JR(I)-2)=XL(3*JR(I)-2)+FX2
0499      XL(3*JR(I)-1)=XL(3*JR(I)-1)+FY2
0500      XL(3*JR(I))=XL(3*JR(I))+XM2(I)
0501
0502      P1(I)=-P1(I)
0503      GOTO 572
0504
0505
0506      566      W(I)=((P1(I)/EI(I))*0.5)
0507      QG(I)=W(I)*L(I)
0508      CW(I)=COSH(QG(I))
0509      SW(I)=SINH(QG(I))
0510      V(I)=(2*W(I)*(1-CW(I)))+(QG(I)*W(I)*SW(I))
0511      CT11(I)=EA(I)/L(I)
0512      CT22(I)=(P1(I)*W(I)*W(I)*SW(I)/V(I))
0513      CT32(I)=-P1(I)*W(I)*(1-CW(I))/V(I)
    
```



```

0514      CT33(I)=- (P1(I)*(SW(I)-(QQ(I)*CW(I)))/V(I))
0515      CT42(I)=CT32(I)
0516      CT43(I)=- (P1(I)*(QQ(I)-SW(I))/V(I))
0517      CT44(I)=CT33(I)
0518
0519      C
0520      C      NON-NODAL LOADING SUBROUTINE
0521      C
0522
0523      CN11=((W(I)*W(I)*L(I)*SW(I))-(W(I)*CW(I))+W(I))/V(I)
0524      CN12=((W(I)*L(I)*CW(I))-SW(I))/V(I)
0525      CN13=(W(I)*(1-CW(I)))/V(I)
0526      CN14=(SW(I)-(W(I)*L(I)))/V(I)
0527      CN21=-(W(I)*W(I)*SW(I))/V(I)
0528      CN22=CN13
0529      CN23=-CN21
0530      CN24=CN13
0531      CN31=-CN21/W(I)
0532      CN32=CN11/W(I)
0533      CN33=CN21/W(I)
0534      CN34=-CN13/W(I)
0535      CN41=CN13
0536      CN42=-CN12
0537      CN43=-CN13
0538      CN44=-CN14
0539
0540      SNN9=(L(I)*CN11)+(CN21*L(I)*L(I)/2)
0541      SNN10=(CN31*(CW(I)-1)/W(I))+(CN41*SW(I)/W(I))
0542      S1=UDL(I)*(SNN9+SNN10)
0543      SNN11=(L(I)*CN12)+(CN22*L(I)*L(I)/2)
0544      SNN12=(CN32*(CW(I)-1)/W(I))+(CN42*SW(I)/W(I))
0545      XM1(I)=UDL(I)*(SNN11+SNN12)
0546      SNN13=(L(I)*CN13)+(CN23*L(I)*L(I)/2)
0547      SNN14=(CN33*(CW(I)-1)/W(I))+(CN43*SW(I)/W(I))
0548      S2=UDL(I)*(SNN13+SNN14)
0549      SNN15=(L(I)*CN14)+(CN24*L(I)*L(I)/2)
0550      SNN16=(CN34*(CW(I)-1)/W(I))+(CN44*SW(I)/W(I))
0551      XM2(I)=UDL(I)*(SNN15+SNN16)
0552      C
0553      C      CONVERSION TO GLOBAL COORDINATES
0554      C
0555      FX1=S1*CB(I)
0556      FY1=S1*CM(I)
0557      XM1(I)=XM1(I)
0558      FX2=S2*CB(I)
0559      FY2=S2*CM(I)
0560      XM2(I)=XM2(I)
0561      XL(3*KR(I)-2)=XL(3*KR(I)-2)+FX1
0562      XL(3*KR(I)-1)=XL(3*KR(I)-1)+FY1
0563      XL(3*KR(I))=XL(3*KR(I))+XM1(I)
0564      XL(3*JR(I)-2)=XL(3*JR(I)-2)+FX2
0565      XL(3*JR(I)-1)=XL(3*JR(I)-1)+FY2
0566      XL(3*JR(I))=XL(3*JR(I))+XM2(I)
0567
0568      GOTO 572
0569
0570

```



```

0571      570      CT11(I)=EA(I)/L(I)
0572      CT22(I)=12*EI(I)/(L(I)**3)
0573      CT32(I)=6*EI(I)/(L(I)**2)
0574      CT33(I)=4*EI(I)/L(I)
0575      CT42(I)=CT32(I)
0576      CT43(I)=2*EI(I)/L(I)
0577      CT44(I)=CT33(I)
0578
0579
0580      C
0581      C      CALCULATION FOR GLOBAL STIFFNESS MATRIX FOR
0582      C      THE NON-LINEAR CASE
0583      C
0584
0585      572      A(I)=(CT11(I)*CA(I)*CA(I))+(CT22(I)*CL(I)*CL(I))
0586      B(I)=(CT11(I)*CB(I)*CB(I))+(CT22(I)*CM(I)*CM(I))
0587      C(I)=(CT11(I)*CA(I)*CB(I))+(CT22(I)*CL(I)*CM(I))
0588      D(I)=(CT32(I)*CL(I))
0589      E(I)=(CT32(I)*CM(I))
0590      F(I)=(CT33(I))
0591      G(I)=(CT43(I))
0592
0593      C
0594      C      GLOBAL STIFFNESS MATRIX
0595      C
0596
0597
0598      S((3*KR(I)-2),(3*KR(I)-2))=S((3*KR(I)-2),(3*KR(I)-2))+A(I)
0599      S((3*KR(I)-1),(3*KR(I)-1))=S((3*KR(I)-1),(3*KR(I)-1))+B(I)
0600      S((3*KR(I)-1),(3*KR(I)-2))=S((3*KR(I)-1),(3*KR(I)-2))+C(I)
0601      S((3*KR(I)),(3*KR(I)))=S((3*KR(I)),(3*KR(I)))+F(I)
0602      S((3*KR(I)),(3*KR(I)-1))=S((3*KR(I)),(3*KR(I)-1))+E(I)
0603      S((3*KR(I)),(3*KR(I)-2))=S((3*KR(I)),(3*KR(I)-2))+D(I)
0604      S((3*JR(I)-2),(3*JR(I)-2))=S((3*JR(I)-2),(3*JR(I)-2))+A(I)
0605      S((3*JR(I)-1),(3*JR(I)-1))=S((3*JR(I)-1),(3*JR(I)-1))+B(I)
0606      S((3*JR(I)-1),(3*JR(I)-2))=S((3*JR(I)-1),(3*JR(I)-2))+C(I)
0607      S((3*JR(I)),(3*JR(I)))=S((3*JR(I)),(3*JR(I)))+F(I)
0608      S((3*JR(I)),(3*JR(I)-1))=S((3*JR(I)),(3*JR(I)-1))-E(I)
0609      S((3*JR(I)),(3*JR(I)-2))=S((3*JR(I)),(3*JR(I)-2))-D(I)
0610      S((3*JR(I)-2),(3*KR(I)-2))=S((3*JR(I)-2),(3*KR(I)-2))-A(I)
0611      S((3*JR(I)-2),(3*KR(I)-1))=S((3*JR(I)-2),(3*KR(I)-1))-C(I)
0612      S((3*JR(I)-2),(3*KR(I)))=S((3*JR(I)-2),(3*KR(I)))-D(I)
0613      S((3*JR(I)-1),(3*KR(I)-2))=S((3*JR(I)-1),(3*KR(I)-2))-C(I)
0614      S((3*JR(I)-1),(3*KR(I)-1))=S((3*JR(I)-1),(3*KR(I)-1))-B(I)
0615      S((3*JR(I)-1),(3*KR(I)))=S((3*JR(I)-1),(3*KR(I)))-E(I)
0616      S((3*JR(I)),(3*KR(I)-2))=S((3*JR(I)),(3*KR(I)-2))+D(I)
0617      S((3*JR(I)),(3*KR(I)-1))=S((3*JR(I)),(3*KR(I)-1))+E(I)
0618      S((3*JR(I)),(3*KR(I)))=S((3*JR(I)),(3*KR(I)))+G(I)
0619      IF (I.LT.NM) GOTO 575
0620      IF (I.EQ.NM) GOTO 580
0621      575      I=I+1
0622      GOTO 560
0623      580      CONTINUE
0624
0625      C
0626      C      RESTRAINTS CONDITIONS
0627      C

```



```

0628          I=1
0629    577    LL(I)=XL(I)
0630          IF (I.LT.(3*NJ)) GOTO 578
0631          IF (I.EQ.(3*NJ)) GOTO 579
0632    578    I=I+1
0633          GOTO 577
0634    579    CONTINUE
0635
0636          I=1
0637    581    IF (IDOF(I).EQ.0) GOTO 583
0638          IF (IDOF(I).EQ.1) GOTO 585
0639    583    S(I,I)=S(I,I)*1.0E20
0640          LL(I)=S(I,I)*IDOF(I)
0641    585    IF (I.EQ.3*NJ) GOTO 590
0642          I=I+1
0643          GOTO 581
0644    590    CONTINUE
0645
0646    C
0647    C      CHOLESKYS SOLUTION ROUTINE
0648    C
0649    C
0650    C      DECOMPOSITION
0651    C
0652
0653          N=3*NJ
0654          J=0
0655    600    J=J+1
0656          I=J-1
0657    610    I=I+1
0658          IF (I.EQ.J) GOTO 650
0659          K=0
0660          SUM=0
0661    620    K=K+1
0662          IF (K.NE.J) GOTO 630
0663          IF (K.EQ.J) GOTO 640
0664    630    SUM=SUM+(S(I,K)*S(J,K))
0665          GOTO 620
0666    640    S(I,J)=(S(I,J)-SUM)/S(J,J)
0667          GOTO 690
0668    650    K=0
0669          SUM=0
0670    660    K=K+1
0671          IF (K.NE.J) GOTO 670
0672          IF (K.EQ.J) GOTO 680
0673    670    SUM=SUM+(S(I,K)**2)
0674          GOTO 660
0675    680    S(I,I)=(S(I,I)-SUM)**0.5)
0676    690    IF (I.NE.N) GOTO 610
0677          IF (I.EQ.N) GOTO 700
0678    700    IF (J.NE.N) GOTO 600
0679          IF (J.EQ.N) GOTO 710
0680    710    CONTINUE
0681
0682    C
0683    C      FORWARD SUBSTUTION
0684    C

```



```

0685
0686      I=1
0687      713      ZZ(I)=LL(I)
0688      IF (I.LT.N) GOTO 715
0689      IF (I.EQ.N) GOTO 717
0690      715      I=I+1
0691      GOTO 713
0692      717      CONTINUE
0693      I=0
0694      720      I=I+1
0695      J=0
0696      SUM=0
0697      730      J=J+1
0698      IF (I.EQ.J) GOTO 740
0699      SUM=SUM+ZZ(J)*S(I,J)
0700      GOTO 730
0701      740      ZZ(I)=(ZZ(I)-SUM)/S(I,I)
0702      IF (I.NE.N) GOTO 720
0703      IF (I.EQ.N) GOTO 750
0704      750      CONTINUE
0705
0706      C
0707      C      BACK SUBSTITUTION
0708      C
0709
0710      I=N+1
0711      760      I=I-1
0712      J=N+1
0713      SUM=0
0714      770      J=J-1
0715      IF (I.EQ.J) GOTO 780
0716      SUM=SUM+S(J,I)*ZZ(J)
0717      GOTO 770
0718      780      ZZ(I)=(ZZ(I)-SUM)/S(I,I)
0719      IF (I.NE.1) GOTO 760
0720      IF (I.EQ.1) GOTO 790
0721      790      CONTINUE
0722
0723      C
0724      C      MEMBER FORCES P,S,M1,M2.
0725      C
0726
0727      I=1
0728      792      FN1=-(CT22(I)*CL(I)*ZZ(3*KR(I)-2))
0729      FN2=-(CT22(I)*CM(I)*ZZ(3*KR(I)-1))
0730      FN3=-(CT32(I)*ZZ(3*KR(I)))
0731      FN4=(CT22(I)*CL(I)*ZZ(3*JR(I)-2))
0732      FN5=(CT22(I)*CM(I)*ZZ(3*JR(I)-1))
0733      FN6=-(CT42(I)*ZZ(3*JR(I)))
0734      SS(I)=FN1+FN2+FN3+FN4+FN5+FN6
0735      FN7=-(CT32(I)*CL(I)*ZZ(3*KR(I)-2))
0736      FN8=-(CT32(I)*CM(I)*ZZ(3*KR(I)-1))
0737      FN9=-(CT33(I)*ZZ(3*KR(I)))
0738      FN10=(CT32(I)*CL(I)*ZZ(3*JR(I)-2))
0739      FN11=(CT32(I)*CM(I)*ZZ(3*JR(I)-1))
0740      FN12=-(CT43(I)*ZZ(3*JR(I)))
0741      MA(I)=(FN7+FN8+FN9+FN10+FN11+FN12)+XM1(I)

```



```

0742      FN13=-(CT42(I)*CL(I)*ZZ(3*KR(I)-2))
0743      FN14=-(CT42(I)*CM(I)*ZZ(3*KR(I)-1))
0744      FN15=-(CT43(I)*ZZ(3*KR(I)))
0745      FN16=(CT42(I)*CL(I)*ZZ(3*JR(I)-2))
0746      FN17=(CT42(I)*CM(I)*ZZ(3*JR(I)-1))
0747      FN18=-(CT44(I)*ZZ(3*JR(I)))
0748      MB(I)=-(FN13+FN14+FN15+FN16+FN17+FN18)-(XM2(I))
0749      FN19=-(CT11(I)*CA(I)*ZZ(3*KR(I)-2))
0750      FN20=-(CT11(I)*CB(I)*ZZ(3*KR(I)-1))
0751      FN21=(CT11(I)*CA(I)*ZZ(3*JR(I)-2))
0752      FN22=(CT11(I)*CB(I)*ZZ(3*JR(I)-1))
0753      P(I)=FN19+FN20+FN21+FN22
0754      IF (I.LT.NM) GOTO 813
0755      IF (I.EQ.NM) GOTO 814
0756      813      I=I+1
0757              GOTO 792
0758      814      CONTINUE
0759
0760      WRITE(6,3800)
0761      WRITE(6,3180)
0762
0763      I=1
0764      900      WRITE(6,3200)I,CA(I),CB(I),CL(I),CM(I)
0765              IF (I.LT.NM) GOTO 910
0766              IF (I.EQ.NM) GOTO 920
0767      910      I=I+1
0768              GOTO 900
0769      920      CONTINUE
0770
0771      WRITE(6,3300)
0772
0773      I=1
0774      930      WRITE(6,3400)I,ZZ(3*I-2),ZZ(3*I-1),ZZ(3*I)
0775              IF (I.LT.NJ) GOTO 940
0776              IF (I.EQ.NJ) GOTO 950
0777      940      I=I+1
0778              GOTO 930
0779      950      CONTINUE
0780
0781      WRITE(6,3500)
0782
0783      I=1
0784      960      WRITE(6,3600)I,SS(I),P(I),MA(I),MB(I)
0785              IF (I.LT.NM) GOTO 970
0786              IF (I.EQ.NM) GOTO 980
0787      970      I=I+1
0788              GOTO 960
0789      980      CONTINUE
0790
0791      WRITE(6,3700)
0792
0793
0794      C
0795      C      NON-LINEAR ANALYSIS STARTS HERE (COUPLING FACTORS)
0796      C
0797
0798

```



```

0799
0800      985      I=1
0801      1211     ZZ(I)=XLX(I)
0802                XL(I)=0
0803                IF (I.LT.(3*NJ)) GOTO 1212
0804                IF (I.EQ.(3*NJ)) GOTO 1213
0805      1212     I=I+1
0806                GOTO 1211
0807      1213     CONTINUE
0808
0809                I=1
0810                J=1
0811      981      S(I,J)=0
0812                IF (I.NE.(3*NJ)) GOTO 982
0813                IF (I.EQ.(3*NJ)) GOTO 983
0814      982      I=I+1
0815                GOTO 981
0816      983      IF (J.NE.(3*NJ)) GOTO 984
0817                IF (J.EQ.(3*NJ)) GOTO 986
0818      984      J=J+1
0819                I=1
0820                GOTO 981
0821      986      CONTINUE
0822
0823
0824      C
0825      C      CALCULATION OF THE LOCAL STIFFNESS MATRIX
0826      C      FOR A NON-LINEAR MEMBER
0827      C
0828                I=1
0829      990      IF (P1(I).EQ.0) GOTO 1015
0830                IF (P1(I).LT.0) GOTO 993
0831                IF (P1(I).GT.0) GOTO 995
0832
0833
0834      993      P1(I)=-P1(I)
0835                W(I)=((P1(I)/EI(I))**.5)
0836                QQ(I)=W(I)*L(I)
0837                CW(I)=COS(QQ(I))
0838                SW(I)=SIN(QQ(I))
0839                V(I)=W(I)*((QQ(I)*SW(I))+(2*CW(I))-2)
0840                GOTO 1500
0841      1010     V(I)=-V(I)
0842                CT11(I)=EA(I)/L(I)
0843                CT22(I)=(P1(I)*W(I)*W(I)*SW(I)/V(I))
0844                CT32(I)=(P1(I)*W(I)*(1-CW(I))/V(I))
0845                CT33(I)=(P1(I)*(SW(I)-(QQ(I)*CW(I)))/V(I))
0846                CT42(I)=CT32(I)
0847                CT43(I)=(P1(I)*(QQ(I)-SW(I))/V(I))
0848                CT44(I)=CT33(I)
0849
0850      C
0851      C      NON-NODAL LOADINGS
0852      C
0853
0854                VN=(2*W(I)*(1-CW(I)))-(W(I)*W(I)*L(I)*SW(I))
0855                CN11=(W(I)-(W(I)*W(I)*L(I)*SW(I))-(W(I)*CW(I)))/VN

```



```

0856      CN12=((W(I)*L(I)*CW(I))-SW(I))/VN
0857      CN13=(W(I)*(1-CW(I)))/VN
0858      CN14=(SW(I)-(W(I)*L(I)))/VN
0859      CN21=W(I)*W(I)*SW(I)/VN
0860      CN22=CN13
0861      CN23=-CN21
0862      CN24=CN13
0863      CN31=-CN21/W(I)
0864      CN32=CN11/W(I)
0865      CN33=CN21/W(I)
0866      CN34=-CN13/W(I)
0867      CN41=CN13
0868      CN42=-CN12
0869      CN43=-CN13
0870      CN44=-CN14
0871
0872      SNN1=(L(I)*CN11)+(CN21*L(I)*L(I)/2)
0873      SNN2=(CN31*(1-CW(I))/W(I))+(CN41*SW(I)/W(I))
0874      S1=UDL(I)*(SNN1+SNN2)
0875      SNN3=(L(I)*CN12)+(CN22*L(I)*L(I)/2)
0876      SNN4=(CN32*(1-CW(I))/W(I))+(CN42*SW(I)/W(I))
0877      XM1(I)=UDL(I)*(SNN3+SNN4)
0878      SNN5=(L(I)*CN13)+(CN23*L(I)*L(I)/2)
0879      SNN6=(CN33*(1-CW(I))/W(I))+(CN43*SW(I)/W(I))
0880      S2=UDL(I)*(SNN5+SNN6)
0881      SNN7=(L(I)*CN14)+(CN24*L(I)*L(I)/2)
0882      SNN8=(CN34*(1-CW(I))/W(I))+(CN44*SW(I)/W(I))
0883      XM2(I)=UDL(I)*(SNN7+SNN8)
0884
0885      FX1=S1*CB(I)
0886      FY1=S1*CM(I)
0887      XM1(I)=XM1(I)
0888      FX2=S2*CB(I)
0889      FY2=S2*CM(I)
0890      XM2(I)=XM2(I)
0891
0892      XL(3*KR(I)-2)=XL(3*KR(I)-2)+FX1
0893      XL(3*KR(I)-1)=XL(3*KR(I)-1)+FY1
0894      XL(3*KR(I))=XL(3*KR(I))+XM1(I)
0895      XL(3*JR(I)-2)=XL(3*JR(I)-2)+FX2
0896      XL(3*JR(I)-1)=XL(3*JR(I)-1)+FY2
0897      XL(3*JR(I))=XL(3*JR(I))+XM2(I)
0898
0899      P1(I)=-P1(I)
0900      GOTO 1020
0901
0902      995      W(I)=((P1(I)/EI(I))**.5)
0903      QQ(I)=W(I)*L(I)
0904      CW(I)=COSH(QQ(I))
0905      SW(I)=SINH(QQ(I))
0906      V(I)=(2*W(I)*(1-CW(I)))+(QQ(I)*W(I)*SW(I))
0907      GOTO 1700
0908      1011     CT11(I)=EA(I)/L(I)
0909      CT22(I)=(P1(I)*W(I)*W(I)*SW(I)/V(I))
0910      CT32(I)=-P1(I)*W(I)*(1-CW(I))/V(I)
0911      CT33(I)=-P1(I)*(SW(I)-(QQ(I)*CW(I)))/V(I)
0912      CT42(I)=CT32(I)

```



```

0913          CT43(I)=- (P1(I)*(QG(I)-SW(I))/V(I))
0914          CT44(I)=CT33(I)
0915
0916          C
0917          C          NON-NODAL LOADINGS
0918          C
0919          CN11=((W(I)*W(I)*L(I)*SW(I))-(W(I)*CW(I))+W(I))/V(I)
0920          CN12=((W(I)*L(I)*CW(I))-SW(I))/V(I)
0921          CN13=(W(I)*(1-CW(I)))/V(I)
0922          CN14=(SW(I)-(W(I)*L(I)))/V(I)
0923          CN21=- (W(I)*W(I)*SW(I)/V(I))
0924          CN22=CN13
0925          CN23=-CN21
0926          CN24=CN13
0927          CN31=-CN21/W(I)
0928          CN32=CN11/W(I)
0929          CN33=CN21/W(I)
0930          CN34=-CN13/W(I)
0931          CN41=CN13
0932          CN42=-CN12
0933          CN43=-CN13
0934          CN44=-CN14
0935
0936          SNN9=(L(I)*CN11)+(CN21*L(I)*L(I)/2)
0937          SNN10=(CN31*(CW(I)-1)/W(I))+(CN41*SW(I)/W(I))
0938          S1=UDL(I)*(SNN9+SNN10)
0939          SNN11=(L(I)*CN12)+(CN22*L(I)*L(I)/2)
0940          SNN12=(CN32*(CW(I)-1)/W(I))+(CN42*SW(I)/W(I))
0941          XM1(I)=UDL(I)*(SNN11+SNN12)
0942          SNN13=(L(I)*CN13)+(CN23*L(I)*L(I)/2)
0943          SNN14=(CN33*(CW(I)-1)/W(I))+(CN43*SW(I)/W(I))
0944          S2=UDL(I)*(SNN13+SNN14)
0945          SNN15=(L(I)*CN14)+(CN24*L(I)*L(I)/2)
0946          SNN16=(CN34*(CW(I)-1)/W(I))+(CN44*SW(I)/W(I))
0947          XM2(I)=UDL(I)*(SNN15+SNN16)
0948
0949          FX1=S1*CB(I)
0950          FY1=S1*CM(I)
0951          XM1(I)=XM1(I)
0952          FX2=S2*CB(I)
0953          FY2=S2*CM(I)
0954          XM2(I)=XM2(I)
0955
0956          XL(3*KR(I)-2)=XL(3*KR(I)-2)+FX1
0957          XL(3*KR(I)-1)=XL(3*KR(I)-1)+FY1
0958          XL(3*KR(I))=XL(3*KR(I))+XM1(I)
0959          XL(3*JR(I)-2)=XL(3*JR(I)-2)+FX2
0960          XL(3*JR(I)-1)=XL(3*JR(I)-1)+FY2
0961          XL(3*JR(I))=XL(3*JR(I))+XM2(I)
0962
0963          GOTO 1020
0964
0965          1015          CT11(I)=EA(I)/L(I)
0966          CT22(I)=12*EI(I)/(L(I)**3)
0967          CT32(I)=6*EI(I)/(L(I)**2)
0968          CT33(I)=4*EI(I)/L(I)
0969          CT42(I)=CT32(I)

```



```

0970          CT43(I)=2*EI(I)/L(I)
0971          CT44(I)=CT33(I)
0972          C
0973          C          CALCULATION FOR GLOBAL STIFFNESS MATRIX
0974          C
0975
0976
0977          1020      A(I)=(CT11(I)*CA(I)*CA(I))+(CT22(I)*CL(I)*CL(I))
0978                  B(I)=(CT11(I)*CB(I)*CB(I))+(CT22(I)*CM(I)*CM(I))
0979                  C(I)=(CT11(I)*CA(I)*CB(I))+(CT22(I)*CL(I)*CM(I))
0980                  D(I)=(CT32(I)*CL(I))
0981                  E(I)=(CT32(I)*CM(I))
0982                  F(I)=CT33(I)
0983                  G(I)=CT43(I)
0984
0985
0986                  S((3*KR(I)-2),(3*KR(I)-2))=S((3*KR(I)-2),(3*KR(I)-2))+A(I)
0987                  S((3*KR(I)-1),(3*KR(I)-1))=S((3*KR(I)-1),(3*KR(I)-1))+B(I)
0988                  S((3*KR(I)-1),(3*KR(I)-2))=S((3*KR(I)-1),(3*KR(I)-2))+C(I)
0989                  S((3*KR(I)),(3*KR(I)))=S((3*KR(I)),(3*KR(I)))+F(I)
0990                  S((3*KR(I)),(3*KR(I)-1))=S((3*KR(I)),(3*KR(I)-1))+E(I)
0991                  S((3*KR(I)),(3*KR(I)-2))=S((3*KR(I)),(3*KR(I)-2))+D(I)
0992                  S((3*JR(I)-2),(3*JR(I)-2))=S((3*JR(I)-2),(3*JR(I)-2))+A(I)
0993                  S((3*JR(I)-1),(3*JR(I)-1))=S((3*JR(I)-1),(3*JR(I)-1))+B(I)
0994                  S((3*JR(I)-1),(3*JR(I)-2))=S((3*JR(I)-1),(3*JR(I)-2))+C(I)
0995                  S((3*JR(I)),(3*JR(I)))=S((3*JR(I)),(3*JR(I)))+F(I)
0996                  S((3*JR(I)),(3*JR(I)-1))=S((3*JR(I)),(3*JR(I)-1))-E(I)
0997                  S((3*JR(I)),(3*JR(I)-2))=S((3*JR(I)),(3*JR(I)-2))-D(I)
0998                  S((3*JR(I)-2),(3*KR(I)-2))=S((3*JR(I)-2),(3*KR(I)-2))-A(I)
0999                  S((3*JR(I)-2),(3*KR(I)-1))=S((3*JR(I)-2),(3*KR(I)-1))-C(I)
1000                  S((3*JR(I)-2),(3*KR(I)))=S((3*JR(I)-2),(3*KR(I)))-D(I)
1001                  S((3*JR(I)-1),(3*KR(I)-2))=S((3*JR(I)-1),(3*KR(I)-2))-C(I)
1002                  S((3*JR(I)-1),(3*KR(I)-1))=S((3*JR(I)-1),(3*KR(I)-1))-B(I)
1003                  S((3*JR(I)-1),(3*KR(I)))=S((3*JR(I)-1),(3*KR(I)))-E(I)
1004                  S((3*JR(I)),(3*KR(I)-2))=S((3*JR(I)),(3*KR(I)-2))+D(I)
1005                  S((3*JR(I)),(3*KR(I)-1))=S((3*JR(I)),(3*KR(I)-1))+E(I)
1006                  S((3*JR(I)),(3*KR(I)))=S((3*JR(I)),(3*KR(I)))+G(I)
1007                  IF (I.LT.NM) GOTO 1030
1008                  IF (I.EQ.NM) GOTO 1040
1009          1030      I=I+1
1010                  GOTO 990
1011          1040      CONTINUE
1012
1013
1014          C
1015          C          RESTRAINTS CONDITIONS
1016          C
1017
1018                  I=1
1019          1045      BB(I)=ZZ(I)+XL(I)
1020                  IF (I.LT.(3*NJ)) GOTO 1046
1021                  IF (I.EQ.(3*NJ)) GOTO 1047
1022          1046      I=I+1
1023                  GOTO 1045
1024          1047      CONTINUE
1025
1026                  I=1

```



```

1027      1050      IF (IDOF(I).EQ.0) GOTO 1060
1028      IF (IDOF(I).EQ.1) GOTO 1070
1029      1060      S(I,I)=S(I,I)*1.0E12
1030      BB(I)=S(I,I)*IDOF(I)
1031      IF (I.EQ.(3*NJ)) GOTO 1090
1032      1070      I=I+1
1033      GOTO 1050
1034      1090      CONTINUE
1035
1036      C
1037      C      DECOMPOSITION
1038      C
1039      J=0
1040      1100      J=J+1
1041      I=J-1
1042      1120      I=I+1
1043      IF (I.EQ.J) GOTO 1160
1044      K=0
1045      SUM=0
1046      1130      K=K+1
1047      IF (K.NE.J) GOTO 1140
1048      IF (K.EQ.J) GOTO 1150
1049      1140      SUM=SUM+(S(I,K)*S(J,K))
1050      GOTO 1130
1051      1150      S(I,J)=(S(I,J)-SUM)/S(J,J)
1052      GOTO 1195
1053      1160      K=0
1054      SUM=0
1055      1170      K=K+1
1056      IF (K.NE.J) GOTO 1180
1057      IF (K.EQ.J) GOTO 1190
1058      1180      SUM=SUM+(S(I,K)**2)
1059      GOTO 1170
1060      1190      S(I,I)=((S(I,I)-SUM)**0.5)
1061      1195      IF (I.NE.(3*NJ)) GOTO 1120
1062      IF (I.EQ.(3*NJ)) GOTO 1200
1063      1200      IF (J.NE.(3*NJ)) GOTO 1100
1064      IF (J.EQ.(3*NJ)) GOTO 1210
1065      1210      CONTINUE
1066      C
1067      C      FORWARD SUBSTITUTION
1068      C
1069      I=0
1070      1220      I=I+1
1071      J=0
1072      SUM=0
1073      1230      J=J+1
1074      IF (I.EQ.J) GOTO 1240
1075      SUM=SUM+BB(J)*S(I,J)
1076      GOTO 1230
1077      1240      BB(I)=(BB(I)-SUM)/S(I,I)
1078      IF (I.NE.(3*NJ)) GOTO 1220
1079      IF (I.EQ.(3*NJ)) GOTO 1250
1080      1250      CONTINUE
1081
1082      C
1083      C      BACK SUBSTITUTION

```



```

1084      C
1085
1086          I=(3*NJ)+1
1087      1260      I=I-1
1088          J=(3*NJ)+1
1089          SUM=0
1090      1270      J=J-1
1091          IF (I.EQ.J) GOTO 1280
1092          SUM=SUM+S(J,I)*BB(J)
1093          GOTO 1270
1094      1280      BB(I)=(BB(I)-SUM)/S(I,I)
1095          IF (I.NE.1) GOTO 1260
1096          IF (I.EQ.1) GOTO 1290
1097      1290      CONTINUE
1098
1099      C
1100      C          MEMBER FORCES P, S, M1, M2.
1101      C
1102
1103          I=1
1104      1300      FN1=-(CT22(I)*CL(I)*BB(3*KR(I)-2))
1105          FN2=-(CT22(I)*CM(I)*BB(3*KR(I)-1))
1106          FN3=-(CT32(I)*BB(3*KR(I)))
1107          FN4=(CT22(I)*CL(I)*BB(3*JR(I)-2))
1108          FN5=(CT22(I)*CM(I)*BB(3*JR(I)-1))
1109          FN6=-(CT42(I)*BB(3*JR(I)))
1110          SS(I)=FN1+FN2+FN3+FN4+FN5+FN6
1111          FN7=-(CT32(I)*CL(I)*BB(3*KR(I)-2))
1112          FN8=-(CT32(I)*CM(I)*BB(3*KR(I)-1))
1113          FN9=-(CT33(I)*BB(3*KR(I)))
1114          FN10=(CT32(I)*CL(I)*BB(3*JR(I)-2))
1115          FN11=(CT32(I)*CM(I)*BB(3*JR(I)-1))
1116          FN12=-(CT43(I)*BB(3*JR(I)))
1117          MA(I)=(FN7+FN8+FN9+FN10+FN11+FN12)+XM1(I)
1118          FN13=-(CT42(I)*CL(I)*BB(3*KR(I)-2))
1119          FN14=-(CT42(I)*CM(I)*BB(3*KR(I)-1))
1120          FN15=-(CT43(I)*BB(3*KR(I)))
1121          FN16=(CT42(I)*CL(I)*BB(3*JR(I)-2))
1122          FN17=(CT42(I)*CM(I)*BB(3*JR(I)-1))
1123          FN18=-(CT44(I)*BB(3*JR(I)))
1124          MB(I)=-(FN13+FN14+FN15+FN16+FN17+FN18)-(XM2(I))
1125          FN19=-(CT11(I)*CA(I)*BB(3*KR(I)-2))
1126          FN20=-(CT11(I)*CB(I)*BB(3*KR(I)-1))
1127          FN21=(CT11(I)*CA(I)*BB(3*JR(I)-2))
1128          FN22=(CT11(I)*CB(I)*BB(3*JR(I)-1))
1129          P1(I)=(FN19+FN20+FN21+FN22)+AMDA(I)
1130          IF (I.LT.NM) GOTO 1310
1131          IF (I.EQ.NM) GOTO 1320
1132      1310      I=I+1
1133          GOTO 1300
1134      1320      CONTINUE
1135
1136          IF (ID.LT.IDCON) GOTO 1325
1137          IF (ID.EQ.IDCON) GOTO 1327
1138      1325      ID=ID+1
1139          GOTO 985
1140      1327      CONTINUE

```



```

1141
1142      WRITE(6,3950)
1143      WRITE(6,3180)
1144
1145      I=1
1146 1330  WRITE(6,3200)I,CA(I),CB(I),CL(I),CM(I)
1147      IF (I.LT.NM) GOTO 1340
1148      IF (I.EQ.NM) GOTO 1350
1149 1340  I=I+1
1150      GOTO 1330
1151 1350  CONTINUE
1152
1153      WRITE(6,3300)
1154
1155      I=1
1156 1360  WRITE(6,3400)I,BB(3*I-2),BB(3*I-1),BB(3*I)
1157      IF (I.LT.NJ) GOTO 1370
1158      IF (I.EQ.NJ) GOTO 1380
1159 1370  I=I+1
1160      GOTO 1360
1161 1380  CONTINUE
1162
1163      WRITE(6,3500)
1164
1165      I=1
1166 1390  WRITE(6,3600)I,SS(I),P1(I),MA(I),MB(I)
1167      IF (I.LT.NM) GOTO 1400
1168      IF (I.EQ.NM) GOTO 1410
1169 1400  I=I+1
1170      GOTO 1390
1171 1410  CONTINUE
1172
1173      WRITE(6,3700)
1174      WRITE(6,3900)
1175      CLOSE (5)
1176      CLOSE (6)
1177 10000 STOP
1178
1179
1180 C
1181 C      SUBROUTINE COUPLING FACTORS
1182 C
1183
1184
1185 1500  W1(I)=(CL(I)*BB(3*KR(I)-2))+(CM(I)*BB(3*KR(I)-1))
1186      W2(I)=(CL(I)*BB(3*JR(I)-2))+(CM(I)*BB(3*JR(I)-1))
1187      R1(I)=BB(3*KR(I))
1188      R2(I)=BB(3*JR(I))
1189
1190      CC(1,1)=(((W(I)*W(I)*L(I)*SW(I))+(W(I)*CW(I))-W(I))/V(I))
1191      CC(1,2)=((SW(I)-(W(I)*L(I)*CW(I)))/V(I))
1192      CC(1,3)=(((W(I)*CW(I))-W(I))/V(I))
1193      CC(1,4)=(((W(I)*L(I))-SW(I))/V(I))
1194      CC(2,1)=-((W(I)*W(I)*SW(I))/V(I))
1195      CC(2,2)=CC(1,3)
1196      CC(2,3)=-CC(2,1)
1197      CC(2,4)=CC(1,3)

```



```

1198      CC(3,1)=(W(I)*SW(I)/V(I))
1199      CC(3,2)=(((W(I)*L(I)*SW(I))+CW(I)-1)/V(I))
1200      CC(3,3)=-CC(3,1)
1201      CC(3,4)=((1-CW(I))/V(I))
1202      CC(4,1)=CC(1,3)
1203      CC(4,2)=(((W(I)*L(I)*CW(I))-SW(I))/V(I))
1204      CC(4,3)=-CC(1,3)
1205      CC(4,4)=((SW(I)-(W(I)*L(I)))/V(I))
1206
1207
1208      M=1
1209      N=1
1210      1510  CNN1=(CC(2,M)*CC(2,N)/2)
1211      1520  CNN2=(((CC(2,M)*CC(3,N))+((CC(3,M)*CC(2,N)))*SW(I)/(2*L(I)))
1212      CNN3=(((CC(2,M)*CC(4,N))+((CC(4,M)*CC(2,N)))*((CW(I)-1)/(2*L(I)))
1213      CNN4=(W(I)*W(I)/4)+((W(I)*SIN(2*W(I)*L(I)))/(8*L(I)))
1214      CNN5=(W(I)*W(I)/4)-((W(I)*SIN(2*W(I)*L(I)))/(8*L(I)))
1215      CNN6=(CC(3,M)*CC(3,N)*CNN4)
1216      CNN7=(((CC(3,M)*CC(4,N))+((CC(4,M)*CC(3,N))))
1217      CNN8=(COS(2*W(I)*L(I))-1)
1218      CNN9=(W(I)/(8*L(I)))*CNN7*CNN8
1219      CNN10=(CC(4,M)*CC(4,N)*CNN5)
1220      Q(M,N)=CNN1+CNN2+CNN3+CNN6+CNN9+CNN10
1221      IF (N.LT.4) GOTO 1530
1222      IF (N.EQ.4) GOTO 1540
1223      1530  N=N+1
1224      GOTO 1520
1225      1540  IF (M.LT.4) GOTO 1550
1226      IF (M.EQ.4) GOTO 1560
1227      1550  M=M+1
1228      GOTO 1510
1229      1560  CONTINUE
1230
1231
1232      CT1=(Q(1,1)*W1(I))+((Q(1,2)*R1(I))
1233      CT2=(Q(1,3)*W2(I))+((Q(1,4)*R2(I))
1234      A1(I)=CT1+CT2
1235      CT3=(Q(2,1)*W1(I))+((Q(2,2)*R1(I))
1236      CT4=(Q(2,3)*W2(I))+((Q(2,4)*R2(I))
1237      A2(I)=CT3+CT4
1238      CT5=(Q(3,1)*W1(I))+((Q(3,2)*R1(I))
1239      CT6=(Q(3,3)*W2(I))+((Q(3,4)*R2(I))
1240      A3(I)=CT5+CT6
1241      CT7=(Q(4,1)*W1(I))+((Q(4,2)*R1(I))
1242      CT8=(Q(4,3)*W2(I))+((Q(4,4)*R2(I))
1243      A4(I)=CT7+CT8
1244      GAMA=(A1(I)*W1(I))+((A2(I)*R1(I)))+(A3(I)*W2(I))+((A4(I)*R2(I))
1245      AMDA(I)=EA(I)*GAMA
1246      A1(I)=A1(I)*EA(I)
1247      A2(I)=A2(I)*EA(I)
1248      A3(I)=A3(I)*EA(I)
1249      A4(I)=A4(I)*EA(I)
1250
1251      ZN1=A1(I)*CA(I)*CL(I)*BB(3*KR(I)-2)
1252      ZN2=A1(I)*CA(I)*CM(I)*BB(3*KR(I)-1)
1253      ZN3=A2(I)*CA(I)*BB(3*KR(I))
1254      ZN4=A2(I)*CB(I)*BB(3*KR(I))

```



```

1255      ZN5=A1(I)*CB(I)*CL(I)*BB(3*KR(I)-2)
1256      ZN6=A1(I)*CB(I)*CM(I)*BB(3*KR(I)-1)
1257      ZN7=A4(I)*CB(I)*BB(3*JR(I))
1258      ZN8=A4(I)*CA(I)*BB(3*JR(I))
1259      ZN9=A3(I)*CA(I)*CL(I)*BB(3*JR(I)-2)
1260      ZN10=A3(I)*CA(I)*CM(I)*BB(3*JR(I)-1)
1261      ZN11=A3(I)*CB(I)*CL(I)*BB(3*JR(I)-2)
1262      ZN12=A3(I)*CB(I)*CM(I)*BB(3*JR(I)-1)
1263
1264      ZN13=ZN1+ZN2+ZN3+ZN9+ZN10+ZN8
1265      ZN14=ZN5+ZN6+ZN4+ZN11+ZN12+ZN7
1266
1267      ZZ(3*KR(I)-2)=ZZ(3*KR(I)-2)+ZN13
1268      ZZ(3*KR(I)-1)=ZZ(3*KR(I)-1)+ZN14
1269      ZZ(3*JR(I)-2)=ZZ(3*JR(I)-2)-ZN13
1270      ZZ(3*JR(I)-1)=ZZ(3*JR(I)-1)-ZN14
1271      GOTO 1010
1272
1273
1274      C
1275      C      SUBROUTINE COUPLING FACTORS FOR TENSION
1276      C
1277
1278
1279      1700      W1(I)=(CL(I)*BB(3*KR(I)-2)+(CM(I)*BB(3*KR(I)-1))
1280      W2(I)=(CL(I)*BB(3*JR(I)-2)+(CM(I)*BB(3*JR(I)-1))
1281      R1(I)=BB(3*KR(I))
1282      R2(I)=BB(3*JR(I))
1283
1284      CC(1,1)=((W(I)*W(I)*L(I)*SW(I))-(W(I)*CW(I))+W(I))/V(I)
1285      CC(1,2)=((W(I)*L(I)*CW(I))-SW(I))/V(I)
1286      CC(1,3)=(W(I)*(1-CW(I)))/V(I)
1287      CC(1,4)=(SW(I)-(W(I)*L(I)))/V(I)
1288      CC(2,1)=-W(I)*W(I)*SW(I)/V(I)
1289      CC(2,2)=CC(1,3)
1290      CC(2,3)=-CC(2,1)
1291      CC(2,4)=CC(1,3)
1292      CC(3,1)=-CC(2,1)/W(I)
1293      CC(3,2)=(CC(1,1)/W(I))
1294      CC(3,3)=(CC(2,1)/W(I))
1295      CC(3,4)=-CC(1,3)/W(I)
1296      CC(4,1)=CC(1,3)
1297      CC(4,2)=-CC(1,2)
1298      CC(4,3)=-CC(1,3)
1299      CC(4,4)=-CC(1,4)
1300
1301
1302      M=1
1303      N=1
1304      1720      CNN1=(CC(2,M)*CC(2,N))/2)
1305      CNN2=((CC(2,M)*CC(3,N))+CC(3,M)*CC(2,N))*SW(I)/(2*L(I))
1306      CNN3=((CC(2,M)*CC(4,N))+CC(4,M)*CC(2,N))*CW(I)/(2*L(I))
1307      CNN4=(W(I)*W(I)/4)+(W(I)*SINH(2*W(I)*L(I)))/(8*L(I))
1308      CNN5=-W(I)*W(I)/4+(W(I)*SINH(2*W(I)*L(I)))/(8*L(I))
1309      CNN6=(CC(3,M)*CC(3,N)*CNN4)
1310      CNN7=((CC(3,M)*CC(4,N))+CC(4,M)*CC(3,N))
1311      CNN8=(COSH(2*W(I)*L(I))-1)

```



```

1312      CNN9=(W(I)/(8*L(I)))*CNN7*CNNB
1313      CNN10=(CC(4,M)*CC(4,N)*CNN5)
1314      Q(M,N)=CNN1+CNN2+CNN3+CNN6+CNN9+CNN10
1315      IF (N.LT.4) GOTO 1730
1316      IF (N.EQ.4) GOTO 1740
1317      1730      N=N+1
1318      GOTO 1720
1319      1740      IF (M.LT.4) GOTO 1750
1320      IF (M.EQ.4) GOTO 1760
1321      1750      M=M+1
1322      GOTO 1710
1323      1760      CONTINUE
1324
1325      CT1=(Q(1,1)*W1(I))+(Q(1,2)*R1(I))
1326      CT2=(Q(1,3)*W2(I))+(Q(1,4)*R2(I))
1327      A1(I)=CT1+CT2
1328      CT3=(Q(2,1)*W1(I))+(Q(2,2)*R1(I))
1329      CT4=(Q(2,3)*W2(I))+(Q(2,4)*R2(I))
1330      A2(I)=CT3+CT4
1331      CT5=(Q(3,1)*W1(I))+(Q(3,2)*R1(I))
1332      CT6=(Q(3,3)*W2(I))+(Q(3,4)*R2(I))
1333      A3(I)=CT5+CT6
1334      CT7=(Q(4,1)*W1(I))+(Q(4,2)*R1(I))
1335      CT8=(Q(4,3)*W2(I))+(Q(4,4)*R2(I))
1336      A4(I)=CT7+CT8
1337      GAMA=(A1(I)*W1(I))+(A2(I)*R1(I))+(A3(I)*W2(I))+(A4(I)*R2(I))
1338      AMDA(I)=EA(I)*GAMA
1339      A1(I)=A1(I)*EA(I)
1340      A2(I)=A2(I)*EA(I)
1341      A3(I)=A3(I)*EA(I)
1342      A4(I)=A4(I)*EA(I)
1343
1344      ZN1=A1(I)*CA(I)*CL(I)*BB(3*KR(I)-2)
1345      ZN2=A1(I)*CA(I)*CM(I)*BB(3*KR(I)-1)
1346      ZN3=A2(I)*CA(I)*BB(3*KR(I))
1347      ZN4=A2(I)*CB(I)*BB(3*KR(I))
1348      ZN5=A1(I)*CB(I)*CL(I)*BB(3*KR(I)-2)
1349      ZN6=A1(I)*CB(I)*CM(I)*BB(3*KR(I)-1)
1350      ZN7=A4(I)*CB(I)*BB(3*JR(I))
1351      ZN8=A4(I)*CA(I)*BB(3*JR(I))
1352      ZN9=A3(I)*CA(I)*CL(I)*BB(3*JR(I)-2)
1353      ZN10=A3(I)*CA(I)*CM(I)*BB(3*JR(I)-1)
1354      ZN11=A3(I)*CB(I)*CL(I)*BB(3*JR(I)-2)
1355      ZN12=A3(I)*CB(I)*CM(I)*BB(3*JR(I)-1)
1356
1357      ZN13=ZN1+ZN2+ZN3+ZN9+ZN10+ZN8
1358      ZN14=ZN5+ZN6+ZN4+ZN11+ZN12+ZN7
1359
1360      ZZ(3*KR(I)-2)=ZZ(3*KR(I)-2)+ZN13
1361      ZZ(3*KR(I)-1)=ZZ(3*KR(I)-1)+ZN14
1362      ZZ(3*JR(I)-2)=ZZ(3*JR(I)-2)-ZN13
1363      ZZ(3*JR(I)-1)=ZZ(3*JR(I)-1)-ZN14
1364      GOTO 1011
1365      C
1366      C      FORMATION SUBROUTINE
1367      C
1368

```



```

1369      2000      FORMAT(48X, '      '//
1370      *          48X, '      '//
1371      *          48X, '      '//
1372      *          48X, '      '//
1373      *          48X, 'DDDDDD  AAAA  TTTT  AAAA '//
1374      *          48X, 'DD  D  A  A  T  A  A '//
1375      *          48X, 'DD  D  A  A  T  A  A '//
1376      *          48X, 'DD  D  AAAA  T  AAAA '//
1377      *          48X, 'DD  D AA  A  T  AA  A '//
1378      *          48X, 'DD  D AA  A  T  AA  A '//
1379      *          48X, 'DD  D AA  A  T  AA  A '//
1380      *          48X, 'DDDDDD AA  A  T  AA  A '//
1381      *          48X, '      '//
1382      *          48X, '      '//
1383      *          48X, '      '//
1384      *          48X, '      '//
1385      *          38X, 'THE DATA FILE CONTAINS THE INPUT DATA OF THE '//
1386      *          38X, '  STRUCTURE, SUCH AS JOINT NUMBERING, JOINT '//
1387      *          38X, '  LOADING & RESTRAINTS, MEMBER POSITION, '//
1388      *          38X, '  AND MEMBER PROPERTIES '//
1389      *          38X, '      '//
1390      *          38X, '      '//
1391      *          38X, '      '//
1392      *          38X, '      ')
1393      2100      FORMAT(28X, 'THE STRUCTURE HAS', 12, ' JOINTS '//
1394      *          28X, '===== '//
1395      *          38X, '      '//
1396      *          38X, '      '//
1397      *          20X, 'JOINT COORDINATES '//
1398      *          20X, '===== '//
1399      *          20X, '      '//
1400      *          20X, '      '//
1401      *          12X, 'ALL COORDINATES ARE IN METRES '//
1402      *          12X, '      '//
1403      *          1X, '-----'
1404      *          1X, '      JOINT          X-COORDINATE          Y-COORDINATE'
1405      *          1X, '-----'
1406      *          1X, '      ')
1407      2200      FORMAT(1X, '      ', 12, '      ', F6.2, '      ', F6.2, '      ')
1408      2300      FORMAT(1X, '      ')
1409      *          1X, '-----'
1410      *          1X, '      '//
1411      *          1X, '      '//
1412      *          1X, '      '//
1413      *          1X, '      '//
1414      *          1X, '      '//
1415      *          15X, 'RESTRAINTS OF JOINTS '//
1416      *          15X, '===== '//
1417      *          15X, '      '//
1418      *          15X, '      '//
1419      *          10X, 'A "0" DENOTES A RESTRAINT & A '//
1420      *          10X, '"1" REPRESENTS FREE MOVEMENT '//
1421      *          10X, '      '//
1422      *          1X, '-----'
1423      *          1X, '      JOINT          X-DIR          Y-DIR          THETA-DIR  '//
1424      *          1X, '-----'
1425      *          1X, '      ')

```



```

1426      2400      FORMAT(1X, '      ', I2, '      ', I2, '      ', I2, '      ', I2, '      ', I2, '      ')
1427      2500      FORMAT(1X, '      //
1428      *          1X, '-----'//
1429      *          1X, '      //
1430      *          1X, '      //
1431      *          1X, '      //
1432      *          1X, '      //
1433      *          1X, '      //
1434      *          15X, 'LOADINGS ON JOINTS'//
1435      *          15X, '=====//
1436      *          15X, '      //
1437      *          15X, '      //
1438      *          10X, 'ALL LOADS ARE IN KN & KNm'//
1439      *          10X, '      //
1440      *          1X, '-----'//
1441      *          1X, '      JOINT      X-DIR      Y-DIR      THETA-DIR
1442      *          1X, '-----'//
1443      *          1X, '      )
1444      2600      FORMAT(1X, '      ', I2, '      ', F9.2, '      ', F9.2, '      ', F9.2, '      ')
1445      2700      FORMAT(1X, '      //
1446      *          1X, '-----'//
1447      *          1X, '      //
1448      *          1X, '      //
1449      *          1X, '      //
1450      *          1X, '      //
1451      *          1X, '      //
1452      *          38X, 'THE STRUCTURE HAS', I2, ' MEMBERS'//
1453      *          38X, '=====//
1454      *          38X, '      //
1455      *          38X, '      //
1456      *          14X, 'MEMBER POSITIONING & LENGTH'//
1457      *          14X, '=====//
1458      *          14X, '      //
1459      *          14X, '      //
1460      *          15X, 'ALL LENGTHS ARE IN METRES'//
1461      *          15X, '      //
1462      *          1X, '-----'//
1463      *          1X, '      MEMBER      JOINT I      JOINT J      LENGTH //
1464      *          1X, '-----'//
1465      *          1X, '      )
1466      2800      FORMAT(1X, '      ', I2, '      ', I2, '      ', I2, '      ', I2, '      ')
1467      2900      FORMAT(1X, '      //
1468      *          1X, '-----'//
1469      *          1X, '      //
1470      *          1X, '      //
1471      *          1X, '      //
1472      *          1X, '      //
1473      *          1X, '      //
1474      *          15X, 'MEMBER PROPERTIES'//
1475      *          15X, '=====//
1476      *          15X, '      //
1477      *          15X, '      //
1478      *          13X, 'ALL VALUES IN KN & m'//
1479      *          13X, '      //
1480      *          1X, '-----'//
1481      *          1X, '      MEMBER      EI VALUE      EA VALUE
1482      *          1X, '-----'//

```



```
1483 *          1X, '      ')
1484 3000  FORMAT(1X, '      ', I2, '      ', F10.2, '      ', F10.2)
1485 3100  FORMAT(1X, '      '//)
1486 *          1X, '-----'
1487 *          1X, '      '//
1488 *          1X, '      '//
1489 *          1X, '      '//
1490 *          20X, '----- E N D   O F   D A T A -----'
1491 *          20X, '      '//
1492 *          20X, '      '//
1493 *          20X, '      '//
1494 *          20X, '      '//
1495 *          20X, '      '//
1496 *          20X, '      '//
1497 *          20X, '      '//
1498 *          20X, '      '//
1499 *          38X, 'RRRRR EEEEE SSSSS UU  U LL  TTTT SSSSS '//
1500 *          38X, 'RR  R EE  SS  UU  U LL  T  SS  '//
1501 *          38X, 'RR  R EE  SS  UU  U LL  T  SS  '//
1502 *          38X, 'RRRRR EEEEE SSSSS UU  U LL  T  SSSSS '//
1503 *          38X, 'RRR  EE  S  UU  U LL  T  S '//
1504 *          38X, 'RR RR EE  S  UU  U LL  T  S '//
1505 *          38X, 'RR  R EE  S  UU  U LL  T  S '//
1506 *          38X, 'RR  R EEEEE SSSSS UUUUU LLLLL T  SSSSS '//
1507 *          38X, '      ')
1508 3150  FORMAT(38X, '      '//)
1509 *          38X, '      '//
1510 *          38X, '      '//
1511 *          44X, 'THE RESULT SECTION CONTAINS THE '//
1512 *          44X, '    DIRECTIONAL COSINES, JOINT  '//
1513 *          44X, '    DEFLECTIONS & MEMBER  '//
1514 *          44X, '    FORCES  '//
1515 *          44X, '      '//
1516 *          44X, '      '//
1517 *          28X, 'ALL DEFLECTIONS & MEMBER FORCES ARE IN '//
1518 *          28X, '    METRES/RADIANS, KN & KNm '//
1519 *          28X, '      '//
1520 *          28X, '      ')
1521 3175  FORMAT(28X, '    L I N E A R    A N A L Y S I S '//)
1522 *          28X, '    ===== '//
1523 *          28X, '    /// '//
1524 *          15X, 'ANALYSIS WITH MUTUALLY INDEPENDENT STIFFNESS '//
1525 *          15X, '    MATRICES IGNORING LARGE DEFLECTIONS '//
1526 *          15X, '    /// '//
1527 3180  FORMAT(15X, 'DIRECTIONAL COSINES '//)
1528 *          15X, '    ===== '//
1529 *          15X, '      '//
1530 *          1X, '-----'
1531 *          1X, ' MEMBER    ALPHA    BETA    LAMDA    MUE '//
1532 *          1X, '-----'
1533 *          1X, '      ')
1534 3200  FORMAT(1X, '      ', I2, '      ', F6.3, '      ', F6.3, '      ', F6.3, '      ', F6.3)
1535 3300  FORMAT(1X, '      '//)
1536 *          1X, '-----'
1537 *          1X, '      '//
1538 *          1X, '      '//
1539 *          1X, '      '//
```

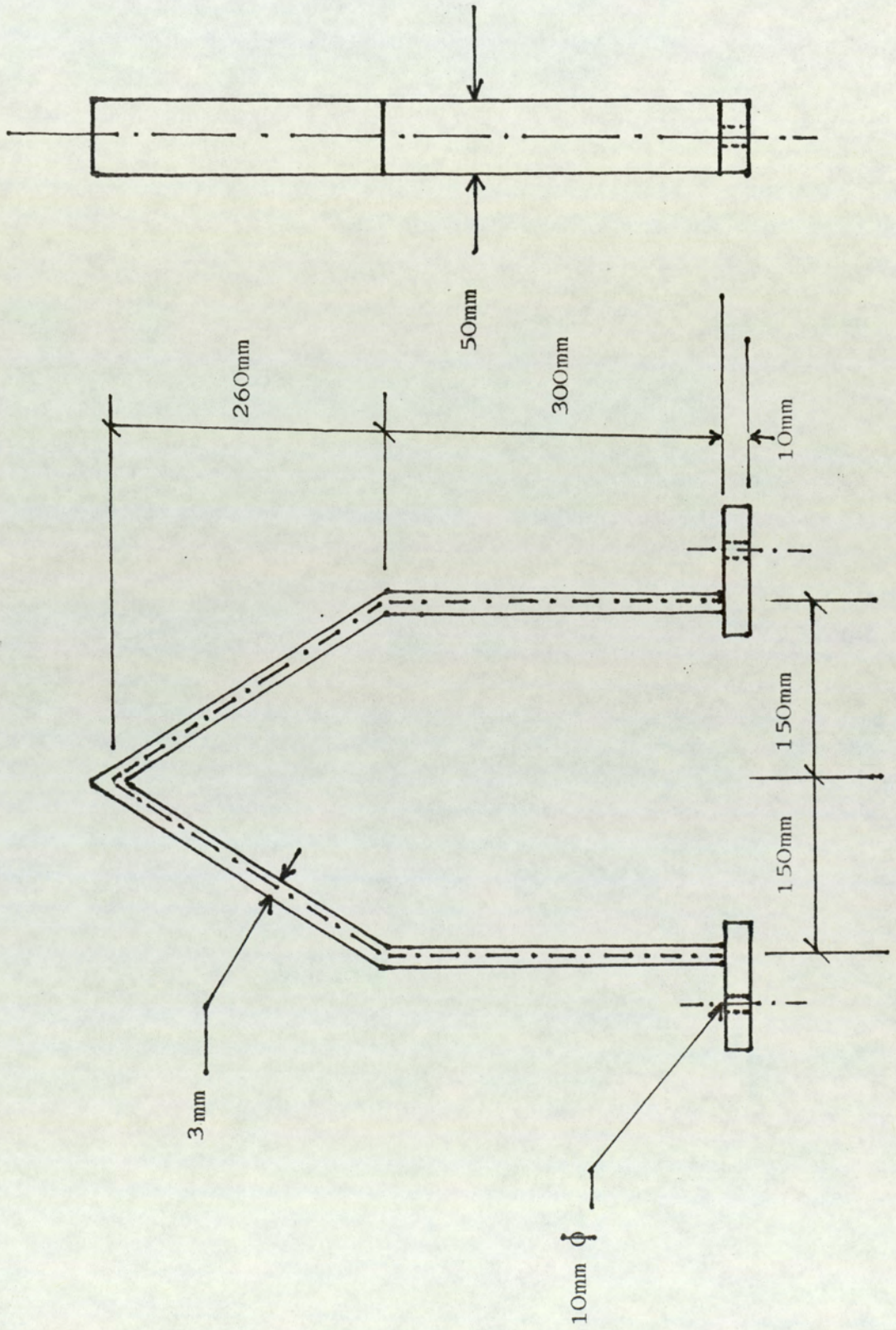


```
1540      *          1X, '      '//
1541      *          1X, '      '//
1542      *          15X, 'JOINT DEFLECTIONS'//
1543      *          15X, '===== '//
1544      *          15X, '      '//
1545      *          1X, '-----'//
1546      *          1X, '  JOINT      X-DEF      Y-DEF      ROTATION'//
1547      *          1X, '-----'//
1548      *          1X, '      ' )
1549      3400      FORMAT(1X, '      ', I2, '      ', F10.4, '      ', F10.4, '      ', F10.4, '      ')
1550      3500      FORMAT(1X, '      '//
1551      *          1X, '-----'//
1552      *          1X, '      '//
1553      *          1X, '      '//
1554      *          1X, '      '//
1555      *          1X, '      '//
1556      *          1X, '      '//
1557      *          18X, 'MEMBER FORCES'//
1558      *          18X, '===== '//
1559      *          18X, '      '//
1560      *          18X, '      '//
1561      *          10X, 'ALL AXIAL FORCES IN MEMBERS ARE'//
1562      *          10X, '      IN TENSION IF POSITIVE'//
1563      *          10X, '      '//
1564      *          1X, '-----'//
1565      *          1X, '  MEMBER      SHEAR      AXIAL      MOMENT      MOMENT'//
1566      *          1X, '      No      FORCE      FORCE      AT I      AT J'//
1567      *          1X, '-----'//
1568      *          1X, '      ' )
1569      3600      FORMAT(1X, '      ', I2, '      ', F9.2, '      ', F9.2, '      ', F10.2, '      ', F10.2, '      ')
1570      3700      FORMAT(1X, '      '//
1571      *          1X, '-----'//
1572      *          1X, '      '//
1573      *          1X, '      '//
1574      *          1X, '      '//
1575      *          1X, '      '//
1576      *          1X, '      ' )
1577      3800      FORMAT(28X, 'NON - LINEAR      ANALYSIS (MAJID)'//
1578      *          28X, '===== '//
1579      *          28X, '      '//
1580      *          28X, '      '//
1581      *          28X, '      '//
1582      *          15X, 'ANALYSIS WITH MUTUALLY INDEPENDENT STIFFNESS'//
1583      *          15X, 'MATRICES INCORPORATING THE LARGE DEFLECTIONS'//
1584      *          15X, '      '///)
1585      3900      FORMAT(48X, '---- END OF FILE ----')
1586      3950      FORMAT(28X, 'NON - LINEAR (COUPLING FACTORS)'//
1587      *          28X, '===== '//
1588      *          28X, '      '//
1589      *          28X, '      '//
1590      *          28X, '      '//
1591      *          15X, 'ANALYSIS INCORPORATING COUPLINGS BETWEEN THE'//
1592      *          15X, '      AXIAL AND FLEXURAL STIFFNESS MATRICES'//
1593      *          15X, '      '///)
1594      4000      FORMAT(1X, '      '//////////)
1595      END
```

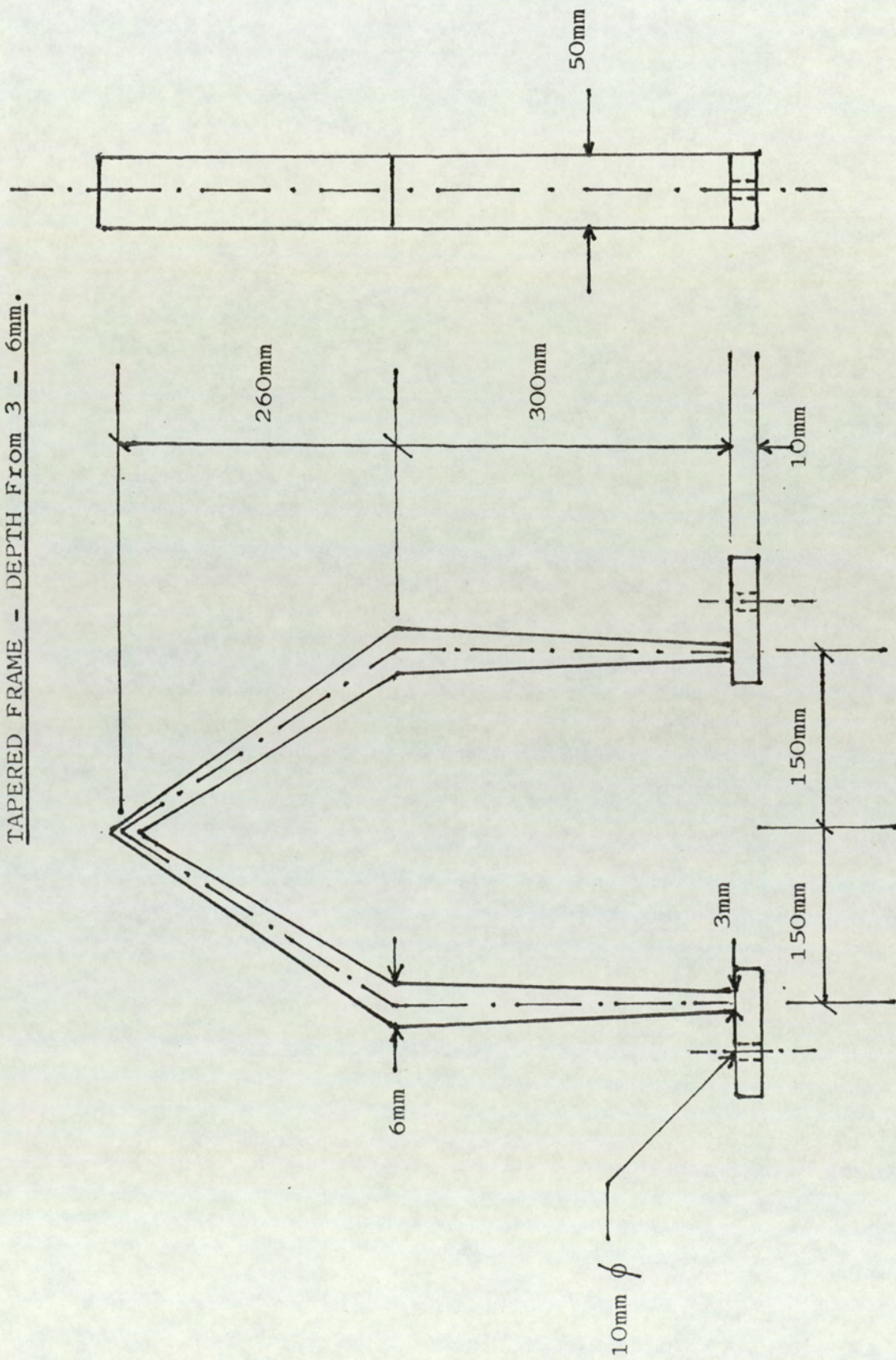

Appendix 4.

Working Drawings of Test Specimens.

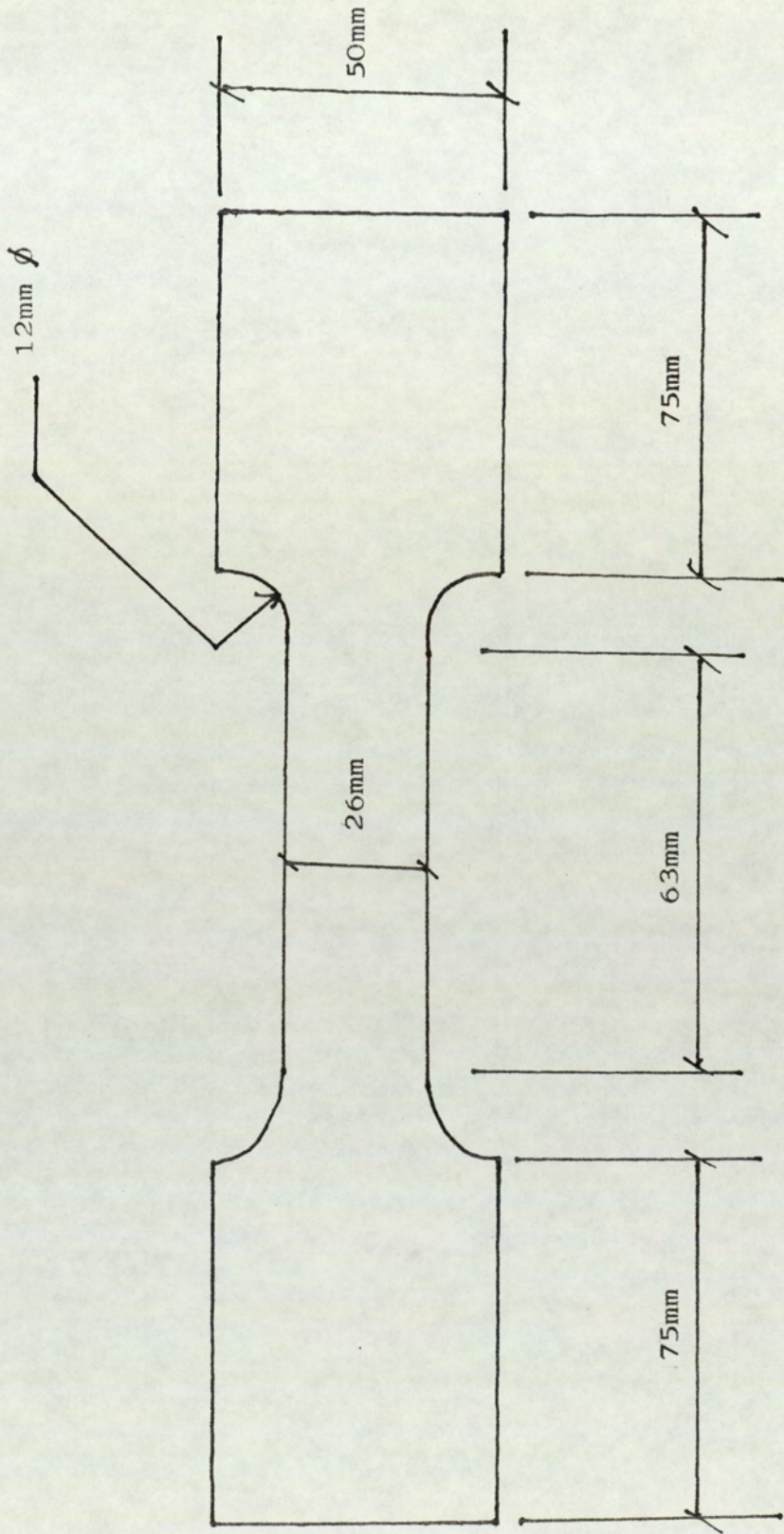
PRISMATIC FRAME WITH 3mm SECTION.



TAPERED FRAME - DEPTH FROM 3 - 6mm.



3mm TENSILE TEST SPECIMAN



6mm TENSILE TEST SPECIMAN.

